

# In the heat of the night: wheat respiration and photosynthesis in a warming world

Bradley Cooper Posch

A thesis submitted for the degree of Doctor of Philosophy of  
The Australian National University  
October 2021

© Copyright by Bradley Cooper Posch, 2021

All Rights Reserved

## Declaration

This thesis is my own original work, and no part of it has been previously submitted for any other tertiary degree. This thesis contains no material previously published by another person, except where acknowledged. Chapters 1, 2, 3, and 4 were co-authored, and author contributions have been specified for each of these chapters on their respective title pages.

A handwritten signature in black ink, appearing to read 'B. Cooper Posch', written in a cursive style.

Bradley Cooper Posch, 29/10/2021

*This thesis is dedicated to the memory of  
Heinrich and Erika Posch*

## Acknowledgements

I begin with grateful thanks to the Grains Research and Development Corporation, the Australian Government Research Training Program, and the Plant Energy Biology ARC Centre of Excellence for their generous support of my research, both financial and otherwise.

My biggest thank you goes to my primary supervisor, Owen Atkin, whose exceptional supervision is the reason I stuck with his lab through the completion of an undergraduate student project, an Honours thesis, and finally a PhD. Owen's passion for plant science is highly infectious, but more impressive is his genuine concern for the wellbeing and success of his lab members – this is what makes being in Owen's lab a true pleasure (the fact that he is a fellow St. Kilda tragic also helps). A special thanks also goes to Onoriode Coast, who has been an ever-reliable source of advice and assistance since I started in the lab. Coast is an exceptional role model, and I am extremely grateful for how generously he donated his time to me. Thank you also to the two other members of my supervisory panel, Helen Bramley and Spencer Whitney. As the original leader of our GRDC project Helen was a great source of crop physiology knowledge, and always encouraged me to follow my research interests. As for Spencer, I consider myself very fortunate to have enjoyed ready access to his frank and insightful advice (advice that always improved my experimental work), as well as his strong advocacy, goodwill, and (mostly) good humour.

There are many past and present members of the Atkin lab that I would like to acknowledge. I was lucky to have crossed paths with Shinichi Asao during my first few years, as he is one of my favourite people to talk science – or anything else – with. I thank Reshmi Gaju for teaching me nearly everything I know about wheat physiology and phenotyping, as well as for giving me the wonderful opportunity to assist her research at CIMMYT in Obregón, Mexico. Thanks also to Andrew Scafaro who provided invaluable tutelage in the lab, and with whom I have enjoyed countless meandering dialogues about films, books, Twin Peaks, and extra-terrestrial life. Thank you to Lingling Zhu, Zara Rashid, and Sally Buck for being patient and generous with their time when teaching me new lab techniques. To the rest of the lab – Yuzhen, Clarissa, Julia, Andy, Buddhima, John, Christina, Deping, Nur, Duncan – thank you for your

comradery and for fostering a fun and welcoming (if not quirky) environment. Special mention also to Cal Bryant, whose technical expertise saved the day on many an occasion.

Our lab was lucky to share a corridor with the folk in the Pogson and Borevitz labs, all of whom were very friendly and helpful when called upon. A special mention for Derek Collinge for being truly selfless and exceptional at his job, as well as just being a genuinely great bloke. Thanks to the RSB Plant Services team (Steve, Chris, Jenny, Darren, and Gavin) and the APPF staff (particularly Richard Poiré) for their expert preparation and management of controlled growth environments. Thanks also to Terry Neeman for her statistical and experimental design consultations.

In addition to all the brilliant people mentioned above, working at RSB also allowed me to work alongside a wider circle of impressive scientists. I thank Adrienne Nicotra for providing the opportunity to work as a demonstrator for her field ecology courses in Kosciuszko National Park and Singapore/Malaysia (alongside the dynamic duo of Megan Head and Wes Keys), for trusting me with the role of editor-in-chief of our undergraduate student journal, and for welcoming me to the Thermal Tolerance Team – a dream-team of temperature tolerance-minded folk! I also feel extremely privileged to have had the chance to learn from some of the very best plant scientists in the world during my time at RSB, and I thank the likes of Dani Way, Elizabeth Vierling, Richard Richards, Marilyn Ball, and John Evans for generously sharing their wisdom with me.

Outside the lab, I have been fortunate to enjoy the unwavering support of a great band of friends and family. My housemates over the last five years Sam H, Oli, Sam C, and Darcy are all great friends, and each a true mensch in their own right. Finally, thank you to Mum, Dad, Jemma, Daniel, Tracey, and Saff, because without their unconditional care and support this thesis would not have been possible.

## Abstract

Temperature is crucial in determining the efficiency of plant respiration and photosynthesis. Given ongoing trends of rising global average temperature, warming nights, and longer and hotter heatwaves, understanding how these key processes respond to high temperature is increasingly important. This rings particularly true for crops, because efforts to improve yields must contend with the consequences of warming. In this thesis, measurements of leaf gas-exchange, chlorophyll fluorescence, gene expression and protein thermostability were used to characterise the responses of respiration and photosynthesis to warming in field and controlled environment grown wheat.

Among 20 wheat genotypes grown over multiple seasons in the Australian wheat belt, elevated growth temperature coincided with reduced leaf dark respiration rate ( $R_{\text{dark}}$ ) when measured as  $\text{O}_2$  consumption ( $R_{\text{dark-O}_2}$ ) at a common temperature, reflecting the predicted acclimation response. However, warming was not associated with declines in either  $R_{\text{dark}}$  when measured as  $\text{CO}_2$  release ( $R_{\text{dark-CO}_2}$ ) or  $\text{CO}_2$  assimilation rate. The critical temperature at which photosystem II becomes damaged ( $T_{\text{crit}}$ ) was also used to quantify wheat photosynthetic heat tolerance and acclimation.  $T_{\text{crit}}$  varied dynamically with time of day and phenological stage, rising from heading to anthesis and grain-fill. Acclimation of  $T_{\text{crit}}$  to a 36°C heat shock was rapid (within two hours of heat stress), before reaching an upper threshold of approximately 43.7°C after three-to-five days. A systematic review of wheat  $T_{\text{crit}}$  data highlighted a 20°C variation in wheat leaf  $T_{\text{crit}}$ , though this was unrelated to the latitude of genotype origin.

Controlled environment experiments were also conducted to examine the effects of night versus day warming on  $R_{\text{dark}}$ . Wheat leaf  $R_{\text{dark-O}_2}$  measured at a common temperature again declined with warming, though this only coincided with night warming rather than day warming. Night warming also led to a lack of acclimation of leaf  $R_{\text{dark-CO}_2}$ , decreased plant biomass at maturity, and an increased capacity of the non-ATP producing alternative oxidase electron transport pathway. Taken together, this illustrated a predominant effect of night warming in reducing wheat growth, potentially via reduced ATP demand. Gene and protein-level analyses explored biochemical mechanisms underpinning physiological responses to elevated night temperature and daytime heatwave. A five-day 38°C daytime heatwave elicited a large and rapid

increase in gene expression for heat shock proteins 70 and 90 (*HSP70* and *HSP90*), as well as for the heat tolerant isoform of Rubisco activase (*Rca1-β*). Elevated night growth temperature seemed to prime these responses; warm night-grown plants increased their expression of *HSP70*, *HSP90*, and *Rca-1β* more rapidly during the heatwave. Additionally, after five days of heatwave, the Rubisco activase of warm night-grown plants displayed a higher thermostability than that of the cool-grown plants.

Overall, the results in this thesis demonstrate the dynamic and rapid responses of wheat respiration and photosynthesis to high temperature, as well as highlighting that night warming exerts greater influence over wheat energy metabolism than daytime warming does. These findings provide a framework for future efforts to improve wheat growth under elevated temperature, and also carry implications for the modelling of leaf carbon flux in a future, warmer world.

## List of publications & thesis format

Chapters 1, 2, and 4 of this thesis are mostly presented in the form in which they have been published, though some minor changes to these chapters have been included for this thesis in accordance with comments from thesis examiners. Similarly, Chapter 3 is presented largely in the form in which it has been accepted for publication, but with moderate changes reflecting the comments of thesis examiners. Minor formatting changes have also been made to these chapters to maintain a consistent format throughout the thesis.

### *Published*

- **Posch BC, Kariyawasam BC, Bramley H, Coast O, Richards RA, Reynolds MP, Trethowan R, Atkin OK.** 2019. Exploring high temperature responses of photosynthesis and respiration to improve heat tolerance in wheat. *Journal of Experimental Botany* **70**, 5051–5069.
- **Coast O, Posch BC, Bramley H, Gaju O, Richards RA, Lu M, Ruan YL, Trethowan R, Atkin OK.** 2021. Acclimation of leaf photosynthesis and respiration to warming in field-grown wheat. *Plant, Cell & Environment* **44**, 2331–2346.
- **Posch BC, Zhai D, Coast O, Scafaro AP, Bramley H, Reich PB, Ruan YL, Trethowan R, Way DA, Atkin OK.** 2021. Wheat respiratory O<sub>2</sub> consumption falls with night warming alongside greater respiratory CO<sub>2</sub> loss and reduced biomass. *Journal of Experimental Botany* **73**, 916–926.

### *Accepted for publication in the Journal of Experimental Botany*

- **Posch BC, Hammer J, Atkin OK, Bramley H, Ruan YL, Trethowan R, Coast O.** 2021. Wheat photosystem II heat tolerance responds dynamically to short and long-term warming.



# Table of Contents

<b><i>Declaration</i></b> .....	<b>2</b>
<b><i>Acknowledgements</i></b> .....	<b>4</b>
<b><i>Abstract</i></b> .....	<b>6</b>
<b><i>List of publications &amp; thesis format</i></b> .....	<b>8</b>
<b><i>Chapter 1 – Exploring high temperature responses of photosynthesis and respiration to improve heat tolerance in wheat</i></b> .....	<b>11</b>
<b>Abstract</b> .....	<b>11</b>
<b>Introduction</b> .....	<b>12</b>
<b>Potential mechanisms underpinning heat tolerance in wheat leaves</b> .....	<b>27</b>
<b>Net carbon balance of wheat – importance of photosynthesis and respiration</b> .....	<b>29</b>
<b>Conclusions and future directions</b> .....	<b>44</b>
<b>Acknowledgements</b> .....	<b>46</b>
<b>References</b> .....	<b>46</b>
<b><i>Chapter 2 – Acclimation of leaf photosynthesis and respiration to warming in field-grown wheat</i></b> .....	<b>58</b>
<b>Abstract</b> .....	<b>58</b>
<b>Introduction</b> .....	<b>59</b>
<b>Materials and methods</b> .....	<b>63</b>
<b>Results</b> .....	<b>68</b>
<b>Discussion</b> .....	<b>81</b>
<b>Acknowledgements</b> .....	<b>87</b>
<b>References</b> .....	<b>87</b>
<b>Supplementary material</b> .....	<b>94</b>
<b><i>Chapter 3 – Wheat photosystem II heat tolerance responds dynamically to short and long-term warming</i></b> .....	<b>111</b>
<b>Abstract</b> .....	<b>111</b>
<b>Introduction</b> .....	<b>112</b>
<b>Materials and methods</b> .....	<b>115</b>
<b>Results</b> .....	<b>122</b>
<b>Discussion</b> .....	<b>130</b>
<b>Acknowledgements</b> .....	<b>137</b>
<b>References</b> .....	<b>137</b>

Supplementary material.....	143
<b>Chapter 4 – Wheat respiratory O<sub>2</sub> consumption falls with night warming alongside greater respiratory CO<sub>2</sub> loss and reduced biomass .....</b>	<b>146</b>
Abstract.....	146
Introduction .....	147
Materials and methods .....	150
Results.....	156
Discussion.....	161
Acknowledgments .....	167
References.....	167
Supplementary material.....	172
<b>Chapter 5 – General discussion.....</b>	<b>177</b>
Recap of results .....	177
The pros and cons of differing approaches to studying heat tolerance of wheat physiology .....	179
Limits to acclimation/limits of life at high temperature .....	181
Implications for crop breeding and wheat yield gains.....	183
Improving models to represent plant carbon flux more accurately under warming .....	185
References.....	188
<b>Appendix .....</b>	<b>192</b>
The effect of night warming on Rubisco activase.....	192

# **Chapter 1 – Exploring high temperature responses of photosynthesis and respiration to improve heat tolerance in wheat**

**Bradley C. Posch, Buddhima C. Kariyawasam, Helen Bramley, Onoriode Coast, Richard A. Richards, Matthew P. Reynolds, Richard Trethowan, and Owen K. Atkin**

Author Contributions: B.C.P. and B.C.K. conducted searches of the literature; and B.C.P. wrote the paper with contributions from all authors.

*This manuscript has been published in the Journal of Experimental Botany (Posch BC, Kariyawasam BC, Bramley H, Coast O, Richards RA, Reynolds MP, Trethowan R, Atkin OK. 2019. Exploring high temperature responses of photosynthesis and respiration to improve heat tolerance in wheat. Journal of Experimental Botany 70, 5051–5069.)*

## **Abstract**

High temperatures account for major wheat yield losses annually and, as the climate continues to warm, these losses will likely increase. Both photosynthesis and respiration are the main determinants of carbon balance and growth in wheat, and both are sensitive to high temperature. Wheat is able to acclimate photosynthesis and respiration to high temperature, and thus reduce the negative affects on growth. The capacity to adjust these processes to better suit warmer conditions stands as a potential avenue toward reducing heat-induced yield losses in the future. However, much remains to be learnt about such phenomena. Here, we review what is known of high temperature tolerance in wheat, particularly in respect to the high temperature responses of photosynthesis and respiration. We also identify the many unknowns that surround this area, particularly in respect to the high temperature response of wheat respiration and the consequences of this for growth and yield. It is concluded that further investigation into the response of photosynthesis and respiration to high temperature could present several methods

of improving wheat high temperature tolerance. Extending our knowledge in this area could also lead to more immediate benefits, such as the enhancement of current crop models.

## Introduction

The warming climate presents a pressing challenge to the global economy and food security, with food production required to increase by 60% to feed the growing world population (Ray *et al.*, 2013). Globally, the climate has been steadily warming over the past century, with the four decades from the 1970s to 2018 each warmer than their predecessor (CSIRO and The Bureau of Meteorology, 2018). Under a high emission scenario, global mean temperature will continue to rise by at least 4°C towards the end of this century (IPCC, 2014). In addition, an increase in frequency, intensity, and durations of heatwaves is predicted, as well as a diurnal asymmetry in the increase of temperatures, with mean daily minimum increasing more rapidly than mean daily maximum (Davy *et al.*, 2017; García *et al.*, 2015; Hatfield and Prueger, 2015; Lobell and Field, 2007). Considering the major role of temperature in determining the rate of plant growth and development (Berry and Raison, 1981; Hatfield and Prueger, 2015), and that exposure to supra-optimal temperatures can cause irreversible damage, and even death, in all plant species (Hoffmann *et al.*, 2013), increases in average temperatures and heatwaves are a considerable concern. High temperatures can cause delayed germination, disruption of metabolic processes, and reproductive failure (Machado and Paulsen, 2001; Wahid *et al.*, 2007). For an economically and culturally valuable crop like wheat, the effect of heat on yield is of particular importance.

Global wheat production exceeds 700 million tonnes annually, making it one of the most widely grown crops in the world (Food and Agriculture Organization of the United Nations, 2018). However, increases in temperatures over recent decades have reduced wheat yields in several regions worldwide, a trend that is predicted to continue (Al-Khatib and Paulsen, 1984; Alexander *et al.*, 2006; Asseng *et al.*, 2015; Barnabás *et al.*, 2008). An example of the global trend can be seen in Australia, where rising temperatures accounted for 17% of the observed 27% decline in average wheat yield potential between 1990 and 2015 (Hochman *et al.*, 2017). Increases in both mean daily maximum and minimum temperatures drive these high temperature-induced yield

declines (Hunt *et al.*, 2018), with mean daily minimum temperatures exerting a proportionally greater influence on grain yields than mean daily maximums (Cossani and Reynolds, 2013; Martre *et al.*, 2017). Teamed with the fact that mean night-time temperatures are rising at a faster rate than those during the daytime (Davy *et al.*, 2017), warming nights loom as a potential source of significant wheat yield reduction in the near future.

#### *Effects of high temperature on wheat vary with development*

Wheat is vulnerable to high temperature throughout its life cycle (Wardlaw *et al.*, 1989b), with the optimal temperature range varying across different phenological phases (Farooq *et al.*, 2011; Porter and Gawith, 1999; Slafer and Rawson, 1995). The consequences of heat stress also vary with development (Table 1). Around reproduction and flowering, high temperature reduces the number of grains per spikelet and thereby grains per unit area (when above-average temperature occurs prior to anthesis) (Ferris *et al.*, 1998; Prasad *et al.*, 2008; Wardlaw *et al.*, 1995; Wheeler *et al.*, 1996), and grain weight (when high temperature occurs following anthesis) (Stone and Nicolas, 1994; Wardlaw *et al.*, 1989a; Wardlaw *et al.*, 1989b). High temperature at anthesis is particularly detrimental to yield because of the narrow optimum temperature range of fertilisation. High temperature disrupts fertilisation (Prasad and Djanaguiraman, 2014) via the abnormal development of reproductive organs, such as the ovule or pollen tube, which in turn increases grain abortion (Saini *et al.*, 1983). It is for these reasons that the effects of high temperature at anthesis have been so heavily studied to date.

**Table 1.** Negative effects of high temperature on wheat across development stages

<b>Developmental stage when heat treatment occurred (approximate Zadok's growth stages)<sup>1</sup></b>	<b>Temperature treatment</b>	<b>Key findings of effects of high temperature</b>	<b>Reference</b>
<u>Pre-anthesis</u>			
Includes Z10 – 60	Natural warming throughout vegetative stage	Shortened pre-anthesis stage, reduced biomass at anthesis	Liu <i>et al.</i> (2010)
No stage listed – model	Increased maximum temperatures during vegetative growth (modelled)	Increased crop evapotranspiration leading to reduced soil moisture later in seasons	(Asseng <i>et al.</i> , 2011)
Z0 – 59	30/23°C for duration of vegetative growth until ear emergence	Decreased duration of vegetative, spikelet, and elongation phases, decreased number of spikelets per ear	Rahman and Wilson (1978)
<u>Anthesis</u>			
~Z41	30°C for 3 days	Greatly decreased grain set, reduced female fertility	Saini <i>et al.</i> (1983)
~Z61 – 91	31/20°C, from anthesis to maturity	Reduced duration of grain filling period	Dias and Lidon (2009)
~Z59 – 65	12 days, max temp +31°C	Decreased root biomass, grain number and yield	Ferris <i>et al.</i> (1998)
~Z51 – 65	5 days, 36/26°C	Decreased floret fertility	Prasad and Djanaguiraman (2014)
<u>Post-anthesis</u>			

~Z69 – 83	3 days, max temp 40°C	Reduced individual grain mass	Stone and Nicolas (1994)
~Z69 – 91	24/19°C or 30/25°C from anthesis to maturity	Reduced grain mass at maturity	Wardlaw and Moncur (1995)
~Z69 - 75	34/26°C for 16 days, beginning 10 days after anthesis	Reduced quantum yield of PSII, reduced individual grain mass and yield	Pradhan and Prasad (2015)
~Z69 – 91	34°C/22°C, 32°C/24°C, 26°C/14°C, and 24°C/16°C from 7 days after anthesis to maturity	Accelerated leaf senescence, reduced single grain mass, increased lipid peroxidation	Zhao <i>et al.</i> (2007)

<sup>1</sup>Zadok's growth stages provided are estimates based on methodology provided in respective papers. Most studies did not provide any kind of growth scoring for their plants and estimates with large ranges of growth stage reflect this.

Wheat yields may also be adversely impacted by high temperatures occurring during developmental stages prior to and following anthesis (Porter and Gawith, 1999; Skylas *et al.*, 2002; Stone and Nicolas, 1994). High temperatures occurring as early as sowing can hamper both germination and seedling emergence (Rebetzke *et al.*, 2004). Supra-optimal temperatures during the vegetative stage speed up development (Al-Khatib and Paulsen, 1984; Asseng *et al.*, 2011; Harding *et al.*, 1990), causing plants to flower earlier in the season and leaving them vulnerable to substantial frost-induced yield losses (Hunt *et al.*, 2018). An acceleration of wheat development also reduces the window in which to capture resources (e.g. radiation and water) (Midmore *et al.*, 1982; Shpiler and Blum, 1986), thus reducing pre-anthesis biomass accumulation (Liu *et al.*, 2010). Up to 80% of total grain production can be drawn from carbohydrates accumulated and stored prior to flowering, and so less biomass at anthesis can reduce grain number (Prasad *et al.*, 2008; Slafer and Rawson, 1994) and overall yield (Blum *et al.*, 1994; Villegas *et al.*, 2001). Furthermore, a plant relies more heavily on stem carbohydrate reserves when experiencing stresses during the grain filling stage (Bidinger *et al.*, 1977). Thus, supra-optimal temperature earlier in development – prior to grain fill – will reduce the carbon supply that a plant is able to draw upon to later produce grain (Blum *et al.*, 1994). Coping with high temperature during vegetative growth thus requires that wheat be more efficient in the processes that control net carbon balance (i.e. photosynthesis and respiration) during vegetative growth. In this review, we explore what is known, and not known, about the impacts of heat on these two core carbon exchange processes in wheat.

#### *High temperature responses of photosynthesis and respiration*

Photosynthesis and respiration are both temperature sensitive. Net photosynthesis ( $A_{\text{net}}$ ) increases as leaf temperature rises, peaking at an optimum temperature ( $T_{\text{opt}}$ ) and then declining (see Fig. 1), reflecting the impact of temperature on photosynthetic  $\text{CO}_2$  fixation, and  $\text{CO}_2$  release by photorespiration and mitochondrial respiration. However, following sustained increases in growth temperature, most plants (including wheat) can adjust, or ‘acclimate’, their photosynthetic characteristics (Berry and Bjorkman, 1980; Yamori *et al.*, 2014). Thermal acclimation is a process by which plants adjust metabolic rates to compensate for a change in



growth temperature, potentially resulting in metabolic homeostasis (i.e. identical metabolic rates in contrasting thermal regimes when measured *in situ*). As discussed in more detail in later sections, photosynthetic thermal acclimation likely involves altered activity of the enzyme responsible for CO<sub>2</sub> fixation – Rubisco, adjustments in electron transport through photosystem II (PSII) in chloroplasts (Yamasaki *et al.*, 2002), and changes in photo-inhibition susceptibility (Hurry and Huner, 1991, 1992; Oquist *et al.*, 1993). While the general temperature response of photosynthesis is well studied, little is known of genotypic variation in wheat photosynthetic thermal acclimation to high temperature, or of the mechanisms regulating it. This is important in the context of determining wheat yield under high temperature, as optimising photosynthesis serves to maximise net carbon gain in the daytime. Even less is known about the temperature-response of the other component of net carbon balance, respiration.

Wheat leaf respiration increases in response to short-term temperature rise (de Vries *et al.*, 1979), generally doubling with every 10°C increase in sub-optimal temperature (Table 2, Fig. 2), with the temperature dependence of respiration likely to be primarily driven by how temperature affects the processes of substrate supply (Azcón-Bieto *et al.*, 1983; Bingham and Stevenson, 1993) and demand for respiratory products, both locally and in remote tissues (Farrar, 1985; Farrar and Williams, 1991; O'Leary *et al.*, 2018). Energy demand is derived from processes such as phloem loading, protein turnover, ion gradient maintenance, and other metabolic activities in leaves and roots (Vos, 1981). Importantly, short-term changes in temperature have a greater effect on leaf respiration than on photosynthesis (Dusenge *et al.*, 2019), a factor with important consequences for leaf carbon economy. Some wheat varieties are able to thermally acclimate respiration to compensate for sustained increases in growth temperature, minimising respiratory carbon losses in leaves under hot growth conditions (Figure 2) (Gifford, 1995; Kurimoto *et al.*, 2004). In wheat, capacity to acclimate leaf respiration has also been linked to homeostasis of relative growth rate with varying growth temperature (Kurimoto *et al.*, 2004). Thus, it seems likely that the temperature response of leaf respiration, both over the short and long-term, is central in determining wheat net carbon balance and biomass accumulation following high temperature exposure. Despite this likelihood, our knowledge of the connection between respiratory thermal acclimation and wheat growth and yield remains limited.

**Table 2.** Summary of past approaches used to quantify the response of wheat respiration to short-term increases in temperature

<b>Approach used to measure short term temperature sensitivity<sup>1</sup></b>	<b>Scope of the study relevant to the present review</b>	<b>Growth stage considered for measurements</b>	<b>Organ/organelle used for respiration measurements</b>	<b>Findings</b>	<b>Reference</b>
Arrhenius plots	To study the effect of temperature on mitochondrial and shoot segment respiration in three wheat varieties grown at 2 and 18°C	Compared germinating seedling at common morphological stage i.e. seedlings grown at 24°C for 2 days with seedlings at 2°C for 4 weeks in the dark	Shoot segments and isolated mitochondria	Respiration decreased sharply beyond the transition temperature of 6-10°C for shoot segments and 10-14°C for isolated mitochondria indicating increased activation energy ( $E_a$ ) for respiration	Pomeroy and Andrews (1975)

---

<p>To explore the cyanide-insensitive respiration among wheat genotypes and the effects of temperature</p>	<p>Etiolated coleoptiles at 20-22°C for 3-4 days in the dark</p>	<p>Isolated mitochondria</p>	<p>Relatively linear increase in respiration increasing temperature. A distinct break noted at ~17.5 °C and alternative respiration was maximal around this point as the state of mitochondrial membrane influenced the alternative oxidase in germinating wheat. Also, respiration declined following this point partly owing to decreased solubility of oxygen when increasing temperature</p>	<p>McCaig and Hill (1977)</p>
<p>To test whether the <math>E_a</math> of wheat mitochondrial oxidative activity is constant across the physiological range of temperature and to explore any phase transition in membrane lipids within this temperature range.</p>	<p>Germinating seedling at 24°C for 24 to 36 hours in the dark</p>	<p>Isolated mitochondria</p>	<p>The <math>E_a</math> for the oxidation of both succinate, <math>\alpha</math>-ketoglutarate and succinate-cytochrome c oxidoreductase activity were constant across the temperature range of 3-27°C and a phase transition has been noted about 0 and 30°C for wheat membrane lipids in chilling resistant varieties being similar to their chilling sensitive counterparts.</p>	<p>Raison <i>et al.</i> (1977)</p>

---

	To explore the effect of carbohydrate status on temperature dependence of respiration in darkened and illuminated wheat leaves	Mature leaves of 30-day-old plants grown at 25/20°C and at day length of 13 hours. Measurement temperatures began at 20°C and increased rapidly up to 42°C	Mature leaves	CO <sub>2</sub> efflux increased following photosynthetic activity due to carbohydrate accumulation and a dramatic change observed in the shape of respiration-temperature showing different $E_a$ above and below 20°C.	Azcón-Bieto and Osmond (1983)
$Q_{10}$	The temperature coefficient of respiration in the short term	Instantaneous temperature response of respiration was measured between 14 and 27°C	Various organs including shoot, roots, stem, sheath, leaf laminae and ears	The $Q_{10}$ remained closer to 2.2 yet varied from 1.8 to 2.4 when tested between 14-27°C. A representative $Q_{10}$ value of 2.2 has been suggested by authors for vegetative organs of wheat irrespective of the treatment, age, organ, and temperature range.	(Vos, 1981)
	Effect of temperature on dark respiration and temperature sensitivity of wheat varieties in vegetative stage	14 hour photoperiod and measurement temperatures ranged from 5 - 35°C, with exposure for between 30 – 60 minutes	Shoots during vegetative stage	Respiration increased when increasing temperature up to 35°C. $Q_{10}$ was 1.89 at 15/5°C (day/night), 1.37 at 25/15°C, and 1.98 at 35/25°C. Respiration rate at 35°C was higher in vegetative stage than at reproductive stage.	(Todd, 1982)

---

Effect of temperature on dark respiration and temperature sensitivity of wheat varieties in reproductive stage	14 hour photoperiod and measurement temperatures ranged from 5 - 35°C, with exposure for between 30 – 60 minutes	Flag leaf and spike during reproductive stage	Respiration gradually increased when increasing temperature from 5°C to 35°C. Consistently higher respiration values than vegetative stage at same measuring temperatures. $Q_{10}$ value decreased from 3.74 for plants at 15/5°C (day/night) to 2.04 at 35/25°C	(Todd, 1982)
Observe response of leaf dark respiration in winter wheat to natural variations in night temperature	Plants experienced ambient night-time temperature fluctuations (10 - 21°C), leaf dark respiration measured at four time points throughout one night during booting stage	Mature flag leaves	From four measurements taken throughout one night, $Q_{10}$ value was 1.977	(Tan <i>et al.</i> , 2013)

---

	Measure relationship between dark respiration of shoots and ears with N, water availability, temperature, and simulated photosynthesis	Shoots measured through vegetative stage to anthesis, ears measured from anthesis to maturity	Main shoots and ears	Although not explicitly provided by the authors, $Q_{10}$ could be estimated from figure. $Q_{10}$ for shoots was roughly 2; for ears, $Q_{10}$ was approximately 2 when measured near anthesis, yet less than 2 when measured closer to maturity	(Mitchell <i>et al.</i> , 1991) <sup>2</sup>
Arrhenius plot and $Q_{10}$	Compare short and long term effects of temperature on dark respiration, its components and its relationship to the ratio of respiration to net assimilation	Plants were grown at 15, 20, 25 and 30°C and then exposed to 15, 20, 25, or 35°C for 4 hours	Whole plants	Arrhenius coefficients of $1.2 \times 10^6$ , $46 \times 10^3$ , $5 \times 10^3$ , $0.3 \times 10^3$ and $Q_{10}$ values of 1.80, 1.59, 1.49 and 1.32 were found at 15, 20, 25, 30°C, respectively. The absolute sensitivity of specific respiration was independent of temperature across 15-25°C and then declined at 30°C	(Gifford, 1995)

<sup>1</sup> $Q_{10}$ , extent of increase in respiratory rate with an increase in temperature of 10 °C; <sup>2</sup> the authors do not mention the term  $Q_{10}$ , but they provided results that allow for the calculation of  $Q_{10}$ .

### *Scope of review*

In this review, we focus on short and long-term responses of wheat net carbon balance to high temperature. Specifically, we examine the high temperature responses of wheat photosynthesis and respiration, and their relationships in the context of crop production. While acknowledging that the effects of high temperature on wheat can depend on the presence of other stresses (abiotic and biotic) - including most notably with water stress, which can cause stomatal closure and increase leaf temperature (Reynolds *et al.*, 2010) - for the purposes of this review we focus solely to the effects of high-temperature. We begin with considering the general mechanisms likely to underpin heat tolerance in wheat, drawing on studies specific to this crop, as well as from other model systems. Thereafter, we discuss the roles of photosynthesis and respiration in determining leaf level and whole-plant net carbon balance. Next, we explore the response of wheat photosynthesis to short- and long-term high temperature exposure, including the biochemical mechanisms potentially underpinning this response. We then review factors that influence respiratory costs of growth and maintenance processes, and how temperature affects these processes, including changes associated with thermal acclimation of mitochondrial respiration. The importance of understanding how both wheat photosynthesis and respiration will respond to rising temperatures is highlighted throughout, particularly in the context of avoiding major yield reductions in a rapidly warming world.

**Box 1. High temperature tolerance and acclimation of photosynthesis and respiration**

Figures 1 and 2 depicts the typical temperature responses of net CO<sub>2</sub> assimilation ( $A_{\text{net}}$ ) and leaf dark respiration ( $R$ ), respectively, with a focus on what occurs at high temperatures when these processes peak (i.e. at the temperature of maximum photosynthetic rate –  $T_{\text{opt}}$ , and respiration rate –  $T_{\text{max}}$ ) and then begin to fall. Figure 1 compares the temperature response of light-saturated  $A_{\text{net}}$  in a cold-acclimated and hot-acclimated plant.  $A_{\text{net}}$  increases with measuring temperature, until it reaches a maximum rate of assimilation ( $T_{\text{opt}}$ ).  $A_{\text{net}}$  reflects the balance between photosynthetic carbon gain and photorespiratory carbon loss. Thus,  $T_{\text{opt}}$  is not necessarily an optimum temperature for photosynthetic carbon gain, but rather the point at which photosynthetic carbon gain is maximized in respect to respiratory carbon loss. Increases in temperature beyond  $T_{\text{opt}}$  result in  $A_{\text{net}}$  sharply declining.  $A_{\text{net}}$  is determined by a combination of the carboxylation rate of Rubisco ( $V_c$ ), the oxygenation rate of Rubisco ( $V_o$ ), and respiration in the light ( $R_{\text{light}}$ ). The equation for this comes from Farquhar *et al.* (1980):

$$A_{\text{net}} = V_c - 0.5V_o - R_{\text{light}}$$

The effects of these factors on  $A_{\text{net}}$  change with temperature, as is represented in the bars below Fig. 1. The increase in  $A_{\text{net}}$  prior to reaching  $T_{\text{opt}}$  is driven by the rise in  $V_c$  outpacing that of  $V_o$  or  $R_{\text{light}}$ . However, beyond  $T_{\text{opt}}$   $V_o$  and  $R_{\text{light}}$  begin to increase with temperature at a rate greater than that of  $V_c$ . This results in carbon loss outpacing carbon gain, and thus the observed decrease in  $A_{\text{net}}$ . As temperature increases beyond  $T_{\text{opt}}$ , the specificity of Rubisco for fixing CO<sub>2</sub> decreases faster than that for fixing O<sub>2</sub>, resulting in less efficient enzyme activity and a lower  $A_{\text{net}}$  (Walker *et al.*, 2016). Leaf CO<sub>2</sub> uptake is also reduced due to stomatal conductance decreasing at these temperatures, which acts to increase the ratio of  $V_o$  to  $V_c$  (Walker *et al.*, 2016). The balance between  $V_o$  and  $V_c$  presents a potential avenue to enhancing wheat  $A_{\text{net}}$  at above-optimum temperatures. Genetic variability in Rubisco catalytic properties, specifically the affinity for CO<sub>2</sub> over O<sub>2</sub>, has been observed among 25 wheat genotypes (Prins *et al.*, 2016). This suggests that this trait could potentially be selected for in the effort to improve  $A_{\text{net}}$  of wheat at temperatures beyond the current temperature optimum.

At low temperatures in light saturated conditions carbon assimilation is limited by the rate of electron transport. When temperatures approach and exceed  $T_{\text{opt}}$  the maximum rate of



carboxylation by Rubisco ( $V_{\text{cmax}}$ ) becomes the predominant factor limiting assimilation. Therefore,  $T_{\text{opt}}$  is partly a reflection of  $V_{\text{cmax}}$ , and so a higher  $T_{\text{opt}}$  may be indicative of a greater  $V_{\text{cmax}}$ . Applying this to Fig. 1, it is likely that the  $V_{\text{cmax}}$  of the cold-acclimated plant is greater than that of the hot-acclimated plant at temperatures below and around its  $T_{\text{opt}}$ . However, as temperatures increase beyond this point, the  $V_{\text{cmax}}$  of the hot-acclimated plant continues to increase, while that of the cold-acclimated plant falls. The difference in  $A_{\text{net}}$  at high measuring temperatures between the cold- and hot-acclimated genotypes in Fig. 1 therefore reflects the difference in  $V_{\text{cmax}}$  between the two plants. Because of the important role of Rubisco Activase (Rca) in maintaining Rubisco function at high temperatures,  $V_{\text{cmax}}$  represents the capacity of Rca to continually activate Rubisco under heat stress. The higher  $T_{\text{opt}}$  of the hot-acclimated plant in Fig. 1 suggests that it has a greater  $V_{\text{cmax}}$  at high measuring temperatures, and thus likely a greater abundance of and/or a more thermally stable Rca.

Figure 2 shows dark respiration plotted against measurement temperature for a hot acclimated and a cold acclimated plant. This figure was generated using the Schoolfield model of temperature-dependent enzyme activity (Schoolfield *et al.*, 1981). The acclimation effect observed was generated within the model by increasing the high temperature tolerance of enzyme activity and decreasing the rate of enzyme activity at 25°C in the hot-acclimated plant when compared to the cold-acclimated plant. As is the case for  $A_{\text{net}}$  in Fig. 1, respiration increases with temperature until it peaks at  $T_{\text{max}}$ , at which point respiration rate decreases with subsequent increases in temperature. The thermal acclimation of respiration can be seen when comparing the curves of the two plants at different measuring temperatures. Respiration in the hot-acclimated plant is lower than the cold-acclimated plant at lower measuring temperatures.  $T_{\text{max}}$  also occurs at a higher temperature in the hot-acclimated plant, and so respiration begins to fall at lower temperatures in the cold-acclimated plant than in the hot-acclimated one. At 30°C,  $R$  is greater in the cold-acclimated plant than the hot-acclimated one. This corresponds to what is occurring at the same temperature in Fig. 1, where  $A_{\text{net}}$  is lower in the cold-acclimated than the hot-acclimated plant. The decrease in  $A_{\text{net}}$  in the cold-acclimated plant at 30°C is likely driven in part by an increase in carbon loss via  $R$ . Similarly, the hot-acclimated plant's ability to maintain

$A_{net}$  at higher temperatures than the cold-acclimated plant is aided by a comparatively lower respiratory rate at these temperatures.

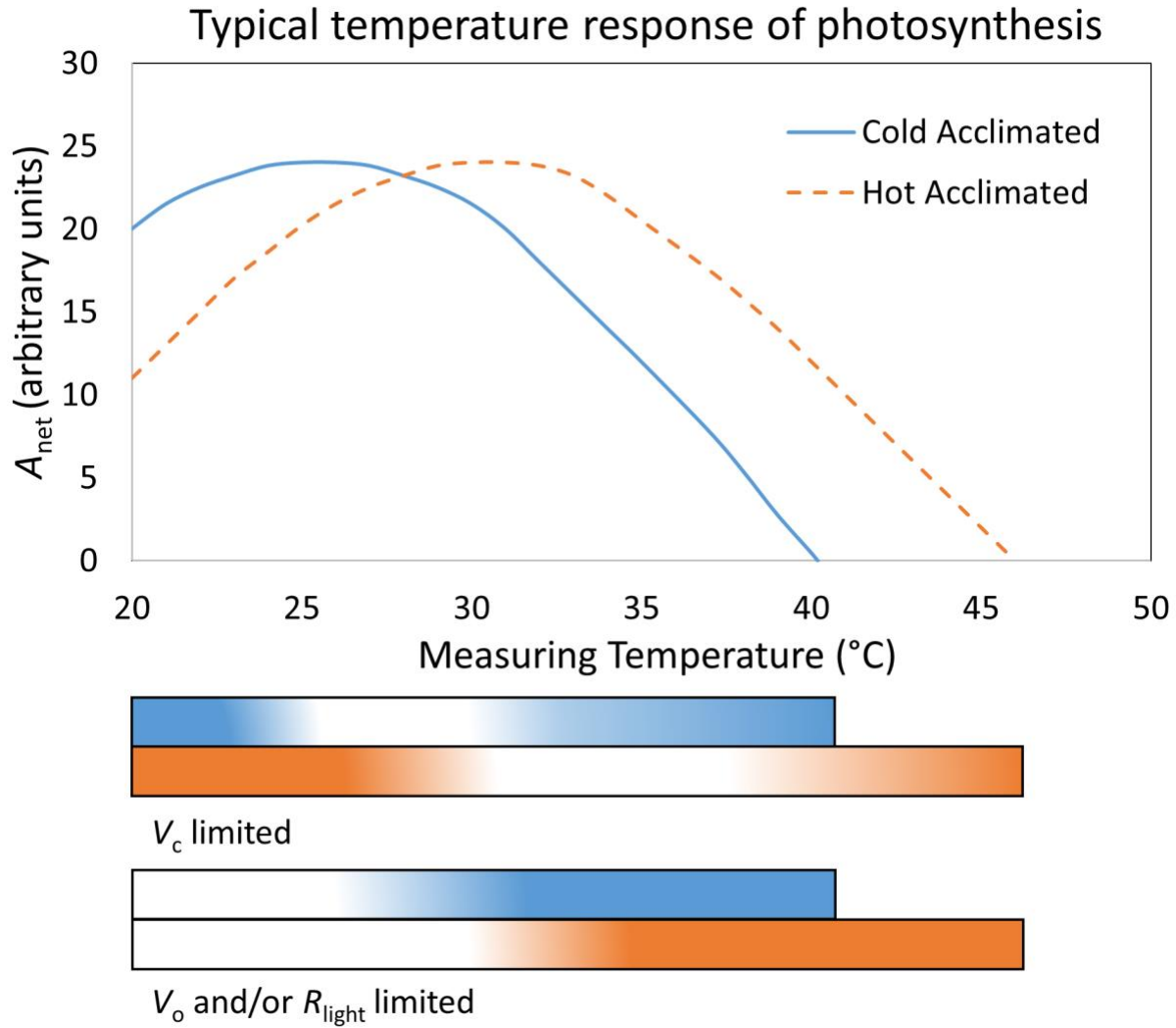


**Figure 1:** Typical temperature response curves of net  $\text{CO}_2$  assimilation ( $A_{net}$ ) for a cold-acclimated plant (blue, solid line) and hot-acclimated plant (orange, dotted line). Bars underneath plot indicate factors limiting  $A_{net}$  as temperature increases.  $A_{net}$  is predominantly limited by Rubisco capacity ( $V_c$ ) at sub-optimal temperatures and by the rates of oxygenation of Rubisco ( $V_o$ ) and respiration in the light ( $R_{light}$ ) at supra-optimal temperatures.

Acclimation of respiration as change in  $V_{25}$  and  $T_H$  — 337 — 347

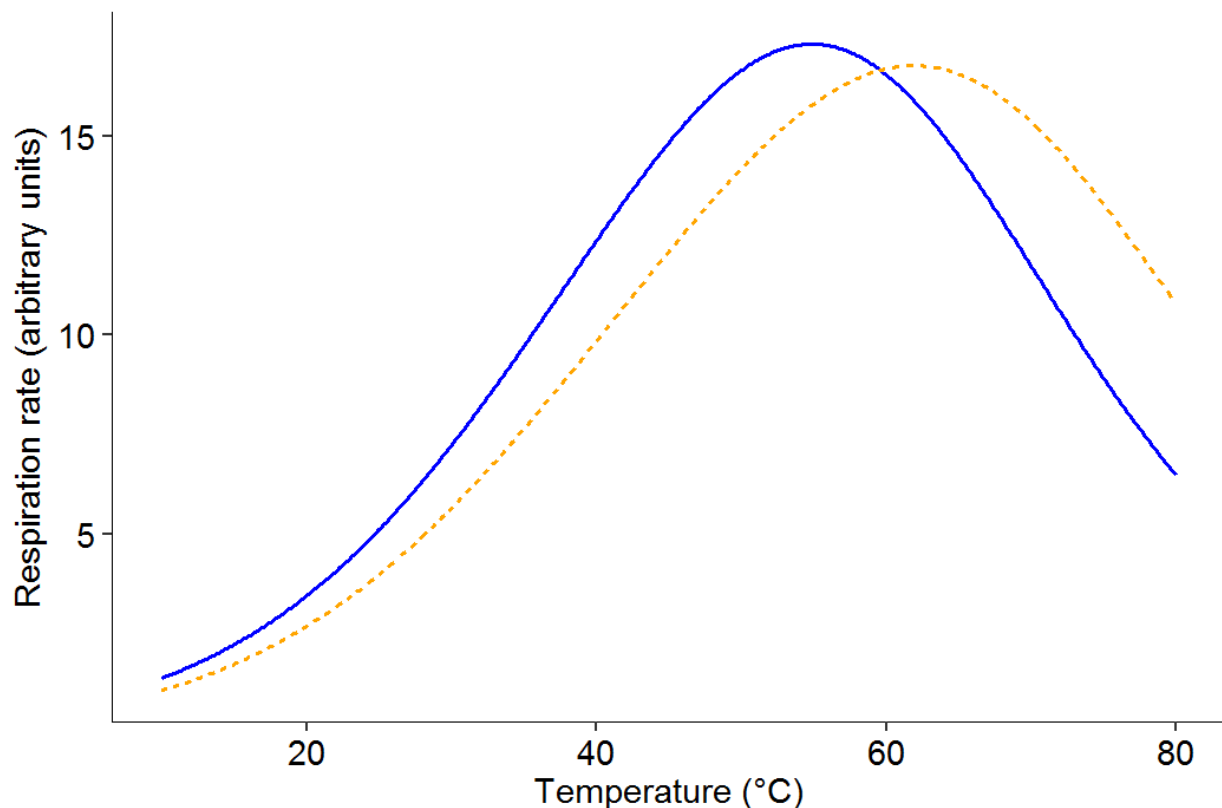


**Figure 2:** Typical high temperature responses of leaf dark respiration in a cold acclimated (blue solid line) and hot-acclimated (orange dashed line) plant. Figure was generated using the Schoolfield model of temperature-dependent enzyme activity (Schoolfield *et al.*, 1981). The parameters of the model that were altered to achieve the acclimation response pictured were enzyme activity (arbitrary units) at 25°C ( $V_{25}$ ) and the high temperature tolerance (in K) of enzyme activity ( $T_H$ ). For the cold acclimated plant,  $V_{25} = 14$ ,  $T_H = 337$  K; for the hot-acclimated plant,  $V_{25} = 18$ ,  $T_H = 347$  K.

### Potential mechanisms underpinning heat tolerance in wheat leaves

Various biochemical mechanisms underpin heat tolerance in plants, including wheat, although the exact nature of these remain unclear. These mechanisms are related to lipid membrane thermostability, heat shock proteins (HSPs), reactive oxygen species (ROS), antioxidants, and the activities of important enzymes (e.g. Rubisco, starch synthase), among other factors. The thermostability of lipid membranes is controlled by the saturation or unsaturation of membrane fatty acids. Membranes with greater thermostability enhance protection against ROS, which are

a by-product of increased respiration under high temperatures (Brestic *et al.*, 2012; Christiansen, 1978; Cossani and Reynolds, 2012; Mohammed and Tarpley, 2009). High temperature causes membranes to become overly fluid and permeable (Fig. 3) (Allakhverdiev *et al.*, 2008). The degree of saturation of membrane fatty acids regulates the structure of the membrane, with higher relative levels of saturated compared to unsaturated fatty acids in a membrane promoting rigidity (Los and Murata, 2004; Narayanan *et al.*, 2016). Therefore, plants that are more adept at increasing the ratio of saturated to unsaturated fatty acids in lipid membranes are likely to be more tolerant of heat stress (Murata and Los, 1997). PSII, a highly heat-susceptible component of the photosynthetic electron transport chain, is embedded in the thylakoid membrane. A higher degree of membrane thermostability is likely to promote heat tolerance of PSII, and thus result in a greater degree of photosynthetic thermal tolerance. Indeed, cell membrane thermostability has been observed to positively correlate with biomass and yield under high temperatures in field conditions, independent of drought or biotic stresses (Blum *et al.*, 2001; Reynolds *et al.*, 1994).

Heat shock proteins are another biochemical mechanism associated with plant thermal tolerance. These proteins are induced rapidly and in large quantities following the onset of heat stress, and are thought to assist other proteins to maintain functionality (Vierling, 1991; Wang *et al.*, 2004). Assistance may include acting as chaperones to other proteins to ensure that they are able to continue to function during bouts of high temperature, as well as preventing the aggregation of misfolded proteins (Trösch *et al.*, 2015). Despite persisting uncertainty about how specific HSPs may confer heat tolerance in wheat, studies in other species have found that they protect PSII during episodes of high temperature (Heckathorn *et al.*, 1998; Schroda *et al.*, 1999). Although no direct causal relationship was observed, Krishnan *et al.* (1989) found a positive correlation between thermal tolerance and the expression of small HSPs in two wheat varieties differing in susceptibility to heat stress. Small HSPs have also been associated with enhancing grain quality (Skylas *et al.*, 2002). Further research is needed to better understand how specific HSPs promote thermal tolerance in wheat, as well as the effect that the expression of these proteins may have on grain yield and quality. More specifically, the role of HSPs and membrane thermostability in protecting respiration and photosynthesis in wheat under high temperatures

remains unclear, although it is likely that they number among the mechanisms that regulate the thermal tolerance of each of these processes.

Some of the potential biochemical explanations for heat-induced declines of chloroplast and mitochondrial function are presented in Fig. 3. High temperature has the effect of increasing the fluidity of cell and organelle lipid membranes, interfering with the membrane's ability to regulate what is allowed to pass in and out of the cell/organelle (Fig. 3). Membrane damage of this kind is common to both chloroplast and mitochondrial-located membranes (Niu and Xiang, 2018). In the context of the chloroplast, heat-induced membrane damage results mainly from the peroxidation of lipids (particularly polyunsaturated fatty acids), which interferes with the maintenance of the pH gradient required for ATP synthesis (Yadav and Pospíšil, 2012). Components of the PSII complex itself are also damaged by ROS under heat stress, most notably the D1 protein (Fig. 3) (Chan *et al.*, 2012). Heat stress to mitochondrial membranes has a similarly negative effect on ATP production. In mitochondria, this stems from the peroxidation of the phospholipid cardiolipin, which in turn inhibits cytochrome c oxidase activity, thus decreasing electron transport and, ultimately, ATP synthesis (Pan *et al.*, 2014; Paradies *et al.*, 1998). However, by increasing the relative amount of saturated fatty acids in cellular and organelle membranes, the membrane is able to preserve its optimal structure at higher temperatures. This fortification of membranes at high temperature offers membrane-bound electron transport greater protection from ROS, therefore enhancing the thermotolerance of photosynthesis and respiration.

### **Net carbon balance of wheat – importance of photosynthesis and respiration**

The net carbon balance within plants is determined by a combination of both photosynthetic assimilation ( $A$ ) and respiration ( $R$ ). The general ratio of  $R/A$  in whole plants likely ranges between 0.35 – 0.80 (when measured at a common temperature), with the exact number varying based on both biotic and abiotic factors during plant growth (Amthor, 2000). For wheat, maize, and rice, the ratio of  $R/A$  generally falls between 0.3 – 0.6 (Amthor, 1989). Even small variations in this ratio can significantly affect plant growth, illustrating the importance of both  $A$  and  $R$  in determining overall productivity. The response of photosynthetic and respiratory carbon

exchange to temperature is crucial in this respect, as  $R/A$  ratios of whole-plants typically increase with measurement temperature (Gifford, 1995). This reflects the fact that respiration is typically more sensitive to rising temperature than is net photosynthesis (Dusenge *et al.*, 2019). Looking ahead, one strategy to improve net carbon gain of wheat, then, could be to screen genotypes for variability in: (1) temperature-normalized  $R/A$  (i.e. of plants grown and measured at 25°C); (2) temperature-sensitive changes in  $R/A$  values (e.g. via having a lower differential in the short-term temperature sensitivity of  $R$  and  $A$ ); and, (3)  $R/A$  values of hot-acclimated plants, where the target is to identify genotypes with lower  $R/A$  following acclimation to hot conditions.

A lower  $R/A$  could be achieved through improving the rate of photosynthetic  $\text{CO}_2$  fixation (e.g. via increasing heat stability of Rubisco activity or improving PSII functionality), reducing the energy costs associated with cellular maintenance and/or biosynthesis (and thus limiting the rate of respiratory  $\text{CO}_2$  release), and/or improving the efficiency of respiratory ATP synthesis per unit of  $\text{CO}_2$  released. There is growing evidence of significant variation in net photosynthetic rate among field-grown wheat varieties (Reynolds *et al.*, 2000); similarly, a recent study (Scafaro *et al.*, 2017) using a high-throughput technique reported substantial genotypic variation in leaf respiration rates in wheat. Together, these observations point to the probability that  $R/A$  does differ among wheat lines. Moreover, there are reports of grain yields being higher in ryegrass, tomato and canola lines that exhibit lower respiratory rates (Hauben *et al.*, 2009; Nunes-Nesi *et al.*, 2005; Wilson and Jones, 1982). While the stability of such traits may vary depending on planting density (Kraus and Lambers, 2001), the possibility remains that variations in photosynthesis and/or respiration could influence wheat yields. More work needs to be done to understand how respiration influences growth and yield in wheat, how these relationships may be impacted by increased temperature, and whether measurement at the plant level extrapolates to field canopies. The capacity to identify varieties that maintain lower respiration rates under high temperatures could be invaluable to efforts to develop new wheat varieties better suited to a future climate that is increasingly warming and unpredictable.

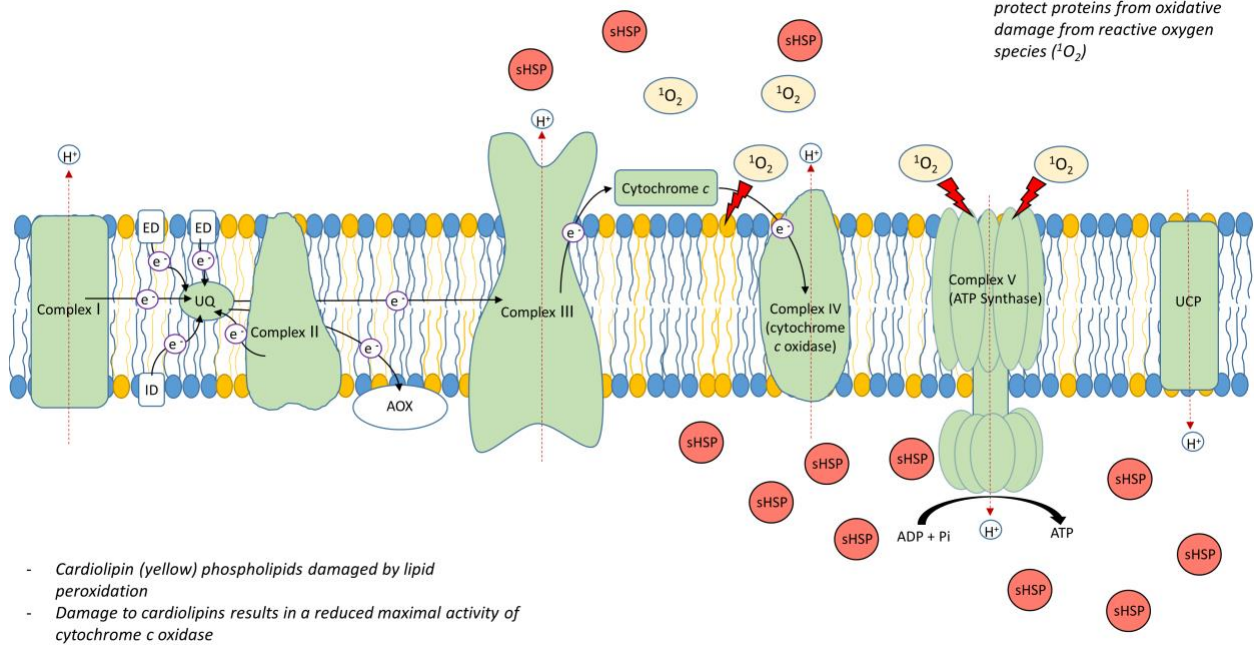
Below, we outline possible ways of maintaining favourable net carbon balance in wheat. We start by focussing on mechanisms underpinning thermal acclimation of photosynthesis; we

then consider factors that could influence respiratory costs associated with maintenance and growth, and finally, we consider what is known about thermal acclimation of respiration in wheat.

### *Thermal tolerance and acclimation of photosynthesis*

Photosynthesis is a highly thermolabile process, which can be influenced or altered by high temperatures in a number of ways. The basic temperature response of photosynthesis has been well documented and, aside from variations based on species or biome differences, is largely conserved across plant species. It generally resembles a parabolic curve, with the photosynthetic rate initially increasing with temperature, before reaching a peak ( $T_{opt}$ ) and then declining with further temperature increases (Fig. 1) (Berry and Bjorkman, 1980). This means that temperature extremes on either side of  $T_{opt}$  can inhibit photosynthesis. Temperatures significantly higher than  $T_{opt}$  can result in a reduction in photosynthesis in both wheat leaves and ears, which in turn impairs grain fill (Blum *et al.*, 1994). However, most plants are equipped to deal with non-optimal temperatures by acclimating their optimal temperature range of photosynthesis to better suit their new climate (Yamori *et al.*, 2014). When a plant experiences a temperature increase, acclimation allows it to become more efficient at fixing carbon at elevated temperatures. Wang *et al.* (2011) investigated the effects that pre-anthesis acclimation can have on photosynthetic characteristics later in winter wheat development. Following two 2-day exposures to 32/28 °C (day/night) pre-anthesis, plants were later exposed to further heat stress 7 days after anthesis. The plants that acclimated to high temperature pre-anthesis had smaller decreases in net photosynthesis, transpiration rate, and stomatal conductance in comparison to those that had not experienced pre-anthesis heat exposure (Wang *et al.*, 2011). Due to the inhibition of photosynthesis being directly associated with reduced yield (Scafaro and Atkin, 2016), the thermal tolerance and acclimation of photosynthesis in a valuable crop like wheat is a crucial area of study.

### Mitochondrial inner membrane under heat stress



### Thylakoid membrane under heat stress

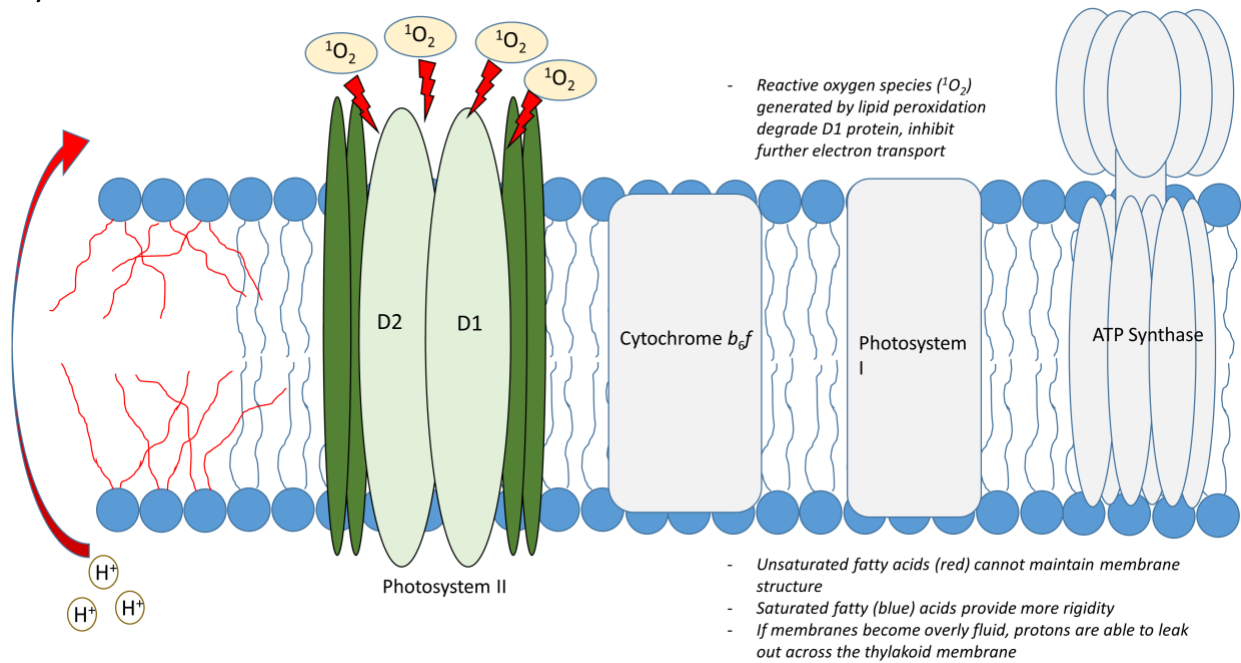


**Figure 3:** Schematic diagrams of thylakoid membrane and inner mitochondrial membrane following heat shock exposure. In both organelles, high temperature-generated reactive oxygen species damage membrane-bound proteins and inhibit electron transfer. In each case this has the effect of decreasing ATP synthesis, and contributes to the falling rates of  $A_{net}$  and  $R$  that are observed at high temperatures in Figures 1 and 2. In the case of the mitochondrial membrane, the plant can also activate an alternative pathway for oxidation when experiencing heat stress. This alternative pathway (represented by the membrane components in white – external



dehydrogenase, *ED*; internal dehydrogenase, *ID*; alternative oxidase, *AOX*) uncouples ATP synthesis from oxidation by not including any of the proton pumping characteristic of Complexes III – IV. This is thought to curb the production of toxic reactive oxygen species (ROS; like  $^1\text{O}_2$ ). The membrane also contains uncoupling proteins which serve to limit the build-up of ROS. The negative effects of ROS are also counteracted by the induction of small HSPs, which assist proteins in maintaining their structure under high temperatures.

#### *Rubisco activation is sensitive to moderate levels of heat stress*

A key limiting factor of photosynthesis is the activity of the carbon-fixing protein Rubisco, and more specifically, its capacity for carboxylation (Demirevska-Kepova and Feller, 2004). Rubisco itself is a fairly thermostable enzyme, even in cold-adapted species (Salvucci and Crafts-Brandner, 2004; Yamori *et al.*, 2006). However, Rubisco activity has been observed to decline under high temperature, including in wheat (Feng *et al.*, 2014; Kobza and Edwards, 1987). Crafts-Brandner and Law (2000) suggested that the adverse effect of high temperature on Rubisco activation is caused by the inhibition of interactions between Rubisco and the enzyme Rubisco Activase (*Rca*). The main function of *Rca* is to clear Rubisco catalytic sites of sugar phosphates, allowing for more efficient activation (Robinson and Portis, 1988). During an episode of high temperature, the inhibition of Rubisco activation is thought to be due predominantly to the rate of *Rca* activity being outpaced by the rate at which Rubisco is being deactivated (Crafts-Brandner and Salvucci, 2000). It is reasonable to hypothesise, then, that *Rca* plays an important role in determining the response of photosynthesis to increasing temperature. Ristic *et al.* (2009) indeed found that, in winter wheat, *Rca* expression was positively correlated with productivity following a 16-day heat stress over the anthesis period. Feller *et al.* (1998) observed a reduction in Rubisco activation in wheat leaf tissue following just 5 minutes of exposure to 30-35 °C. *Rca* also began to aggregate at high temperature, as well as becoming insoluble as temperatures rose above 37 °C (Feller *et al.*, 1998). There has been debate as to whether the heat lability of *Rca* is the predominant factor in decreasing C assimilation at high temperature, with many suggesting that this decline could instead be due to limitations to RuBP regeneration (Cen & Sage 2005). However, more recent work from Busch and Sage (2017) has lent strong support to the notion that *Rca* deactivation is the major factor behind declining  $A_{\text{net}}$  under high temperature. Although investigations into the link between *Rca* and productivity in wheat have thus far been limited, findings such as these suggest that *Rca* plays a key role in the high temperature response of photosynthesis in wheat.

A correlation between the thermal stability of Rca and the temperature that rice species are adapted to has been observed across wild and domesticated rice species (Scafaro *et al.*, 2016). This lends further support to the notion that genetic variability in the temperature optimum of Rubisco activation could potentially be exploited in wheat. Whether the expression and activity of this protein during periods of supra-optimal temperatures exerts a significant influence on growth and yield remains unknown.

#### *Damage to photosystem II when leaves become very hot*

Another way that high temperature can inhibit photosynthetic rate is by damaging PSII, a central component of the chloroplast electron transfer chain (Bukhov *et al.*, 1999). Specifically, it is thought that high temperature may lead to the loss of two manganese ions from the oxygen-evolving complex of PSII (Enami *et al.*, 1994). PSII is embedded in the chloroplast thylakoid membrane, which is itself also susceptible to heat-induced damage (Gounaris *et al.*, 1984), compounding the thermal sensitivity of PSII. Damage to PSII is a commonly used gauge of photosynthetic heat tolerance, as it is a trait that can be easily measured (Knight and Ackerly, 2002; O'Sullivan *et al.*, 2013; Zhu *et al.*, 2018). An increase in variable chlorophyll fluorescence indicates a decrease in the proportion of light energy used to drive electron transport, and thus an inhibition of the rate of photosynthesis (Atwell *et al.*, 1999). More specifically, there are a number of chlorophyll fluorescence parameters that are used to determine heat tolerance, including  $F_o$  (minimum fluorescence yield) and  $F_v/F_m$  (the maximum quantum efficiency of PSII). Both traits are commonly used as indicators of the heat tolerance of photosynthetic machinery in dark-adapted leaves and correlate strongly with each other (Sharma *et al.*, 2012), despite providing slightly different insights into the consequences of high temperature.  $F_o$  is the minimum fluorescence, achieved while all PSII reaction centres are open, and provides an indication of non-photochemical quenching (Maxwell and Johnson, 2000). The difference between  $F_o$  and the maximum fluorescence ( $F_m$ ) is termed the variable fluorescence ( $F_v$ ). The  $F_v/F_m$  ratio is taken following a high intensity pulse of light that causes PSII reaction centres to close. Decreases in this trait may reflect damage to PSII reaction centres or slowly relaxing quenching processes (Baker and Rosenqvist, 2004). The primary role that PSII plays in the

electron transfer chain, along with the relative efficiency with which damage to this complex can be measured, make PSII thermostability a valuable indicator of photosynthetic thermal tolerance. As a result, a number of studies have employed these techniques when measuring high temperature tolerance in wheat (Brestic *et al.*, 2012; Haque *et al.*, 2014; Shanmugam *et al.*, 2013; Sharma *et al.*, 2012; Sharma *et al.*, 2015; Sharma *et al.*, 2014).

*Understanding impact of high temperature on photosynthesis through modelling limitations in the maximum rates of electron transport and Rubisco activity*

Two of the main limitations of photosynthesis are the maximum rate of electron transport ( $J_{\max}$ ), and the maximum carboxylation rate of Rubisco ( $V_{\text{cmax}}$ ). These two processes determine the upper limit of the photosynthetic rate, assuming there are no limitations on vascular flow of water within the plant. In light saturated conditions and elevated  $\text{CO}_2$ , photosynthesis may be limited by the capacity to regenerate RuBP, which reflects  $J_{\max}$  (Sage and Kubien, 2007). Alternatively, as temperature increases,  $V_{\text{cmax}}$  acts as the limiting factor on the rate of photosynthesis (Fig. 1). As mentioned previously,  $J_{\max}$  may be inhibited by heat stress via damage incurred by the thermally-sensitive PSII. For  $V_{\text{cmax}}$ , temperature increases between approximately 15 – 30°C lead to an exponential increase; however, a rapid decline in  $V_{\text{cmax}}$  follows as temperatures continue to rise (Hikosaka *et al.*, 2005). This decline in  $V_{\text{cmax}}$  is likely due to the dysfunction of Rubisco Activase, resulting in a decline in Rubisco activity. The capacity to photosynthetically acclimate to high temperature in wheat is likely driven by the ability to adjust  $V_{\text{cmax}}$  and  $J_{\max}$  in response to increasing temperature. Photosynthetic rate has been observed to correlate with leaf area index and yield (Chakrabarti *et al.*, 2013), meaning that limiting high temperature-induced reductions in photosynthesis and leaf area (likely symptoms of accelerated development) could potentially protect against yield losses in hot conditions. The capacity to maintain a high photosynthetic rate at high temperature could aid plants in compensating for a reduction in net carbon gain resulting from an acceleration in development. Research into the relationship between leaf-level photosynthesis and yield in wheat must be explored further in order to determine the influence of photosynthetic acclimation upon grain yield, as this link has yet to be demonstrated convincingly in the field.

### *Reducing the respiratory costs of maintenance and growth*

As outlined earlier, one way of enhancing biomass accumulation (and thus yield) is through minimizing the ratio of respiratory carbon release compared to how much CO<sub>2</sub> is fixed by photosynthesis. From a respiratory perspective, this could be achieved by reducing the energy demands of growth and maintenance processes, both of which are crucial components of a plant's carbon economy (Wohl and James, 1942). Growth respiration refers to the respiratory products that are utilised in the conversion of existing materials into new plant structures (Amthor, 2000). Maintenance respiration encapsulates all respiration that contributes to the turnover of pre-existing plant proteins and the preservation of ionic gradients (Penning de Vries, 1975). In the context of improving yields in wheat and other crops, one strategy is to minimize the energy costs associated with cellular maintenance, while maintaining the allocation of respiratory products to growth processes. For such a strategy to work in field conditions, consideration needs to be given to the extent to which respiratory rates vary throughout development and among organs, as well as the factors that influence the amount of respiratory ATP produced per unit CO<sub>2</sub> released. The response of growth and maintenance respiration to short- and long-term changes in temperature – particularly high air temperatures - also needs to be characterised.

### *Developmental and organ-to-organ variation in respiration*

Wheat respiration varies across developmental stages, and between different plant organs. Variation in leaf respiratory rates between developmental stages is unsurprising, given that a plant's energy demands change as it progresses through its life cycle. When measuring dark respiration in glasshouse-grown winter wheat, Todd (1982) observed lower shoot and leaf respiration rates in three week-old plants in the vegetative stage when compared with individuals in the midst of reproduction. Similarly, canopy respiration of Chinese winter wheat varieties increased following stem elongation, peaked at anthesis, and then decreased as the dough stage was approached (Shuting, 1994). Pinto et al. (2017) found leaf dark respiration decreased as spring wheat progressed from booting and anthesis toward the latter stages of grain filling. These

findings support the notion that wheat leaf respiration varies phenologically; increasing through the vegetative stage up until anthesis, then declining in subsequent stages. This trajectory mirrors the pattern of biomass accumulation throughout the life of many seasonal crops. Ontogenetic changes in respiration also parallel changes observed in tissue composition over time. McCullough and Hunt (1993) found that, between the early vegetative stage and anthesis, stores of structural and non-structural carbohydrates increased in spring and winter wheat, while protein and lipid levels declined over the same period. Such changes in substrate supply likely contribute to the observed variation in respiratory rates throughout wheat development.

As well as varying with phenological stage, wheat respiratory rates also differ across plant organs. Given the different physiological roles of leaves, shoots, and roots, it follows that respiratory rates would differ between these tissue types. While leaf respiration appears to increase through development up to anthesis, Mitchell et al. (1991) found that shoot respiration decreased as field-grown winter wheat approached anthesis. Developmental stage and leaf organ also play a role in determining the balance between growth and maintenance respiration. As wheat approaches maturity, ear respiration effectively accounts for the entirety of above-ground plant growth respiration (Mitchell *et al.*, 1991). This is likely typical of most domesticated cereals, having been selected for high yield over thousands of years. Considering the evidence that respiration varies across wheat developmental stage and plant organ, it is probable that the effect of high temperature on net carbon balance would differ in a similar fashion. However, to date there has been little work comparing the effects of high temperature on wheat respiration across leaves, shoots, and roots, as well as across phenological stages. It is likely that the differences between the rates at which air and soil temperatures respond to changes in weather would result in differences in the high temperature response of respiration between above and below ground organs. Whether variations in wheat respiration rates are driven predominantly by substrate supply or energy demand is likely to depend on the extent to which environmental conditions regulate photosynthesis (influencing substrate supply), and/or influence the processes that use respiratory products.

*Temperature dependence of growth and maintenance respiration*

Temperature is one of the most important abiotic factors that influence plant respiration (Berry and Raison, 1981). When considering growth and maintenance respiration independently, both processes are responsive to changes in temperature; however, maintenance respiration is thought to be more sensitive to temperature change than growth respiration in mature tissue (Johnson and Thornley, 1985; Slot and Kitajima, 2015a; Vos, 1981). As ambient temperature rises, so too does the rate of activity of temperature-dependent plant processes, including growth, maintenance, and ion uptake. Along with this, enzymatic reactions are accelerated, and an increase in demand for respiratory products ensues. As a result, when measured at low to optimal temperatures, respiration rate rapidly increases in response to short-term increases in temperature (Fig. 2) (Penning de Vries *et al.*, 1979). In an experiment that incorporated wheat, maize, and ryegrass, Penning De Vries *et al.* (1979) observed wheat whole plant growth respiration (calculated as total whole plant respiration minus an approximation of maintenance respiration) increased with temperature from 10 °C, before reaching a maximal rate ( $T_{max}$ ) at just beyond 30 °C. Following this peak, growth respiration decreased sharply in those plants experiencing long-term exposure to temperatures above 30 °C (Penning de Vries *et al.*, 1979). Penning De Vries *et al.* (1979) also found leaf elongation responded to temperature increases in a similar fashion, perhaps indicative of restricted cell division rates as temperatures approached 30 °C, although this possibility was not investigated. A linear relationship was observed between whole plant above-ground respiration rate and temperature when measured between 10 – 20 °C (below the temperature at which growth respiration reaches its maximum rate) (Mitchell *et al.*, 1991). A similar relationship was observed for canopy respiration in both spring and winter wheat across the range of 5 – 35 °C (McCullough and Hunt, 1993). In both instances, the rate of respiration roughly doubled with every 10 °C increase in measurement temperature. Such relationships are reflected in numerous crop growth models that include a respiratory component (Table 3). These models generally represent the relationship between plant respiration and temperature as close to the assumption of  $Q_{10} = 2$  (i.e. a doubling of respiration rate with a 10 °C increase in temperature). Along with the Arrhenius approach,  $Q_{10}$  has been the most commonly used way to model the temperature response of respiration in wheat (Table 2). However, models such as these often fail to capture the complexity inherent in the temperature

response of respiration, notably overlooking the fact that: (1) respiration exhibits a decelerating function as leaves warm, reflecting a declining sensitivity to higher temperatures (Heskel *et al.*, 2016; Kruse and Adams, 2008); and (2) that respiration acclimates to sustained periods of warming (Atkin and Tjoelker, 2003; Reich *et al.*, 2016; Slot and Kitajima, 2015a).

Previous studies have found increasing daily minimum temperatures to drive yield loss in wheat and other crops (Cossani and Reynolds, 2012; Mohammed and Tarpley, 2009), and it is likely that higher respiration rates contribute to this. An increased respiration rate can increase carbon loss – and therefore, reduce yield – in a number of ways. Higher rates of night-time respiratory CO<sub>2</sub> release could reduce daily rates of net C gain (and biomass accumulation) during vegetative growth, and thus negatively affect yield. Thus, one strategy for improving wheat yields will be to select lines with reduced rates of respiratory CO<sub>2</sub> release during period of warmer nights. Another factor is the production of ROS, which damage cell and organelle membranes (Narayanan *et al.*, 2015). It has been suggested that one way that plants manage ROS is to use an alternative pathway of mitochondrial electron transport, one that uncouples respiratory oxidation from ATP production (Dahal and Vanlerberghe, 2017; O'Leary *et al.*, 2018; van Aken *et al.*, 2009; Vanlerberghe, 2013). The use of the alternative cyanide-insensitive pathway may also fulfil other roles during abiotic stress, such as synthesising carbon skeletons as sources of phosphate or to aid in osmoregulation (Del-Saz *et al.*, 2018; O'Leary *et al.*, 2018). Our knowledge of the role that the alternative pathway plays in wheat during episodes of high temperature is still developing; however, recent studies have begun to explore this area. Results suggested that the activation of the alternative pathway protects photosynthetic machinery within developing wheat leaves following short-term exposure of seedlings to 42 °C (Batjuka *et al.*, 2017), and that the alternative pathway – specifically the alternative oxidase protein – assists in the acclimation of wheat seedling leaves to high temperature (Borovik and Grabelnych, 2018). While these results hold for seedlings, it remains unknown whether the alternative oxidase protein continues to aid thermal tolerance throughout later stages of wheat development.

#### *Thermal acclimation of respiration – general features*

As the global climate becomes more erratic and the frequency and intensity of heatwaves increase, the trait of thermal acclimation is becoming increasingly relevant. Elevated growth temperatures – particularly night-time minimums – and exposure to heatwaves may elicit greater respiratory carbon losses in plants, so the capacity to thermally acclimate respiration rate will likely be important in determining wheat productivity going forward. High temperature acclimation is dynamic, and can refer to short-term, rapid responses to heat shock, as well as longer-term responses to prolonged exposure to elevated temperature. Acclimation in this sense is distinct from adaptation, which is a process that takes place on a scale of generations. In the context of the high temperature response of wheat respiration, adaptation is what breeders exploit in order to develop varieties better suited to hot conditions. It is believed the biochemical mechanisms that underpin rapid acclimation likely differ from those that drive gradual thermal acclimation (Atkin and Tjoelker, 2003; O'Leary *et al.*, 2018; Zhu *et al.*, 2018), although understanding of these mechanisms remains limited. Thermal acclimation of respiration is characterised by a change in  $T_{max}$ , or the intercept or slope of the respiratory temperature response curve in order to compensate for a shift in growth temperature (Fig. 2; (Atkin *et al.*, 2005; Atkin and Tjoelker, 2003). It has long been assumed that leaf respiration rates double for every 10 °C rise in temperature, however thermal acclimation prevents respiration from increasing to an inefficient level and causing excessive losses of carbon when there is no corresponding demand for such a large increase in ATP (Atkin *et al.*, 2000a; Covey-Crump *et al.*, 2002). An example of this is a Reich *et al.* (2016) field study of boreal and temperate trees, in which acclimation to a 3.4 °C increase in growth temperature resulted in an 80% reduction in the observed respiration rate compared to what was expected sans acclimation.



**Table 3:** Selection of popular crop growth models and how these models incorporate photosynthesis, respiration, and the temperature responses of each.

Model	Species modelled	Incorporation of respiration ( <i>R</i> )	Incorporation of CO <sub>2</sub> assimilation ( <i>A</i> )	Temperature responses of <i>R</i> & <i>A</i>	References
APSIM	Wheat, maize, rice, and others	When modelling transpiration demand for wheat, potential biomass accumulation is intercepted radiation minus <i>R</i> , divided by transpiration efficiency. Assumes <i>R</i> is 0.	<i>A</i> represented as potential biomass accumulation resulting from radiation interception, accounting for stress factors.	Includes temperature factor in models of biomass accumulation, calculated based on mean daily temperature. No temperature response of <i>R</i> included.	(Zheng <i>et al.</i> , 2014)
CERES-wheat	Over 42 crops (mainly annual crops such as wheat, rice, maize, and grain legumes)	<i>R</i> is calculated as proportional to <i>A</i> rather than calculated individually. It is assumed to increase exponentially with temperature up until the maximal rate is reached.	Represented as potential daily carbohydrate production, minus low temperature, water stress, and N stress.	Temperature stress component of photosynthesis calculation is based on weighted mean of daily maximum and minimum temperatures. The optimum daytime temperature for photosynthesis is considered to be 18°C.	(White, 2001)
DAISY	Spring barley, winter wheat	Respiration considered as a combination of growth respiration and temperature dependent maintenance respiration.	Daily gross canopy photosynthesis based on assumptions that gross leaf photosynthesis is described as a single light response curve, and that Beer's law describes crop canopy light distribution.	Assumes <i>Q</i> <sub>10</sub> of maintenance respiration is 2, and therefore a constant relationship between <i>R</i> / <i>T</i> (i.e. for every 10°C increase, <i>R</i> doubles).	(Hansen <i>et al.</i> , 1991)

MONICA (derived from HERMES)	Wheat and eight crops	Maintenance respiration is calculated separately for day and night periods using AGROSIM algorithms.	A based on gross canopy CO <sub>2</sub> assimilation, consisting of light response curve of leaves, green area of canopy, leaf arrangement, and incident irradiation.	Estimations of impacts of extreme heat on growth and yield via reduction of biomass accumulation based on Challinor <i>et al.</i> (2005). Maintenance R Q <sub>10</sub> = 2.	(Mirschel and Wenkel, 2007; Nendel <i>et al.</i> , 2011; van Keulen <i>et al.</i> , 1982) (de Wit <i>et al.</i> , 2018)
WOFOST	Wheat, barley, rice, maize and others	Maintenance R calculation based on plant organ dry weight and chemical composition. Assumes maintenance R cannot outstrip gross A.	Calculation of daily gross CO <sub>2</sub> -assimilation rate is based on absorbed radiation (incoming radiation and leaf area) and photosynthesis-light response curve of leaves. Leaf age and temperature also influence A.	Maintenance R Q <sub>10</sub> = 2. Daily minimum temperature can reduce A, based on low temperature inhibiting transition of assimilates to structural biomass in the night.	(Stöckle <i>et al.</i> , 2003)
CropSyst	Most crops (including wheat)	Has no respiration component. Daily biomass accumulation is mediated only by N, transpiration, and temperature factors.	Represents A as unstressed biomass accumulation, calculated as intercepted PAR-dependent biomass growth, which comprises of RUE, intercepted PAR.	The RUE component of A is limited by low temperature during early growth. RUE is assumed to linearly increase with increases in air temperature from base temperature for development to an optimum temperature for early growth. There are no high temperature limitations on growth.	

Abbreviations: Respiration rate, R; photosynthetic rate, A; nitrogen, N; radiation use efficiency, RUE; photosynthetically active radiation, PAR; Q<sub>10</sub>, extent of increase in respiratory rate with an increase in temperature of 10°C.

Atkin and Tjoelker (2003) suggested that long-term respiratory acclimation can occur in one of two ways. The first is 'type I' acclimation, in which the slope ( $Q_{10}$ ) of a respiratory temperature response curve changes, but the intercept of the curve remains unchanged. In a high temperature situation, this would manifest as a decrease in the  $Q_{10}$  when plants acclimate to warmer conditions. In 'type II' acclimation, the intercept of the temperature response curve is shifted, resulting in altered respiration rates at both high and low measuring temperatures (Atkin and Tjoelker, 2003). Type II acclimation may also include a change in  $Q_{10}$ , although this is not necessary for this form of acclimation. Type I acclimation is thought to be driven by changes in the respiratory substrate supply, the restriction of adenylates to leaf respiration, and/or changes in protein abundance within existing organelles (Atkin and Tjoelker, 2003). Contrastingly, type II acclimation is more likely a product of altered leaf morphology and biochemistry in newly-developed leaves, leading to a change in respiratory capacity (Atkin and Tjoelker, 2003). Around the world, plants vary in their  $T_{max}$ , and those from colder biomes exhibit greater leaf respiration rates and higher intercepts of their respiratory temperature response curves in comparison to warmer biomes (Heskel *et al.*, 2016; O'Sullivan *et al.*, 2017). It has been suggested that there are no systematic differences among species in acclimating root respiration (Atkinson *et al.*, 2007), or leaf respiration and photosynthesis (Campbell *et al.*, 2007). However, Atkin *et al.* (2007) and Loveys *et al.* (2002) both found that, while whole-plant  $R/A$  ratio remained constant at moderate growth temperatures, the ratio markedly increased at high growth temperatures due to increased respiratory costs associated with ion uptake and cellular maintenance.

#### *Accounting for variability in the temperature response of respiration*

A range of factors drive variation in the shape of the temperature response of plant respiration (i.e. variations in  $Q_{10}$  values), including temperature itself (Covey-Crump *et al.*, 2002; Loveys *et al.*, 2003; O'Sullivan *et al.*, 2013), water availability (Turnbull *et al.*, 2001), light availability, and soil nutrients (Turnbull *et al.*, 2005). In wheat, the effects of drought (Liu *et al.*, 2004), elevated  $CO_2$  (Gifford, 1995), light (McCashin *et al.*, 1988; Vos, 1981), and N supply (Vos, 1981) on respiration have been investigated. However, the temperature sensitivity and response of wheat respiration remains largely unexplored. Variation in  $Q_{10}$  values may reflect the temperature

sensitivity of respiratory enzymes, or a transition from enzymatic control to limitations imposed by adenylate or substrate demands (Atkin *et al.*, 2005; Atkin and Tjoelker, 2003). Respiration tends to be limited by enzyme capacity at lower temperatures, while the availability of substrates and adenylates limit respiration at high temperatures (Atkin *et al.*, 2005). As part of the energy demand that influences respiratory flux, adenylates can control respiration rates via the energy requirements of processes such as growth, maintenance, and ion uptake (van der Werf *et al.*, 1988). Therefore, temperature-driven changes in these processes can influence the extent to which respiration is regulated by adenylates, particularly at high temperatures. In fact, Slot and Kitajima (2015b) suggested that the observed decline in  $Q_{10}$  at high temperatures likely reflects the declining carbon pool which limits further increases in respiration. Similarly, given the large scope for adjustments of respiration rate via thermal acclimation, as well as the increasing variability of the climate, crop growth models should be improved to predict productivity more accurately in a future, warmer world. Current models (Table 3) should look to incorporate more realistic representations of the high temperature response of respiration, including a plant's capacity to thermally acclimate its respiration rate. This will require extending research into the high temperature response of, and variation in, respiration rates amongst wheat varieties, on which there has been little work to date. Assuming varieties do vary in their high temperature acclimation of respiration, it is still unknown whether this trait is associated with an increase in growth or yield in heat stressed wheat. However, considering that respiration is more sensitive to increases in temperature than is photosynthesis (Way and Yamori, 2014), the ability to minimise respiratory carbon loss under high temperature would likely have a direct impact on growth and yield. By minimising respiratory carbon losses, particularly at night, the  $R/A$  ratio could be prevented from moving past the point at which the plant experiences net carbon losses induced by high temperature.

## **Conclusions and future directions**

Despite growing awareness of the negative impacts of high temperature on both respiration and photosynthesis, as well as the continued warming of the climate, understanding of how these processes respond to high temperature in wheat remains limited. In addition, the response of

wheat net carbon balance to increases in daily maximum and minimum temperature looms as a crucial, yet poorly understood area. Given that the diurnal asymmetry in climate warming favours night-time temperature rises, there is potential for increased night-time carbon loss via respiration amongst wheat lines and other major crops going forward. When combined with the possibility of increasing daily maximum temperatures leading to a reduction in carbon fixed during the day, wheat biomass accumulation will likely be compromised in a future warming climate. A better understanding of how plants protect photosynthetic processes against high temperature may contribute to maintaining net carbon gain over a 24-hour period, and ultimately productivity. However, because of the more rapid rate of increase of night-time temperatures, the higher thermal sensitivity of respiration, and the previously observed links between high night temperatures and yield loss, the thermal response of leaf respiration will likely be even more influential in determining heat-induced decreases in wheat biomass accumulation. Plants with a greater capacity for respiratory acclimation to high temperature could stand to lose 1.5 times less carbon via CO<sub>2</sub> efflux (Atkin *et al.*, 2000b). Because of this, the ability to adjust respiratory rates in the face of supra-optimal temperatures is a highly desirable trait for future wheat varieties. Such varieties could potentially compensate for a reduced period of biomass accumulation via greater efficiency in managing net carbon balance under high temperature (i.e. maximising photosynthetic carbon gain through the day and minimising respiratory carbon losses at night). Developing new varieties that are more adept at thermally acclimating respiration and photosynthesis may therefore help to avoid the yield losses that are projected with increasing average day and night-time temperatures. In order to successfully develop varieties equipped for high temperature acclimation, identifying the extent of genetic variation that exists for these traits in wheat is a necessity.

In pursuit of this, future work must determine the extent to which wheat thermal acclimation of net carbon balance is associated with increased production in hot conditions. By identifying the biochemical mechanisms that confer chloroplast and mitochondrial heat tolerance and acclimation, we could then seek to quantify the effect of these on growth and yield. Screening large numbers of varieties for variability in acclimation potential and respiratory thermal tolerance (i.e. screening for  $T_{max}$ , see Fig. 2) will also be valuable moving forward, with

genome wide association studies a potential option for understanding the genetic basis of such traits. The benefits of better thermally acclimating varieties could also be enhanced by delayed-flowering mechanisms. The combination of increasing net carbon gain over a 24-hour period with a delay in flowering time could aid plants in maximizing their resource capture, particularly when high temperatures have accelerated phenological development. Finally, incorporating this knowledge into current crop growth models would also allow for more accurate predictions of wheat productivity in a future warmer climate. The increasing volatility of the climate means that high resolution predictions of crop growth and yield will likely become more difficult. Models of greater accuracy may better inform growers about which varieties are more suited to cope with either warmer growth temperatures, or the sudden onset of heatwaves. Such models could also improve yield estimates for wheat varieties during growing seasons, including when heatwaves have been experienced, or are anticipated.

## **Acknowledgements**

This work was supported by grants from the Grains Research Development Corporation grant (2016.02.01G), and the ARC Centre of Excellence in Plant Energy Biology (CE140100008). The first author is also supported by the Australian Government Research Training Program.

## **References**

- Al-Khatib K, Paulsen G.** 1984. Mode of high temperature injury to wheat during grain development. *Physiologia Plantarum* **61**, 363-368.
- Alexander L, Zhang X, Peterson T, Caesar J, Gleason B, Klein Tank A, Haylock M, Collins D, Trewin B, Rahimzadeh F.** 2006. Global observed changes in daily climate extremes of temperature and precipitation. *Journal of Geophysical Research: Atmospheres* **111**.
- Allakhverdiev SI, Kreslavski VD, Klimov VV, Los DA, Carpentier R, Mohanty P.** 2008. Heat stress: an overview of molecular responses in photosynthesis. *Photosynthesis Research* **98**, 541-550.
- Amthor JS.** 1989. *Respiration and crop productivity*. New York, NY: Springer-Verlag.
- Amthor JS.** 2000. The McCree-de Wit-Penning de Vries-Thornley respiration paradigms: 30 years later. *Annals of Botany* **86**, 1-20.
- Asseng S, Ewert F, Martre P, Rotter RP, Lobell DB, Cammarano D, Kimball BA, Ottman MJ, Wall GW, White JW, Reynolds MP, Alderman PD, Prasad PVV, Aggarwal PK, Anothai J, Basso B, Biernath C, Challinor AJ, De Sanctis G, Doltra J, Fereres E, Garcia-Vila M, Gayler S, Hoogenboom G, Hunt LA, Izaurralde RC, Jabloun M, Jones CD, Kersebaum KC, Koehler AK, Muller C, Naresh**

- Kumar S, Nendel C, O'Leary G, Olesen JE, Palosuo T, Priesack E, Eyshi Rezaei E, Ruane AC, Semenov MA, Shcherbak I, Stockle C, Stratonovitch P, Streck T, Supit I, Tao F, Thorburn PJ, Waha K, Wang E, Wallach D, Wolf J, Zhao Z, Zhu Y.** 2015. Rising temperatures reduce global wheat production. *Nature Climate Change* **5**, 143-147.
- Asseng S, Foster I, Turner NC.** 2011. The impact of temperature variability on wheat yields. *Global Change Biology* **17**, 997-1012.
- Atkin O, Holly C, Ball M.** 2000a. Acclimation of snow gum (*Eucalyptus pauciflora*) leaf respiration to seasonal and diurnal variations in temperature: the importance of changes in the capacity and temperature sensitivity of respiration. *Plant, Cell & Environment* **23**, 15-26.
- Atkin O, Scheurwater I, Pons T.** 2007. Respiration as a percentage of daily photosynthesis in whole plants is homeostatic at moderate, but not high, growth temperatures. *New Phytologist* **174**, 367-380.
- Atkin OK, Bruhn D, Tjoelker MG.** 2005. Response of plant respiration to changes in temperature: mechanisms and consequences of variations in  $Q_{10}$  values and acclimation. In: Lambers H, Ribas-Carbo M, eds. *Plant Respiration: From Cell to Ecosystem*. Dordrecht: Springer Netherlands, 95-135.
- Atkin OK, Edwards EJ, Loveys BR.** 2000b. Response of root respiration to changes in temperature and its relevance to global warming. *The New Phytologist* **147**, 141-154.
- Atkin OK, Tjoelker MG.** 2003. Thermal acclimation and the dynamic response of plant respiration to temperature. *Trends in plant science* **8**, 343-351.
- Atkinson LJ, Hellicar MA, Fitter AH, Atkin OK.** 2007. Impact of temperature on the relationship between respiration and nitrogen concentration in roots: an analysis of scaling relationships,  $Q_{10}$  values and thermal acclimation ratios. *New Phytologist* **173**, 110-120.
- Atwell B, Kriedemann P, Turnbull C.** 1999. *Plants in Action: Adaptation in Nature, Performance in Cultivation*. Melbourne, Australia: Macmillan Education Australia Pty Ltd.
- Azcón-Bieto J, Lambers H, Day DA.** 1983. Effect of photosynthesis and carbohydrate status on respiratory rates and the involvement of the alternative pathway in leaf respiration. *Plant Physiology* **72**, 598-603.
- Azcón-Bieto J, Osmond CB.** 1983. Relationship between photosynthesis and respiration. The effect of carbohydrate status on the rate of  $\text{CO}_2$  production by respiration in darkened and illuminated wheat leaves. *Plant Physiology* **71**, 574-581.
- Baker NR, Rosenqvist E.** 2004. Applications of chlorophyll fluorescence can improve crop production strategies: an examination of future possibilities. *Journal of Experimental Botany* **55**, 1607-1621.
- Barnabás B, Jäger K, Fehér A.** 2008. The effect of drought and heat stress on reproductive processes in cereals. *Plant, Cell & Environment* **31**, 11-38.
- Batjuka A, Škute N, Petjukevičs A.** 2017. The influence of antimycin A on pigment composition and functional activity of photosynthetic apparatus in *Triticum aestivum* L. under high temperature. *Photosynthetica* **55**, 251-263.
- Berry J, Bjorkman O.** 1980. Photosynthetic response and adaptation to temperature in higher plants. *Annual Review of Plant Physiology* **31**, 491-543.
- Berry J, Raison J.** 1981. Responses of macrophytes to temperature. *Physiological plant ecology I*: Springer, 277-338.

- Bidinger F, Musgrave R, Fischer R.** 1977. Contribution of stored pre-anthesis assimilate to grain yield in wheat and barley. *Nature* **270**, 431.
- Bingham I, Stevenson E.** 1993. Control of root growth: effects of carbohydrates on the extension, branching and rate of respiration of different fractions of wheat roots. *Physiologia Plantarum* **88**, 149-158.
- Blum A, Klueva N, Nguyen H.** 2001. Wheat cellular thermotolerance is related to yield under heat stress. *Euphytica* **117**, 117-123.
- Blum A, Sinmena B, Mayer J, Golan G, Shpiler L.** 1994. Stem reserve mobilisation supports wheat-grain filling under heat stress. *Functional Plant Biology* **21**, 771-781.
- Borovik OA, Grabelnych OI.** 2018. Mitochondrial alternative cyanide-resistant oxidase is involved in an increase of heat stress tolerance in spring wheat. *Journal of plant physiology* **231**, 310-317.
- Brestic M, Zivcak M, Kalaji HM, Carpentier R, Allakhverdiev SI.** 2012. Photosystem II thermostability *in situ*: environmentally induced acclimation and genotype-specific reactions in *Triticum aestivum* L. *Plant Physiology and Biochemistry* **57**, 93-105.
- Bukhov NG, Wiese C, Neimanis S, Heber U.** 1999. Heat sensitivity of chloroplasts and leaves: leakage of protons from thylakoids and reversible activation of cyclic electron transport. *Photosynthesis Research* **59**, 81-93.
- Campbell C, Atkinson L, Zaragoza-Castells J, Lundmark M, Atkin O, Hurry V.** 2007. Acclimation of photosynthesis and respiration is asynchronous in response to changes in temperature regardless of plant functional group. *New Phytologist* **176**, 375-389.
- Chakrabarti B, Singh S, Kumar V, Harit R, Misra S.** 2013. Growth and yield response of wheat and chickpea crops under high temperature. *Indian Journal of Plant Physiology* **18**, 7-14.
- Challinor A, Wheeler T, Craufurd P, Slingo J.** 2005. Simulation of the impact of high temperature stress on annual crop yields. *Agricultural and Forest Meteorology* **135**, 180-189.
- Chan T, Shimizu Y, Pospíšil P, Nijo N, Fujiwara A, Taninaka Y, Ishikawa T, Hori H, Nanba D, Imai A.** 2012. Quality control of photosystem II: lipid peroxidation accelerates photoinhibition under excessive illumination. *PLoS ONE* **7**, e52100.
- Christiansen M.** 1978. The physiology of plant tolerance to temperature extremes. In: Jung G, ed. *Crop tolerance to suboptimal land conditions*. Madison, WI.: ASA, 173-191.
- Cossani CM, Reynolds MP.** 2012. Physiological traits for improving heat tolerance in wheat. *Plant Physiology* **160**, 1710-1718.
- Cossani CM, Reynolds MP.** 2013. What physiological traits should we focus on in breeding for heat tolerance? In: Alderman PD, Quilligan E, Asseng S, Ewert F, Reynolds MP, eds. *Modeling Wheat Response to High Temperature*. CIMMYT, El Batan, Texcoco, Mexico, 24.
- Covey-Crump E, Attwood R, Atkin O.** 2002. Regulation of root respiration in two species of *Plantago* that differ in relative growth rate: the effect of short-and long-term changes in temperature. *Plant, Cell & Environment* **25**, 1501-1513.
- Crafts-Brandner S, Law R.** 2000. Effect of heat stress on the inhibition and recovery of the ribulose-1, 5-bisphosphate carboxylase/oxygenase activation state. *Planta* **212**, 67-74.
- Crafts-Brandner SJ, Salvucci ME.** 2000. Rubisco activase constrains the photosynthetic potential of leaves at high temperature and CO<sub>2</sub>. *Proceedings of the National Academy of Sciences of the United States of America* **97**, 13430-13435.
- CSIRO, The Bureau of Meteorology.** 2018. *State of the Climate 2018*. Canberra, Australia: Australian Government.



- Dahal K, Vanlerberghe GC.** 2017. Alternative oxidase respiration maintains both mitochondrial and chloroplast function during drought. *New Phytologist* **213**, 560-571.
- Davy R, Esau I, Chernokulsky A, Outten S, Zilitinkevich S.** 2017. Diurnal asymmetry to the observed global warming. *International Journal of Climatology* **37**, 79-93.
- de Vries F, Witlage J, Kremer D.** 1979. Rates of respiration and of increase in structural dry matter in young wheat, ryegrass and maize plants in relation to temperature, to water stress and to their sugar content. *Annals of Botany* **44**, 595-609.
- de Wit A, Boogaard H, Fumagalli D, Janssen S, Knapen R, van Kraalingen D, Supit I, van der Wijngaart R, van Diepen K.** 2018. 25 years of the WOFOST cropping systems model. *Agricultural Systems* **168**, 154-167.
- Del-Saz NF, Ribas-Carbo M, McDonald AE, Lambers H, Fernie AR, Florez-Sarasa I.** 2018. An *in vivo* perspective of the role(s) of the alternative oxidase pathway. *Trends in plant science* **23**, 206-219.
- Demirevska-Kepova K, Feller U.** 2004. Heat sensitivity of Rubisco, Rubisco activase and Rubisco binding protein in higher plants. *Acta Physiologiae Plantarum* **26**, 103-114.
- Dias A, Lidon F.** 2009. Evaluation of grain filling rate and duration in bread and durum wheat, under heat stress after anthesis. *Journal of Agronomy and Crop Science* **195**, 137-147.
- Dusenge ME, Duarte AG, Way DA.** 2019. Plant carbon metabolism and climate change: elevated CO<sub>2</sub> and temperature impacts on photosynthesis, photorespiration and respiration. *New Phytologist* **221**, 32-49.
- Enami I, Kitamura M, Tomo T, Isokawa Y, Ohta H, Katoh S.** 1994. Is the primary cause of thermal inactivation of oxygen evolution in spinach PSII membranes release of the extrinsic 33 kDa protein or of Mn? *Biochimica et Biophysica Acta (BBA)-Bioenergetics* **1186**, 52-58.
- Farooq M, Bramley H, Palta JA, Siddique KH.** 2011. Heat stress in wheat during reproductive and grain-filling phases. *Critical Reviews in Plant Sciences* **30**, 491-507.
- Farquhar GD, von Caemmerer S, Berry JA.** 1980. A biochemical model of photosynthetic CO<sub>2</sub> assimilation in leaves of C<sub>3</sub> species. *Planta* **149**, 78-90.
- Farrar J.** 1985. The respiratory source of CO<sub>2</sub>. *Plant, Cell & Environment* **8**, 427-438.
- Farrar J, Williams M.** 1991. The effects of increased atmospheric carbon dioxide and temperature on carbon partitioning, source-sink relations and respiration. *Plant, Cell & Environment* **14**, 819-830.
- Feller U, Crafts-Brandner SJ, Salvucci ME.** 1998. Moderately high temperatures inhibit ribulose-1, 5-bisphosphate carboxylase/oxygenase (Rubisco) activase-mediated activation of Rubisco. *Plant Physiology* **116**, 539-546.
- Feng B, Liu P, Li G, Dong S, Wang F, Kong L, Zhang J.** 2014. Effect of heat stress on the photosynthetic characteristics in flag leaves at the grain-filling stage of different heat-resistant winter wheat varieties. *Journal of Agronomy and Crop Science* **200**, 143-155.
- Ferris R, Ellis R, Wheeler T, Hadley P.** 1998. Effect of high temperature stress at anthesis on grain yield and biomass of field-grown crops of wheat. *Annals of Botany* **82**, 631-639.
- Food and Agriculture Organization of the United Nations.** 2018. *FAO Cereal Supply and Demand Brief*. Vol. 2018.
- García GA, Dreccer MF, Miralles DJ, Serrago RA.** 2015. High night temperatures during grain number determination reduce wheat and barley grain yield: a field study. *Global Change Biology* **21**, 4153-4164.

- Gifford RM.** 1995. Whole plant respiration and photosynthesis of wheat under increased CO<sub>2</sub> concentration and temperature: long-term vs. short-term distinctions for modelling. *Global Change Biology* **1**, 385-396.
- Gounaris K, Brain A, Quinn P, Williams W.** 1984. Structural reorganisation of chloroplast thylakoid membranes in response to heat-stress. *Biochimica et Biophysica Acta (BBA)-Bioenergetics* **766**, 198-208.
- Hansen S, Jensen H, Nielsen N, Svendsen H.** 1991. Simulation of nitrogen dynamics and biomass production in winter wheat using the Danish simulation model DAISY. *Fertilizer research* **27**, 245-259.
- Haque MS, Kjaer KH, Rosenqvist E, Sharma DK, Ottosen C-O.** 2014. Heat stress and recovery of photosystem II efficiency in wheat (*Triticum aestivum* L.) cultivars acclimated to different growth temperatures. *Environmental and Experimental Botany* **99**, 1-8.
- Harding SA, Guikema JA, Paulsen GM.** 1990. Photosynthetic decline from high temperature stress during maturation of wheat I. Interaction with senescence processes. *Plant Physiology* **92**, 648-653.
- Hatfield JL, Prueger JH.** 2015. Temperature extremes: effect on plant growth and development. *Weather and Climate Extremes* **10, Part A**, 4-10.
- Hauben M, Haesendonckx B, Standaert E, Van Der Kelen K, Azmi A, Akpo H, Van Breusegem F, Guisez Y, Bots M, Lambert B, Laga B, De Block M.** 2009. Energy use efficiency is characterized by an epigenetic component that can be directed through artificial selection to increase yield. *Proceedings of the National Academy of Sciences of the United States of America* **106**, 20109-20114.
- Heckathorn SA, Downs CA, Sharkey TD, Coleman JS.** 1998. The small, methionine-rich chloroplast heat-shock protein protects photosystem II electron transport during heat stress. *Plant Physiology* **116**, 439-444.
- Heskel MA, O'Sullivan OS, Reich PB, Tjoelker MG, Weerasinghe LK, Penillard A, Egerton JJ, Creek D, Bloomfield KJ, Xiang J.** 2016. Convergence in the temperature response of leaf respiration across biomes and plant functional types. *Proceedings of the National Academy of Sciences of the United States of America* **113**, 3832-3837.
- Hikosaka K, Ishikawa K, Borjigidai A, Muller O, Onoda Y.** 2005. Temperature acclimation of photosynthesis: mechanisms involved in the changes in temperature dependence of photosynthetic rate. *Journal of Experimental Botany* **57**, 291-302.
- Hochman Z, Gobbett DL, Horan H.** 2017. Climate trends account for stalled wheat yields in Australia since 1990. *Global Change Biology*, n/a-n/a.
- Hoffmann AA, Chown SL, Clusella-Trullas S.** 2013. Upper thermal limits in terrestrial ectotherms: how constrained are they? *Functional Ecology* **27**, 934-949.
- Hunt JR, Hayman PT, Richards RA, Passioura JB.** 2018. Opportunities to reduce heat damage in rain-fed wheat crops based on plant breeding and agronomic management. *Field Crops Research* **224**, 126-138.
- Hurry V, Huner N.** 1991. Low growth temperature effects a differential inhibition of photosynthesis in spring and winter wheat. *Plant Physiology* **96**, 491-497.
- Hurry V, Huner N.** 1992. Effect of cold hardening on sensitivity of winter and spring wheat leaves to short-term photoinhibition and recovery of photosynthesis. *Plant Physiology* **100**, 1283-1290.

- IPCC.** 2014. *Climate Change 2014: Synthesis Report. Contribution of Working Groups I, II and III to the Fifth Assessment Report of the Intergovernmental Panel on Climate Change*. In: R.K. P, L.A. M, eds. Geneva, Switzerland: IPCC, 151.
- Johnson I, Thornley J.** 1985. Temperature dependence of plant and crop process. *Annals of Botany* **55**, 1-24.
- Knight CA, Ackerly DD.** 2002. An ecological and evolutionary analysis of photosynthetic thermotolerance using the temperature-dependent increase in fluorescence. *Oecologia* **130**, 505-514.
- Kobza J, Edwards GE.** 1987. Influences of leaf temperature on photosynthetic carbon metabolism in wheat. *Plant Physiology* **83**, 69-74.
- Kraus E, Lambers H.** 2001. Leaf and root respiration of *Lolium perenne* populations selected for contrasting leaf respiration rates are affected by intra- and interpopulation interactions. *Plant and Soil* **231**, 267-274.
- Krishnan M, Nguyen HT, Burke JJ.** 1989. Heat shock protein synthesis and thermal tolerance in wheat. *Plant Physiology* **90**, 140-145.
- Kruse J, Adams MA.** 2008. Three parameters comprehensively describe the temperature response of respiratory oxygen reduction. *Plant, Cell & Environment* **31**, 954-967.
- Kurimoto K, Day DA, Lambers H, Noguchi K.** 2004. Effect of respiratory homeostasis on plant growth in cultivars of wheat and rice. *Plant Cell and Environment* **27**, 853-862.
- Liu H-S, Li F-M, Xu H.** 2004. Deficiency of water can enhance root respiration rate of drought-sensitive but not drought-tolerant spring wheat. *Agricultural water management* **64**, 41-48.
- Liu Y, Wang E, Yang X, Wang J.** 2010. Contributions of climatic and crop varietal changes to crop production in the North China Plain, since 1980s. *Global Change Biology* **16**, 2287-2299.
- Lobell DB, Field CB.** 2007. Global scale climate–crop yield relationships and the impacts of recent warming. *Environmental research letters* **2**, 014002.
- Los DA, Murata N.** 2004. Membrane fluidity and its roles in the perception of environmental signals. *Biochimica et Biophysica Acta (BBA)–Biomembranes* **1666**, 142-157.
- Loveys B, Atkinson LJ, Sherlock D, Roberts RL, Fitter AH, Atkin OK.** 2003. Thermal acclimation of leaf and root respiration: an investigation comparing inherently fast- and slow-growing plant species. *Global Change Biology* **9**, 895-910.
- Loveys B, Scheurwater I, Pons T, Fitter A, Atkin O.** 2002. Growth temperature influences the underlying components of relative growth rate: an investigation using inherently fast- and slow-growing plant species. *Plant, Cell & Environment* **25**, 975-988.
- Machado S, Paulsen GM.** 2001. Combined effects of drought and high temperature on water relations of wheat and sorghum. *Plant and Soil* **233**, 179-187.
- Martre P, Reynolds MP, Asseng S, Ewert F, Alderman PD, Cammarano D, Maiorano A, Ruane AC, Aggarwal PK, Anothai J.** 2017. The International Heat Stress Genotype Experiment for modeling wheat response to heat: field experiments and AgMIP-Wheat multi-model simulations. *Open Data Journal for Agricultural Research* **3**, 23-28.
- Maxwell K, Johnson GN.** 2000. Chlorophyll fluorescence—a practical guide. *Journal of Experimental Botany* **51**, 659-668.
- McCaig T, Hill R.** 1977. Cyanide-insensitive respiration in wheat: cultivar differences and effects of temperature, carbon dioxide, and oxygen. *Canadian Journal of Botany* **55**, 549-555.

- McCashin BG, Cossins EA, Canvin DT.** 1988. Dark respiration during photosynthesis in wheat leaf slices. *Plant Physiology* **87**, 155-161.
- McCullough D, Hunt L.** 1993. Mature tissue and crop canopy respiratory characteristics of rye, triticale and wheat. *Annals of Botany* **72**, 269-282.
- Midmore D, Cartwright P, Fischer R.** 1982. Wheat in tropical environments. I. Phasic development and spike size. *Field Crops Research* **5**, 185-200.
- Mirschel W, Wenkel K-O.** 2007. Modelling soil–crop interactions with AGROSIM model family. *Modelling water and nutrient dynamics in soil–crop systems*: Springer, 59-73.
- Mitchell RA, Lawlor DW, Young AT.** 1991. Dark respiration of winter wheat crops in relation to temperature and simulated photosynthesis. *Annals of Botany* **67**, 7-16.
- Mohammed A-R, Tarpley L.** 2009. Impact of high nighttime temperature on respiration, membrane stability, antioxidant capacity, and yield of rice plants. *Crop Science* **49**, 313-322.
- Murata N, Los DA.** 1997. Membrane fluidity and temperature perception. *Plant Physiology* **115**, 875.
- Narayanan S, Prasad P, Fritz A, Boyle D, Gill B.** 2015. Impact of high night-time and high daytime temperature stress on winter wheat. *Journal of Agronomy and Crop Science* **201**, 206-218.
- Narayanan S, Tamura PJ, Roth MR, Prasad P, Welti R.** 2016. Wheat leaf lipids during heat stress: I. High day and night temperatures result in major lipid alterations. *Plant, Cell & Environment* **39**, 787-803.
- Nendel C, Berg M, Kersebaum K, Mirschel W, Specka X, Wegehenkel M, Wenkel K, Wieland R.** 2011. The MONICA model: Testing predictability for crop growth, soil moisture and nitrogen dynamics. *Ecological Modelling* **222**, 1614-1625.
- Niu Y, Xiang Y.** 2018. An overview of biomembrane functions in plant responses to high-temperature stress. *Frontiers in plant science* **9**, 915.
- Nunes-Nesi A, Carrari F, Lytovchenko A, Smith AM, Loureiro ME, Ratcliffe RG, Sweetlove LJ, Fernie AR.** 2005. Enhanced photosynthetic performance and growth as a consequence of decreasing mitochondrial malate dehydrogenase activity in transgenic tomato plants. *Plant Physiology* **137**, 611-622.
- O'Leary BM, Asao S, Millar AH, Atkin OK.** 2018. Core principles which explain variation in respiration across biological scales. *New Phytologist*.
- O'Sullivan OS, Heskell MA, Reich PB, Tjoelker MG, Weerasinghe LK, Penillard A, Zhu L, Egerton JGG, Bloomfield KJ, Creek D, Bahar NHA, Griffin KL, Hurry V, Meir P, Turnbull MH, Atkin OK.** 2017. Thermal limits of leaf metabolism across biomes. *Global Change Biology* **23**, 209-223.
- O'Sullivan OS, Weerasinghe KLK, Evans JR, Egerton JJ, Tjoelker MG, Atkin OK.** 2013. High-resolution temperature responses of leaf respiration in snow gum (*Eucalyptus pauciflora*) reveal high-temperature limits to respiratory function. *Plant, Cell & Environment* **36**, 1268-1284.
- Oquist G, Hurry V, Huner N.** 1993. Low-temperature effects on photosynthesis and correlation with freezing tolerance in spring and winter cultivars of wheat and rye. *Plant Physiology* **101**, 245-250.
- Pan R, Jones AD, Hu J.** 2014. Cardiolipin-mediated mitochondrial dynamics and stress response in Arabidopsis. *The Plant Cell*, tpc. 113.121095.
- Paradies G, Ruggiero FM, Petrosillo G, Quagliariello E.** 1998. Peroxidative damage to cardiac mitochondria: cytochrome oxidase and cardiolipin alterations. *FEBS letters* **424**, 155-158.

**Penning de Vries F.** 1975. The cost of maintenance processes in plant cells. *Annals of Botany* **39**, 77-92.

**Penning de Vries F, Witlage J, Kremer D.** 1979. Rates of respiration and of increase in structural dry matter in young wheat, ryegrass and maize plants in relation to temperature, to water stress and to their sugar content. *Annals of Botany* **44**, 595-609.

**Pinto RS, Molero G, Reynolds MP.** 2017. Identification of heat tolerant wheat lines showing genetic variation in leaf respiration and other physiological traits. *Euphytica* **213**, 76.

**Pomeroy MK, Andrews CJ.** 1975. Effect of temperature on respiration of mitochondria and shoot segments from cold-hardened and nonhardened wheat and rye seedlings. *Plant Physiology* **56**, 703-706.

**Porter JR, Gawith M.** 1999. Temperatures and the growth and development of wheat: a review. *European Journal of Agronomy* **10**, 23-36.

**Pradhan GP, Prasad PV.** 2015. Evaluation of wheat chromosome translocation lines for high temperature stress tolerance at grain filling stage. *PLoS ONE* **10**, e0116620.

**Prasad PV, Djanaguiraman M.** 2014. Response of floret fertility and individual grain weight of wheat to high temperature stress: sensitive stages and thresholds for temperature and duration. *Functional Plant Biology* **41**, 1261-1269.

**Prasad PV, Pisipati S, Ristic Z, Bukovnik U, Fritz A.** 2008. Impact of nighttime temperature on physiology and growth of spring wheat. *Crop Science* **48**, 2372-2380.

**Prins A, Orr DJ, Andralojc PJ, Reynolds MP, Carmo-Silva E, and Parry MA.** 2016. Rubisco catalytic properties of wild and domesticated relatives provide scope for improving wheat photosynthesis. *Journal of Experimental Botany* **67**, 1827-1838.

**Rahman M, Wilson J.** 1978. Determination of spikelet number in wheat. III.\* Effect of varying temperature on ear development. *Australian Journal of Agricultural Research* **29**, 459-467.

**Raison JK, Chapman EA, White P.** 1977. Wheat mitochondria oxidative activity and membrane lipid structure as a function of temperature. *Plant Physiology* **59**, 623-627.

**Ray DK, Mueller ND, West PC, Foley JA.** 2013. Yield trends are insufficient to double global crop production by 2050. *PLoS ONE* **8**, e66428.

**Rebetzke G, Richards R, Sirault X, Morrison A.** 2004. Genetic analysis of coleoptile length and diameter in wheat. *Australian Journal of Agricultural Research* **55**, 733-743.

**Reich PB, Sendall KM, Stefanski A, Wei X, Rich RL, Montgomery RA.** 2016. Boreal and temperate trees show strong acclimation of respiration to warming. *Nature* **531**, 633-636.

**Reynolds M, Balota M, Delgado M, Amani I, Fischer R.** 1994. Physiological and morphological traits associated with spring wheat yield under hot, irrigated conditions. *Functional Plant Biology* **21**, 717-730.

**Reynolds M, Gutiérrez-Rodríguez M, Larqué-Saavedra A.** 2000. Photosynthesis of wheat in a warm, irrigated environment: I: genetic diversity and crop productivity. *Field Crops Research* **66**, 37-50.

**Reynolds MP, Hays D, Chapman S.** 2010. Breeding for adaptation to heat and drought stress. *Climate change and crop production* **1**, 71-91.

**Ristic Z, Momčilović I, Bukovnik U, Prasad PV, Fu J, DeRidder BP, Elthon TE, Mladenov N.** 2009. Rubisco activase and wheat productivity under heat-stress conditions. *Journal of Experimental Botany* **60**, 4003-4014.

- Robinson SP, Portis AR.** 1988. Release of the nocturnal inhibitor, carboxyarabinitol-1-phosphate, from ribulose biphosphate carboxylase/oxygenase by rubisco activase. *FEBS letters* **233**, 413-416.
- Sage RF, Kubien DS.** 2007. The temperature response of C<sub>3</sub> and C<sub>4</sub> photosynthesis. *Plant, Cell & Environment* **30**, 1086-1106.
- Saini H, Sedgley M, Aspinall D.** 1983. Effect of heat stress during floral development on pollen tube growth and ovary anatomy in wheat (*Triticum aestivum* L.). *Functional Plant Biology* **10**, 137-144.
- Salvucci ME, Crafts-Brandner SJ.** 2004. Relationship between the heat tolerance of photosynthesis and the thermal stability of Rubisco activase in plants from contrasting thermal environments. *Plant Physiology* **134**, 1460-1470.
- Scafaro AP, Atkin OK.** 2016. The Impact of Heat Stress on the Proteome of Crop Species. In: Salekdeh GH, ed. *Agricultural Proteomics Volume 2: Environmental Stresses*. Cham: Springer International Publishing, 155-175.
- Scafaro AP, Gallé A, Van Rie J, Carmo-Silva E, Salvucci ME, Atwell BJ.** 2016. Heat tolerance in a wild *Oryza* species is attributed to maintenance of Rubisco activation by a thermally stable Rubisco activase ortholog. *New Phytologist* **211**, 899-911.
- Scafaro AP, Negrini ACA, O'Leary B, Rashid FAA, Hayes L, Fan Y, Zhang Y, Chochois V, Badger MR, Millar AH.** 2017. The combination of gas-phase fluorophore technology and automation to enable high-throughput analysis of plant respiration. *Plant Methods* **13**, 16.
- Schoolfield R, Sharpe P, Magnuson C.** 1981. Non-linear regression of biological temperature-dependent rate models based on absolute reaction-rate theory. *Journal of theoretical biology* **88**, 719-731.
- Schroda M, Vallon O, Wollman F-A, Beck CF.** 1999. A chloroplast-targeted heat shock protein 70 (HSP70) contributes to the photoprotection and repair of photosystem II during and after photoinhibition. *The Plant Cell* **11**, 1165-1178.
- Shanmugam S, Kjaer KH, Ottosen CO, Rosenqvist E, Kumari Sharma D, Wollenweber B.** 2013. The Alleviating effect of elevated CO<sub>2</sub> on heat stress susceptibility of two wheat (*Triticum aestivum* L.) cultivars. *Journal of Agronomy and Crop Science* **199**, 340-350.
- Sharma DK, Andersen SB, Ottosen C-O, Rosenqvist E.** 2012. Phenotyping of wheat cultivars for heat tolerance using chlorophyll a fluorescence. *Functional Plant Biology* **39**, 936-947.
- Sharma DK, Andersen SB, Ottosen CO, Rosenqvist E.** 2015. Wheat cultivars selected for high Fv/Fm under heat stress maintain high photosynthesis, total chlorophyll, stomatal conductance, transpiration and dry matter. *Physiologia Plantarum* **153**, 284-298.
- Sharma DK, Fernández JO, Rosenqvist E, Ottosen C-O, Andersen SB.** 2014. Genotypic response of detached leaves versus intact plants for chlorophyll fluorescence parameters under high temperature stress in wheat. *Journal of plant physiology* **171**, 576-586.
- Shpiler L, Blum A.** 1986. Differential reaction of wheat cultivars to hot environments. *Euphytica* **35**, 483-492.
- Shuting D.** 1994. Canopy apparent photosynthesis, respiration and yield in wheat. *The Journal of Agricultural Science* **122**, 7-12.
- Skylas D, Cordwell S, Hains P, Larsen M, Basseal D, Walsh B, Blumenthal C, Rathmell W, Copeland L, Wrigley C.** 2002. Heat shock of wheat during grain filling: proteins associated with heat-tolerance. *Journal of Cereal Science* **35**, 175-188.

- Slafer G, Rawson H.** 1995. Base and optimum temperatures vary with genotype and stage of development in wheat. *Plant, Cell & Environment* **18**, 671-679.
- Slafer GA, Rawson H.** 1994. Sensitivity of wheat phasic development to major environmental factors: a re-examination of some assumptions made by physiologists and modellers. *Functional Plant Biology* **21**, 393-426.
- Slot M, Kitajima K.** 2015a. General patterns of acclimation of leaf respiration to elevated temperatures across biomes and plant types. *Oecologia* **177**, 885-900.
- Slot M, Kitajima K.** 2015b. Whole-plant respiration and its temperature sensitivity during progressive carbon starvation. *Functional Plant Biology* **42**, 579-588.
- Stöckle CO, Donatelli M, Nelson R.** 2003. CropSyst, a cropping systems simulation model. *European Journal of Agronomy* **18**, 289-307.
- Stone P, Nicolas M.** 1994. Wheat cultivars vary widely in their responses of grain yield and quality to short periods of post-anthesis heat stress. *Functional Plant Biology* **21**, 887-900.
- Tan K, Zhou G, Ren S.** 2013. Response of leaf dark respiration of winter wheat to changes in CO<sub>2</sub> concentration and temperature. *Chinese Science Bulletin* **58**, 1795-1800.
- Todd GW.** 1982. Photosynthesis and respiration of vegetative and reproductive parts of wheat and barley plants in response to increasing temperature. *Proceedings of the Oklahoma Academy of Science* **62**, 57-62.
- Trösch R, Mühlhaus T, Schroda M, Willmund F.** 2015. ATP-dependent molecular chaperones in plastids—More complex than expected. *Biochimica et Biophysica Acta (BBA)-Bioenergetics* **1847**, 872-888.
- Turnbull MH, Tissue DT, Griffin KL, Richardson SJ, Peltzer DA, Whitehead D.** 2005. Respiration characteristics in temperate rainforest tree species differ along a long-term soil-development chronosequence. *Oecologia* **143**, 271-279.
- Turnbull MH, Whitehead D, Tissue DT, Schuster WS, Brown KJ, Griffin KL.** 2001. Responses of leaf respiration to temperature and leaf characteristics in three deciduous tree species vary with site water availability. *Tree physiology* **21**, 571-578.
- van Aken O, Giraud E, Clifton R, Whelan J.** 2009. Alternative oxidase: a target and regulator of stress responses. *Physiologia Plantarum* **137**, 354-361.
- van der Werf A, Kooijman A, Welschen R, Lambers H.** 1988. Respiratory energy costs for the maintenance of biomass, for growth and for ion uptake in roots of *Carex diandra* and *Carex acutiformis*. *Physiologia Plantarum* **72**, 483-491.
- van Keulen H, Penning de Vries F, Drees E.** 1982. A summary model for crop growth. *Simulation of plant growth and crop production: Pudoc*, 87-97.
- Vanlerberghe GC.** 2013. Alternative oxidase: a mitochondrial respiratory pathway to maintain metabolic and signaling homeostasis during abiotic and biotic stress in plants. *International Journal of Molecular Sciences* **14**, 6805-6847.
- Vierling E.** 1991. The roles of heat shock proteins in plants. *Annual review of plant biology* **42**, 579-620.
- Villegas D, Aparicio N, Blanco R, Royo C.** 2001. Biomass accumulation and main stem elongation of durum wheat grown under Mediterranean conditions. *Annals of Botany* **88**, 617-627.
- Vos J.** 1981. Effects of temperature and nitrogen supply on post-floral growth of wheat: measurements and simulations, Pudoc.

- Wahid A, Gelani S, Ashraf M, Foolad MR.** 2007. Heat tolerance in plants: An overview. *Environmental and Experimental Botany* **61**, 199-223.
- Walker BJ, VanLoocke A, Bernacchi CJ, Ort DR.** 2016. The costs of photorespiration to food production now and in the future. *Annual review of plant biology* **67**, 107-129.
- Wang W, Vinocur B, Shoseyov O, Altman A.** 2004. Role of plant heat-shock proteins and molecular chaperones in the abiotic stress response. *Trends in plant science* **9**, 244-252.
- Wang X, Cai J, Jiang D, Liu F, Dai T, Cao W.** 2011. Pre-anthesis high-temperature acclimation alleviates damage to the flag leaf caused by post-anthesis heat stress in wheat. *Journal of plant physiology* **168**, 585-593.
- Wardlaw I, Dawson I, Munibi P.** 1989a. The tolerance of wheat to high temperatures during reproductive growth. 2. Grain development. *Crop and Pasture Science* **40**, 15-24.
- Wardlaw I, Dawson I, Munibi P, Fewster R.** 1989b. The tolerance of wheat to high temperatures during reproductive growth. I. Survey procedures and general response patterns. *Australian Journal of Agricultural Research* **40**, 1-13.
- Wardlaw I, Moncur L.** 1995. The response of wheat to high temperature following anthesis. I. The rate and duration of kernel filling. *Functional Plant Biology* **22**, 391-397.
- Wardlaw I, Moncur L, Patrick J.** 1995. The response of wheat to high temperature following anthesis. II. Sucrose accumulation and metabolism by isolated kernels. *Functional Plant Biology* **22**, 399-407.
- Way DA, Yamori W.** 2014. Thermal acclimation of photosynthesis: on the importance of adjusting our definitions and accounting for thermal acclimation of respiration. *Photosynthesis Research* **119**, 89-100.
- Wheeler T, Hong T, Ellis R, Batts G, Morison J, Hadley P.** 1996. The duration and rate of grain growth, and harvest index, of wheat (*Triticum aestivum* L.) in response to temperature and CO<sub>2</sub>. *Journal of Experimental Botany* **47**, 623-630.
- White JW.** 2001. Modeling temperature response in wheat and maize. In: White JW, ed. *Modeling Temperature Response in Wheat and Maize*. El Batan, Mexico.
- Wilson D, Jones JG.** 1982. Effect of selection for dark respiration rate of mature leaves on crop yields of *Lolium perenne* cv. S23. *Annals of Botany* **49**, 313-320.
- Wohl K, James W.** 1942. The energy changes associated with plant respiration. *New Phytologist* **41**, 230-256.
- Yadav DK, Pospíšil P.** 2012. Role of chloride ion in hydroxyl radical production in photosystem II under heat stress: electron paramagnetic resonance spin-trapping study. *Journal of bioenergetics and biomembranes* **44**, 365-372.
- Yamasaki T, Yamakawa T, Yamane Y, Koike H, Satoh K, Katoh S.** 2002. Temperature acclimation of photosynthesis and related changes in photosystem II electron transport in winter wheat. *Plant Physiology* **128**, 1087-1097.
- Yamori W, Hikosaka K, Way DA.** 2014. Temperature response of photosynthesis in C<sub>3</sub>, C<sub>4</sub>, and CAM plants: temperature acclimation and temperature adaptation. *Photosynthesis Research* **119**, 101-117.
- Yamori W, Suzuki K, Noguchi K, Nakai M, Terashima I.** 2006. Effects of Rubisco kinetics and Rubisco activation state on the temperature dependence of the photosynthetic rate in spinach leaves from contrasting growth temperatures. *Plant, Cell & Environment* **29**, 1659-1670.



**Zhao H, Dai T, Jing Q, Jiang D, Cao W.** 2007. Leaf senescence and grain filling affected by post-anthesis high temperatures in two different wheat cultivars. *Plant Growth Regulation* **51**, 149-158.

**Zheng B, Chenu K, Doherty A, Chapman S.** 2014. The APSIM-Wheat module (7.5 R3008). *Agricultural Production Systems Simulator (APSIM) Initiative*.

**Zhu L, Bloomfield KJ, Hocart CH, Egerton JJ, O'Sullivan OS, Penillard A, Weerasinghe LK, Atkin OK.** 2018. Plasticity of photosynthetic heat tolerance in plants adapted to thermally contrasting biomes. *Plant, Cell & Environment*.

## Statement of Contribution

This thesis is submitted as a Thesis by Compilation in accordance with [https://policies.anu.edu.au/ppl/document/ANUP\\_003405](https://policies.anu.edu.au/ppl/document/ANUP_003405)

I declare that the research presented in this Thesis represents original work that I carried out during my candidature at the Australian National University, except for contributions to multi-author papers incorporated in the Thesis where my contributions are specified in this Statement of Contribution.

Title: Exploring high temperature responses of photosynthesis and respiration to improve heat tolerance in wheat \_\_\_\_\_

Authors: Bradley C. Posch, Buddhima C. Kariyawasam, Helen Bramley, Onoriode Coast, Richard A. Richards, Matthew P. Reynolds, Richard Trethowan, and Owen K. Atkin \_\_\_\_\_

Publication outlet: Journal of Experimental Botany \_\_\_\_\_

Current status of paper: Published

Contribution to paper: B.C.P. and B.C.K. conducted searches of the literature; and B.C.P. wrote the paper with contributions from all authors \_\_\_\_\_

Senior author or collaborating authors endorsement: Owen Atkin April 2nd 2022

Bradley C. Posch

Candidate – Print Name



Signature

01-04-2022

Date

### Endorsed

PROFESSOR OWEN ATKIN

Primary Supervisor – Print Name



Signature

April 2nd 2022

Date

## Chapter 2 – Acclimation of leaf photosynthesis and respiration to warming in field-grown wheat

Onoriode Coast\*, Bradley C. Posch\*, Helen Bramley, Oorbessy Gaju, Richard A. Richards, Meiqin Lu, Yong-Ling Ruan, Richard Trethowan, and Owen K. Atkin

\* Onoriode Coast and Bradley C. Posch should be considered joint first author

Author Contributions: O.K.A., H.B., and Y-L.R. secured grants; R.T. developed the seed materials; O.C., H.B., and O.K.A. designed experiments; O.C. and B.C.P. collected data; O.C. and B.C.P. analysed data; and O.C. and B.C.P. wrote the paper with contributions from all authors.

*This manuscript has been published in Plant, Cell & Environment (Coast O, Posch BC, Bramley H, Gaju O, Richards RA, Lu M, Ruan YL, Trethowan R, Atkin OK. 2021. Acclimation of leaf photosynthesis and respiration to warming in field-grown wheat. Plant, Cell & Environment 44, 2331–2346.)*

### Abstract

Climate change and future warming will significantly affect crop yield. The capacity of crops to dynamically adjust physiological processes (i.e. acclimate) to warming might improve overall performance. Understanding and quantifying the degree of acclimation in field crops could ensure better parameterization of crop and Earth System models and predictions of crop performance. We hypothesized that for field-grown wheat, when measured at a common temperature (25°C), crops grown under warmer conditions would exhibit acclimation, leading to enhanced crop performance and yield. Acclimation was defined as: (i) decreased rates of net photosynthesis at 25°C ( $A^{25}$ ) coupled with lower maximum carboxylation capacity ( $V_{cmax}^{25}$ ); (ii) reduced leaf dark respiration at 25°C (both in terms of  $O_2$  consumption,  $R_{dark\_O_2}^{25}$ ; and  $CO_2$  efflux,  $R_{dark\_CO_2}^{25}$ ); and (iii) lower  $R_{dark\_CO_2}^{25}:V_{cmax}^{25}$ . Field experiments were conducted over two seasons with 20 wheat genotypes, sown at three different planting dates, to test these hypotheses. Leaf-level  $CO_2$  based traits ( $A^{25}$ ,  $R_{dark\_CO_2}^{25}$ ,

and  $V_{\text{cmax}}^{25}$ ) did not show the classic acclimation responses that we hypothesized; by contrast, the hypothesized changes in  $R_{\text{dark\_O}_2}$  were observed. These findings have implications for predictive crop models that assume similar temperature response among these physiological processes, and for predictions of crop performance in a future warmer world.

## Introduction

Anthropogenic activities have increased atmospheric CO<sub>2</sub> concentration resulting in global warming. Earth System Models (ESMs) predict that average annual global land surface temperatures will rise by 0.3–4.8°C by 2100 (Collins et al., 2013). This increase in temperature is likely to affect the growth of plants in natural and managed ecosystems, with the effect of climate change on crops being of particular importance. Understanding how key physiological processes in crops – particularly leaf photosynthesis and respiration - respond to rising temperatures, including quantifying their capacity to thermally acclimate, will be critical for global food security (Lobell & Gourdjji, 2012) and modelling crop responses to climate change (Huntingford et al., 2017; Smith & Dukes, 2013; Wang et al., 2017).

Leaf dark respiration [ $R_{\text{dark}}$ , defined here either as non-photorespiratory mitochondrial CO<sub>2</sub> release in darkness ( $R_{\text{dark\_CO}_2}$ ) or dark O<sub>2</sub> consumption ( $R_{\text{dark\_O}_2}$ )] and photosynthesis (net CO<sub>2</sub> assimilation rate,  $A$ ) differ in their response to temperature. Short-term (minutes to hours) elevations in temperature induce a near-exponential increase in  $R_{\text{dark}}$  (Atkin & Tjoelker, 2003) up to a maximum at around 50–60°C, followed by a rapid decline in  $R_{\text{dark}}$  indicating irreversible damage to the respiratory apparatus (O'Sullivan et al., 2013). For net photosynthesis,  $A$  increases in response to short-term elevations in temperature until it reaches its optimum (often in the 25–35 °C range) and then decreases at supra-optimal temperatures. Under long-term (several days or longer) warming, plants dynamically adjust (i.e. acclimate) rates of  $A$  and  $R_{\text{dark}}$  to maintain fixation of CO<sub>2</sub> and/or limit CO<sub>2</sub> release, respectively. Acclimation to long-term warming should improve plant performance through constructive adjustment that maximise daytime net CO<sub>2</sub> assimilation and minimize daily respiratory CO<sub>2</sub> loss (Way & Yamori, 2014). Most studies that have shown beneficial effects of adjustment on plant performance have been for acclimation to light in non-crop plants (Athanasίου, Dyson, Webster, & Johnson, 2010; Frenkel, Bellafiore, Rochaix, & Jansson, 2007).

The opposite of constructive adjustment is detractive adjustment such as unsustainable increase in rates of  $R_{\text{dark}}$  or decline in rates of photosynthesis of warmed plants at high temperature, which does not improve a plant's ability to grow and/or survive in its new growth regime (Slot & Winter, 2016; Way & Yamori, 2014). It remains unknown whether annual field crops respond to temperature through constructive adjustment.

Acclimation to elevated temperatures might be partial or full, the latter potentially leading to reset of metabolic homeostasis, when cool and warm grown plants are compared at their respective growth temperatures. Acclimation of  $R_{\text{dark}}$  to sustained warming is characterised by decreases in  $R_{\text{dark}}$ 's temperature sensitivity (e.g.  $Q_{10}$ , the proportional change in  $R_{\text{dark}}$  per 10°C change in temperature; Type I acclimation) or the downward regulation of the basal rate of  $R_{\text{dark}}$  at a reference temperature (e.g. at 25°C,  $R_{\text{dark}}^{25}$ ; Type II acclimation) or a combination of both (Atkin & Tjoelker, 2003). Altered  $Q_{10}$  values reflect changes in the underlying factors regulating respiratory flux (e.g. substrate availability and/or the turnover of ATP to ADP) (Atkin & Tjoelker, 2003). Type II acclimation is likely underpinned by decreases in respiratory capacity associated with changes in mitochondrial abundance, structure and/or protein composition (Armstrong, Logan, & Atkin, 2006; Campbell et al., 2007; Rashid et al., 2020). For photosynthesis, growth under warm conditions is characterised by a number of changes (relative to plants grown at lower temperatures) including: lower rates of  $A$  measured at temperatures below the thermal optimum of  $A$  (i.e. leaf temperature where maximal rates of  $A$  occur); higher or similar rates of  $A$  at the thermal optimum (Way & Yamori, 2014); an increase in the leaf temperature at which the thermal optimum of  $A$  occurs (Berry & Bjorkman, 1980); and, a down-regulation of photosynthetic capacity (maximum carboxylation rate,  $V_{\text{cmax}}$  and/or maximum electron transport rate,  $J_{\text{max}}$ ), when measured at a set temperature (e.g.  $V_{\text{cmax}}$  at 25°C,  $V_{\text{cmax}}^{25}$ ) (Ghannoum et al., 2010). For plants that are growing near or above their optimum temperature, the downregulation of  $V_{\text{cmax}}^{25}$  can lead to decreases in daily net  $\text{CO}_2$  uptake (Way & Sage, 2008) that may compromise plant performance.

The greatest source of uncertainty in models used to simulate the impact of climate change on crop yields (Bassu et al., 2014; Li et al., 2015; Rosenzweig et al., 2013; Wang et al., 2017) is attributed to contrasting differences in the temperature response functions of key physiological processes (Senthold Asseng et al., 2013; Wang et al., 2017). Most models assuming a fixed temperature response of key physiological processes. In many ESMs,  $R_{\text{dark}}$  is

modelled from  $A$  or  $V_{\text{cmax}}$ . For example, in MOSES-TRIFFID (now JULES), BIOME3, and BETHY,  $R_{\text{dark}}$  is estimated to be 0.011-0.015 (for  $C_3$  plants) or 0.025-0.042 (for  $C_4$  plants) of  $V_{\text{cmax}}$  at a common temperature of 25°C (Cox, 2001; Haxeltine & Prentice, 1996; Knorr, 2000; Ziehn, Kattge, Knorr, & Scholze, 2011). But  $R_{\text{dark}}^{25}:V_{\text{cmax}}^{25}$  varies between cold and hot acclimated plants. A global study of 899 species across 100 sites from the tropics, reported greater  $R_{\text{dark}}:V_{\text{cmax}}$  in species at cold sites compared to species at warmer sites, with faster rates of  $R_{\text{dark}}^{25}$  at a given  $V_{\text{cmax}}^{25}$  for  $C_3$  herbs/grasses compared with broadleaved/needle-leaved plants and shrubs (Atkin et al., 2015). These acclimation responses and the change in  $R_{\text{dark}}^{25}:V_{\text{cmax}}^{25}$  are rarely accounted for by models when predicting crop responses under warmer field conditions (Li et al., 2015). One reason for this deficiency in crop models is in part due to the difficulty in obtaining relevant field data for model evaluation. The extent to which acclimation changes  $R_{\text{dark}}^{25}:V_{\text{cmax}}^{25}$  in crops grown under thermally contrasting field settings remains untested.

Wheat is an ideal annual crop species for examining the acclimation response of leaf  $R_{\text{dark}}$  and  $A$  to warming and its relationships with plant performance (or crop yield) under realistic field settings. There is increasing evidence that warming in many wheat producing regions (including China, India, USA, France and Australia) is resulting in either stalled or reduced wheat yields (Hochman, Gobbett, & Horan, 2017; Zhao, Li, Yu, Cheng, & He, 2016). Some of the ways that warming can affect crop yield include accelerating phenological development, consequently shortening the time available for crops to efficiently capture and convert natural resources into yield (Slafer & Rawson, 1994); altering the rates of  $R_{\text{dark}}$  (Atkin & Tjoelker, 2003) and  $A$  (Crafts-Brandner & Salvucci, 2002; Sage & Kubien, 2007), potentially reducing daily net  $\text{CO}_2$  uptake; reducing  $A$  due to stomatal closure with increasing atmospheric vapour pressure deficit (Lin, Medlyn, & Ellsworth, 2012); and, directly disrupting reproductive development leading to floral and grain abortion (Ruan, Patrick, Bouzayen, Osorio, & Fernie, 2012). Although genotypic variation exists for wheat sensitivity to high temperature, the degree of variation in acclimation of leaf  $R_{\text{dark}}$  and  $A$  to warming is unknown.

Our understanding of acclimation responses to warming has improved over time (Atkin & Tjoelker, 2003; Berry & Bjorkman, 1980; Hikosaka, Ishikawa, Borjigidai, Muller, & Onoda, 2006; Larigauderie & Körner, 1995; Sage & McKown, 2006; Way & Yamori, 2014). This gain has come from experiments predominantly conducted either in temperature-controlled settings or by exploiting natural temperature variations. Some examples of the latter include

studies conducted along regional climatic gradients or across different seasons (Drake et al., 2015; Tjoelker, Oleksyn, Reich, & Żytkowiak, 2008). Another example involves the use of different times of sowing (TOS) within a cropping season. The TOS concept is commonly used by crop modelers and agronomists as a surrogate for generating different thermal environments in studies of crop responses to temperature (Hunt et al., 2019; Kirkegaard et al., 2016; Wang et al., 2019). Adjusting TOS has also been suggested as one of the most convenient management strategies for climate change impact at the field level (Donatelli, Srivastava, Duveiller, Niemeier, & Fumagalli, 2015). While its use is complicated by the difficulty in isolating the effect of temperature from other environmental factors, adjusting TOS can nonetheless, provide insights into the response of crops to changes in growth temperature under typical field conditions.

Considering the points described above, we used wheat crops sown on three planting dates (three TOS) and two cropping seasons to test if the assumption of fixed temperature responses of  $R_{\text{dark}}$  and  $A$  with temperature used in crop and Earth System models (Cox, 2001; Hansen, Jensen, Nielsen, & Svendsen, 1991; Oleson et al., 2013; Ruimy, Dedieu, & Saugier, 1996) holds true for wheat. We hypothesized that, when measured at a commonly reported standardized temperature of 25°C, plants grown under warmer field settings would – relative to cooler grown plants - show: (i) decreased leaf  $A^{25}$  coupled with lower  $V_{\text{cmax}}^{25}$  due to acclimation to higher growth temperature; (ii) lower leaf  $R_{\text{dark}}^{25}$  when measured on both  $\text{O}_2$  and  $\text{CO}_2$  bases, i.e. exhibit a downward shift in the  $R_{\text{dark}}$ -temperature response curve due to acclimation; and (iii) lower  $R_{\text{dark\_CO}_2^{25}:A^{25}}$  and  $R_{\text{dark\_CO}_2^{25}:V_{\text{cmax}}^{25}}$ . We normalised measurements to 25°C, which is close to the optimum temperature of 27.5°C for  $A$  in wheat (Wang et al., 2017). To quantify the extent to which acclimation of leaf  $R_{\text{dark}}$  was Type I or Type II (Atkin and Tjoelker 2003), we estimated short-term temperature responses of  $R_{\text{dark}}$  at anthesis of TOS 1-3 plants. Finally, we examined if the temperature response of leaf  $R_{\text{dark}}$  and  $A$  at anthesis was reflective of overall crop performance at harvest.

## Materials and methods

### *Experimental sites*

Two field experiments were conducted over a 2-year period to investigate variation in acclimation to temperature of  $R_{\text{dark}}$  and  $A^{25}$  of wheat. The experiments were located in commercial wheat farms in Dingwall (35°48'22.2" S, 143°47'3.3" E) and Barraport West (36°2'38.6" S, 143°32'20.9" E), Victoria, Australia, during the spring of 2017 and 2018, respectively. Dingwall and Barraport West are 49 km apart but both in the Mallee district of the SE region of Australia. Soils within the region are relatively infertile (Isbell, 1996).

### *Plant materials and growing conditions*

The trials consisted of 20 wheat genotypes, including four commercial cultivars (Corak, Trojan, Mace, and Suntop) and 16 breeding lines developed by the University of Sydney's Plant Breeding Institute for the Australian environment (Table S1). The 16 breeding lines cover a diverse genetic background, including hexaploid genotypes derived from crosses to emmer wheat-based hexaploid lines (*Triticum dicoccon* Schrank ex Schübl.) (Ullah et al., 2018) and genotypes with pedigrees originating from hot climates, such as Sudan, India and Mexico. Seeds were sown on three dates in 2017 (02 May, 02 June and 01 July) and 2018 (09 May, 01 June and 03 July) in order to expose crops to different growth temperatures at a common developmental stage. The first times of sowing (TOS) for both experiments were within the locally recommended periods for sowing. For brevity, the first, second and third TOS will henceforth be referred to as TOS1, TOS2 and TOS3, respectively.

The 2017 and 2018 experiments conducted primarily under rainfed conditions, with supplemental watering provided by an overhead centre pivot (2017) or overhead lateral move (2018) irrigator. Rainfall and irrigation at both sites are given in Table S3. The trials were managed by the Birchip Cropping Group (BCG; [www.bcg.org.au](http://www.bcg.org.au)) following standard agronomic practices for the region. Daily maximum and minimum temperatures, and rainfall data were obtained from the closest Australian Bureau of Meteorology (BOM) weather station, which was ~0.7 km from the experimental site, for the first 140 days after sowing (DAS) for Experiment I. From 141 DAS onwards in 2017 and throughout 2018 a weather



station was placed on site to record temperature, relative humidity, rainfall, solar radiation and evapotranspiration at 15-minute intervals.

### *Experimental design*

The experiments were sown using a 6-row planter at a rate of 130 plants m<sup>-2</sup> and each row spaced 30 cm apart. Each experiment was sown as three adjacent fields, one for each TOS. Each field consisted of four replicate blocks and each block had 20 plots that were 2.15 x 4 m. Individual fields were buffered on all sides with the commercial cultivar Mace using the same spacing and plant density as in the plots. The wheat lines were randomly allocated to the plots using Digger biometrics software (<http://nswdpiom.org/austatgen/software/>). Samples for physiological measurements were collected from plants in rows 3 or 4 of plots.

### *Measurement of physiological traits*

All physiological measurements were carried out at Zadok growth scale between 59-70 (Zadoks, Chang, & Konzak, 1974; when about 50% of plants in each TOS were between early and late flowering). In 2017, measurements were conducted over three-day periods on 26–28 September (147–149 DAS) for TOS1, 17–19 October (137–139 DAS) for TOS2 and 24–26 October (115–117 DAS) for TOS3. In 2018, measurements were made on 03–05 October (147–149 DAS) for TOS1, 17–19 October (138–140 DAS) for TOS2 and 30 October–01 November (119–121 DAS) for TOS3. In both 2017 and 2018, leaf  $R_{\text{dark\_O}_2^{25}}$  of all 20 genotypes were completed over two days, with two replicates sampled on the first day and two replicates on the second. Flag leaves were harvested between 0830 and 1030 h. Samples were stored temporarily for at least 30 minutes in cool, moist darkened containers prior to sample preparation and measurements for dark adaptation. Measurements were concluded within 6 h of harvesting leaves.

*Measurement of  $A^{25}$  and  $R_{\text{dark\_CO}_2^{25}}$ :* Leaf CO<sub>2</sub> gas exchange measurements were limited to six genotypes, which included the two commercial cultivars Mace and Suntop. Unpublished data from previous studies show that these six lines were representative of the diversity of the set of 20 lines. Leaf CO<sub>2</sub> gas exchange measurements were conducted for all TOS in 2017 and 2018. Leaf  $A^{25}$  and  $R_{\text{dark\_CO}_2^{25}}$  were measured using Licor 6400XT Portable Photosynthesis Systems (Li-6400XT, Licor, Lincoln, NE, USA). Licor units with a 6 cm<sup>2</sup> leaf

chamber and red-blue light source (6400-18 RGB Light Source, Licor) were used, with the chamber temperature set to 25°C, reference line atmospheric [CO<sub>2</sub>] to 400 ppm and a flow rate of 500 μmol s<sup>-1</sup>. Flag leaves of the main stems, from one plant per plot, were used for all measurements. To determine A<sup>25</sup>, leaves in chambers were exposed to saturating irradiance of 1500 μmol photons m<sup>-2</sup> s<sup>-1</sup> for at least five min, after which A<sup>25</sup> was measured following equilibrium (stable readings for at least one minute). Immediately after measuring A<sup>25</sup>, light within the chamber was turned off and leaves dark adapted for at least 30 min (to avoid post-illumination transients; Atkin, Evans, and Siebke (1998); Azcon-Bieto, Day, and Lambers (1983)) then R<sub>dark\_CO2</sub><sup>25</sup> was measured. Relative humidity (RH) within the chamber was maintained between 40 and 75% for all measurements. These measurements were taken within a day between 0900 and 1730 h (~40 min before sunset) for each TOS.

*Estimates of V<sub>cm<sub>max</sub></sub>* using the ‘one-point-method’:

To assess whether TOS influenced net photosynthetic rates (A) in the absence of limitations in stomatal conductance (and thus limitations in C<sub>i</sub>), we estimated the catalytic capacity of Rubisco (V<sub>cm<sub>max</sub>) using the ‘one-point method’ (Wilson, Baldocchi, & Hanson, 2000), which was recently validated by (De Kauwe et al., 2016). These V<sub>cm<sub>max</sub> values were then used to obtain estimates of A at a set internal CO<sub>2</sub> concentration (C<sub>i</sub>) of 250 ppm (De Kauwe et al., 2016), using Eqn 1:</sub></sub>

$$V_{cm_{max}} = A_{sat} + R_{light} (C_i + K_c[1 + O/K_o]) / (C_i - \Gamma^*) \quad \text{Eqn 1}$$

where  $\Gamma^*$  is the CO<sub>2</sub> compensation point in the absence of nonphotorespiratory mitochondrial CO<sub>2</sub> release (36.9 μbar at 25°C), O is the partial pressure of oxygen (kPa), C<sub>i</sub> is the intercellular CO<sub>2</sub> partial pressure (Pa), R<sub>light</sub> is the rate of nonphotorespiratory mitochondrial CO<sub>2</sub> release (here assumed to be equal to R<sub>dark\_CO2</sub><sup>25</sup>), and K<sub>c</sub> (59.4 kJ mol<sup>-1</sup>) and K<sub>o</sub> (36 kJ mol<sup>-1</sup>) are the Michaelis–Menten constants (K<sub>m</sub>) of Rubisco for CO<sub>2</sub> (404 μbar) and O<sub>2</sub> (248 mbar), respectively, at 25°C (Evans, von Caemmerer, Setchell, & Hudson, 1994; von Caemmerer, Evans, Hudson, & Andrews, 1994). Using this approach, we assumed that A at saturating irradiance and ambient CO<sub>2</sub> is limited by Rubisco carboxylation rather than by ribulose 1,5-bisphosphate (RuBP) regeneration. Moreover, we assumed that leaf mitochondrial respiration in the light (R<sub>light</sub>) can be equal to those measured on the same leaf in darkness. Because leaf temperatures were not always at 25°C during gas exchange measurements we standardized V<sub>cm<sub>max</sub> to 25°C (V<sub>cm<sub>max</sub><sup>25</sup>) following:</sub></sub>

$$V_{\text{cmax}}^{25} = V_{\text{cmax}} / [\exp ((T - 25) * \Delta E_a) / (R * 298(T + 273.15)))] \quad \text{Eqn } 2$$

where  $T$  is the leaf temperature at which  $A$  was measured (and  $V_{\text{cmax}}$  was initially estimated),  $\Delta E_a$  is the activation energy [assuming = 64.8 kJ mol<sup>-1</sup>, Badger and Collatz (1977)], and  $R$  is the universal gas constant (8.314 J mol<sup>-1</sup> K<sup>-1</sup>).

*Leaf  $R_{\text{dark\_O}_2}$ :* For all 20 genotypes, four 4 cm<sup>2</sup> sections of flag leaf tissue from one stem per plot, cut from the middle of the leaf, were used to estimate flag leaf  $R_{\text{dark\_O}_2}$  at 20, 25, 30 and 35°C. Measurements were taken using an automated Q<sub>2</sub> O<sub>2</sub>-sensor (Astec Global, Maarsse, the Netherlands) described in Scafaro et al. (2017) and previously used for wheat (Coast et al., 2019). Briefly, a LED excitation pulse is emitted onto an O<sub>2</sub>-sensitive fluorophore embedded on the lid of a sealed tube, and the subsequent fluorescence signal is detected by a fibre-optic sensor, providing a measurement of O<sub>2</sub> concentration inside the tube. These measurements are taken at regular intervals to track the rate of O<sub>2</sub> consumption of tissue over time.

*Leaf traits:* Leaf mass per unit area (LMA) and leaf N were determined using leaf sections covered within the cuvette of the Licor head during the gas exchange measurements. The leaf sections were oven-dried at 60°C for 72 h then weighed. The same leaf sections were used to determine leaf N content (%), by combustion using a Carlo-Erba elemental analyser (NA1500, Thermo Fisher Scientific, Milan, Italy). Leaf N content and LMA were used to estimate leaf N per unit dry mass ( $N_{\text{mass}}$ ) and N per unit leaf area ( $N_{\text{area}}$ ).

*Yield:* At harvest maturity when grain moisture was approximately 9–11%, all plots (each 8.6 m<sup>2</sup>) were harvested using a combine harvester. Final yield of each plot was determined based on machine harvests of three adjacent inner rows. Grain yield measured in grams per plot was converted to tonnes per hectare and used for all analyses.

#### *Statistical analysis*

The 2017 and 2018 experiments were treated as different experiments and their data analysed separately. We conducted ANOVA on all physiological variables, leaf traits and ratios of  $R_{\text{dark\_CO}_2}^{25}$  to  $A^{25}$  and  $V_{\text{cmax}}^{25}$  using the General Treatment Structure in Randomized Blocks Design function in GENSTAT (18<sup>th</sup> edn, VSN International Ltd, Hemel Hempstead, UK). Genotype, TOS and their interaction term were taken as the treatment terms and block as the replicate term. Means were separated by l.s.d. ( $P=0.05$ , unless otherwise stated).

Slopes of log-transformed temperature response curves (20–35°C) of  $R_{\text{dark\_O}_2}$  were used to compute  $Q_{10}$ . To assess the type of acclimation of  $R_{\text{dark\_O}_2}$  that occurred we compared the slopes of the log  $R_{\text{dark}}$ -temperature response curves. Lower slopes for TOS2 and TOS3 compared to TOS1 would indicate Type I acclimation; the absence of significantly lower slopes but lower intercepts for TOS2 and TOS3 would indicate Type II acclimation (Slot & Kitajima, 2015).

Relationships of leaf physiological characteristics ( $A^{25}$ ,  $R_{\text{dark\_CO}_2^{25}}$  and  $R_{\text{dark\_O}_2^{25}}$ ) with LMA,  $N_{\text{mass}}$  and  $N_{\text{area}}$  or measured environmental variables were explored using bivariate and multiple linear regressions. The measured environmental factors were daily average minimum temperature ( $T_{\text{min}}$ ) or maximum temperature ( $T_{\text{max}}$ ) over the 1–10 day period before 50% of plants had achieved anthesis (DBA) and 1–3 day period when 50% of plants were at anthesis (DAA). Other measured variables were mean photosynthetically active radiation and total solar radiation during the 1–3 DAA. To test if TOS or experiments influenced these relationships, analyses were initially conducted separately for 2017 and 2018 and later with data from both experiments combined. Multiple linear regressions were also conducted to explain variation in grain yield by measured and estimated leaf traits. Stepwise regression was used to select the best-fitting equation given the set of input leaf traits.

## Results

### *Environmental conditions during vegetative growth and at anthesis*

From sowing to anthesis, average  $T_{\min}$  and  $T_{\max}$  were similar for TOS1 and TOS2 across the two experiments, but  $T_{\max}$  of TOS3 was warmer in 2018 than 2017 (Table 1). During the 1–3 DAA period,  $T_{\min}$  was generally warmer in 2017 than in 2018. Rainfall between sowing and anthesis was 19–44% higher in 2017 compared to 2018 (Table 1 and S2). Rainfall was supplemented by irrigation, with less irrigation (in terms of quantity and application times) and overall water supplied to 2017 (Table S3). However, the combination of rainfall and irrigation provided sufficient moisture to the plants except for a brief period of water deficit stress (with visible signs of leaf rolling) during the period of physiological measurements for TOS2 and just prior to that of TOS3 for 2018. This is not reflected in total water supplied (Supplementary Table S3). The sum of daily solar radiation from sowing to anthesis was 477–502 kWh m<sup>-2</sup> in Experiment I, with this range being narrower than that for 2018 which was 420–606 kWh m<sup>-2</sup>.

During the 1–3 DAA period  $T_{\min}/T_{\max}$  of TOS2/TOS3 were warmer than TOS1 by 6–10°C in 2017 and 1–10°C in 2018. Total solar radiation was 4–5 kWh m<sup>-2</sup> more and photosynthetically active radiation was 60–160% higher in TOS2/TOS3 than TOS1 for 2017 (Table 1). For the same period of 2018,  $T_{\min}$  of TOS2/TOS3 were approximately 2°C warmer than TOS1,  $T_{\max}$  of TOS3 was more than 10°C warmer than TOS1, and solar radiation was 4–5 kWh m<sup>-2</sup> more in TOS2/TOS3 than for TOS1. Mean photosynthetically active radiation of the three TOS for 2018 were about the same (Table 1).

**Table 1.** Environmental conditions during defined periods for each time of sowing (TOS) during 2017 and 2018.

Weather parameter/Period	TOS	Average $T_{\max}/T_{\min}^1$ (°C)		Total rainfall (mm)		Total solar radiation (kWh m <sup>-2</sup> )		PAR <sup>2</sup> (μmol (photons) m <sup>-2</sup> s <sup>-1</sup> )	
		2017	2018	2017	2018	2017	2018	2017	2018
Sowing to anthesis <sup>3</sup>	1	16.8/4.7	16.4/3.5	123	69	477	420	---	---
	2	17.7/4.8	17.4/3.9	90	73	499	491	---	---
	3	18.7/5.6	20.1/5.2	97	67	502	606	---	---
Anthesis <sup>4</sup>	1	21.4/ 5.1	22.8/7.2	0	0	14	15	1394	2331
	2	31.6/12.3	23.0/8.7	0	0	19	20	1934	1706
	3	26.6/11.2	33.4/9.2	0	0	18	19	1632	2041

<sup>1</sup>Average daily maximum or minimum temperature, actual daily temperature and other environmental variables are given in supplementary Table S2. <sup>2</sup>Mean maximum photosynthetically active radiation measured with Licor 6400XTs light sensors during gas exchange measurements.

<sup>3</sup>Data from closest Australian Bureau of Meteorology weather station in 2017 and on-site weather station in 2018; <sup>4</sup>Mean values of the three-day period when physiological measurements were taken and during which at least 50% of plants had visible anther.

### *Temperature responses of leaf CO<sub>2</sub> exchange among six wheat genotypes*

For Experiment I, there was no significant genotype by TOS interaction effects ( $P>0.05$ ) on leaf  $A^{25}$ ,  $V_{\text{cmax}}^{25}$  or  $R_{\text{dark\_CO}_2}^{25}$  (Table 2) but all three variables were significantly greater under TOS2 and TOS3 compared with TOS1 (Fig. 1, Table 2). Mean leaf  $A^{25}$  was significantly higher ( $P<0.001$ ) by 10% for TOS2 and 23% for TOS3 than TOS1. Stomatal conductance mirrored the increases with TOS seen in leaf  $A^{25}$ , with mean values being  $0.24 \text{ mol m}^{-2} \text{ s}^{-1}$  at TOS1,  $0.31 \text{ mol m}^{-2} \text{ s}^{-1}$  at TOS2 and  $0.41 \text{ mol m}^{-2} \text{ s}^{-1}$  at TOS3 (i.e. 34–67% higher,  $P<0.001$ ). Similarly,  $V_{\text{cmax}}^{25}$  and leaf  $R_{\text{dark\_CO}_2}^{25}$  were 11–46% and 15–18% greater at TOS2 and TOS3 compared with TOS1 (Fig. 1c, e). Genotypes only differed for  $V_{\text{cmax}}^{25}$ , there were no other significant genotype effects (Table 2).

There was no significant genotype x TOS effect for  $A^{25}$  and  $R_{\text{dark\_CO}_2}^{25}$  in 2018, consistent with 2017 (Table 2). However, TOS responses of leaf  $A^{25}$  and  $R_{\text{dark\_CO}_2}^{25}$  for 2018 were not consistent with those of 2017 (Fig. 1). Mean leaf  $A^{25}$  reduced in TOS2 and TOS3 compared with TOS1. The reduction was greater in TOS2 than TOS3 due to lower stomatal conductance. Mean stomatal conductance for TOS2 at  $0.064 \text{ mol m}^{-2} \text{ s}^{-1}$  and TOS3 at  $0.098$  were 56 and 33% less ( $P<0.001$ ) than that of TOS1 ( $0.145 \text{ mol m}^{-2} \text{ s}^{-1}$ ), respectively. The reduced stomatal conductance was in response to apparent water deficit stress during the period of physiological measurement for TOS2. However, estimates of  $V_{\text{cmax}}^{25}$  showed consistent increases (46–55%) from TOS1 to TOS2 and TOS3 (Fig. 1d). Compared with TOS1, leaf  $R_{\text{dark\_CO}_2}^{25}$  increased slightly at TOS2 but was similar at TOS3 (Fig. 1f). As was the case for Experiment I, there was no significant effect of genotype on leaf  $A^{25}$  and  $R_{\text{dark\_CO}_2}^{25}$  in 2018, but there was for  $V_{\text{cmax}}^{25}$  (Table 2).

**Table 2.** Analysis of variance of thermal acclimation-related traits for wheat genotypes grown under three thermal regimes, achieved by varying time of sowing (TOS) during 2017 and 2018.

	Genotype		TOS		Genotype x TOS	
	d.f.	v.r	d.f.	v.r	d.f.	v.r
<b>2017</b>						
Six genotypes						
$A^{25}$	5	1.03 <sup>ns</sup>	2	<b>25.48***</b>	10	0.46 <sup>ns</sup>
$V_{cmax}^{25}$	5	<b>3.05*</b>	2	<b>66.72***</b>	10	0.45 <sup>ns</sup>
$R_{dark\_CO_2}^{25}$	5	0.45 <sup>ns</sup>	2	<b>7.28**</b>	10	0.98 <sup>ns</sup>
$R_{dark\_O_2}^{25}$	5	1.73 <sup>ns</sup>	2	<b>31.55***</b>	10	0.34 <sup>ns</sup>
20 genotypes						
$R_{dark\_O_2}^{20}$	19	0.52 <sup>ns</sup>	2	<b>14.28***</b>	38	0.27 <sup>ns</sup>
$R_{dark\_O_2}^{25}$	19	1.53 <sup>ns</sup>	2	<b>50.43***</b>	38	0.49 <sup>ns</sup>
$R_{dark\_O_2}^{30}$	19	1.34 <sup>ns</sup>	2	<b>28.18***</b>	38	0.54 <sup>ns</sup>
$R_{dark\_O_2}^{35}$	19	<b>1.95*</b>	2	<b>19.58***</b>	38	0.60 <sup>ns</sup>
<b>2018</b>						
Six genotypes						
$A^{25}$	5	1.54 <sup>ns</sup>	2	<b>49.56***</b>	10	0.93 <sup>ns</sup>
$V_{cmax}^{25}$	5	<b>4.15**</b>	2	<b>10.89***</b>	10	<b>2.18*</b>
$R_{dark\_CO_2}^{25}$	5	2.07 <sup>ns</sup>	2	<b>10.21***</b>	10	0.45 <sup>ns</sup>
$R_{dark\_O_2}^{25}$	5	0.05 <sup>ns</sup>	2	0.96 <sup>ns</sup>	10	0.42 <sup>ns</sup>
20 genotypes						
$R_{dark\_O_2}^{20}$	19	<b>1.72*</b>	2	<b>46.45***</b>	38	1.09 <sup>ns</sup>
$R_{dark\_O_2}^{25}$	19	0.47 <sup>ns</sup>	2	2.52 <sup>ns</sup>	38	0.57 <sup>ns</sup>
$R_{dark\_O_2}^{30}$	19	1.02 <sup>ns</sup>	2	<b>26.19***</b>	38	0.84 <sup>ns</sup>
$R_{dark\_O_2}^{35}$	19	1.38 <sup>ns</sup>	2	<b>44.94***</b>	38	0.79 <sup>ns</sup>

$A^{25}$  ( $\mu\text{mol CO}_2 \text{ m}^{-2} \text{ s}^{-1}$ ), net  $\text{CO}_2$  assimilation rate measured at 25°C;  $V_{cmax}^{25}$  ( $\mu\text{mol CO}_2 \text{ m}^{-2} \text{ s}^{-1}$ ) maximum carboxylation capacity of photosynthetic capacity at 25°C;  $R_{dark\_CO_2}^{25}$  ( $\mu\text{mol CO}_2 \text{ m}^{-2} \text{ s}^{-1}$ ), dark respiration ( $\text{CO}_2$  efflux) rate measured at 25°C;  $R_{dark\_O_2}$  ( $\mu\text{mol O}_2 \text{ m}_{LA}^{-2} \text{ s}^{-1}$ ), dark respiration ( $\text{O}_2$  consumption) rate measured at 20, 25, 30 or 35°C. The respiration flux values are area-based. <sup>ns</sup>=not significant. \* $P < 0.05$ . \*\* $P < 0.01$ . \*\*\* $P < 0.001$ . Significant effects are indicated in bold.



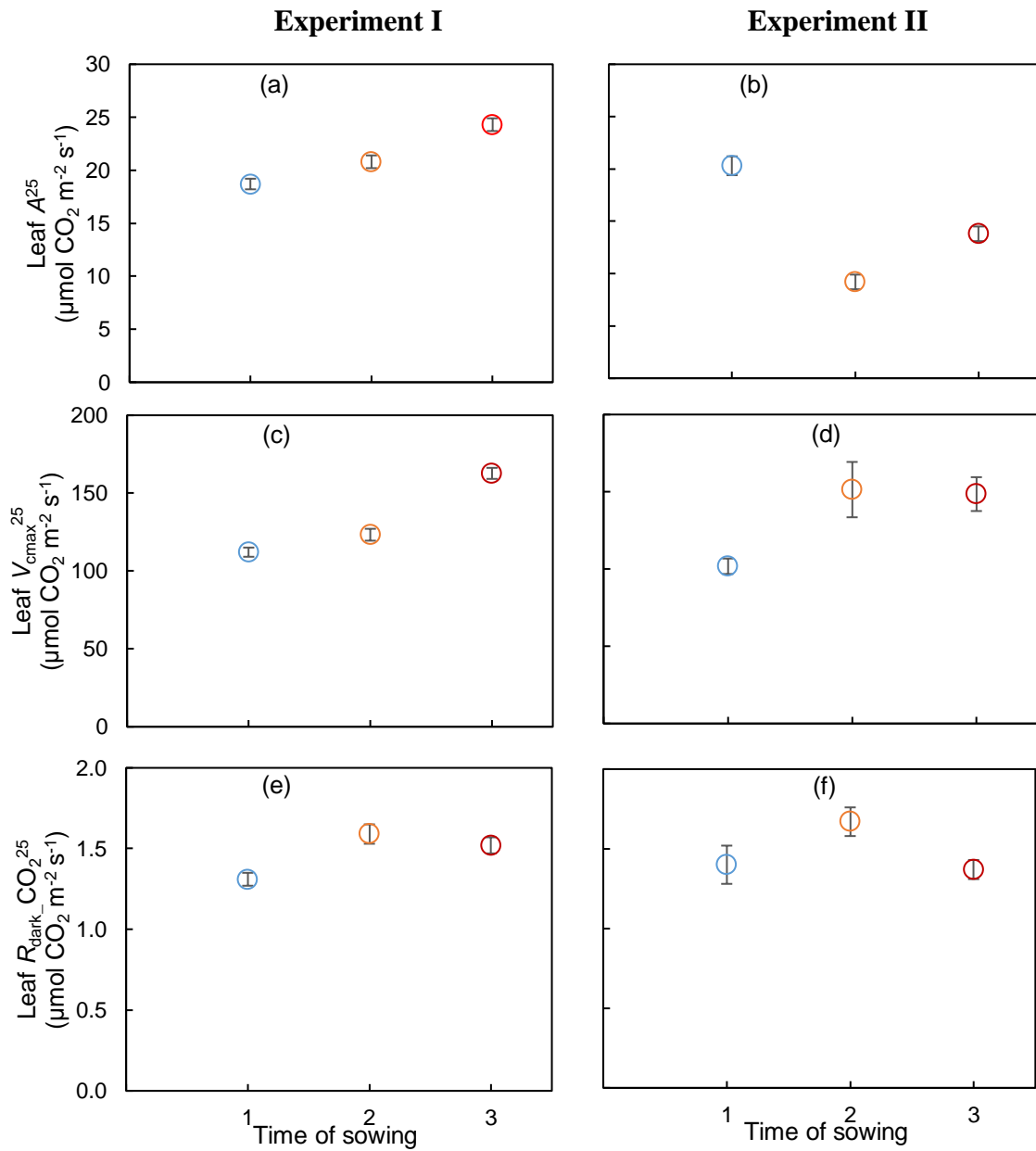


**Figure 1.** Mean rates of area-based net CO<sub>2</sub> assimilation rates at 25°C ( $A^{25}$ ), maximum carboxylation capacity of photosynthetic capacity ( $V_{\text{cmax}}^{25}$ ), and leaf dark respiration at 25°C taken as rate of CO<sub>2</sub> efflux ( $R_{\text{dark\_CO}_2}^{25}$ ) for six selected wheat genotypes. Genotypes were grown under three thermal regimes (by varying time of sowing, TOS) during 2017 (a, c and e) and 2018 (b, d and f). Values are the mean of four plants ( $\pm$ standard error of mean).

### Temperature responses of leaf $R_{\text{dark\_O}_2}$ across 20 wheat genotypes

Leaf  $R_{\text{dark\_O}_2}^{25}$  of the six selected genotypes were representative of the whole set of 20 genotypes (Fig. 2). Generally, leaf  $R_{\text{dark\_O}_2}^{25}$  reduced in TOS2 and TOS3 compared to TOS1 in Experiment I, whereas for 2018 there was no significant difference among the three TOS (Fig. 2). There was neither genotype effect nor genotype by TOS interaction on leaf  $R_{\text{dark\_O}_2}^{25}$  for the six or 20 genotypes (Table 2). However, leaf  $R_{\text{dark\_O}_2}$  of all 20 genotypes and at the other three measurement temperatures (20, 30 and 35°C) revealed differences which were not apparent with just the selected six genotypes at 25°C. For example, while there was no TOS effect on leaf  $R_{\text{dark\_O}_2}$  at 25°C in 2018, measurements at 20, 30 and 35°C showed highly significant differences among TOS (Fig. 3).

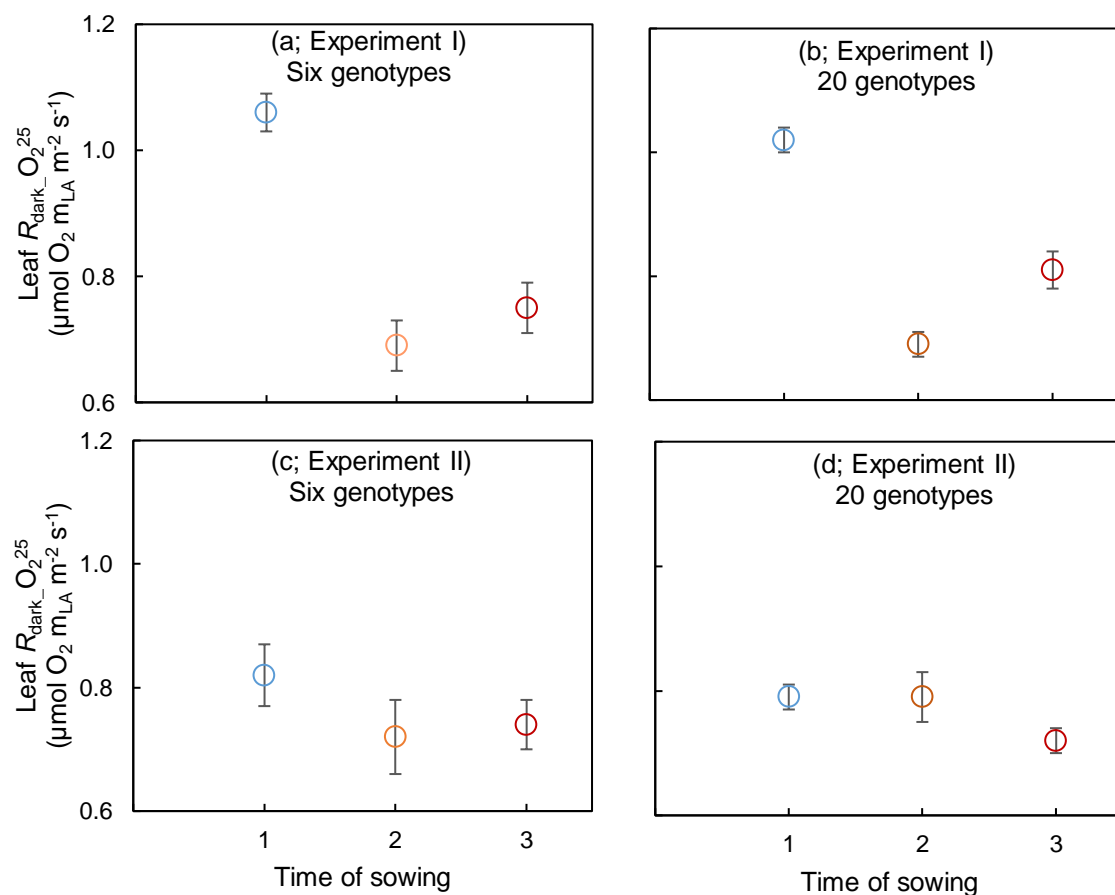


**Figure 2.** Mean rates of leaf dark respiration on O<sub>2</sub> consumption basis at 25°C ( $R_{\text{dark\_O}_2}^{25}$ ) for six selected and the whole set of 20 wheat genotypes. Genotypes were grown under three thermal regimes (by varying time of sowing, TOS) during 2017 (a, b) and 2018 (c, d). Values are the mean of four plants ( $\pm$ standard error of mean).

Regression of log transformed leaf  $R_{\text{dark\_O}_2}$  by measurement temperature showed substantial genotypic and TOS variation for both 2017 and 2018 (Fig. 3, Tables S4 and S5). For both experiments, TOS1 had higher  $R_{\text{dark\_O}_2}$  than TOS2 and TOS3 (Fig. 3), and significantly different slopes or intercepts from TOS2 and TOS3 (Table S6). In Experiment I, across all times of sowing,  $Q_{10}$  values of the different genotypes ranged from 2.03–2.64 (Table S4), and across all genotypes TOS1 exhibited the lowest  $Q_{10}$  (Fig. 3a). For 2018, the range of  $Q_{10}$  for the genotypes was 1.85–2.53 (Table S5). Across genotypes, TOS1 had a higher  $Q_{10}$  than TOS3 but not statistically different from TOS2 (Fig. 3b).

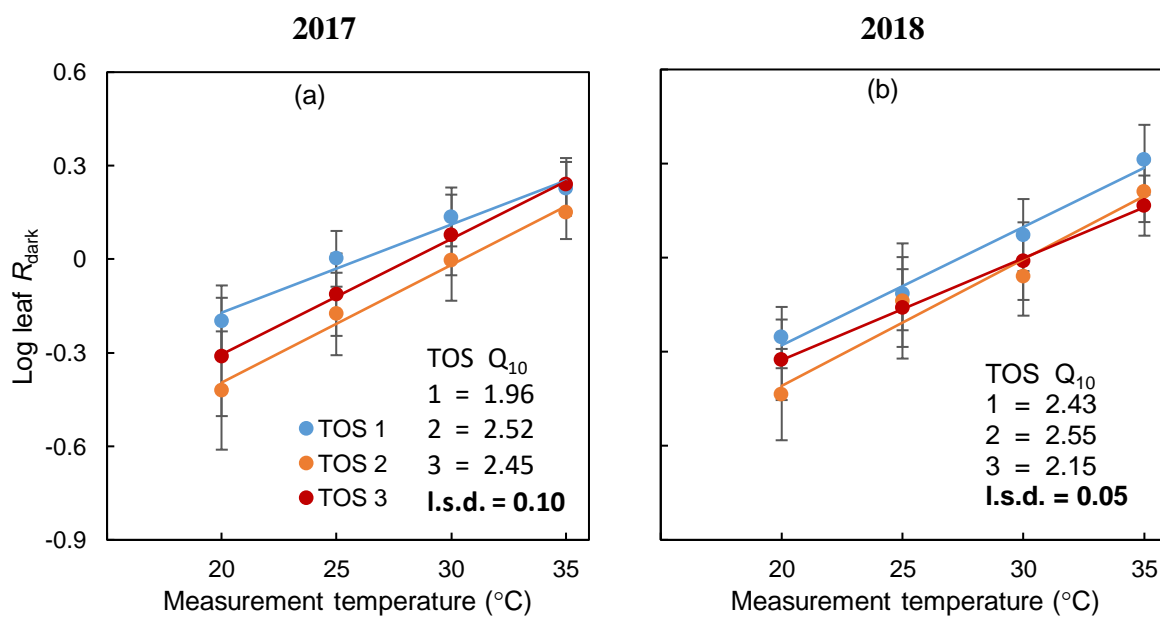


**Figure 3.** Mean temperature response of leaf dark respiration ( $\text{O}_2$  consumption; values shown on a log scale) expressed per leaf area ( $R_{\text{dark}}$ ) of 20 wheat genotypes grown under three thermal regimes (by varying time of sowing, TOS) during 2017 (a) and 2018 (b). Values are the means of four plants ( $\pm$ standard deviation) from each of 20 genotypes at the different TOS. Treatments (or TOS) are significantly different ( $P < 0.05$ ) if the difference in their  $Q_{10}$  values is greater than the indicated least significant difference (l.s.d.) value. Parameter estimates of the log-transformed instantaneous leaf  $R_{\text{dark}}$ -temperature responses are given in Table S6.

*Relationship of wheat leaf photosynthetic and respiratory traits with growth temperatures and other environmental factors*

For Experiment I,  $A^{25}$  and  $V_{cmax}^{25}$  were significantly associated with  $T_{max}$  during the 1-10 DBA and  $T_{min}$  of the 1-5 DBA (for  $A^{25}$ ) or 1-3 DBA (for  $V_{cmax}^{25}$ ; Fig. 4). Mean rate of  $A^{25}$  increased with increasing pre-anthesis growth temperature with the rate of the increase greater for night-time temperatures than day-time. Leaf  $R_{dark\_CO_2}^{25}$  was positively associated with anthesis  $T_{max}$  and  $T_{min}$  with close to 50% of the variation explained by the growth temperature. Including photosynthetically active radiation and/or solar radiation in the regression models of leaf  $A^{25}$  or  $R_{dark\_CO_2}^{25}$  with,  $T_{min}$  and  $T_{max}$  did not result in better goodness of fits than without the parameters included (data not shown). Leaf  $R_{dark\_O_2}^{25}$  was associated with  $T_{min}$  and  $T_{max}$  of the 1-3 DAA, decreasing with rise in growth temperature (Fig. 5). The relationship of  $R_{dark\_O_2}$  over the 1-3 DAA period was weaker with photosynthetically active radiation ( $r^2=0.33-0.40$ ), in a broader but similar range to that with solar radiation ( $r^2=0.44-0.69$ ) or all four environmental variables combined ( $r^2=0.54-0.69$ ).

For 2018, the strength of the associations of these leaf traits with  $T_{min}$  or  $T_{max}$  were of the order  $A^{25} > R_{dark\_CO_2}^{25} > R_{dark\_O_2}^{25}$ . The slopes and intercepts that describe the relationships of the leaf traits with  $T_{min}$  and  $T_{max}$  were significant and different. Leaf  $A^{25}$  and  $R_{dark\_O_2}$  decreased with  $T_{min}$  or  $T_{max}$ , while  $R_{dark\_CO_2}^{25}$  increased with  $T_{min}$  only (no significant relationship vs  $T_{max}$ ; Fig. 4 and 5). The slope of the  $A^{25}$  vs  $T_{min}$  or  $T_{max}$  regression was higher for  $T_{max}$  than  $T_{min}$ , whereas that for leaf  $R_{dark}^{25}$  was steeper for  $T_{min}$  than  $T_{max}$  (Fig. 4 and 5).

Across genotypes, TOS and experiments, multiple linear regression models with combined  $T_{min}$ ,  $T_{max}$ , photosynthetically active radiation and solar radiation of the 1-3DAA accounted for 72 and 25%, respectively, of the variation in wheat flag leaf  $A^{25}$ , and  $R_{dark\_CO_2}^{25}$ . For  $R_{dark\_O_2}$  (depending on the measurement temperature) the variation accounted for was 40-48% for all 20 genotypes or 39-64% for the six genotypes (Table S7).

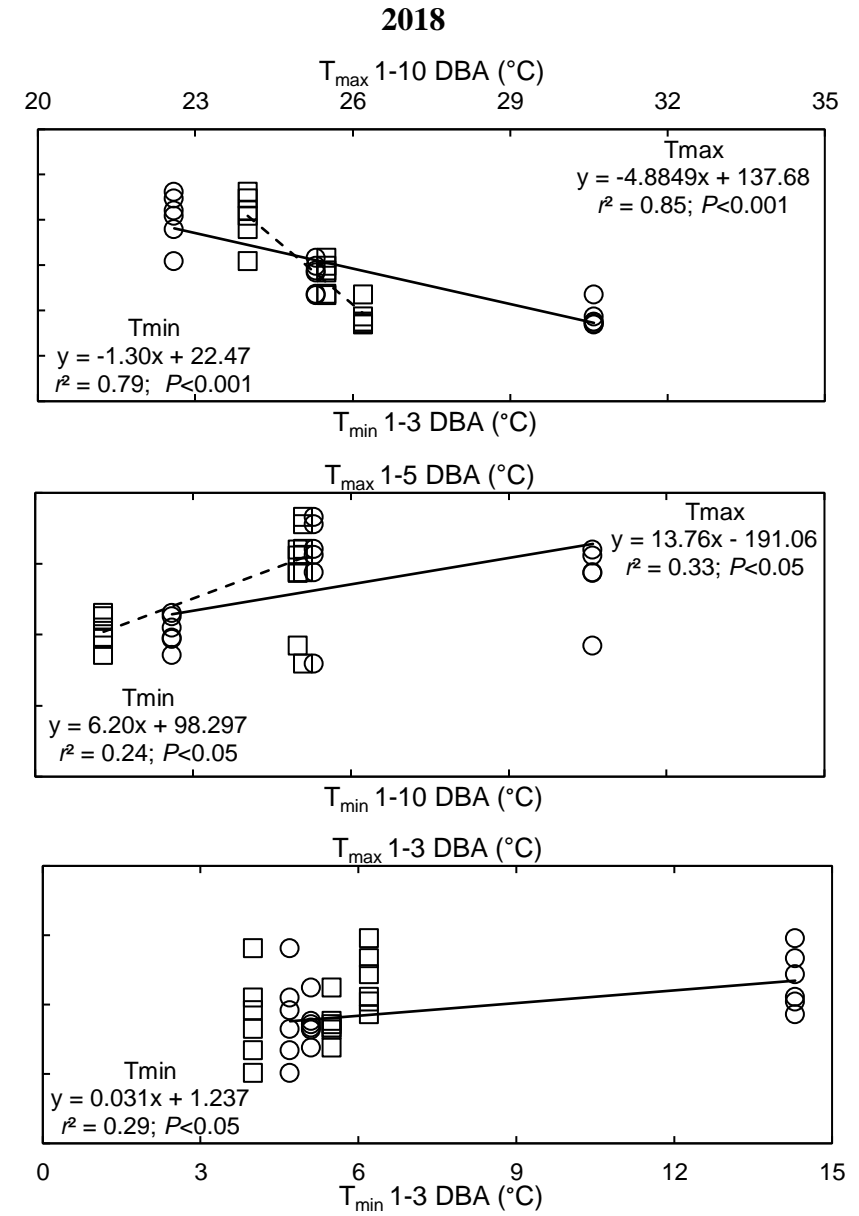
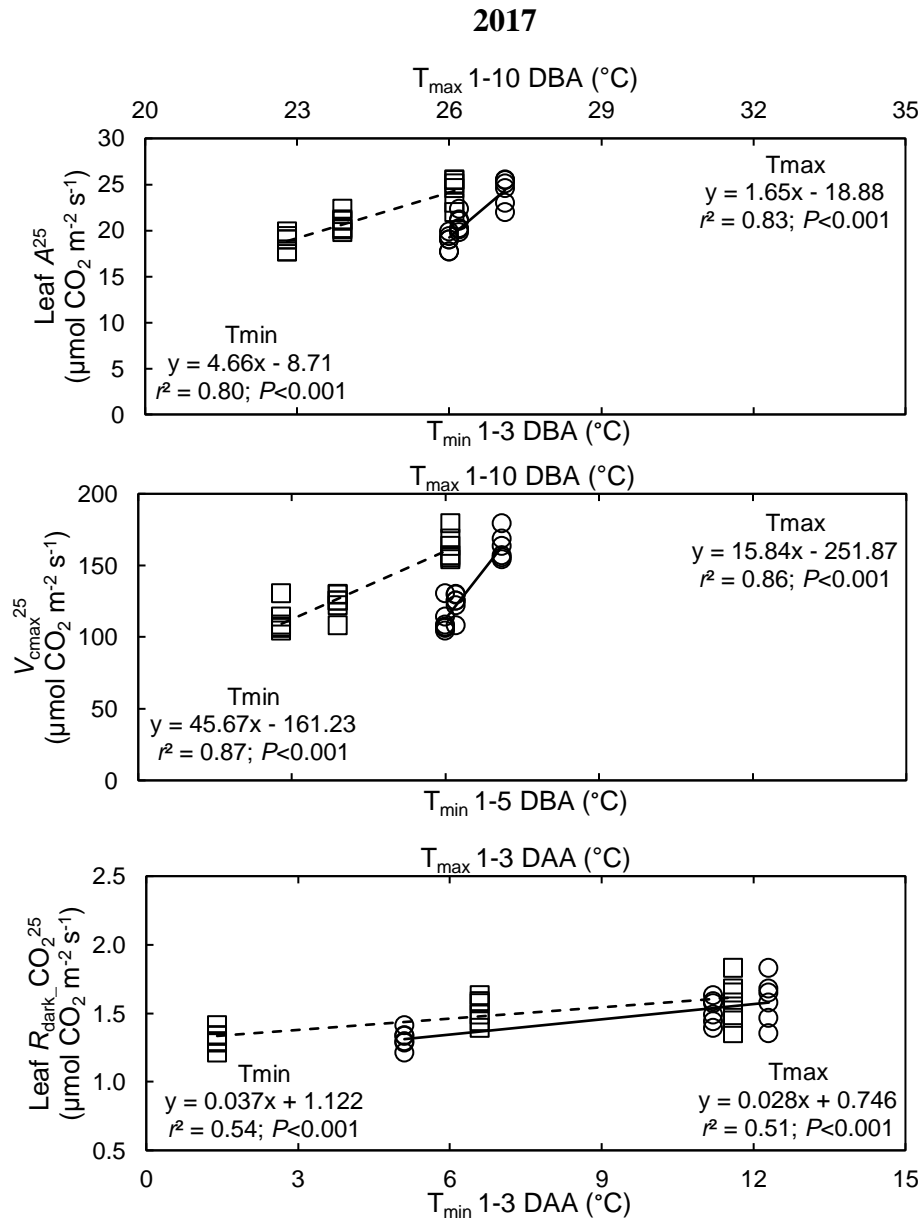


**Figure 4.** Relationship of mean area-based leaf net CO<sub>2</sub> assimilation rate ( $A^{25}$ ), maximum carboxylation capacity of photosynthetic capacity ( $V_{cmax}^{25}$ ) and rate of CO<sub>2</sub> efflux ( $R_{dark\_CO_2^{25}}$ ) at 25°C with average minimum temperature (open circles and solid lines) or maximum temperature (open squares and dashed lines) of period before 50% of plants had achieved anthesis (DBA) or period when 50% of plants were at anthesis (DAA) for 2017 (left panel) and 2018 (right panel). Note the different night and day periods on the primary and secondary x-axes.

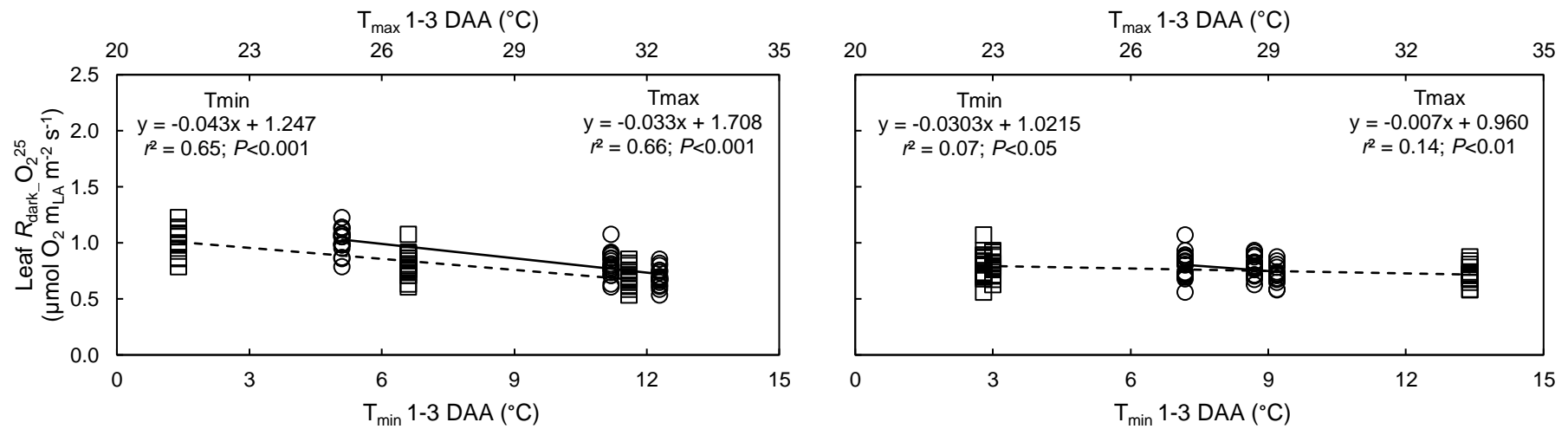


**Figure 5.** Relationship of rate of O<sub>2</sub> consumption at 25°C ( $R_{dark\_O_2^{25}}$ ) with average daily minimum temperature (open circles and solid lines) or maximum temperature (open squares and dashed lines) of the 1–3 day period when 50% of plants were at anthesis (DAA) for 2017 (left panel) and 2018 (right panel).

### *Acclimation of $R_{\text{dark\_CO}_2^{25}}:A^{25}$ and $R_{\text{dark\_CO}_2^{25}}:V_{\text{cmax}}^{25}$ among six wheat genotypes*

The asynchronous degree and/or direction of the response of  $R_{\text{dark\_CO}_2^{25}}$  and  $A^{25}$  or  $V_{\text{cmax}}^{25}$  to TOS resulted in significant changes in the ratios of  $R_{\text{dark\_CO}_2^{25}}:A^{25}$  and  $R_{\text{dark\_CO}_2^{25}}:V_{\text{cmax}}^{25}$  with change in TOS in both Experiments (Table 3). The general pattern was one of consistent reductions in the ratios when comparing TOS3 vs TOS2, and less so for TOS3 vs TOS1 or TOS2 vs TOS1. In Experiment I,  $R_{\text{dark\_CO}_2^{25}}:A^{25}$  and  $R_{\text{dark\_CO}_2^{25}}:V_{\text{cmax}}^{25}$  reduced by 19 and 31%, respectively, from TOS2 to TOS3 (Table 3). In 2018,  $R_{\text{dark\_CO}_2^{25}}:A^{25}$  of TOS3 was 52% lower compared to TOS2. Between TOS3 and TOS1, the differences in the ratios varied, from significant reduction for  $R_{\text{dark\_CO}_2^{25}}:V_{\text{cmax}}^{25}$  irrespective of the experiment, to marginally different for  $R_{\text{dark\_CO}_2^{25}}:A^{25}$  in 2017 and no difference for  $R_{\text{dark\_CO}_2^{25}}:A^{25}$  in 2018 (Table 3).

### *Leaf trait-trait relationships among six wheat genotypes*

There were significant variations in leaf N and LMA in both experiments with genotype or TOS (Table S8). In 2017 and 2018, bivariate relationships between leaf physiological traits ( $A^{25}$ ,  $R_{\text{dark\_CO}_2^{25}}$  and  $R_{\text{dark\_O}_2^{25}}$ ) and chemical ( $N_{\text{area}}$  and  $N_{\text{mass}}$ ) or morphological (LMA) traits, expressed on either an area- or mass-basis, were not significantly altered by TOS (in terms of differences in both slope and intercepts from TOS1). The only exceptions were: mass-based  $R_{\text{dark\_O}_2^{25}}$  vs LMA of TOS2 in 2017 (Table S9); area-based  $A^{25}$  vs  $N_{\text{area}}$  for TOS2 in 2018; and mass-based  $R_{\text{dark\_CO}_2^{25}}$  vs LMA of TOS2 in 2017 (Table S10). In 2017 and 2018, and across both experiments, singular regressions of LMA,  $N_{\text{area}}$ ,  $N_{\text{mass}}$  or  $V_{\text{cmax}}^{25}$  with  $A^{25}$ ,  $R_{\text{dark\_CO}_2^{25}}$  or  $R_{\text{dark\_O}_2^{25}}$  were in most cases significant but also weak ( $r^2=0.05-0.29$ ). Across experiments, the strongest bivariate relationship (in terms of  $r^2$ ) for  $A^{25}$  or  $R_{\text{dark\_CO}_2^{25}}$  was with LMA when  $A^{25}$  or  $R_{\text{dark\_CO}_2^{25}}$  was expressed per leaf area (Fig. S1-S3). Leaf N,  $V_{\text{cmax}}^{25}$  and LMA were better correlated with  $A^{25}$ ,  $R_{\text{dark\_CO}_2^{25}}$  or  $R_{\text{dark\_O}_2^{25}}$  when combined than when treated independently (Table S11). However, the addition of  $V_{\text{cmax}}^{25}$  to regressions of  $R_{\text{dark}}^{25}$  vs leaf N and LMA did not significantly improve the relationships. For leaf  $A^{25}$ , correlations with LMA and N either independently or combined were stronger on an area basis than on a mass basis. Whereas for  $R_{\text{dark\_CO}_2^{25}}$  and  $R_{\text{dark\_O}_2^{25}}$  there was no clear difference between area- and mass-based relationships (Table S11).

**Table 3.** Back-transformed means of the ratios of leaf dark respiration rates at 25°C (CO<sub>2</sub> efflux,  $R_{\text{dark\_CO}_2^{25}}$ ) to net, area-based, CO<sub>2</sub> assimilation rates measured at 25°C ( $A^{25}$ ) and maximum carboxylation capacity of photosynthesis at 25°C ( $V_{\text{cmax}}^{25}$ ) of six wheat genotypes grown under three thermal regimes (by varying time of sowing, TOS) during 2017 and 2018.  $n=4$ .

Time of sowing	2017		2018	
	$R_{\text{dark\_CO}_2^{25}}:A^{25}$	$R_{\text{dark\_CO}_2^{25}}:V_{\text{cmax}}^{25}$	$R_{\text{dark\_CO}_2^{25}}:A^{25}$	$R_{\text{dark\_CO}_2^{25}}:V_{\text{cmax}}^{25}$
1	0.072	0.012	0.075	0.015
2	0.078	0.013	0.215	0.013
3	0.063	0.009	0.104	0.010
Mean	0.071	0.012	0.132	0.013
l.s.d ( $F$ pr.)				
TOS	<b>0.010*</b>	<b>0.001***</b>	<b>0.044***</b>	<b>0.005*</b>
Other terms				
Genotype	0.014 <sup>ns</sup>	0.002 <sup>ns</sup>	0.063 <sup>ns</sup>	0.007 <sup>ns</sup>
Genotype x TOS	0.024 <sup>ns</sup>	0.003 <sup>ns</sup>	0.108 <sup>ns</sup>	0.012 <sup>ns</sup>

Levels of significant differences for the treatment terms are indicated by <sup>ns</sup>=not significant,  $P>0.05$ ; \* $P < 0.05$ ; \*\*\* $P < 0.001$ .



*Grain yield at harvest and links with leaf traits at anthesis*

Grain yield varied ( $P < 0.001$ ) with TOS for Experiment I, being 5.1, 5.3 and 4.8 t ha<sup>-1</sup> for TOS1, TOS2 and TOS3, respectively, but not for 2018 ( $P = 0.102$ ) with yields of 2.4 (TOS1), 2.5 (TOS2) and 2.6 t ha<sup>-1</sup> (TOS3). The relative change in yield for 2017 (range of -24 to +36%) was less than that of 2018 (-25 to +105%). Ranking of genotypes based on their relative change in mean yields from TOS1 for both TOS2 and TOS3 were similar for 2017 and 2018 (Fig. 6). Spearman's Rank correlations of the relative change in yield were 0.84 ( $P < 0.001$ ) for 2017 and 0.93 ( $P < 0.001$ ) for 2018. Changes in individual leaf traits did not correlate with changes in yield in response to growth under warmer conditions in 2017 or 2018 (Fig. S4).

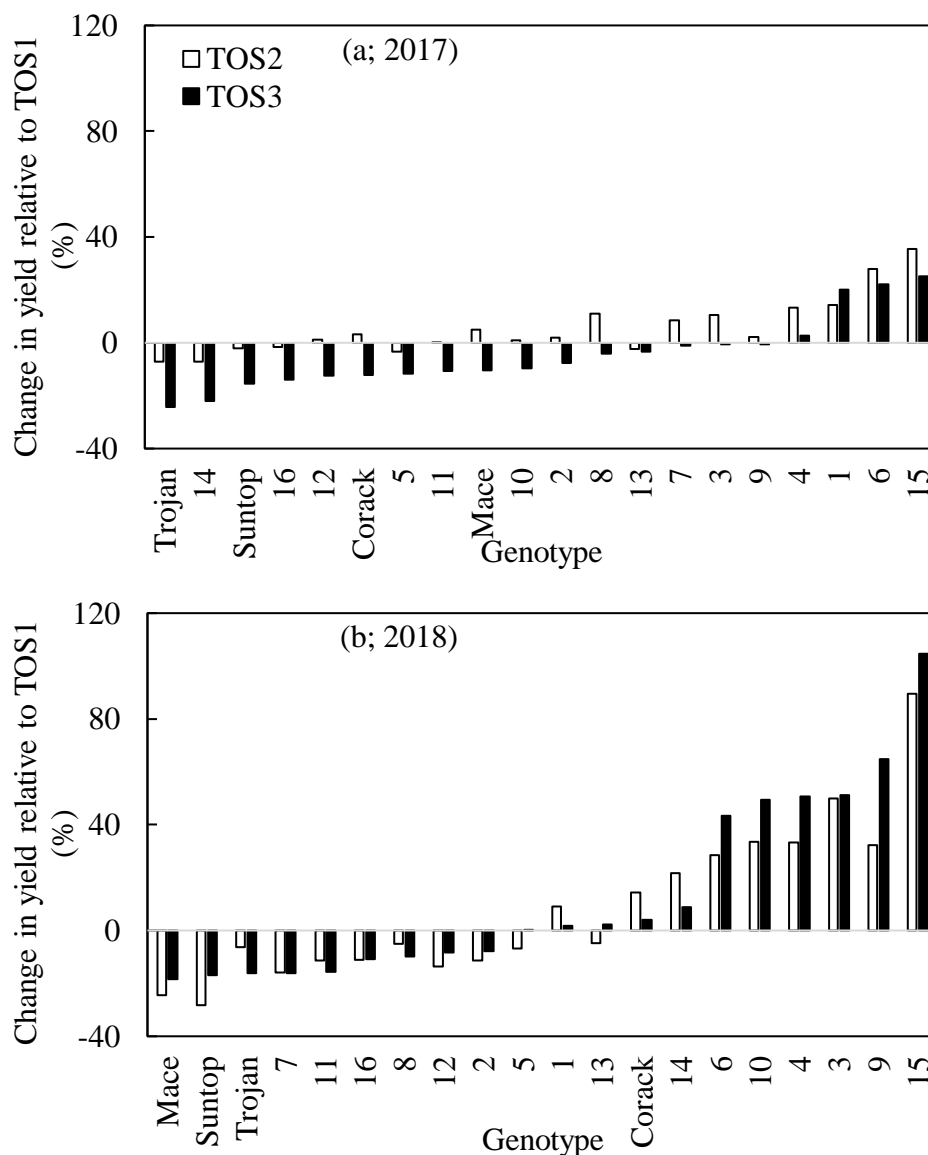


**Figure 6.** Relative change in mean yield of 20 genotypes for time of sowing (TOS) 2 (white bars) and TOS3 (black bars) compared to TOS1 in 2017 (a) and 2018 (b). Spearman's Rank correlations of the relative change in yield of TOS2 and TOS3 from TOS1 were 0.84 ( $P < 0.001$ ) for 2017 and 0.93 ( $P < 0.001$ ) for 2018.

## Discussion

We used time of sowing (TOS) as a proxy for generating different thermal environments for field-grown wheat (Table 1 and S1) and tested if responses of temperature-normalized values of photosynthetic CO<sub>2</sub> uptake ( $A^{25}$  and  $V_{cmax}^{25}$ ) and leaf dark respiration – measured as both CO<sub>2</sub> release and O<sub>2</sub> uptake ( $R_{dark}$ ) – were consistent with generalized patterns of thermal acclimation. We observed that for the CO<sub>2</sub>-exchange traits, warming (i.e. later dates of TOS) did not result in our hypothesized decreases in flag leaf  $A^{25}$ ,  $V_{cmax}^{25}$  or  $R_{dark}^{25}$  (Fig. 1). Rather, these traits increased and/or remained unchanged response to warming with later sowing. The only exception was the reduced  $A^{25}$  at later TOS in 2018; however, in that case, the reduction in  $A^{25}$  was not due to a direct effect of warming on photosynthetic metabolism, but rather was a consequence of reduced stomatal conductance (with TOS 2 and 3 stomatal conductance being 56 and 33% less than that of TOS1, respectively) reflecting limitations in water availability during the few days of measurements in 2018 (Supplementary Table S3). Differences in the temperature sensitivities of the three CO<sub>2</sub> exchange traits meant that the balance between  $R_{dark\_CO_2}^{25}$  and  $A^{25}$  or  $V_{cmax}^{25}$  was altered by warming, with consistently lower  $R_{dark\_CO_2}^{25}:A^{25}$  and  $R_{dark\_CO_2}^{25}:V_{cmax}^{25}$  at the warmest TOS relative to the earlier, cooler TOS (Table 3). Importantly, in contrast to the results for  $R_{dark\_CO_2}^{25}$ , O<sub>2</sub>-based measures of leaf  $R_{dark}$  were lower at TOS2/3 compared with TOS1 (Fig. 2 and 3) - a result that supported our hypothesis that acclimation to warming is characterised by a downward shift in the  $R_{dark}$ -temperature response curve. The divergent temperature responses of CO<sub>2</sub>- and O<sub>2</sub>-based  $R_{dark}$  suggests different substrates drive respiratory processes in leaves of warmer-grown plants, as changes in the ratio of CO<sub>2</sub> efflux to O<sub>2</sub> uptake (i.e. respiratory quotient, RQ) are known to occur in response to shifts in the type of substrates used by respiratory metabolism (Dieuaide-Noubhani, Canioni, & Raymond, 1997; Lambers, Robinson, & Ribas-Carbo, 2005). Interestingly, there were only weak, albeit significant, relationships between the leaf gas exchange and chemical/structural traits, with these relationships being unaffected by warming (Fig. S1-S3). We have previously reported similar weak relationships of  $R_{dark\_O_2}$  with

LMA,  $N_{\text{area}}$  and  $N_{\text{mass}}$  in wheat leaves across multiple genotypes from both glasshouse and field experiments (Coast et al., 2019). The weak  $R_{\text{dark}}$ -N relationships indicates that rates of  $R_{\text{dark}}$  are not contingent on increases in N concentration *per se* (Atkinson, Hellicar, Fitter, & Atkin, 2007) or are necessarily directly linked with rates of protein turnover. The varied TOS responses of wheat flag leaf gas exchange at anthesis were not reflective of overall crop performance, in terms of yield at harvest maturity (Fig. S4).

The use of TOS to investigate wheat responses to high growth temperature was probably confounded by changes in other environmental variables. We note that: (1) agronomic traits (days to flowering and plant height at harvest) were influenced by TOS (data not shown); (2) that such traits could have been due to not just temperature but also differences in photoperiod, input of solar radiation and soil temperature; and (3) that such trait differences could influence leaf and whole plant carbon dynamics.

#### *Carbon-based leaf physiological processes did not acclimate to warming*

Our results did not support our working hypothesis that acclimation of leaf  $\text{CO}_2$  exchange traits, measured at a common temperature of  $25^\circ\text{C}$  (i.e.  $A^{25}$ ,  $V_{\text{cmax}}^{25}$  and  $R_{\text{dark\_CO}_2^{25}}$ ), would be lower in leaves experiencing higher growth temperatures (i.e. TOS2/3) than in leaves developed under cooler conditions (i.e. TOS 1; Fig. 1). In support of this finding, leaf  $\text{CO}_2$  exchange also did not acclimate to night-time warming in field-grown wheat (Impa et al., 2019). By contrast, previous studies have reported lower rates of temperature-normalized  $\text{CO}_2$  exchange in warm vs cold acclimated plants across a range of species (Atkin & Tjoelker, 2003; Berry & Bjorkman, 1980; Way & Yamori, 2014), but, more widely, the leaf physiology responses of crop plants to elevated temperatures in field experiments have been inconsistent (Cai et al., 2020; Cai et al., 2018; Zheng et al., 2018; Zhou et al., 2018), suggesting that crops do not always exhibit classical thermal acclimation responses in the field. While the reason(s) for the disparity in acclimation responses of crop plants is unclear, it is likely that differences in the warming techniques, degree and duration of warming used in the field might be factors. For example, in experiments where warming is imposed by heating only the air around leaves or the crop canopy [e.g. by infrared radiators or with T-FACE (temperature with free-air  $\text{CO}_2$  enrichment)], warming is restricted to the above-ground part of the plant, not the whole plant. By contrast, when varying TOS, both air and soil temperature increase

simultaneously, likely promoting changes in growth and carbon demand of above- and below-ground tissues. Moreover, use of TOS as a warming treatment introduces other variables (e.g. different day lengths and input of solar radiation) that may, in themselves, influence rates of leaf gas exchange, reduce the period of vegetative development and affect source activities. Seasonal changes in day length can influence the temperature responses of leaf biochemical processes (Stinziano, Way, & Bauerle, 2018; Yamaguchi, Nakaji, Hiura, & Hikosaka, 2016). Thus, there is a need to disentangle the effect of temperature from changes in day length and solar radiation.

Why were temperature-normalized rates of CO<sub>2</sub> exchange higher in TOS2/3 plants compared to their TOS1 counterparts (Fig. 1, Table 2)? Later sowing is associated with warmer days and longer photoperiods – conditions that increase the rate of development of sink tissues (i.e. meristematic regions of shoots and roots) in wheat canopies (Angus, Mackenzie, Morton, & Schafer, 1981; Baker & Gallagher, 1983; Slafer & Rawson, 1996). This increase in sink tissue development could increase the demand for photosynthetically fixed carbon from source leaves creating a positive feedback effect on  $A^{25}$  and  $V_{cmax}^{25}$  (Asao & Ryan, 2015; King, Wardlaw, & Evans, 1967; Pinkard, Eyles, & O'Grady, 2011). Faster developmental rates in sink tissues would also increase demand for respiratory products (e.g. ATP, NADH and carbon skeletons) in source leaves – products needed to fuel higher rates of amino acid and sucrose synthesis/export (Bouma, De Visser, Van Leeuwen, De Kock, & Lambers, 1995; Edwards, Roberts, & Atwell, 2012; Li et al., 2017). Increased photosynthetic capacity (as indicated by higher  $V_{cmax}^{25}$ ) could also increase the demand for respiratory ATP needed to support processes such as protein turnover and maintenance of ion gradients in source leaves (Atkin et al., 2017; Fatichi, Leuzinger, & Körner, 2014; Lambers et al., 2005). Together, such factors – which point to a tight coupling of metabolism in source and sink tissues of field grown wheat - may explain why rates of CO<sub>2</sub> exchange were higher at TOS2/3 than at TOS1.

Along with the finding that rates of CO<sub>2</sub> exchange increased with increasing TOS, we observed a positive relationship of leaf photosynthetic capacity and  $R_{dark\_CO_2}$  with the recent  $T_{min}$  and  $T_{max}$  values experienced by plants at anthesis (Fig. 4). Global observed trends and model projections show greater increases in land surface  $T_{min}$  than  $T_{max}$  (Vose, Easterling, & Gleason, 2005), with the increase in  $T_{min}$  being more strongly related to global yield decline of major crops than increases in  $T_{max}$  (García, Dreccer, Miralles, & Serrago, 2015; García, Serrago,

Dreccer, & Miralles, 2016; Peng et al., 2004). The  $T_{\min}$  during anthesis may act to stimulate leaf  $R_{\text{dark\_CO}_2}$  by altering biosynthetic processes such as rates of protein turnover and costs associated with sucrose export, increasing carbon loss in source leaves and reducing carbohydrate translocation from leaves to sink organs, with negative effects on plant growth and yield (Sadok & Jagadish, 2020). A recent analysis of metabolite profiles of leaves of wheat exposed to high  $T_{\min}$  showed increased concentrations of tricarboxylic acid cycle related metabolites, which support increased rates of leaf  $R_{\text{dark\_CO}_2}$  (Impa et al., 2019).

*The balance of  $R_{\text{dark\_CO}_2}^{25}$  to  $A^{25}$  or  $V_{\text{cmax}}^{25}$  was reduced by warming*

The processes of carbon release by leaf respiration and carbon uptake by photosynthesis are often correlated (Loveys et al., 2003; Reich et al., 1998; Whitehead et al., 2004). This reflects a physiological interdependence of the two processes (Hurry et al., 2005; Kromer, 1995; Way & Yamori, 2014), such as the dependence of respiratory metabolism on photosynthesis for substrates, the demands for ATP associated with exporting assimilates, and the need for respiration-generated energy to maintain photosynthetic activity including sucrose synthesis and transport or phloem loading (Bouma et al., 1995). Based on these observations, several studies have assumed that the temperature-normalized ratios of  $R_{\text{dark\_CO}_2}$  to  $A$ , and by extension  $V_{\text{cmax}}$ , should be constant among plants experiencing a range of different growth temperatures. This assumption is incorporated in some Earth System modelling frameworks such as MOSES-TRIFFID (now JULES), CLM and Century (Cox, 2001; Melillo et al., 1993; Oleson et al., 2013). However, temperature-normalized values of leaf  $R_{\text{dark\_CO}_2}$ ,  $A$  and  $V_{\text{cmax}}$  may not acclimate to sustained warming to the same degree. These differences would alter the balance between  $R_{\text{dark\_CO}_2}^{25}$  and  $A^{25}$  ( $R_{\text{dark\_CO}_2}^{25}:A^{25}$ ) or  $R_{\text{dark\_CO}_2}^{25}$  and  $V_{\text{cmax}}$  ( $R_{\text{dark\_CO}_2}^{25}:V_{\text{cmax}}^{25}$ ). In our study, the range of  $R_{\text{dark\_CO}_2}^{25}:V_{\text{cmax}}^{25}$  for TOS1 was 0.012–0.015, values that are consistent with the assumed  $R_{\text{dark\_CO}_2}^{25}:V_{\text{cmax}}^{25}$  value (0.015) used in JULES and other ESM, but considerably lower than the mean for  $C_3$  herbs/grasses (0.078) reported for plants growing in natural ecosystems across the globe (Atkin et al., 2015). Our findings that  $R_{\text{dark\_CO}_2}^{25}:A^{25}$  and  $R_{\text{dark\_CO}_2}^{25}:V_{\text{cmax}}^{25}$  were lower in the warmest thermal regime (i.e. TOS3; Table 3) are, however, in agreement with the global pattern (Atkin et al., 2015) and that observed in cucumber and tomato (Ikkonen, Shibaeva, & Titov, 2018). Moreover, our results showed  $R_{\text{dark\_CO}_2}^{25}:A^{25}$  increasing in leaves experiencing water-deficit (as shown by the

higher  $R_{\text{dark\_CO}_2^{25}}:A^{25}$  ratios in plants that had low stomatal conductance in 2018, Table 3), yet  $R_{\text{dark\_CO}_2^{25}}:V_{\text{cmax}}^{25}$  was unchanged under these conditions. This suggests that variations in leaf respiration are more closely tied to variations in Rubisco capacity, rather than to the limits of net photosynthesis.

#### *Oxygen based measure of leaf respiration acclimated to warming*

In contrast to the growing number of studies that have investigated acclimation of  $R_{\text{dark\_CO}_2}$  to warming by a range of field-grown plants in natural and managed environments, studies on acclimation of  $R_{\text{dark\_O}_2}$  to warming by field-grown plants – including crops - have been limited. This is probably because techniques for measuring leaf  $R_{\text{dark\_O}_2}$  are generally cumbersome and low throughput. To overcome this, we used a high-throughput technique described by Scafaro et al. (2017) – and used for wheat (Coast et al., 2019), *Arabidopsis thaliana* (O'Leary et al., 2017) and *Eucalyptus camaldulensis* (Asao et al., 2020) - to measure wheat flag leaf  $R_{\text{dark\_O}_2}$  at four temperatures over the 20-35°C range. In addition to allowing comparisons of temperature-normalized (i.e. at 25°C) rates of  $R_{\text{dark\_O}_2}$ , this enabled us to test whether the slope and elevation of the short-term response of leaf  $R_{\text{dark\_O}_2}$  in 20 wheat genotypes was affected by growth environment in two experiments. The results showed that wheat flag leaf  $R_{\text{dark\_O}_2}$  decreased with increasing growth temperature (Fig. 2) – a result that contrasted with the responses of  $R_{\text{dark\_CO}_2^{25}}$  (see above and Fig. 1). The leaf  $R_{\text{dark\_O}_2}$  response in our study is consistent with expectations for  $R_{\text{dark\_O}_2}$  (see reviews by Atkin & Tjoelker, 2003; Slot & Kitajima, 2015) and earlier observations on how rates of CO<sub>2</sub>-based leaf  $R_{\text{dark}}$  of tree species respond to warming under field settings (Drake et al., 2015; Reich et al., 2016). In both experiments within our study, flag leaves which developed under the warmer conditions of TOS2 and TOS3 generally exhibited lower rates of leaf  $R_{\text{dark\_O}_2}$  across a range of measuring temperatures (i.e. Type II acclimation; Atkin and Tjoelker, 2003), with the exception being TOS3 of 2018 where Type I acclimation (i.e. warm-grown plants exhibit a lower  $Q_{10}$  value than their cold-grown counterparts; Atkin and Tjoelker, 2003) was observed (Fig. 3). Type II acclimation is the more common type of acclimation for leaves that develop under warmer conditions (Slot & Kitajima, 2015), and is likely the result of changes in mitochondrial number, structure and/or protein composition (Atkin, Bruhn, & Tjoelker, 2005). On the other hand, with Type I acclimation (i.e. declining  $Q_{10}$ ), the reduction in  $R_{\text{dark\_O}_2}$  at high measuring

temperatures is likely due to underlying factors regulating respiratory flux, including depletion of available substrate and/or reduction in turnover of ATP to ADP (Atkin & Tjoelker, 2003). On average, the  $Q_{10}$  (the short-term temperature response) of  $R_{\text{dark\_O}_2}$  at TOS1 in both experiments were close to the mean reported for crops including field beans and wheat (2.3; Larigauderie & Körner, 1995) – being 2.0 and 2.4 in 2017 and 2018, respectively.

*The varied temperature responses of CO<sub>2</sub> and O<sub>2</sub> based leaf respiration suggests switch in respiratory substrates*

As noted above, differences in the growth temperature responses of  $R_{\text{dark\_CO}_2}$  (no acclimation, increasing with warming; Fig. 1) and  $R_{\text{dark\_O}_2}$  (acclimation, decreasing with warming; Fig. 2 and 3) suggest changes in the substrate used by respiration. In plants, the main respiratory substrates are soluble carbohydrates (Plaxton & Podestá, 2006), with oxidation of glucose resulting in a respiratory quotient (RQ, the molar ratio of CO<sub>2</sub> produced per O<sub>2</sub> consumed during  $R_{\text{dark}}$ ) of 1.0. Under stress and conditions that reduce rates of photosynthetic fixation of carbon, the source of respiratory substrate can shift from carbohydrates to other stored organic compounds (Araújo, Tohge, Ishizaki, Leaver, & Fernie, 2011). We observed consistent increases in RQ with warming (when comparing late vs early TOS) in both experiments. Increases in RQ point to a switch to more oxidised substrates such as organic acids. Further work is needed to investigate the nature of the respiratory substrate used during warming in crops. This would involve concurrent measurements of gas exchange (O<sub>2</sub> and CO<sub>2</sub> fluxes, which is difficult) and complementary estimates of respiratory substrate pool sizes. However, current techniques for such measurements are cumbersome (e.g. membrane inlet mass spectrometers and the cavity-enhanced Raman multi-gas spectrometry (Keiner, Frosch, Massad, Trumbore, & Popp, 2014), limiting their application in large-scale field studies.

In conclusion, our study has shown that the response of leaf gas exchange to warming is not fixed in field-grown wheat. The oxygen-based measurement of leaf respiration,  $R_{\text{dark\_O}_2}$ , acclimated to warming. By contrast, the CO<sub>2</sub>-based measure of  $R_{\text{dark}}$ ,  $R_{\text{dark\_CO}_2}$ , did not acclimate but instead increased with TOS/warming, suggesting that the substrates used by leaf respiration changed with TOS/warming. These varied physiological responses to warming

have implications for crop models that assume a fixed temperature response of leaf physiological processes.

## Acknowledgements

The authors have no conflicts of interest to declare. The authors are grateful for the support of the ARC Centre of Excellence in Plant Energy Biology (CE140100008), and the Grains Research and Development Corporation National Wheat Heat Tolerance Project US00080. We thank Claire Brown and Amy Smith of Birchip Cropping Group, Victoria for managing field trials in Victoria and Sabina Yasmin of The University of Sydney Plant Breeding Institute, Narrabri for data management. We are also grateful to the farmers who generously provided us with field sites for 2017 and 2018.

## References

- Angus JF, Mackenzie DH, Morton R, Schafer CA.** 1981. Phasic development in field crops II. Thermal and photoperiodic responses of spring wheat. *Field Crops Research* **4**, 269–283.
- Anna FA, Logan DC, Atkin OK.** 2006. On the developmental dependence of leaf respiration: responses to short- and long-term changes in growth temperature. *American Journal of Botany* **93**, 1633–1639.
- Araújo WL, Tohge T, Ishizaki K, Leaver CJ, Fernie AR.** 2011. Protein degradation—an alternative respiratory substrate for stressed plants. *Trends in Plant Science* **16**, 489–498.
- Asao S, Hayes L, Aspinwall MJ, Rymer PD, Blackman C, Bryant CJ, Cullerne D, Egerton JJG, Fan Y, Innes P, Millar AH, Tucker J, Shah S, Wright IJ, Yvon-Durocher G, Tissue D, Atkin OK.** 2020. Leaf trait variation is similar among genotypes of *Eucalyptus camaldulensis* from differing climates and arises as plastic response to season rather than water availability. *New Phytologist* **227**, 780–793.
- Asao S, Ryan MG.** 2015. Carbohydrate regulation of photosynthesis and respiration from branch girdling in four species of wet tropical rain forest trees. *Tree Physiology* **35**, 608–620.
- Asseng S, Ewert F, Rosenzweig C, Jones JW, Hatfield JL, Ruane AC, Boote KJ, Thorburn PJ, Rötter RP, Cammarano D, Brisson N.** 2013. Uncertainty in simulating wheat yields under climate change. *Nature Climate Change* **3**, 827–832.
- Athanasiou K, Dyson BC, Webster RE, Johnson GN** 2010. Dynamic acclimation of photosynthesis increases plant fitness in changing environments. *Plant Physiology*, **152**, 366–373.



- Atkin O, Bruhn D, Tjoelker M.** 2005. Response of plant respiration to changes in temperature: mechanisms and consequences of variations in  $Q_{10}$  values and acclimation. In: Lambers H, Ribas-Carbo M, eds. *Plant Respiration: from cell to ecosystem*. Dordrecht: Springer Netherlands, 95–135.
- Atkin OK, Bahar NHA, Bloomfield KJ, Griffin KL, Heskell MA, Huntingford C, de la Torre AM, Turnbull MH.** 2017. Leaf respiration in terrestrial biosphere models. In: Tcherkez G, Ghashghaie J, eds. *Plant respiration: metabolic fluxes and carbon balance*. Cham, Switzerland: Springer Nature, 109–145.
- Atkin OK, Bloomfield KJ, Reich PB, Tjoelker MG, Asner GP, Bonal D, . . . Zaragoza-Castells J.** 2015. Global variability in leaf respiration in relation to climate, plant functional types and leaf traits. *New Phytologist* **206**, 614–636.
- Atkin OK, Evans JR, Siebke K.** 1998. Relationship between the inhibition of leaf respiration by light and enhancement of leaf dark respiration following light treatment. *Australian Journal of Plant Physiology* **25**, 437–443.
- Atkin OK, Tjoelker MG.** 2003. Thermal acclimation and the dynamic response of plant respiration to temperature. *Trends in Plant Science* **8**, 343–351.
- Atkinson LJ, Hellicar MA, Fitter AH, Atkin OK.** 2007. Impact of temperature on the relationship between respiration and nitrogen concentration in roots: an analysis of scaling relationships,  $Q_{10}$  values and thermal acclimation ratios. *New Phytologist* **173**, 110–120.
- Azcon-Bieto J, Day DA, Lambers H.** 1983. The regulation of respiration in the dark in wheat leaf slices. *Plant Science Letters* **32**, 313–320.
- Badger MR, Collatz GJ.** 1977. Studies on the kinetic mechanism of ribulose-1, 5-bisphosphate carboxylase and oxygenase reactions, with particular reference to the effect of temperature on kinetic parameters. *Carnegie Institute of Washington Yearbook* **76**, 355–361.
- Baker CK, Gallagher JN.** 1983. The development of winter wheat in the field. 2. The control of primordium initiation rate by temperature and photoperiod. *The Journal of Agricultural Science* **101**, 337–344.
- Bassu S, Brisson N, Durand JL, Boote K, Lizaso J, Jones JW, . . . Waha K.** 2014. How do various maize crop models vary in their responses to climate change factors? *Global Change Biology* **20**, 2301–2320.
- Berry J, Bjorkman O.** 1980. Photosynthetic response and adaptation to temperature in higher-plants. *Annual Review of Plant Physiology and Plant Molecular Biology* **31**, 491–543.
- Bouma T, De Visser R, Van Leeuwen P, De Kock M, Lambers H.** 1995. The respiratory energy requirements involved in nocturnal carbohydrate export from starch-storing mature source leaves and their contribution to leaf dark respiration. *Journal of Experimental Botany* **46**, 1185–1194.
- Cai C, Li G, Di L, Ding Y, Fu L, Guo X, ...Yin X.** 2020. The acclimation of leaf photosynthesis of wheat and rice to seasonal temperature changes in T-FACE environments. *Global Change Biology* **26**, 539–556.
- Cai C, Li G, Yang H, Yang J, Liu H, Struik PC, ...Zhu J.** 2018. Do all leaf photosynthesis parameters of rice acclimate to elevated  $CO_2$ , elevated temperature, and their combination, in FACE environments? *Global Change Biology* **24**, 1685–1707.

- Campbell C, Atkinson L, Zaragoza-Castells J, Lundmark M, Atkin O, Hurry V.** 2007. Acclimation of photosynthesis and respiration is asynchronous in response to changes in temperature regardless of plant functional group. *New Phytologist* **176**, 375–389.
- Coast O, Shah S, Ivakov A, Gaju O, Wilson PB, Posch BC, Bryant CJ, Negrini ACA, Evans JR, Condon AG, Silva-Pérez V, Reynolds MP, Pogson BJ, Millar AH, Furbank RT, Atkin OK.** 2019. Predicting dark respiration rates of wheat leaves from hyperspectral reflectance. *Plant, Cell & Environment* **42**, 2133–2150.
- Collins M, Knutti R, Arblaster J, Dufresne JL, Fichet T, Friedlingstein P, ...Krinner G.** 2013. Long-term climate change: projections, commitments and irreversibility. In: *Climate Change 2013–The Physical Science Basis: Contribution of Working Group I to the Fifth Assessment Report of the Intergovernmental Panel on Climate Change*: Cambridge University Press, 1029–1136.
- Cox P.** (2001). Description of the “TRIFFID” dynamic global vegetation model. Bracknell: Hadley Centre, Met Office.
- Crafts-Brandner SJ, Salvucci ME.** 2002. Sensitivity of photosynthesis in a C<sub>4</sub> plant, maize, to heat stress. *Plant Physiology* **129**, 1773–1780.
- de Kauwe MG, Lin YS, Wright IJ, Medlyn BE, Crous KY, Ellsworth DS, ...Domingues TF.** 2016. A test of the ‘one-point method’ for estimating maximum carboxylation capacity from field-measured, light-saturated photosynthesis. *New Phytologist* **210**, 1130–1144.
- Dieuaide-Noubhani M, Canioni P, Raymond P.** 1997. Sugar-starvation-induced changes of carbon metabolism in excised maize root tips. *Plant Physiology* **115**, 1505–1513.
- Donatelli M, Srivastava AK, Duveiller G, Niemeyer S, Fumagalli D.** 2015. Climate change impact and potential adaptation strategies under alternate realizations of climate scenarios for three major crops in Europe. *Environmental Research Letters* **10**, 075005.
- Drake JE, Aspinwall MJ, Pfautsch S, Rymer PD, Reich PB, Smith RA, Crous KY, Tissue DT, Ghannoum O, Tjoelker MG.** 2015. The capacity to cope with climate warming declines from temperate to tropical latitudes in two widely distributed Eucalyptus species. *Global Change Biology* **21**, 459–472.
- Edwards JM, Roberts TH, Atwell BJ.** 2012. Quantifying ATP turnover in anoxic coleoptiles of rice (*Oryza sativa*) demonstrates preferential allocation of energy to protein synthesis. *Journal of Experimental Botany* **63**, 4389–4402.
- Evans JR, von Caemmerer S, Setchell BA, Hudson GS.** 1994. The relationship between CO<sub>2</sub> transfer conductance and leaf anatomy in transgenic tobacco with a reduced content of rubisco. *Australian Journal of Plant Physiology* **21**, 475–495.
- Fatichi S, Leuzinger S, Körner C.** 2014. Moving beyond photosynthesis: from carbon source to sink-driven vegetation modeling. *New Phytologist* **201**, 1086–1095.
- Frenkel M, Bellafiore S, Rochaix JD, Jansson S.** 2007. Hierarchy amongst photosynthetic acclimation responses for plant fitness. *Physiologia Plantarum* **129**, 455–459.
- García GA, Dreccer MF, Miralles DJ, Serrago RA.** 2015. High night temperatures during grain number determination reduce wheat and barley grain yield: a field study. *Global Change Biology* **21**, 4153–4164.
- García GA, Serrago RA, Dreccer MF, Miralles DJ.** 2016. Post-anthesis warm nights reduce grain weight in field-grown wheat and barley. *Field Crops Research* **195**, 50–59.
- Ghannoum O, Phillips NG, Sears MA, Logan BA, Lewis JD, Conroy JP, Tissue DT.** 2010. Photosynthetic responses of two eucalypts to industrial-age changes in atmospheric [CO<sub>2</sub>] and temperature. *Plant, Cell & Environment* **33**, 1671–1681.

- Hansen S, Jensen H, Nielsen N, Svendsen H.** 1991. Simulation of nitrogen dynamics and biomass production in winter wheat using the Danish simulation model DAISY. *Fertilizer Research* **27**, 245–259.
- Haxeltine A, Prentice IC.** 1996. BIOME3: An equilibrium terrestrial biosphere model based on ecophysiological constraints, resource availability, and competition among plant functional types. *Global Biogeochemical Cycles* **10**, 693–709.
- Hikosaka K, Ishikawa K, Borjigidai A, Muller O, Onoda Y.** 2006. Temperature acclimation of photosynthesis: mechanisms involved in the changes in temperature dependence of photosynthetic rate. *Journal of Experimental Botany* **57**, 291–302.
- Hochman Z, Gobbett DL, Horan H.** 2017. Climate trends account for stalled wheat yields in Australia since 1990. *Global Change Biology* **23**, 2071–2081.
- Hunt JR, Lilley JM, Trevaskis B, Flohr BM, Peake A, Fletcher A, Zwart AB, Gobbett D, Kirkegaard JA.** 2019. Early sowing systems can boost Australian wheat yields despite recent climate change. *Nature Climate Change* **9**, 244–247.
- Huntingford C, Atkin OK, Martinez-de la Torre A, Mercado LM, Heskell MA, Harper AB, ...Malhi, Y.** 2017. Implications of improved representations of plant respiration in a changing climate. *Nature Communications* **8**, 1602.
- Hurry V, Igamberdiev A, Keerberg O, Pärnik T, Atkin OK, Zaragoza-Castells J, Gardeström P.** 2005. Respiration in photosynthetic cells: gas exchange components, interactions with photorespiration and the operation of mitochondria in the light. In: *Plant Respiration*. Dordrecht: Springer, 43–61.
- Ikkonen EN, Shibaeva TG, Titov AF.** 2018. Influence of daily short-term temperature drops on respiration to photosynthesis ratio in chilling-sensitive plants. *Russian Journal of Plant Physiology* **65**, 78–83.
- Impa SM, Sunoj VSJ, Krassovskaya I, Bheemanahalli R, Obata T, Jagadish SVK.** 2019. Carbon balance and source-sink metabolic changes in winter wheat exposed to high night-time temperature. *Plant, Cell & Environment* **42**, 1233–1246.
- Isbell RF.** 1996. *The Australian Soil Classification*. Melbourne, Australia: CSIRO Publishing.
- Keiner R, Frosch T, Massad T, Trumbore S, Popp J.** 2014. Enhanced Raman multigas sensing—a novel tool for control and analysis of <sup>13</sup>CO<sub>2</sub> labeling experiments in environmental research. *Analyst* **139**, 3879–3884.
- King RW, Wardlaw IF, Evans LT.** 1967. Effect of assimilate utilization on photosynthetic rate in wheat. *Planta* **77**, 261–276.
- Kirkegaard JA, Lilley JM, Brill RD, Sprague SJ, Fettell NA, Pengilley GC.** 2016. Re-evaluating sowing time of spring canola (*Brassica napus* L.) in South-Eastern Australia—how early is too early? *Crop and Pasture Science* **67**, 381–396.
- Knorr W.** 2000. Annual and interannual CO<sub>2</sub> exchanges of the terrestrial biosphere: process-based simulations and uncertainties. *Global Ecology and Biogeography* **9**, 225–252.
- Kromer S.** 1995. Respiration during photosynthesis. *Annual Review of Plant Biology* **46**, 45–70.
- Lambers H, Robinson SA, Ribas-Carbo M.** 2005. Regulation of respiration *in vivo*. In: *Advances in Photosynthesis and Respiration*. Dordrecht: Springer Netherlands, 1–15.
- Larigauderie A, Körner C.** 1995. Acclimation of leaf dark respiration to temperature in alpine and lowland plant species. *Annals of Botany* **76**, 245–252.
- Li L, Nelson CJ, Trösch J, Castleden I, Huang S, Millar AH.** 2017. Protein degradation rate in *Arabidopsis thaliana* leaf growth and development. *The Plant Cell* **29**, 207–228.

- Li T, Hasegawa T, Yin X, Zhu Y, Boote K, Adam M, . . . Bouman B.** 2015. Uncertainties in predicting rice yield by current crop models under a wide range of climatic conditions. *Global Change Biology* **21**, 1328–1341.
- Lin YS, Medlyn BE, Ellsworth, DS.** 2012. Temperature responses of leaf net photosynthesis: the role of component processes. *Tree Physiology* **32**, 219–231.
- Liu B, Asseng S, Müller C, Ewert F, Elliott J, Lobell DB, ...Zhu Y.** 2016. Similar estimates of temperature impacts on global wheat yield by three independent methods. *Nature Climate Change* **6**, 1130–1136.
- Lobell DB, Gourdji SM.** 2012. The influence of climate change on global crop productivity. *Plant Physiology* **160**, 1686–1697.
- Loveys BR, Atkinson LJ, Sherlock DJ, Roberts RL, Fitter AH, Atkin OK.** 2003. Thermal acclimation of leaf and root respiration: an investigation comparing inherently fast- and slow-growing plant species. *Global Change Biology* **9**, 895–910.
- Melillo JM, McGuire AD, Kicklighter DW, Moore B, Vorosmarty CJ, Schloss AL.** 1993. Global climate change and terrestrial net primary production. *Nature* **363**, 234–240.
- O'Leary BM, Lee CP, Atkin OK, Cheng RY, Brown TB, Millar AH.** 2017. Variation in leaf respiration rates at night correlates with carbohydrate and amino acid supply. *Plant Physiology* **174**, 2261–2273.
- O'Sullivan OS, Weerasinghe KWLK, Evans JR, Egerton JGG, Tjoelker MG, Atkin OK.** 2013. High-resolution temperature responses of leaf respiration in snow gum (*Eucalyptus pauciflora*) reveal high-temperature limits to respiratory function. *Plant, Cell & Environment* **36**, 1268–1284.
- Oleson K, Lawrence DM, Bonan GB, Drewniak B, Huang M, Koven CD, ...Yang ZL.** 2013. Technical Description of version 4.5 of the Community Land Model (CLM), NCAR Tech. Note. NCAR/TN-503+ STR, 420. <https://doi.org/10.5065/D6RR1W7M>.
- Peng S, Huang J, Sheehy JE, Laza RC, Visperas RM, Zhong X, ...Cassman KG.** 2004. Rice yields decline with higher night temperature from global warming. *Proceedings of the National Academy of Sciences* **101**, 9971–9975.
- Pinkard EA, Eyles A, O'Grady AP.** 2011. Are gas exchange responses to resource limitation and defoliation linked to source:sink relationships? *Plant, Cell & Environment* **34**, 1652–1665.
- Plaxton WC, Podestá FE.** 2006. The functional organization and control of plant respiration. *Critical Reviews in Plant Sciences* **25**, 159–198.
- Rashid FAA, Crisp PA, Zhang Y, Berkowitz O, Pogson BJ, Day DA, Masle J, Dewar RC, Whelan J, Atkin OK, Scafaro AP.** 2020. Molecular and physiological responses during thermal acclimation of leaf photosynthesis and respiration in rice. *Plant, Cell & Environment* **43**, 594–610.
- Reich PB, Ellsworth DS, Walters MB.** 1998. Leaf structure (specific leaf area) modulates photosynthesis–nitrogen relations: evidence from within and across species and functional groups. *Functional Ecology* **12**, 948–958.
- Reich PB, Sendall KM, Stefanski A, Wei X, Rich RL, Montgomery RA.** 2016. Boreal and temperate trees show strong acclimation of respiration to warming. *Nature* **531**, 633–636.
- Reich PB, Tjoelker MG, Pregitzer KS, Wright IJ, Oleksyn J, Machado JL.** 2008. Scaling of respiration to nitrogen in leaves, stems and roots of higher land plants. *Ecology Letters* **11**, 793–801.

- Reich PB, Walters MB, Ellsworth DS, Vose JM, Volin JC, Gresham C, Bowman WD.** 1998. Relationships of leaf dark respiration to leaf nitrogen, specific leaf area and leaf life-span: a test across biomes and functional groups. *Oecologia* **114**, 471–482.
- Rosenzweig C, Jones JW, Hatfield JL, Ruane AC, Boote KJ, Thorburn P, Antle JM, Nelson GC, Porter C, Janssen S, Asseng S, Basso B, Ewert F, Wallach D, Baigorria G, Winter JM.** 2013. The Agricultural Model Intercomparison and Improvement Project (AgMIP): Protocols and pilot studies. *Agricultural and Forest Meteorology* **170**, 166–182.
- Ruan YL, Patrick JW, Bouzayen M, Osorio S, Fernie AR.** 2012. Molecular regulation of seed and fruit set. *Trends in Plant Science* **17**, 656–665.
- Ruimy A, Dedieu G, Saugier B.** 1996. TURC: A diagnostic model of continental gross primary productivity and net primary productivity. *Global Biogeochemical Cycles* **10**, 269–285.
- Sadok W, Jagadish K.** 2020. The hidden costs of nighttime warming on yields. *Trends in Plant Science* **25**, 644–651.
- Sage RF, Kubien DS.** 2007. The temperature response of C<sub>3</sub> and C<sub>4</sub> photosynthesis. *Plant, Cell & Environment* **30**, 1086–1106.
- Sage RF, McKown AD.** 2006. Is C<sub>4</sub> photosynthesis less phenotypically plastic than C<sub>3</sub> photosynthesis? *Journal of Experimental Botany* **57**, 303–317.
- Scafaro AP, Negrini ACA, O'Leary B, Rashid FAA, Hayes L, Fan Y, Zhang Y, Chochois V, Badger MR, Millar AH, Atkin OK.** 2017. The combination of gas-phase fluorophore technology and automation to enable high-throughput analysis of plant respiration. *Plant Methods* **13**, 1–13.
- Slafer GA, Rawson HM.** 1996. Responses to photoperiod change with phenophase and temperature during wheat development. *Field Crops Research* **46**, 1–13.
- Slot M, Winter K.** 2016. The Effects of Rising Temperature on the Ecophysiology of Tropical Forest Trees. In: Goldstein G., Santiago L., eds. *Tropical Tree Physiology: Adaptations and Responses in a Changing Environment*. Springer Cham: 385–412.
- Slot M, Kitajima K.** 2015. General patterns of acclimation of leaf respiration to elevated temperatures across biomes and plant types. *Oecologia* **177**, 885–900.
- Smith NG, Dukes JS.** 2013. Plant respiration and photosynthesis in global-scale models: incorporating acclimation to temperature and CO<sub>2</sub>. *Global Change Biology* **19**, 45–63.
- Stinziano JR, Way DA, Bauerle WL.** 2018. Improving models of photosynthetic thermal acclimation: Which parameters are most important and how many should be modified? *Global Change Biology* **24**, 1580–1598.
- Tjoelker MG, Oleksyn J, Reich PB, Żytkowiak R.** 2008. Coupling of respiration, nitrogen, and sugars underlies convergent temperature acclimation in *Pinus banksiana* across wide-ranging sites and populations. *Global Change Biology* **14**, 782–797.
- Ullah S, Bramley H, Daetwyler H, He S, Mahmood T, Thistlethwaite R, Trethowan R.** 2018. Genetic contribution of Emmer wheat (*Triticum dicoccon* Schrank) to heat tolerance of bread wheat. *Frontiers in Plant Science* **9**, 1529.
- von Caemmerer S, Evans JR, Hudson GS, Andrews TJ.** 1994. The kinetics of ribulose-1,5-bisphosphate carboxylase/oxygenase *in vivo* inferred from measurements of photosynthesis in leaves of transgenic tobacco. *Planta* **195**, 88–97.
- Vose RS, Easterling DR, Gleason B.** 2005. Maximum and minimum temperature trends for the globe: An update through 2004. *Geophysical Research Letters* **32**.
- Wang B, Feng P, Chen C, Li Liu D, Waters C, Yu Q.** 2019. Designing wheat ideotypes to cope with future changing climate in South-Eastern Australia. *Agricultural Systems* **170**, 9–18.

- Wang E, Martre P, Zhao Z, Ewert F, Maiorano A, Rötter RP, ...White JW.** 2017. The uncertainty of crop yield projections is reduced by improved temperature response functions. *Nature Plants* **3**, 1–13.
- Way DA, Sage RF.** 2008. Thermal acclimation of photosynthesis in black spruce [*Picea mariana* (Mill.) BSP]. *Plant, Cell & Environment* **31**, 1250–1262.
- Way DA, Yamori W.** 2014. Thermal acclimation of photosynthesis: on the importance of adjusting our definitions and accounting for thermal acclimation of respiration. *Photosynthesis Research* **119**, 89–100.
- Whitehead D, Griffin KL, Turnbull MH, Tissue DT, Engel VC, Brown KJ, Schuster WSF, Walcroft AS.** 2004. Response of total night-time respiration to differences in total daily photosynthesis for leaves in a *Quercus rubra* L. canopy: implications for modelling canopy CO<sub>2</sub> exchange. *Global Change Biology* **10**, 925–938.
- Wilson KB, Baldocchi DD, Hanson PJ.** 2000. Spatial and seasonal variability of photosynthetic parameters and their relationship to leaf nitrogen in a deciduous forest. *Tree Physiology* **20**, 565–578.
- Yamaguchi DP, Nakaji T, Hiura T, Hikosaka K.** 2016. Effects of seasonal change and experimental warming on the temperature dependence of photosynthesis in the canopy leaves of *Quercus serrata*. *Tree Physiology* **36**, 1283–1295.
- Zadoks JC, Chang TT, Konzak CF.** 1974. A decimal code for the growth stages of cereals. *Weed Research* **14**, 415–421.
- Zhao YR, Li X, Yu KQ, Cheng F, He Y.** 2016. Hyperspectral imaging for determining pigment contents in cucumber leaves in response to angular leaf spot disease. *Scientific Reports* **6**, 27790.
- Zheng YP, Li RQ, Guo LL, Hao LH, Zhou HR, Li F, Peng ZP, Cheng DJ, Xu M.** 2018. Temperature responses of photosynthesis and respiration of maize (*Zea mays*) plants to experimental warming. *Russian Journal of Plant Physiology* **65**, 524–531.
- Zhou H, Xu M, Hou R, Zheng Y, Chi Y, Ouyang Z.** 2018. Thermal acclimation of photosynthesis to experimental warming is season dependent for winter wheat (*Triticum aestivum* L.). *Environmental and Experimental Botany* **150**, 249–259.
- Ziehn T, Kattge J, Knorr W, Scholze M.** 2011. Improving the predictability of global CO<sub>2</sub> assimilation rates under climate change. *Geophysical Research Letters* **38**.

## Supplementary material

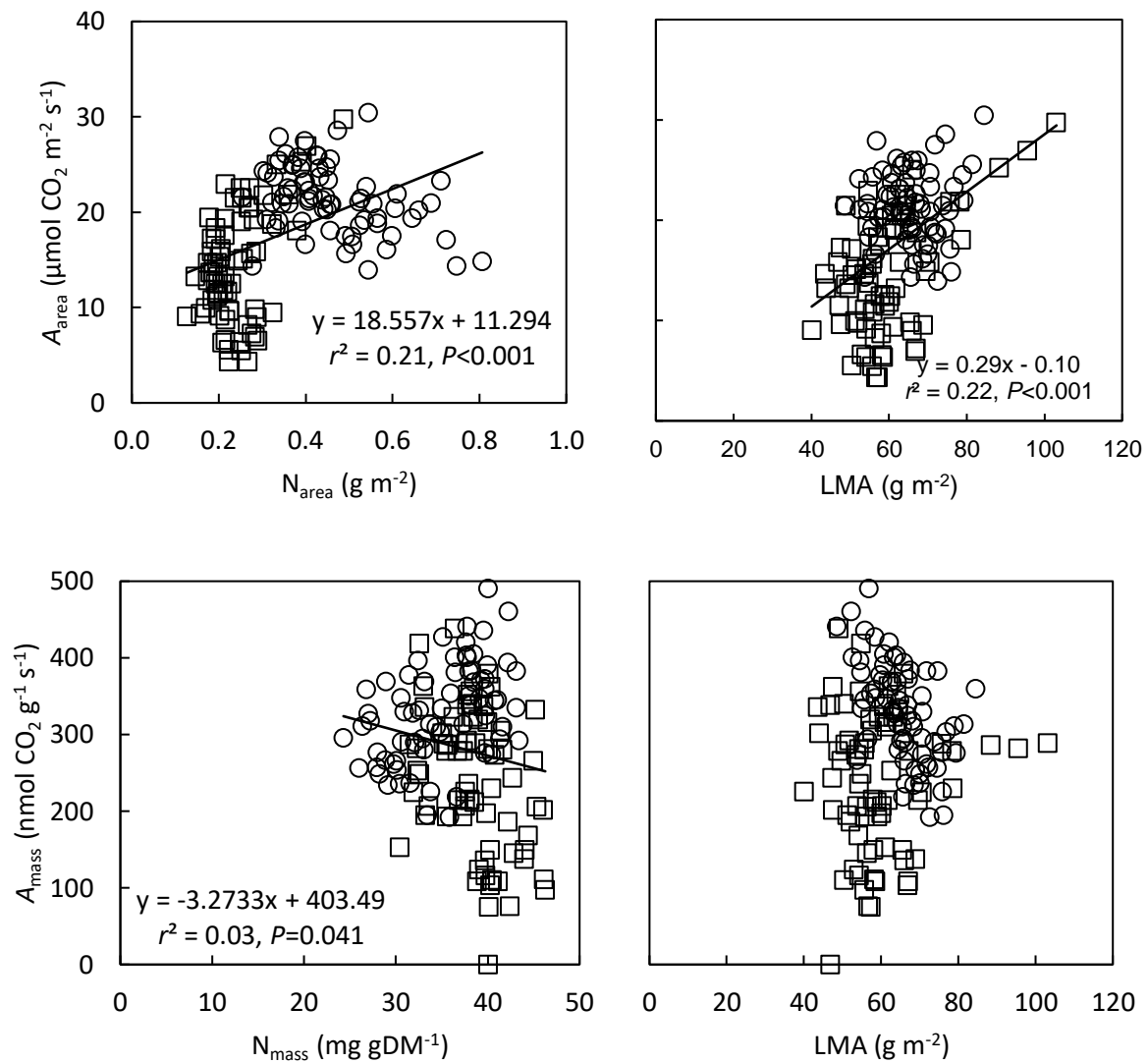


**Figure S1.** Bivariate plots of net CO<sub>2</sub> assimilation rates measured at 25°C (area based,  $A_{area}^{25}$ , top panels; and mass based,  $A_{mass}^{25}$ , bottom panels) with leaf N (area based,  $N_{area}$ , top left panel; and mass based,  $N_{mass}$ , bottom left panel) and leaf mass per unit area (LMA, right panels). Circles and squares represent data from 2017 and 2018, respectively.

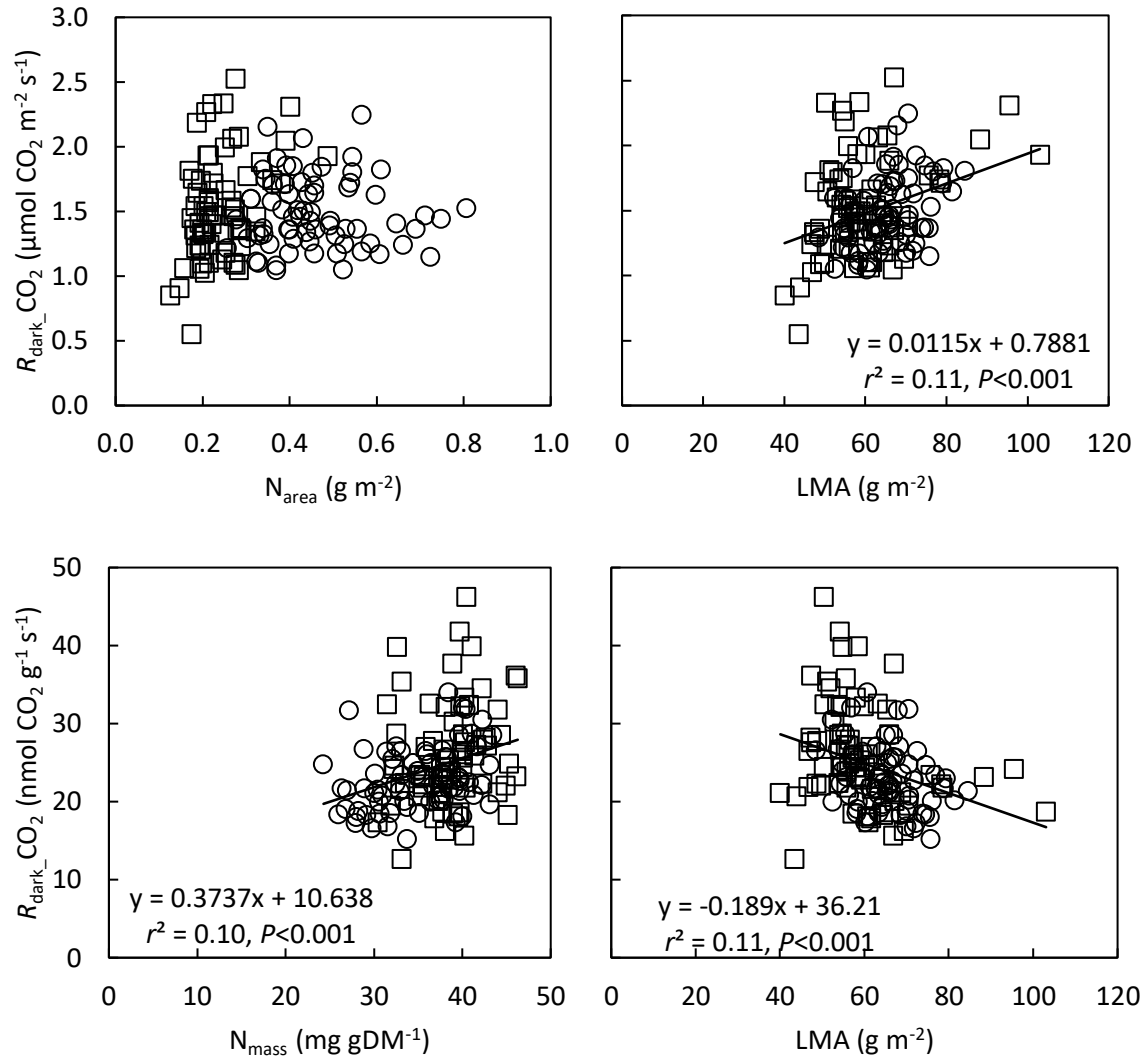


**Figure S2.** Bivariate plots of leaf dark respiration taken as rate of  $\text{CO}_2$  efflux ( $R_{\text{dark\_CO}_2}$ ) measured at  $25^\circ\text{C}$  (area based, top panels; and mass based, bottom panels) with leaf N (area based,  $N_{\text{area}}$ , top left panel; and mass based,  $N_{\text{mass}}$ , bottom left panel) and leaf mass per unit area (LMA, right panels). Circles and squares represent data from 2017 and 2018, respectively.



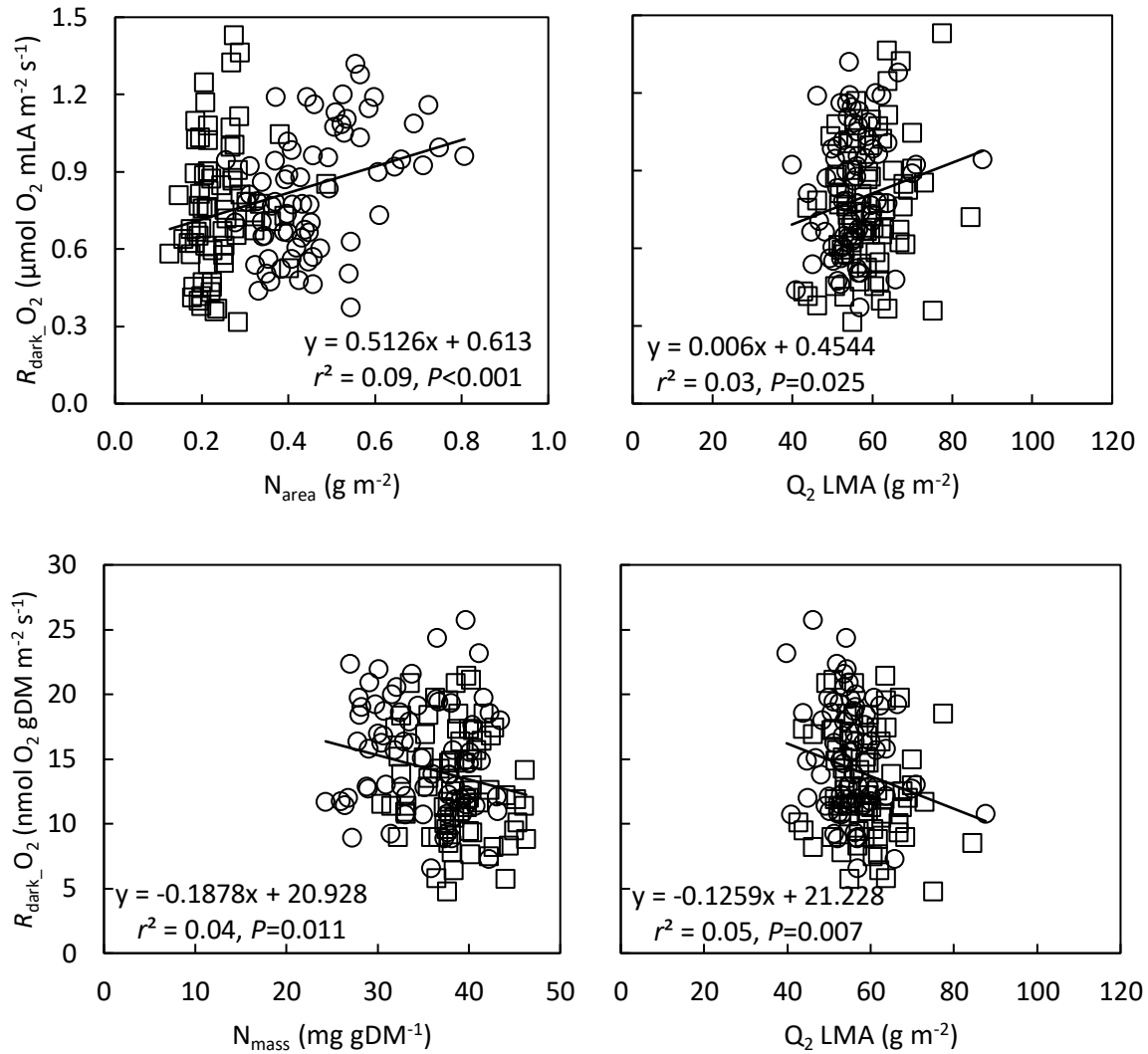


**Figure S3.** Bivariate plots of leaf dark respiration taken as rate of  $\text{O}_2$  consumption ( $R_{\text{dark\_O}_2}$ ) measured at  $25^\circ\text{C}$  (area based, top panels; and mass based, bottom panels) with leaf N (area based,  $N_{\text{area}}$ , top left panel; and mass based,  $N_{\text{mass}}$ , bottom left panel) and leaf mass per unit area (LMA, right panels). Circles and squares represent data from 2017 and 2018, respectively.

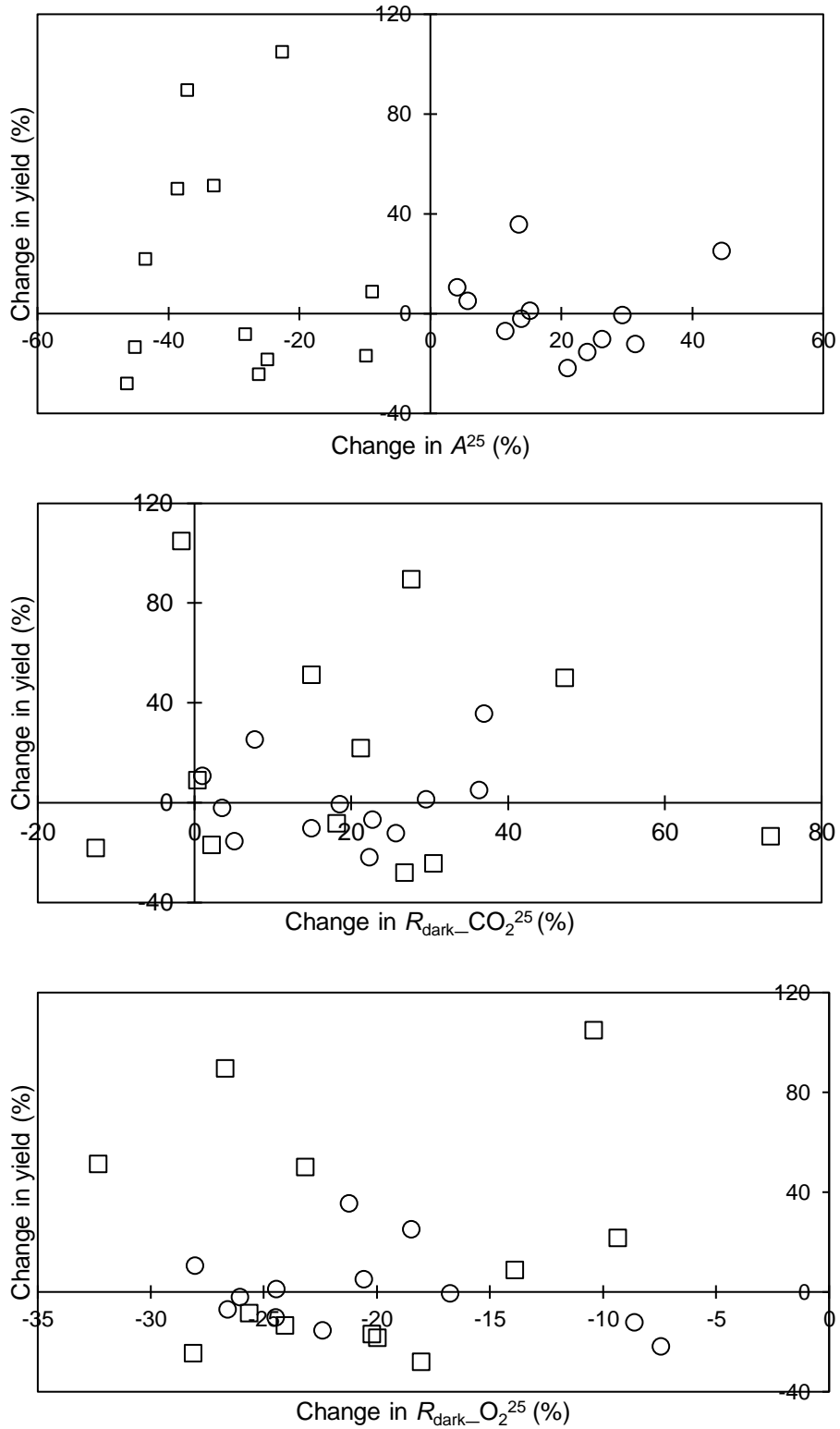


**Figure S4.** Plots of change in mean grain yield versus changes in mean net CO<sub>2</sub> assimilation rate ( $A^{25}$ , top panel) and leaf dark respiration (rate of CO<sub>2</sub> efflux,  $R_{\text{dark\_CO}_2^{25}}$ , middle panel; and rate of O<sub>2</sub> consumption  $R_{\text{dark\_O}_2^{25}}$ , bottom panel). Circles and squares represent data from 2017 and 2018, respectively.

**Table S1.** Genotypes used in study.

Entry	Name (Origin)	Pedigree	Note
1	PBI09C004-BC-DH43 (USyd)	Berkut/2/Berkut/35883 M500110	Backcross of a hexaploid wheat to a heat tolerant tetraploid <i>T. dicoccum</i> and a hexaploid type selected
2	PBI09C009-BC-DH51 (USyd)	Sokoll/2/Sokoll/ 35888 M 500132	Same as above
3	PBI09C026-BC-DH41 (USyd)	Waxwing*2/Kiritati /3/Waxwing*2/Kiritati /2/ 35888 M 500132	Same as above
4	ACIAR09PBI C04-17C-DH10 (USyd)	PBW550//C80.1/*2Batavia	Cross of heat tolerant Indian cultivar with rust resistant sources
5	ACIAR09PBI C38-115C-DH9 (USyd)	PBW343+L24+LR28/Lang	Same as above
6	ACIAR09PBI C29-51C-DH1 (USyd)	DBW16/Sunstate	Same as above
7	ACIAR09PBI C27-0C-0N-3N (USyd)	DBW16/Annuello	Same as above
8	ACIAR09PBI C26-0C-0N-2N (USyd)	DBW16/Gladius	Same as above
9	PBI07C101-DH64 (USyd)	ISR 812.8/Carinya	Heat tolerant Mexican hexaploid landrace cross to Australian cultivar
10	PBI07C101-DH154 (USyd)	ISR 812.8/Carinya	Same as above
11	PBI07C201-BC-DH66 (USyd)	Ventura/Ido 637//Ventura	Low phytate mutant crossed to Australian cultivar - pre-screened for heat tolerance
12	8:ZWW11 (CIMMYT)	D67.2/P66.270//AE.Squarrosa (320)/3/Cunningham/4/Vorb	Heat tolerant in Mexico (Ciudad Obregon) and Narrabri, Australia
13	77:ZWW11 (CIMMYT)	SLVS/Attila//WBLL1*2/3/Gondo/CBRD	Heat tolerant in Mexico (Ciudad Obregon) and Narrabri, Australia
14	45:ZIZ12 (ICARDA)	Hubara-8///Mon's'/Ald's'//Bow's'	Heat tolerant hexaploid; good performance in Sudan and Narrabri
15	267:ZWB13 (CIMMYT)	RAC 1192/4/2*Attila/3/Weaver*2/TSC//Weaver	Heat tolerant hexaploid; good performance in Mexico (Ciudad Obregon) and Narrabri, Australia
16	PBI09C009-BC-DH56 (USyd)	Sokoll/2/Sokoll/35888 M 500132	Backcross of a hexaploid wheat to a heat tolerant tetraploid <i>T. dicoccum</i> and a hexaploid type selected
17	Corak (AGT)		Commercial cultivar, released in 2012
18	Suntop (AGT)		Commercial cultivar, released in 2012
19	Trojan (LongReach)		Commercial cultivar, released in 2013
20	Mace (AGT)	Wyalkatchem/Stylet//Wyalkatchem	Commercial cultivar, released in 2008

USyd, The University of Sydney, Australia; CIMMYT, The International Maize and Wheat Improvement Center, Mexico; ICARDA, The International Centre for Agricultural Research in the Dry Areas, Syria; AGT, Australian Grains Technology, Australia; LongReach, LongReach Plant Breeders, Australia.

**Table S2.** Daily environmental conditions at anthesis for each time of sowing (TOS) during 2017 and 2018.

Weather parameter/Period	Day	T <sub>max</sub> /T <sub>min</sub> (°C)		Total solar radiation (kWh m <sup>-2</sup> )		Maximum photosynthetically active radiation <sup>1</sup> (μmol (photons) m <sup>-2</sup> s <sup>-1</sup> )	
		2017	2018	2017	2018	2017	2018
TOS1	1	18.4/ 1.2	24.1/10.6	5.83	3.40	2119	2331
	2	28.1/ 8.4	21.1/ 7.4	5.19	6.10	668	---
	3	17.6/ 5.7	23.3/ 3.7	3.49	5.34	---	---
TOS2	1	31.0/11.3	19.7/ 8.7	6.87	3.51	1924	1442
	2	32.9/10.9	19.1/10.3	6.69	2.72	1943	1970
	3	30.9/14.8	30.3/ 7.1	4.96	5.62	---	---
TOS3	1	29.0/10.9	30.2/ 4.7	4.85	7.07	1552	2041
	2	26.4/13.1	32.8/ 9.6	4.23	6.80	1712	---
	3	24.5/ 9.6	37.3/13.4	5.06	4.45	---	---

<sup>1</sup>Photosynthetically active radiation measured with Licor 6400XTs light sensors during gas exchange measurements.

**Table S3.** Rainfall and irrigation data from sowing to anthesis for different times of sowing (TOS) during 2017 and 2018.

Water supply (mm)	TOS1	TOS2	TOS3
<b>2017<sup>1</sup></b>			
Rainfall	123	90	97
Irrigation amount	62	62	62
Total water supplied	<b>185</b>	<b>152</b>	<b>159</b>
<b>2018</b>			
Rainfall	69	73	67
Irrigation amount	148	148 <sup>2</sup>	168 <sup>2</sup>
Total water supplied	<b>217</b>	<b>221</b>	<b>235</b>

<sup>1</sup>data from closest Australian Bureau of Meteorology weather station for 2017 and on-site weather station for 2018. <sup>2</sup>There was a brief period of water deficit stress (with visible signs of leaf rolling) prior to and including the period of physiological measurements of TOS2 and TOS3 in 2018 that is not reflected by these irrigation data.

**Table S4. 2017.** Proportional change in leaf dark respiration (rate of oxygen consumption expressed per unit of leaf area) for a 10°C increase in temperature ( $Q_{10}$ ) between 20 and 35°C of 20 wheat genotypes grown under three thermal regimes, achieved by varying time of sowing (TOS), at anthesis.

Genotype	$Q_{10}$			Mean
	TOS1	TOS2	TOS3	
1	2.08	<b>2.91</b>	<b>2.48</b>	<b>2.49</b>
2	1.88	<b>2.58</b>	<b>2.25</b>	<b>2.24</b>
3	2.13	<b>2.68</b>	<b>2.76</b>	<b>2.52</b>
4	2.02	<b>2.28</b>	2.10	<b>2.13</b>
5	2.11	<b>2.47</b>	<b>2.36</b>	<b>2.31</b>
6	1.78	<b>2.43</b>	<b>2.43</b>	<b>2.21</b>
7	2.05	<b>2.26</b>	<b>2.47</b>	<b>2.26</b>
8	1.92	<b>2.79</b>	<b>3.19</b>	<b>2.63</b>
9	1.82	<b>2.72</b>	<b>2.68</b>	<b>2.41</b>
10	1.89	<b>2.69</b>	<b>2.09</b>	<b>2.23</b>
11	1.93	<b>2.52</b>	<b>2.31</b>	<b>2.25</b>
12	1.92	<b>2.54</b>	<b>2.49</b>	<b>2.32</b>
13	1.71	<b>2.18</b>	<b>2.19</b>	<b>2.03</b>
14	1.79	<b>2.39</b>	<b>2.59</b>	<b>2.26</b>
15	1.83	<b>2.39</b>	<b>2.24</b>	<b>2.15</b>
16	2.09	<b>2.70</b>	<b>2.33</b>	<b>2.37</b>
Corak	2.18	<b>2.47</b>	<b>2.40</b>	<b>2.35</b>
Suntop	2.08	<b>2.70</b>	<b>2.59</b>	<b>2.46</b>
Trojan	1.83	<b>2.52</b>	<b>2.37</b>	<b>2.24</b>
Mace	2.12	2.11	<b>2.71</b>	<b>2.31</b>
	<b>Mean</b>	<b>1.96</b>	<b>2.52</b>	<b>2.45</b>
I.s.d. Genotype			0.27 <sup><i>P</i>=0.003</sup>	
I.s.d. TOS			0.10 <sup><i>P</i>≤0.001</sup>	
I.s.d. Genotype x TOS			0.47 <sup><i>P</i>=0.191</sup>	

Significant change in  $Q_{10}$  from TOS1 to TOS2 or TOS3 is highlighted in bold.

**Table S5. 2018.** Proportional change in leaf dark respiration (rate of oxygen consumption expressed per unit of leaf area) for a 10°C increase in temperature ( $Q_{10}$ ) between 20 and 35°C of 20 wheat genotypes grown under three thermal regimes, achieved by varying time of sowing (TOS), at anthesis.

Genotype	$Q_{10}$			Mean
	TOS1	TOS2	TOS3	
1	2.44	2.40	<b>1.88</b>	<b>2.24</b>
2	2.77	<b>2.08</b>	<b>2.34</b>	<b>2.40</b>
3	2.15	<b>3.22</b>	<b>2.21</b>	<b>2.53</b>
4	2.38	2.37	<b>2.04</b>	<b>2.26</b>
5	2.70	<b>2.44</b>	<b>2.21</b>	<b>2.45</b>
6	2.38	<b>2.60</b>	<b>2.20</b>	<b>2.39</b>
7	2.22	<b>2.52</b>	2.22	<b>2.32</b>
8	2.27	<b>2.47</b>	<b>1.85</b>	<b>2.20</b>
9	2.89	<b>2.19</b>	<b>2.56</b>	<b>2.55</b>
10	2.18	<b>2.49</b>	<b>2.12</b>	<b>2.26</b>
11	2.43	<b>3.07</b>	<b>1.88</b>	<b>2.46</b>
12	2.71	2.73	<b>2.25</b>	<b>2.56</b>
13	2.48	2.52	<b>2.00</b>	<b>2.33</b>
14	2.02	<b>2.59</b>	2.04	<b>2.22</b>
15	2.19	<b>2.46</b>	<b>1.99</b>	<b>2.21</b>
16	2.57	2.52	<b>2.09</b>	<b>2.39</b>
Corak	2.36	<b>2.70</b>	<b>2.23</b>	<b>2.43</b>
Suntop	2.40	2.59	<b>2.03</b>	<b>2.34</b>
Trojan	2.75	<b>2.29</b>	<b>2.53</b>	<b>2.52</b>
Mace	2.25	<b>2.77</b>	2.23	<b>2.42</b>
	<b>Mean</b>	<b>2.43</b>	<b>2.55</b>	<b>2.15</b>
I.s.d. Genotype			0.14 <sup><i>P</i>≤0.001</sup>	
I.s.d. TOS			0.05 <sup><i>P</i>≤0.001</sup>	
I.s.d. Genotype x TOS			0.24 <sup><i>P</i>≤0.001</sup>	

Significant change in  $Q_{10}$  from TOS1 to TOS2 or TOS3 is highlighted in bold.

**Table S6.** Parameter estimates of log-transformed instantaneous leaf dark respiration-temperature responses of 20 wheat genotypes grown under three thermal regimes, achieved by varying time of sowing (TOS) during 2017 and 2018. Values of leaf dark respiration presented are based on rate of O<sub>2</sub> consumption expressed per unit of leaf area of 20 genotypes.

Experiment	$R_{\text{dark\_O}_2}$	slope	intercept	Q <sub>10</sub>
<b>2017</b>				
TOS1	0.041	0.028***	-0.74***	1.96
TOS2	<b>-0.111</b>	<b>0.038***</b>	<b>-1.15***</b>	<b>2.52</b>
TOS3	<b>-0.027</b>	<b>0.037***</b>	<b>-1.04***</b>	<b>2.45</b>
<b>2018</b>				
TOS1	0.003	0.038***	-1.04***	2.43
TOS2	-0.106	<b>0.040***</b>	<b>-1.22***</b>	2.55
TOS3	-0.083	<b>0.033***</b>	<b>-0.98***</b>	<b>2.15</b>

Log  $R_{\text{dark\_O}_2}$  ( $\mu\text{mol O}_2 \text{ m}_{\text{LA}}^{-2} \text{ s}^{-1}$ ), log-transformed dark respiration (O<sub>2</sub> consumption) rate measured at 25°C. Slopes and intercept values are the means of 20 wheat genotypes with four replicates across four temperatures (20, 25, 30 and 35°C). \*\*\* $P < 0.001$ . Parameter estimates significantly different from TOS1 are indicated in bold.



**Table S7.** Estimates of parameters and goodness of fit for equations of multiple linear regressions of leaf traits explained by environmental variables over the 1–3 days of 50% anthesis of 6–20 wheat genotypes grown in 2017 and 2018, each with three different thermal regimes (achieved by varying time of sowing).

Leaf traits	Six genotypes					
	Constant	Average $T_{\max}$ ( $^{\circ}\text{C}$ ) <sup>1</sup>	Average $T_{\min}$ ( $^{\circ}\text{C}$ ) <sup>2</sup>	Total solar radiation ( $\text{kWh m}^{-2}$ )	Mean photosynthetically active radiation ( $\mu\text{mol (photons) m}^{-2} \text{s}^{-1}$ )	Goodness of fit ( $r^2$ )
$A^{25}$	48.1***	-0.212	3.117***	-2.909***	-0.002	0.72***
$R_{\text{dark\_CO}_2}^{25}$	1.092**	-0.021*	0.030	0.032	0.000	0.25*
$R_{\text{dark\_O}_2}^{20}$	1.197***	0.005	0.002	-0.054***	0.000	0.64***
$R_{\text{dark\_O}_2}^{25}$	1.471***	0.000	-0.027*	-0.028	0.000	0.55***
$R_{\text{dark\_O}_2}^{30}$	2.057***	0.000	-0.005	-0.042	-0.000	0.39***
$R_{\text{dark\_O}_2}^{35}$	3.426***	-0.035***	0.046*	-0.080**	0.000	0.55***
20 Genotypes						
	Constant	Average $T_{\max}$ ( $^{\circ}\text{C}$ )	Average $T_{\min}$ ( $^{\circ}\text{C}$ )	Total solar radiation ( $\text{kWh m}^{-2}$ )	Mean photosynthetically active radiation ( $\mu\text{mol (photons) m}^{-2} \text{s}^{-1}$ )	Goodness of fit ( $r^2$ )
$R_{\text{dark\_O}_2}^{20}$	1.105***	0.003	0.004	-0.039***	-0.000	0.48***
$R_{\text{dark\_O}_2}^{25}$	1.331***	-0.009**	-0.016*	-0.003	-0.000	0.41***
$R_{\text{dark\_O}_2}^{30}$	2.380***	-0.006	0.030*	-0.074***	-0.000	0.40***
$R_{\text{dark\_O}_2}^{35}$	3.451***	-0.030***	0.060***	-0.083***	-0.000	0.41***

<sup>1</sup>Daily Average daily maximum temperature. <sup>2</sup>Average daily minimum temperature. Asterisks besides parameter estimates and  $r^2$  indicates level of significance (\*= $P<0.05$ , \*\*= $P<0.01$  and \*\*\*= $P<0.001$ ) based on t. probability for terms in the regression models and overall F probability for the full regression model, respectively.

**Table S8.** Leaf mass per unit area (LMA) and leaf nitrogen (N) concentration of six wheat genotypes grown under three thermal regimes, achieved by varying time of sowing (TOS) during 2017 and 2018.

	Genotype (G)	LMA (g m <sup>-2</sup> )			Leaf N <sub>area</sub> (g m <sup>-2</sup> )			Leaf N <sub>mass</sub> (mg gDM <sup>-1</sup> )		
		TOS1	TOS2	TOS3	TOS1	TOS2	TOS3	TOS1	TOS2	TOS3
<b>2017</b>										
	3	64	55	62	0.55	0.34	0.38	30	31	40
	12	70	64	67	0.62	0.39	0.41	29	30	40
	14	72	70	66	0.60	0.38	0.40	29	28	40
	15	74	63	65	0.64	0.45	0.38	32	37	38
	Suntop	64	63	58	0.59	0.46	0.38	34	38	41
	Mace	62	72	67	0.53	0.49	0.38	33	36	38
	<b>Mean</b>	<b>67</b>	<b>64</b>	<b>64</b>	<b>0.59</b>	<b>0.42</b>	<b>0.39</b>	<b>31</b>	<b>34</b>	<b>40</b>
l.s.d.										
	Genotype	6*			0.05 <sup>ns</sup>			2***		
	TOS	4 <sup>ns</sup>			0.03***			2***		
	Genotype x TOS	10 <sup>ns</sup>			0.08 <sup>ns</sup>			4*		
<b>2018</b>										
	3	52	55	52	0.24	0.25	0.20	36	44	41
	12	54	60	57	0.25	0.26	0.20	37	42	39
	14	64	62	62	0.34	0.26	0.19	38	41	35
	15	73	53	57	0.34	0.20	0.19	36	37	37
	Suntop	62	53	58	0.28	0.20	0.22	36	36	43
	Mace	64	54	55	0.28	0.23	0.19	36	41	39
	<b>Mean</b>	<b>61</b>	<b>56</b>	<b>57</b>	<b>0.29</b>	<b>0.24</b>	<b>0.20</b>	<b>37</b>	<b>40</b>	<b>39</b>
l.s.d.										
	Genotype	6*			0.04 <sup>ns</sup>			3 <sup>ns</sup>		
	TOS	4*			0.02***			2***		
	Genotype x TOS	11 <sup>ns</sup>			0.06*			5*		

l.s.d.=least significant differences of means (5% level). The superscripts and asterisks indicate the level of significance. <sup>ns</sup>=not significant. \**P* < 0.05. \*\**P* < 0.01. \*\*\**P* < 0.001. *n*=4.

**Table S9. 2017:** Parameter estimates of regression models of leaf functional traits (net CO<sub>2</sub> assimilation rate,  $A^{25}$ ; rate of CO<sub>2</sub> efflux,  $R_{\text{dark\_CO}_2^{25}}$ ; and rate of O<sub>2</sub> consumption,  $R_{\text{dark\_O}_2^{25}}$ ) with leaf mass per unit area (LMA) or leaf N concentration grouped by time of sowing (TOS). Estimates are given for trait-trait relationships on an area or mass basis.

Structural or chemical traits		Area-based functional leaf traits					
		$A^{25}$		$R_{\text{dark\_CO}_2^{25}}$		$R_{\text{dark\_O}_2^{25}}$	
		Intercept	Slope	Intercept	Slope	Intercept	Slope
LMA	TOS1	26.6	-0.12	0.93	0.006	1.05	0.000
	TOS2	16.9	0.06	0.18	0.022	<b>-0.16</b>	0.015
	TOS3	12.6	<b>0.18</b>	0.59	0.014	0.81	-0.001
N	TOS1	21.8	-5.16	1.12	0.358	1.21	-0.254
	TOS2	20.2	1.42	0.81	1.879	<b>0.54</b>	0.360
	TOS3	17.1	<b>18.42</b>	0.90	1.597	1.27	-1.328
$V_{\text{cmax}}^{25}$	TOS1	---	---	1.66	-0.003	1.25	-0.002
	TOS2	---	---	0.79	0.007	<b>0.29</b>	0.003
	TOS3	---	---	1.33	0.001	1.00	-0.002
		Mass-based functional leaf traits					
		$A^{25}$		$R_{\text{dark\_CO}_2^{25}}$		$R_{\text{dark\_O}_2^{25}}$	
		Intercept	Slope	Intercept	Slope	Intercept	Slope
LMA	TOS1	724.2	-6.57	34.05	-0.210	35.16	-0.290
	TOS2	587.7	-4.06	26.70	-0.030	<b>9.82</b>	<b>0.044</b>
	TOS3	574.4	-3.05	32.76	-0.143	28.43	-0.263
N	TOS1	139.0	4.53	11.54	0.267	13.93	0.150
	TOS2	283.8	1.26	18.72	0.180	7.55	0.141
	TOS3	519.0	-3.60	1.40	0.556	13.10	0.034
$V_{\text{cmax}}^{25}$							

TOS1	---	---	16.69	0.002	20.39	-0.001
TOS2	---	---	19.42	0.003	<b>6.05</b>	0.003
TOS3	---	---	18.95	0.002	8.14	0.002

For each trait-trait relationship, significantly different slopes or intercepts of TOS2 or TOS3 from TOS1 are indicated in bold. ---, not estimated.

**Table S10. 2018:** Parameter estimates of regression models of leaf functional traits (net CO<sub>2</sub> assimilation rate,  $A^{25}$ ; rate of CO<sub>2</sub> efflux,  $R_{\text{dark\_CO}_2^{25}}$ ; and rate of O<sub>2</sub> consumption,  $R_{\text{dark\_O}_2^{25}}$ ) with leaf mass per unit area (LMA) or leaf N concentration grouped by time of sowing (TOS). Estimates are given for trait-trait relationships on an area or mass basis.

Structural or chemical traits		Area-based functional leaf traits					
		$A^{25}$		$R_{\text{dark\_CO}_2^{25}}$		$R_{\text{dark\_O}_2^{25}}$	
		Intercept	Slope	Intercept	Slope	Intercept	Slope
LMA	TOS1	7.37	0.20	0.29	0.019	0.14	0.011
	TOS2	20.10	<b>-0.19</b>	1.46	0.004	0.64	0.001
	TOS3	3.71	0.18	0.61	0.013	0.32	0.008
N	TOS1	9.10	38.40	0.52	3.479	0.85	-0.117
	TOS2	<b>19.58</b>	<b>-44.00</b>	<b>1.67</b>	0.030	0.23	2.110
	TOS3	4.03	49.40	0.68	3.480	0.47	1.370
$V_{\text{cmax}}^{25}$	TOS1	---	---	1.91	-0.003	0.81	0.000
	TOS2	---	---	1.54	0.001	0.95	-0.001
	TOS3	---	---	1.44	-0.001	0.62	0.001
		Mass-based functional leaf traits					
		$A^{25}$		$R_{\text{dark\_CO}_2^{25}}$		$R_{\text{dark\_O}_2^{25}}$	
		Intercept	Slope	Intercept	Slope	Intercept	Slope
LMA	TOS1	332.8	-0.49	19.0	0.073	15.08	-0.033
	TOS2	540.0	<b>-6.59</b>	<b>62.2</b>	<b>-0.550</b>	21.58	-0.156
	TOS3	315.0	-1.25	32.5	-0.150	18.20	-0.087
N	TOS1	529.0	-6.24	24.2	-0.018	6.10	0.187
	TOS2	475.0	-7.58	33.7	-0.089	25.61	-0.325
	TOS3	121.0	3.17	10.2	0.359	22.21	-0.227
$V_{\text{cmax}}^{25}$							

TOS1	---	---	24.9	-0.001	13.18	0.000
TOS2	---	---	26.9	0.001	16.47	-0.001
TOS3	---	---	26.4	-0.001	13.29	0.000

For each trait-trait relationship, significantly different slopes or intercepts of TOS2 or TOS3 from TOS1 are indicated in bold.

**Table S11.** Regression coefficients ( $r^2$ ) for leaf trait-trait relationships with data combined for 2017 and 2018.

Structural or chemical traits	Area based functional traits			Mass based functional traits		
	$A^{25}$	$R_{\text{dark\_CO}_2^{25}}$	$R_{\text{dark\_O}_2^{25}}$	$A^{25}$	$R_{\text{dark\_CO}_2^{25}}$	$R_{\text{dark\_O}_2^{25}}$
LMA	0.22***	0.11***	0.03*	0.00 <sup>ns</sup>	0.10***	0.04**
N	0.20***	0.00 <sup>ns</sup>	0.09***	0.02*	0.09***	0.04*
$V_{\text{cmax}}^{25}$	---	0.00 <sup>ns</sup>	0.02 <sup>ns</sup>	---	0.02 <sup>ns</sup>	0.01 <sup>ns</sup>
LMA+N	0.26***	0.14***	0.12***	0.02 <sup>ns</sup>	0.15***	0.09***
LMA+N+ $V_{\text{cmax}}^{25}$	---	0.15***	0.10***	---	0.10***	0.10***

$A^{25}$  ( $\mu\text{mol CO}_2 \text{ m}^{-2} \text{ s}^{-1}$ ), net  $\text{CO}_2$  assimilation rate measured at 25°C;  $R_{\text{dark\_CO}_2^{25}}$  ( $\mu\text{mol CO}_2 \text{ m}^{-2} \text{ s}^{-1}$ ), dark respiration ( $\text{CO}_2$  efflux) rate measured at 25°C;  $R_{\text{dark\_O}_2}$  ( $\mu\text{mol O}_2 \text{ m}_{\text{LA}}^{-2} \text{ s}^{-1}$ ), dark respiration ( $\text{O}_2$  consumption); LMA ( $\text{g m}^{-2}$ ), leaf mass per unit area; Leaf N expressed on either area basis ( $\text{g m}^{-2}$ ) or mass basis ( $\text{mg gDM}^{-1}$ );  $V_{\text{cmax}}^{25}$ , maximum carboxylation capacity of photosynthetic capacity at 25°C ( $\mu\text{mol CO}_2 \text{ m}^{-2} \text{ s}^{-1}$ ). ---, not estimated. <sup>ns</sup>=not significant.

\* $P < 0.05$ . \*\* $P < 0.01$ . \*\*\* $P < 0.001$ .

## Statement of Contribution

This thesis is submitted as a Thesis by Compilation in accordance with [https://policies.anu.edu.au/ppl/document/ANUP\\_003405](https://policies.anu.edu.au/ppl/document/ANUP_003405)

I declare that the research presented in this Thesis represents original work that I carried out during my candidature at the Australian National University, except for contributions to multi-author papers incorporated in the Thesis where my contributions are specified in this Statement of Contribution.

Title: Acclimation of leaf photosynthesis and respiration to warming in field-grown wheat \_\_\_\_\_

Authors: Onoriode Coast\*, Bradley C. Posch\*, Helen Bramley, Oorbessy Gaju, Richard A. Richards, Meqin Lu, Yong-Ling Ruan, Richard Trethowan, and Owen K. Atkin \_\_\_\_\_

\*Onoriode Coast and Bradley C. Posch should be considered joint first author \_\_\_\_\_

Publication outlet: Plant, Cell & Environment \_\_\_\_\_

Current status of paper: Published

Contribution to paper: O.K.A., H.B., and Y-L.R. secured grants; R.T. developed the seed materials; O.C., H.B., and O.K.A. designed experiments; O.C. and B.C.P. collected data; O.C. and B.C.P. analysed data; and O.C. and B.C.P. wrote the paper with contributions from all authors. \_\_\_\_\_

Senior author or collaborating authors endorsement: Owen Atkin April 2nd 2022

Bradley C. Posch

Candidate – Print Name

*BP*

Signature

01-04-2022

Date

### Endorsed

PROFESSOR OWEN ATKIN

Primary Supervisor – Print Name

*Owen Atkin*

Signature

April 2nd 2022

Date



## Chapter 3 – Wheat photosystem II heat tolerance responds dynamically to short- and long-term warming

Bradley C. Posch, Julia Hammer, Owen K. Atkin, Helen Bramley, Yong-Ling Ruan, Richard Trethowan, and Onoriode Coast

Author Contributions: O.K.A., H.B., and Y-L.R. secured grants; R.T. developed the seed materials; B.C.P., J.H., O.C., H.B., and O.K.A. designed experiments; B.C.P., J.H. and O.C. collected data; B.C.P., J.H. and O.C. analysed data; and B.C.P. and O.C. wrote the paper with contributions from all authors.

*This manuscript has been accepted for publication at the Journal of Experimental Botany and is in press at the time of thesis submission.*

### Abstract

Heat-induced inhibition of photosynthesis is a key factor in declining wheat performance and yield. Variation in wheat heat tolerance can be characterised using the critical temperature ( $T_{crit}$ ) at which incipient damage to the photosynthetic machinery occurs. We investigated intraspecies variation and plasticity of wheat  $T_{crit}$  under elevated temperature in field and controlled environment experiments. We also assessed whether intraspecies variation in wheat  $T_{crit}$  mirrors patterns of global interspecies variation in heat tolerance reported for mostly wild, woody plants. In the field, wheat  $T_{crit}$  varied through the course of a day, peaking at noon and lowest at sunrise, and increased as plants developed from heading to anthesis and grain filling. Under controlled temperature conditions, heat stress (36°C) was associated with a rapid rise in wheat  $T_{crit}$  (i.e. within two hours of heat stress) that peaked after 3–4 days. These peaks in  $T_{crit}$  indicate a physiological limitation to photosystem II heat tolerance. Analysis of a global dataset (comprising 183 *Triticum* and wild wheat (*Aegilops*) species) generated from the current study and a systematic literature review showed that wheat leaf  $T_{crit}$  varied by up to 20°C (about two-thirds of reported global plant interspecies variation). However, unlike global patterns of interspecies  $T_{crit}$  variation which has been linked to latitude

of genotype origin, intraspecific variation in wheat  $T_{crit}$  was unrelated to that. Yet, the observed genotypic variation and plasticity of wheat  $T_{crit}$  suggests that this trait could be a useful tool for high-throughput phenotyping of wheat photosynthetic heat tolerance.

## Introduction

As the climate changes, global mean land-surface temperature has continued to rise, alongside more frequent, longer, and more intense heatwaves (Perkins-Kirkpatrick and Lewis, 2020). This is particularly concerning for the prospect of improving crop yields, as heat stress is associated with significant declines in the yield of widely-cultivated crops, including wheat (Asseng *et al.*, 2015; Tack *et al.*, 2015; Hochman *et al.*, 2017; Liu *et al.*, 2019; Ortiz-Bobea *et al.*, 2019). Photosynthesis is a primary determinant of wheat yield and it is particularly sensitive to heat stress (Berry and Bjorkman, 1980; Way and Yamori, 2014). Improving the heat tolerance of photosynthesis could future-proof wheat yield in a warming world (Cossani and Reynolds, 2012; Scafaro and Atkin, 2016; Iqbal *et al.*, 2017). To realise improvements in wheat photosynthetic heat tolerance, it is paramount that we first understand and quantify patterns of wheat photosynthetic heat tolerance so that we can then successfully exploit them.

Decreased leaf photosynthetic rate under high temperature is partially linked to disruption of the chloroplast electron transport chain, of which the thylakoid membrane-embedded photosystem II (PSII) considered the most sensitive component (Sharkey, 2005; Brestic *et al.*, 2012). Heat-induced reactive oxygen species and lipid peroxidation both cause cleavage of the reaction centre-binding D1 protein of PSII (Yamashita *et al.*, 2008), inhibiting electron flow and thus the production of ATP. For decades PSII damage has been measured with chlorophyll *a* fluorescence metrics, including  $T_{crit}$  of  $F_0$  (Schreiber *et al.*, 1975; Schreiber and Berry, 1977; Hüve *et al.*, 2011; Geange *et al.*, 2021).  $T_{crit}$  of  $F_0$  (henceforth  $T_{crit}$ ) is the critical temperature above which minimal chlorophyll *a* fluorescence ( $F_0$ ) rises rapidly, indicating incipient damage to PSII (Schreiber and Berry, 1977; Melcarek and Brown, 1979; Neuner and Pramsöhler, 2006; Slot *et al.*, 2019).  $T_{crit}$  is associated with increased thylakoid membrane fluidity, disruption of the light-harvesting antennae (Raison *et al.*, 1982; Figueroa *et al.*, 2003), dissociation of chloroplast membrane-bound proteins (Berry and Bjorkman, 1980), and loss of chloroplast thermostability (Armond *et al.*, 1978). As a standardized metric,

$T_{crit}$  has been used to examine global patterns of heat tolerance, quantify phenotypic plasticity in response to warming, and assess vulnerability to climate change across plant species (O'Sullivan *et al.*, 2017; Zhu *et al.*, 2018; Lancaster and Humphreys, 2020; Geange *et al.*, 2021). While the number of publications examining plant  $T_{crit}$  is growing (Ferguson *et al.*, 2020; Arnold *et al.*, 2021; Slot *et al.*, 2021), most studies focused on woody, non-crop species, and characterisation of intraspecies variation in  $T_{crit}$  of crop species has been limited (see Ferguson *et al.*, 2020 for a recent exception). Wheat, as the most widely-cultivated crop (with over 220 million ha cultivated worldwide) with a diverse range of genotypes originating from across the globe, is an ideal crop species for examining intraspecies variation and acclimation of  $T_{crit}$ . In addition, although wheat is a temperate crop, there is increasing evidence of warming in many wheat-producing regions, including China, the USA, and Australia, resulting in either stalled or reduced wheat yield (Hochman *et al.*, 2017; Zhao *et al.*, 2017). Understanding the response of  $T_{crit}$  to warming and the magnitude of intraspecies variation in  $T_{crit}$  could thus provide opportunities for improving photosynthetic heat tolerance and yield resilience in wheat and other crops.

Quantification of intraspecific variation in physiological traits of crops commonly encounters bottlenecks at the phenotyping stage. However, high-throughput phenotyping techniques are being developed, including a robotic system offering a ten-fold increase in the measurement speed of dark respiration (Scafaro *et al.*, 2017; Coast *et al.*, 2019, 2021), and the proximal remote sensing of leaf hyperspectral reflectance signatures for rapidly assaying photosynthetic characteristics and dark respiration (Silva-Pérez *et al.*, 2018; Coast *et al.*, 2019; Fu *et al.*, 2019). Though chlorophyll fluorescence techniques are well-established for assessing photosynthetic heat tolerance, they are typically cumbersome. This limits their incorporation in breeding programmes that screen hundreds of genotypes for heat tolerance. But recently, Arnold *et al.* (2021) described a high-throughput chlorophyll fluorescence screening technique for a diversity of wild species.

Previous studies of photosynthetic thermal tolerance have also largely assumed that  $T_{crit}$  is diurnally and phenologically constant. However, reports of substantial variation in metabolic capacity and demand for photosynthetic products diurnally, with phenological development, and in response to fluctuations in temperature (Steer, 1973; Rashid *et al.*, 2020) suggest that these assumptions may be flawed. The fact that a specific phenological stage –

anthesis – is widely agreed to mark the time at which wheat is most vulnerable to the effects of heat stress (Ferris *et al.*, 1998; Thistlethwaite *et al.*, 2020) also raises the question as to whether heat tolerance varies in a similar fashion with development to provide protection at more critical stages. Furthermore, there have also been numerous studies that have described diurnal variation in plant heat tolerance as measured by tissue damage and plant survival (Colombo *et al.*, 1995; Dickinson *et al.*, 2018), including the chlorophyll fluorescence-based measure  $F_v/F_m$  (Li and Guy, 2001). Based on this evidence it seems reasonable that  $T_{crit}$  might demonstrate similar variation, though this has yet to be verified.

The extent to which plants physiologically adjust to warming is important in determining productivity and survival (Scheiner, 1993; Leung *et al.*, 2020). Acclimation of photosynthetic electron transport to elevated temperature is evidenced by an increase in  $T_{crit}$ . Zhu *et al.* (2018) reported acclimation at a rate of 0.34°C increase in  $T_{crit}$  for every 1°C increase in average temperature over the growing season for a range of native Australian species. Acclimation of  $T_{crit}$  may also increase plant thermal safety margins, thus protecting against damage to PSII under future heat stress. Thermal safety margins are estimated as the difference between the upper limit of leaf function (e.g.  $T_{crit}$ ) and the maximum growth temperature experienced in an environment (Sastry and Barua, 2017), and they provide a useful representation of a species' potential vulnerability to global warming (Sunday *et al.*, 2014). A reduction in this margin indicates increasing vulnerability to heat stress, while an increase in this margin indicates better capacity to tolerate the effects of climate warming (Hoffmann *et al.*, 2013). Thermal safety margins of 10–15°C have been reported for many plant species (Weng and Lai, 2005; O'Sullivan *et al.*, 2017; Perez and Feeley, 2020), with some as high as 12–31°C (Leon-Garcia and Lasso, 2019) when leaf temperature, rather than air temperature, was used. However, many plant species have low thermal safety margins (e.g.  $\leq 5^\circ\text{C}$ ; Sastry and Barua, 2017). Unfortunately, reports quantifying the acclimation capacity and thermal safety margins of food crops are scarce. Reports on acclimation of  $T_{crit}$  to warming have been in response to a sustained increase in long-term growth temperature. Similar descriptions of  $T_{crit}$  acclimation to short-term heat stress (e.g. heatwaves) are not well documented. Considering heatwaves are predicted to become more frequent and intense (Perkins-Kirkpatrick and Lewis, 2020), it is pertinent that we understand if and how  $T_{crit}$

responds to heatwaves. Whether acclimation of  $T_{crit}$  to heatwaves has an upper threshold (i.e. a ceiling temperature) is currently unknown.

Previous uses of  $T_{crit}$  to assess global patterns of heat tolerance have been underpinned by ecological theories established in terrestrial ectotherms and endotherms (Addo-Bediako *et al.*, 2000; Deutsch *et al.*, 2008; Sunday *et al.*, 2011; Araújo *et al.*, 2013). One such theory is that organism physiology correlates closely with large-scale geographical patterns in the thermal environment where populations of an individual species evolved (Gabriel and Lynch, 1992). Indeed, greater photosynthetic heat tolerance of non-crop plants originating from hotter, equatorial environments has been reported for numerous species (O’Sullivan *et al.*, 2017; Drake *et al.*, 2018; Zhu *et al.*, 2018; Lancaster and Humphreys, 2020). It remains unknown whether such global patterns of interspecies variation hold for intraspecific comparisons – e.g. in a widely-cultivated crop like wheat, with genotypes originating from across the globe.

In this study, we employed a high-throughput system to describe intraspecies variation and high temperature acclimation of  $T_{crit}$  in wheat. Our objectives were to: (i) examine whether leaf  $T_{crit}$  varies diurnally and across phenological stages; (ii) determine the thermal safety margins and assess vulnerability of wheat to high temperatures in the Australian grain belt; and (iii) to assess if there is an upper threshold for leaf  $T_{crit}$  exposed to a sustained heat shock. To achieve these objectives, we conducted three field studies and one controlled environment experiment. In addition, we conducted a systematic literature review of wheat  $T_{crit}$  and used the global data we generated to investigate if intraspecies variation in wheat leaf  $T_{crit}$  is related to the latitude of genotype (as a proxy for climate of origin) of wheat genotypes or species.

## Materials and methods

*Field experiments: Assessing diel and phenological variation in wheat  $T_{crit}$  and estimating thermal safety margins of Australian wheat*

*Germplasm:* A set of 20–24 wheat genotypes (Table S1) were used in three field experiments conducted in Australia across three years. Twenty of these genotypes were used in Coast *et al.* (2021) to assess acclimation of wheat photosynthesis and respiration to warming in two

of the fields. The genotypes included: commercial Australian cultivars; heat tolerant materials developed by the centres of the Consultative Group on International Agricultural Research (CGIAR) in Mexico and Morocco and tested in warm areas globally; materials derived from targeted crosses between adapted hexaploid cultivars and heat tolerant Mexican hexaploid landraces, tetraploid emmer wheat (*T. dicoccon* Schrank ex Schübl.), Indian cultivars and synthetic wheat derived by crossing *Aegilops tauchii* with modern tetraploid durum wheat. All genotypes evaluated were hexaploid and chosen for their contrasting heat tolerance under high temperature conditions in Sudan (Gezira; 14.9°N 33°E), Australia (Narrabri, NSW; 30.27°S, 149.81°E) and Mexico (Ciudad Obregón; 27.5°N, 109.90°W).

*Experimental design and husbandry:* The first two years of field experiments were undertaken in regional Victoria (2017, Dingwall; and 2018, Barraport West), and the third was in regional New South Wales (2019, Narrabri). A detailed description of the experimental designs for the 2017 and 2018 experiments are reported in Coast *et al.* (2021). Briefly, a diverse panel of genotypes were sown on three dates each in 2017 (20 genotypes) and 2018 (24 genotypes) to expose crops to different growth temperatures at a common developmental stage. The first time of sowing (TOS) for both experiments were within the locally recommended periods for sowing (early May). Subsequent sowing times were one month apart in June and July. Experiments were sown in three adjacent strips, one for each TOS. Each strip consisted of four replicate blocks. The 2019 field experiment was similar in all aspects to the 2018 field experiment, except for the following: (i) only two times of sowing were incorporated in the design; (ii) the sowing times were approximately two months apart (17 May 2019 and 15 July 2019); and (iii) the soil of the two sites in Victoria were relatively infertile (Isbell, 1996), while the soil at the Narrabri site is comparatively more fertile and is a uniform grey cracking clay (USDA soil taxonomy: Typic Haplustert; Australian soil taxonomy: Grey Vertosol). Of the 24 genotypes sown in 2018 only 20, which were common to the 2017 and 2019 experiments, were assessed for  $T_{crit}$ . All three field experiments were managed following standard agronomic practices for the region by the Birchip Cropping Group ([www.bcg.org.au](http://www.bcg.org.au)) in regional Victoria, and staff of the IA Watson Grains Research Centre at The University of Sydney and AGT, in Narrabri. A summary of the field experiments is presented in Table 1.

**Table 1.** Information on field experiments in Australia

Experiment location and year	Year	Genotypes studied <sup>a</sup>	TOS <sup>b</sup>	Mean daily maximum temperature at anthesis (°C)	PAR at anthesis ( $\mu\text{mol photons m}^{-2} \text{s}^{-1}$ ) <sup>c</sup>	Rainfall (total to anthesis; mm)
Dingwall, Victoria	2017	20	1	21.4	1394	123
			2	31.6	1934	90
			3	26.6	1632	97
Barraport West, Victoria	2018	20	1	22.8	2331	69
			2	23.0	1706	73
			3	33.4	2041	67
Narrabri, New South Wales	2019	24	1	25.1	1541	362
			2	32.0	1988	162
Experiment objective	TOS <sup>b</sup>	Genotypes studied <sup>a</sup>	Brief description of method			
<i>Diurnal variation in <math>T_{crit}</math></i>						
Dingwall, Victoria	3	6	Flag leaf $T_{crit}$ determined at anthesis at four consecutive time points occurring every six hours over an 18-hour period (i.e. solar noon, sunset, midnight, and sunrise).			
<i>Phenological variation in <math>T_{crit}</math></i>						
Barraport West, Victoria	1–3	4	Flag leaf $T_{crit}$ determined at heading, anthesis, and grain filling on the same day at 10 am from all three time of sowing plots.			
<i>Rate of acclimation of <math>T_{crit}</math><sup>+d</sup> and calculation of thermal safety margins</i>						
Dingwall, Victoria	1–3	20	Times of sowing varied so that plants sown later experienced warmer growth environments at a common developmental stage. Flag leaf $T_{crit}$ determined at anthesis. Thermal safety margins were estimated as the difference between genotype mean flag leaf $T_{crit}$ at anthesis and the maximum recorded air temperature at Dingwall/Barraport West (40°C) or Narrabri (40.8°C) in October (typical month of peak wheat anthesis).			
Barraport West, Victoria	1–3	20				
Narrabri, New South Wales	1–2	24				

<sup>a</sup>Twenty genotypes were common to all experiments. The designation of all genotypes used in this study is provided in Supplementary Table S1; <sup>b</sup>Time of sowing, where the first time of sowing was within the locally recommended sowing window, with subsequent times of sowing separated in one month intervals at Victoria, or two months at New South Wales; <sup>c</sup>Mean maximum photosynthetically active radiation measured at anthesis with Licor 6400XTs light sensors; <sup>+d</sup>an additional  $T_{crit}$  high temperature acclimation study was conducted under controlled environments with two of the 24 genotypes.



*Diel measurements of wheat  $T_{crit}$ :* Six of the 20 genotypes in the 2017 field experiment at Dingwall, Victoria were used to investigate diel variation. The six genotypes were two commercial cultivars (Mace and Suntop) and four breeding lines (with reference numbers 143, 2254, 2267, and 2316). These were chosen because they are representative of the diversity of the set of 20 genotypes (Coast *et al.*, 2021). To determine if  $T_{crit}$  varied diurnally, one flag leaf from each of four replicate plants was harvested at anthesis (Zadok GS60–69; Zadoks *et al.*, 1974) from plants of TOS 3 at four consecutive time points occurring every six hours over an 18–hour period (solar noon, sunset, midnight, and sunrise).

*Phenological measurements of wheat  $T_{crit}$ :* A subset of four genotypes from the 20 in the 2018 field experiment at Barraport West, Victoria was used to assess phenological variation in  $T_{crit}$ . The four genotypes were the breeding lines 2062, 2150, 2254, and 2267, the latter two of which were also used for diel measurements as described in the previous paragraph. Plants at heading (Zadok GS50–59), anthesis (Zadok GS60–69), and grain filling (Zadok GS70–79) were respectively chosen from fields of the three times of sowing. One flag leaf was harvested from the tallest tillers of each replicate plant (minimum eight replicates) at the different phenological stages at 10 am on the same day and used to determine  $T_{crit}$ .

*Estimation of thermal safety margin of Australian wheat:* All 20 genotypes in the 2017 and 2018 field experiments in Dingwall and Barraport West respectively, as well as all 24 genotypes in the 2019 field experiment in Narrabri were used to estimate thermal safety margins. Thermal safety margins were estimated as the difference between individual genotype  $T_{crit}$  and the maximum recorded air temperature at either Dingwall or Narrabri in October. Similar definitions of thermal safety margins as the difference between the measured temperature at which a species experiences irreversible physiological damage and the maximum measured temperature of the species' habitat have been used in studies of animal ectotherms and plants (Deutsch *et al.*, 2008; Sunday *et al.*, 2014; O'Sullivan *et al.*, 2017; Sastry and Barua, 2017). We considered Barraport West and Dingwall together for their historical weather records as they are in close proximity to one another in the Mallee district of Victoria, Australia. Weather data for Dingwall and Barraport West were obtained from the Australian Bureau of Meteorology covering the period 1910–2020. We used 40°C and 40.8°C (the maximum recorded air temperature for October) in Dingwall/Barraport West and Narrabri, respectively, to quantify thermal safety margins under current climatic scenarios. October was chosen as the upper threshold of exposure of field plants at anthesis to heat

because all the later sown plants in this study were at anthesis in October. For future climatic conditions we added 2.6°C and 5°C to the current maximum temperature, with the 2.6°C addition representing the top end of the intermediate emission Representative Concentration Pathway (RCP) 4.5 IPCC scenario predicted for Eastern Australia by 2090 (1.3–2.6°C), and the 5°C addition similarly representing the top end of the high emission RCP 8.5 IPCC scenario predicted for Eastern Australia by 2090 (2.8–5°C; Climate Change Australia, 2021). Across all times of sowings in the three field experiments, flag leaves were harvested at anthesis (Zadok GS60-69) at a standardised time of 9–10 am to determine  $T_{crit}$  and estimate thermal safety margins.

*Controlled environment experiment: speed of acclimation and upper limit of leaf  $T_{crit}$  during heat shock*

A controlled environment experiment was conducted to determine the speed and threshold of the response of  $T_{crit}$  to a sudden heat shock. Two wheat genotypes – 29 and 2267 (Table S1) – which contrasted in  $T_{crit}$  under common conditions were used to assess the speed and potential threshold of the response of wheat leaf  $T_{crit}$  to sudden heat shock. This experiment was conducted at the Controlled Environment Facilities of the Australian National University (ANU), Canberra, Australia.

*Plant husbandry:* Seeds were germinated on saturated paper towel in covered plastic containers under darkness for one week. Germinated seedlings were planted in 1.05 L pots (130 mm diameter) filled with potting mix (80% composted bark, 10% sharp sand, 10% coir) with 4g L<sup>-1</sup> fertiliser (Osmocote Exact Mini fertiliser, ICL, Tel Aviv, Israel) mixed through.

*Temperature treatment:* Potted plants were grown in glasshouses in which a 24/18°C day/night temperature regime with a 12-hour photo-thermal period was maintained until tillering. At tillering, when all plants had a fully-extended third leaf (Zadok growth scale 22–29; Zadoks *et al.*, 1974), plants were moved into growth cabinets (TPG-2400-TH, Thermoline Scientific, Wetherill Park, NSW, Australia) for temperature treatment. One of two temperature conditions were imposed: a day/night regime of 24/18°C, or a heat shock with day/night temperatures of 36/24°C. White fluorescent tubes provided a 12 h photoperiod of photosynthetically active radiation of 720–750  $\mu\text{mol m}^{-2} \text{s}^{-1}$  at plant height. Leaf discs were sampled from fully extended third leaves from main tillers and used to determine  $T_{crit}$  after 2, 4, 24, 48, 72, and 120 hours in the growth cabinets. Four replicate plants were used for  $T_{crit}$

measurement at each sampling time and for each temperature condition. Plant husbandry followed standard practice at the ANU Controlled Environment Facilities.

*Meta-study (field experiments, glasshouse studies and a systematic literature review) of wheat  $T_{crit}$  relationship with origins of genotypes*

To explore how our results compare with previous studies that have assessed wheat leaf  $T_{crit}$ , and whether genotypes from hot habitats exhibit higher  $T_{crit}$ , we undertook a systematic review of the published literature and compiled data from over 30 years (1988 to 2020) of wheat leaf  $T_{crit}$  studies. A database was generated using information from a recently published systematic review on global plant thermal tolerance (Geange *et al.*, 2021) and additional literature search. These published data were combined with data from the three field experiments described above. The multiple times of sowings in each of the three Australian field experiments provided us with eight thermal environments for obtaining wheat leaf  $T_{crit}$  from a total of 24 wheat genotypes. We also included unpublished wheat leaf  $T_{crit}$  data from nine other experiments conducted in controlled environment facilities at the Australian National University. Overall, our global dataset included 3223 leaf  $T_{crit}$  samples from 183 wheat genotypes of various species (*T. aestivum* L., *T. turgidum* L., ssp. durum Desf., *T. turgidum* L., ssp. diococcoides Thell.) and wild wheat (*Aegilops* species).

*Determination of leaf  $T_{crit}$*

Leaves were harvested and stored in plastic bags alongside a saturated paper towel and were left to dark adapt for a minimum of 20 minutes. Water (90  $\mu$ l) was placed in each well of a 48-well Peltier heating block in order to ensure leaf samples remained hydrated throughout the assay. A single 6 mm diameter leaf disc was excised from the middle of each harvested dark-adapted leaf and placed within each well of the heating block. Once discs were all loaded into the heating block, a glass plate was used to enclose the wells to prevent leaf pieces from drying out during the assay. The block was then placed directly beneath the lens of an imaging fluorometer (*FluorCam 800MF*, Photon Systems Instruments, Brno, Czech Republic) and programmed to heat from 20 to 65°C at a rate of 1°C min<sup>-1</sup>. The fluorometer recorded  $F_0$  throughout the heating period (approximately one record per minute). Following the conclusion of the temperature ramp, fluorescence data was processed and used to estimate  $T_{crit}$ , which was calculated according to the method detailed by Schreiber & Berry (1977), using

the R package ‘segmented’ (Muggeo 2008). Briefly, the package identifies the breakpoint in data containing a broken-line relationship by estimating linear and generalised linear models. This breakpoint in the  $F_0$  curve was recorded as  $T_{crit}$ .

### *Statistical analysis*

Statistical analyses were carried out within the R statistical environment (v. 3.4.4; R Core Team, 2018) with R Studio. For analysis of the field data we employed linear mixed models in R using the packages lmerTest (Kuznetsova *et al.*, 2017) and emmeans (Lenth, 2020). Genotype was a fixed term in all models, as was time of day (for the analysis of diel variation), developmental stage (for the analysis of phenological variation), and time of sowing (for the analysis of growth temperature variation), while replicate was included as a random term. The ceiling threshold of  $T_{crit}$  under heat stress (of 36°C), in the controlled environment experiment, was determined by fitting a non-linear regression to the  $T_{crit}$  by time relationship. Then using the coefficients of the fitted regressions we estimated the time at which the fitted  $T_{crit}$  was highest, and this was taken as the time to peak acclimation. To test the relationships between  $T_{crit}$  and growth environment temperature, we only used data from the three field experiments in Australia, for which we had reliable data. The 24 genotypes studied under field conditions in Australia were grouped based on the region of origin of their pedigree (Aleppo, Syria; Gezira, Sudan; Narrabri, Australia; Obregón, Mexico; Pune, India; and Roseworthy, Australia) and the relationship examined using linear or bivariate regressions. Our global dataset (see Table 2 for sources) was used to ascertain the link between wheat leaf  $T_{crit}$  and climate of origin by regressing mean genotype  $T_{crit}$  with genotype latitude (as a proxy for climate) of origin.

## **Results**

### *Diel and phenological variation in $T_{crit}$*

There was significant genotype by time of day interaction for  $T_{crit}$  ( $P=0.042$ ; Table S2), highlighting the heterogeneity in this diel variation of  $T_{crit}$  among our genotypes. In all but genotype 2316,  $T_{crit}$  tended to be highest at solar noon before then declining through sunset, midnight, and sunrise. The slope of these trends was only significant for genotype 2267, with

$T_{crit}$  declining by 3.1°C from solar noon to sunrise. By contrast, genotypes 143 exhibited the narrowest diel range in  $T_{crit}$ , with difference of 1.1°C between solar noon and sunrise. Irrespective of genotype,  $T_{crit}$  at solar noon was significantly higher than at sunrise ( $P < 0.001$  for time of day).  $T_{crit}$  also showed a significant genotype by phenology interaction, and highly significant differences for the main effects of genotype as well as phenological stage (Table S2). The interaction effect was largely due to the increasing trend in  $T_{crit}$  as plants developed from heading to anthesis and grain filling for genotypes 2267, 2254 and 2062 but not for 2150 (Fig. 1B).  $T_{crit}$  of genotype 2150 rose slightly between heading and anthesis then declined significantly at grain filling relative to anthesis. Genotype 2254 showed the largest increase in  $T_{crit}$  between heading and anthesis, rising 1.8°C from 44.4°C to 46.2°C.

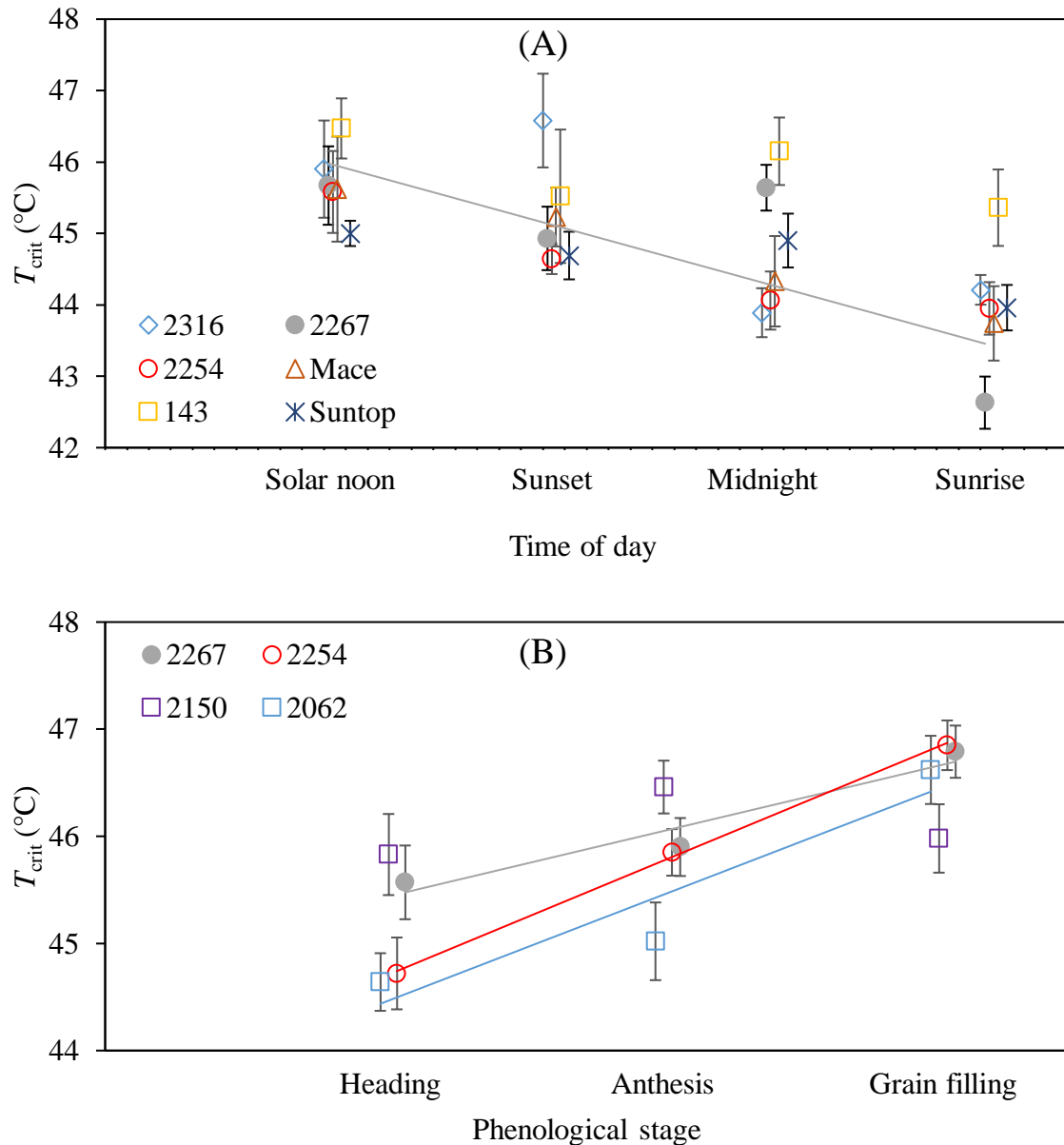


**Figure 1.** Variation in flag leaf  $T_{crit}$  (°C) of wheat genotypes over the course of an 18 h period (A), and across three phenological stages (B). Solid lines indicate significant linear trends. Plants were grown at field sites in Dingwall, Victoria in 2017 (A), and in Barraport West, Victoria in 2018 (B). Points represent mean  $\pm$  se,  $n = 4$  for (A) and  $n = 8-18$  for (B).

#### *Thermal safety margins of Australian wheat*

At Dingwall, only the main effect of TOS was significant (Table S3). In comparison to TOS 1,  $T_{crit}$  of TOS 2 tended to be higher and TOS 3 tended to be lower (Fig. 2A). At Barraport,  $T_{crit}$  varied amongst the genotypes over a range of about 2°C and the effect of TOS on  $T_{crit}$  depended on the genotype ( $P < 0.01$  for Genotype by TOS interaction).  $T_{crit}$  increased more in

some genotypes (e.g. 1132, 143 and Trojan) under later sowing than others (e.g. 2267 and 29), but also did not change significantly in some (e.g. 1898 and 1943; Fig. 2B). At Narrabri, only the main effects were significant, i.e. genotypes varied in their  $T_{crit}$  and TOS 3  $T_{crit}$  was higher than TOS 1 (Table S3, Fig. 2C). Across TOS, the genotypes with the lowest and highest mean  $T_{crit}$  were 1704 (45.3°C) and 143 (46.7°C) respectively. Across the 24 genotypes,  $T_{crit}$  increased by 0.5°C from TOS 1 (at 45.7°C) to TOS 3 (at 46.2°C). An analysis of variance run on a linear mixed effects model of the entire field data set revealed field site to be the largest source of variation in  $T_{crit}$  of all our independent variables (d.f. = 2,  $F$  value = 190.9,  $P$  < 0.001). The overall mean  $T_{crit}$  at each of the field sites was 45.1°C at Barraport West, 44.1°C at Dingwall, and 45.9°C at Narrabri.

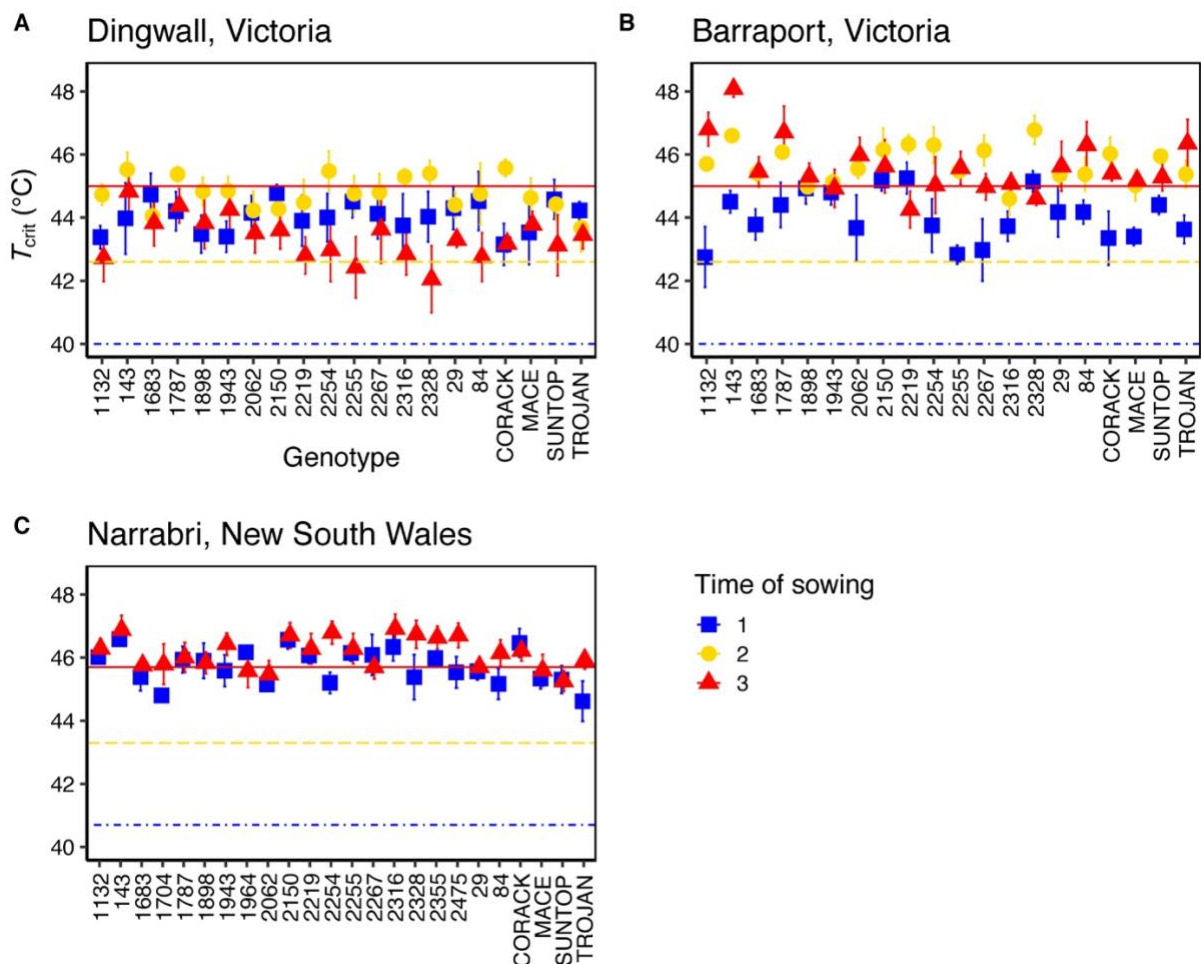


**Figure 2.** Phenotypic plasticity of leaf  $T_{crit}$  and thermal safety margins of 20–24 wheat genotypes. The genotypes were sown at either the locally recommended time of year (time of sowing 1; blue squares); one month after the recommended time (time of sowing 2; yellow circles); or two months after the recommended time (time of sowing 3; red triangles) at three Australian field sites. Delayed times of sowing were used to impose warmer average growth

temperatures for plants sown at times of sowing 2 and 3. The field sites were Dingwall (A) and Barraport West (B), Victoria, and Narrabri, New South Wales (C). Twenty genotypes were sown at Dingwall in 2017 and Barraport West in 2018, and the same 20 plus an additional four genotypes were sown at Narrabri in 2019. The dash-dot blue lines mark the hottest recorded maximum temperature during the typical anthesis month (October) at each field site (40.7°C for Narrabri, and 40°C for Dingwall, data from the Australian Bureau of Meteorology; due to the close proximity of Dingwall and Barraport West we used the same climate records for these sites) while the yellow dashed line and the red solid line mark the RCP 4.5 IPCC and RCP 8.5 IPCC emission scenarios (+2.6 and +5°C), respectively. The difference between the observed  $T_{crit}$  and these current and future maximum temperatures is termed the thermal safety margin. Here we assume that leaf temperature is equal to air temperature. Points represent mean  $\pm$  s.e., minimum  $n = 4$ .

Thermal safety margins were calculated for all field-grown genotypes by quantifying the difference between  $T_{crit}$  and the maximum air temperature recorded during October. All genotypes demonstrated a higher  $T_{crit}$  than the historical maximum October air temperatures recorded at each field site (Fig. 2, dash-dot blue line). Thermal safety margins in the TOS 1 fields ranged from 3.2–4.8°C in Dingwall (Fig. 2A), to 2.8–5.3°C in Barraport West (Fig. 2B) and from 3.8–5.8°C in Narrabri (Fig. 2C). For the later grown crops (i.e. TOS 2 and 3) which experienced warmer growth temperatures, thermal safety margins increased relative to TOS 1 in Dingwall (3.7–5.6°C for TOS 2), in Barraport West (4.6–6.8°C for TOS 2, and 4.3–8.1°C for TOS 3) and in Narrabri (4.5–6.1°C). The exception to this pattern was TOS 3 at Dingwall where the lower end of the thermal safety margin range declined, resulting in a range of 2.1–4.8°C. At both Narrabri and Barraport West, mean  $T_{crit}$  of all genotypes was above the +2.6°C mark associated with the RCP 4.5 intermediate emission scenario (Fig. 2B & 2C, dashed yellow line). Most genotypes were also largely clear of the RCP 4.5 mark at Dingwall, except the  $T_{crit}$  of genotypes 2255 and 2328 sown at TOS 3 were below this threshold. The +5°C warming mark associated with the high emission RCP 8.5 scenario was equal to or above the  $T_{crit}$  of many genotypes at all three field sites, though there was some variation across the locations. At Narrabri, half of the genotypes were below the RCP 8.5 threshold when sown at TOS 1, while this fell to a quarter of genotypes when sown at TOS 3 (Fig. 2C). At TOS 1 in Barraport West, 17 genotypes fell below the RCP 8.5 threshold, with only one and three genotypes below this mark for TOS 2 and 3, respectively (Fig. 2B). At Dingwall,  $T_{crit}$  of all genotypes sown at TOS 1 and TOS 3 was below the RCP 8.5 threshold, while 14 genotypes at TOS 2 were below this mark (Fig. 2A).



*Genotype origin does not predict variation or acclimation in  $T_{crit}$*

The 24 genotypes grown across the three field sites were grouped by the regions from which they originated (Table S1; Aleppo, Syria; Gezira, Sudan; Narrabri, Australia; Obregón, Mexico; Pune, India; and Roseworthy, Australia) in order to determine if this explained any of the observed variation in  $T_{crit}$ . Genotype origin had a significant effect on  $T_{crit}$  at both Barraport West and Narrabri (Table S4). At Barraport West, genotypes that originated in Narrabri had the highest  $T_{crit}$  and Sudan the lowest (Fig. 3). At Narrabri, the genotype that originated from Syria had the highest  $T_{crit}$  whereas those from Roseworthy had the lowest. By contrast, genotype origin had no significant effect on  $T_{crit}$  at Dingwall. TOS had a significant effect on  $T_{crit}$  at all three sites irrespective of origin. In Dingwall  $T_{crit}$  was lower for TOS 3 relative to TOS 1 and 2, while in Barraport West  $T_{crit}$  was lower for TOS 1 than for TOS 2 and 3 (Fig. 3). At the Narrabri site,  $T_{crit}$  increased from TOS 1 to TOS 3 for all origin groupings (Fig. 3C). No interaction between time of sowing and genotype origin was observed at any field site (Table S4).

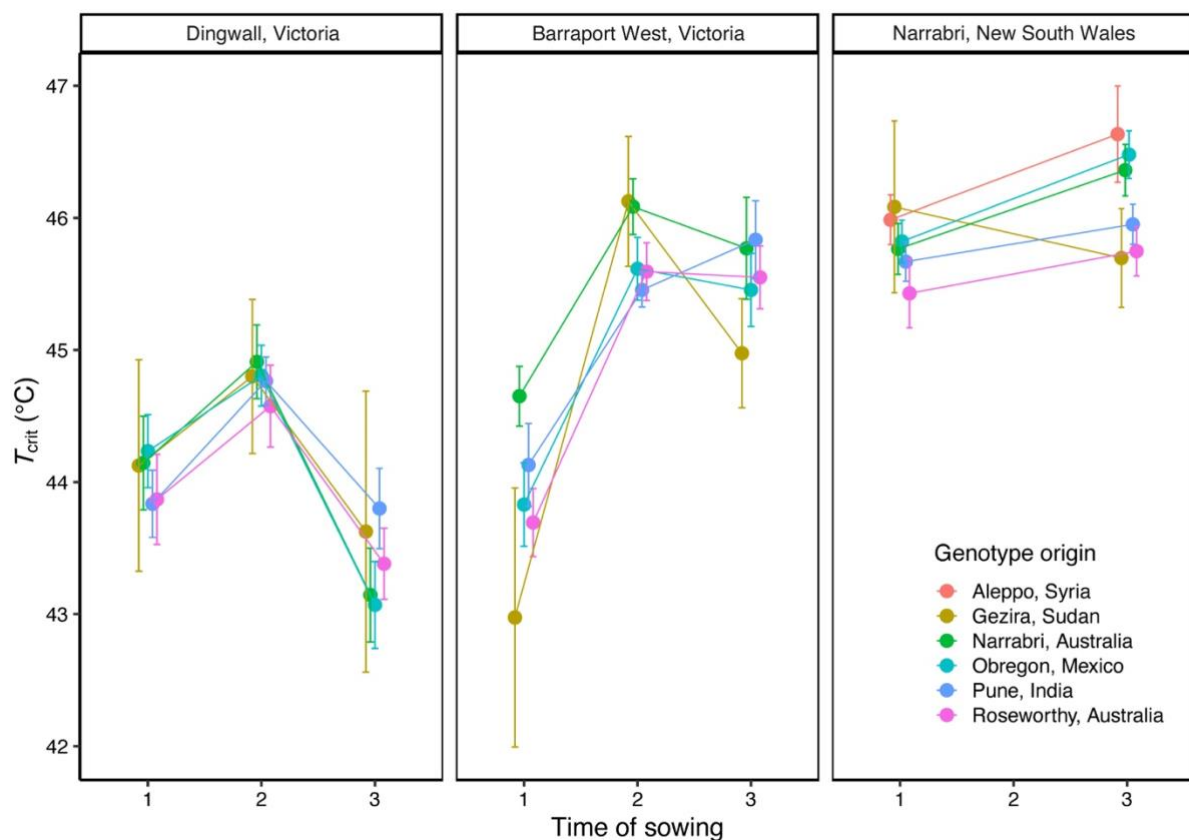


**Figure 3.** Phenotypic response of wheat flag leaf  $T_{crit}$  to time of sowing at three Australian field sites: Dingwall, Victoria; Barraport West, Victoria; and Narrabri, New South Wales.

Genotypes are grouped according to the six locations of the breeding programmes where they were developed. Twenty genotypes were grown at Dingwall in 2017 and at Barraport West in 2018, while the same 20 plus an additional four genotypes were grown in Narrabri in 2019. In order to generate increasingly warmer growth temperature regimes plants were sown at one of three times of sowing: time of sowing 1 (TOS 1) was in May, the locally recommended time of sowing, while time of sowing 2 (TOS 2) and time of sowing 3 (TOS 3) were one and two months after TOS 1, respectively. Points represent mean  $\pm$  se, minimum  $n = 4$ .

*Response of  $T_{crit}$  to short-term exposure to high temperature and upper limit of  $T_{crit}$  plasticity*

In the two genotypes studied,  $T_{crit}$  increased significantly following two hours of heat shock (Fig. 4). In both genotypes,  $T_{crit}$  increased during the heat shock following a curvilinear pattern which peaked after 3.4 days for genotype 2267 and 4.2 days for genotype 54. Although the time to reach peak  $T_{crit}$  during the heat shock differed for the two genotypes, their maximum  $T_{crit}$  values were similar, being 43.8°C for genotype 29 and 43.6°C for genotype 2267 (Fig. 4).  $T_{crit}$  for both genotypes remained largely constant over the 120 hour period for those plants that were maintained at the control day/night temperature regime of 24/12°C.

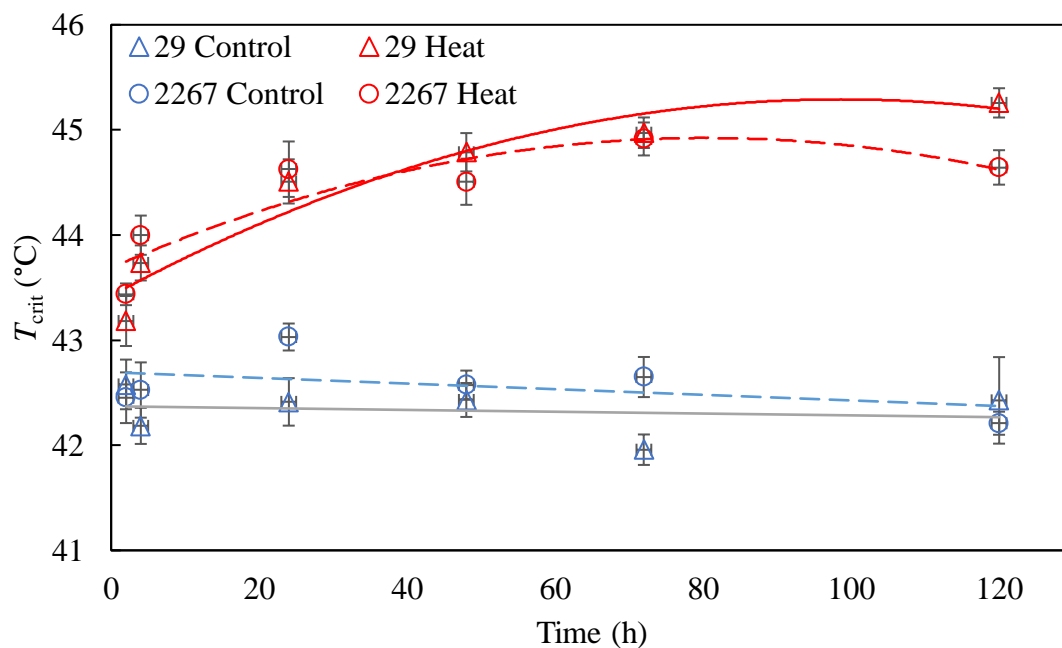


**Figure 4.** Leaf  $T_{crit}$  (°C) of two wheat genotypes – 29 (triangles and solid lines) and 2267 (circles and dashed lines) exposed to 24°C (control; blue shapes and lines) or 36°C (heat; red shapes and lines) for varying durations (2, 4, 24, 48, 72, or 120 h) in a growth cabinet. Leaf samples for  $T_{crit}$  were from the third fully extended leaves on the main stem. Equations for the curvilinear relationships between  $T_{crit}$  at 36°C ( $T_{crit}^{36}$ , °C) and time ( $t$ ; hour) under heat for genotype 29 is  $T_{crit}^{36} = 43.42 + 0.038t - 0.00019t^2$  and for genotype 2267 is  $T_{crit}^{36} = 43.69 + 0.031t - 0.00019t^2$ . Points represent mean  $\pm$  se,  $n = 4$ .

### Global variation in wheat $T_{crit}$

We combined data from our experiments with previously published data (covering genotypes grown across field and controlled environment experiments) to examine the degree of variation in  $T_{crit}$  in wheat genotypes on a global scale based on the latitude of origin as a proxy for climate of origin of their pedigree (Fig. 5). We found three studies (Havaux *et al.*, 1988; Rekika *et al.*, 1997; Végh *et al.*, 2018) that reported wheat leaf  $T_{crit}$  using similar fluorescence temperature response curves (with ramp rates of 1–1.5°C min<sup>-1</sup> between 20–65°C) to estimate  $T_{crit}$ . Our final data collation comprised 183 wheat species/varieties (comprising *T. aestivum* L., *T. turgidum* L., *ssp. durum* Desf., *T. turgidum* L., *ssp. diococcoides* Thell., and wild wheat – *Aegilops* species) originating from all continents except Antarctica (Table 2). Globally, wheat leaf  $T_{crit}$  varied by up to 20°C (35–55°C) and there were more data for studies under warm conditions for genotypes originating from the lower latitudes than high latitudes (Fig 5). The larger variation in  $T_{crit}$  for genotypes originating from the higher latitudes coincided with the cooler growth conditions. Overall, there was less variation in  $T_{crit}$  under the warm conditions. We found no relationship between wheat leaf  $T_{crit}$  and the absolute latitude of genotype climate of origin (Fig. 5).

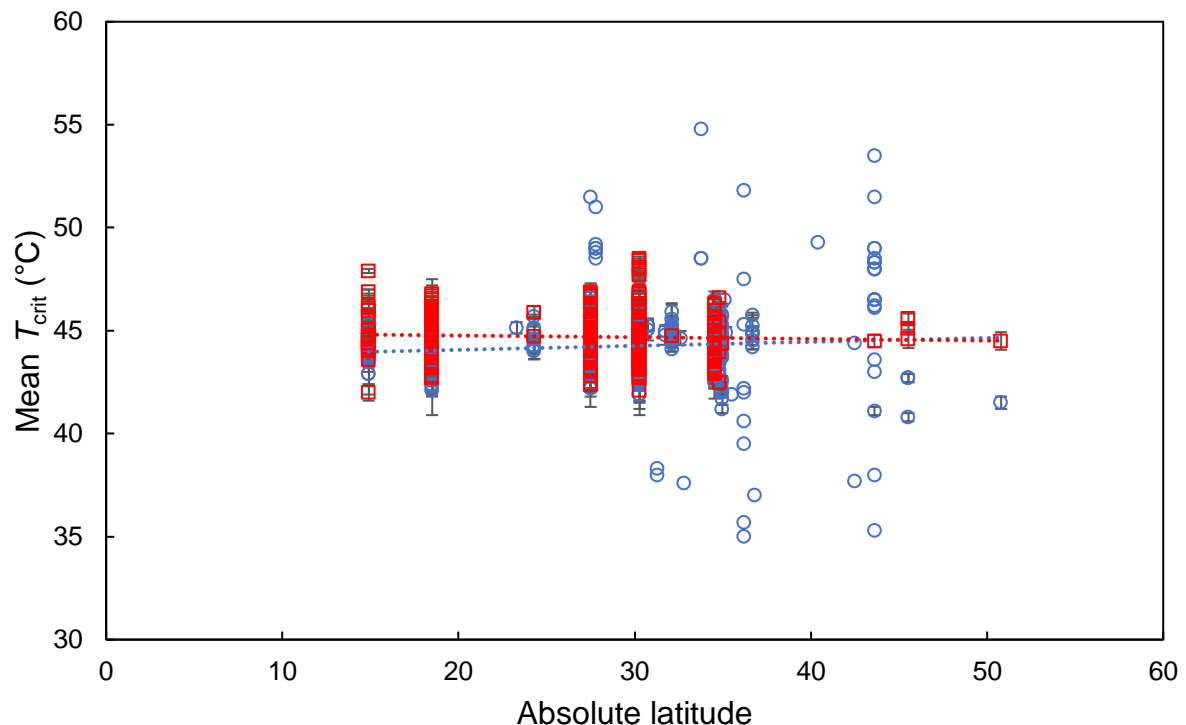


**Figure 5.** Relationship between  $T_{crit}$  and the absolute latitude of the climate of origin for wheat genotypes when grown under cool (blue circles) and warm (red squares) conditions. Data obtained from 183 wheat genotypes (3223 measurements of leaf  $T_{crit}$  overall) from experiments in Australia (this study) and published literature (Havaux *et al.*, 1988; Rekika *et*

*al.*, 1997; Végh *et al.*, 2018). Data points represent mean  $T_{crit}$  ( $\pm$  SE where visible) for each genotype.

**Table 2.** Source of data used for assessment of global variation in leaf photosynthetic heat tolerance ( $T_{crit}$ ).

Study <sup>1</sup>	Origin	Species	Mean $T_{crit}$ (n)
This study	Asia	<i>Triticum aestivum</i> L.	45.1 (8)
	Africa	<i>T. aestivum</i> L.	44.6 (1)
	Australia	<i>T. aestivum</i> L. and <i>T. dicoccum</i> Schrank	44.7 (9)
	North America	<i>T. aestivum</i> L.	45.0 (6)
<b>Average</b>			<b>44.8 (24)</b>
Havaux <i>et al.</i> (1988)	Africa	<i>T. turgidum</i> L., ssp. <i>durum</i> Desf.	49.7 (9)
	Europe	<i>T. turgidum</i> L., ssp. <i>durum</i> Desf.	48.1 (19)
	North America	<i>T. turgidum</i> L., ssp. <i>durum</i> Desf.	51.8 (1)
	South America	<i>T. turgidum</i> L., ssp. <i>durum</i> Desf.	49.0 (2)
<b>Average</b>			<b>48.7 (31)</b>
Végh <i>et al.</i> (2018)	Europe	<i>T. aestivum</i> L.	<b>41.8 (5)</b>
Rekika <i>et al.</i> (1997)	Africa	<i>T. turgidum</i> L., ssp. <i>durum</i> Desf.	37.0 (1)
	North America	<i>T. turgidum</i> L., ssp. <i>durum</i> Desf.	35.0 (1)
	Europe	<i>T. turgidum</i> L., ssp. <i>durum</i> Desf.	37.2 (3)
		<i>T. turgidum</i> L., ssp. <i>diococcoides</i> Thell.	38.0 (1)
	Europe (wild wheat)	<i>Aegilops species</i>	38.2 (5)
<b>Average</b>			<b>37.5 (11)</b>
Unpublished data from our group	Asia	<i>T. aestivum</i> L.	43.8 (21)
	Africa	<i>T. aestivum</i> L.	45.2 (1)
	Australia	<i>T. aestivum</i> L. and <i>T. dicoccum</i> Schrank	44.5 (79)
	North America		43.9 (32)
<b>Average</b>			<b>44.2 (133)</b>

<sup>1</sup>The fluorescence temperature response curves used in these studies were similar (ramp rate of 1–1.5°C min<sup>-1</sup>, in the 20–65°C range). Values in bold are study averages and those in parentheses indicate number of genotypes/species used.

## Discussion

Given the increasing pressure that wheat yields are experiencing from continued warming and heat stress events, identifying existing variation in wheat photosynthetic heat tolerance is an important step in the process of future-proofing wheat yield. In this study we used a

high-throughput technique to record minimal chlorophyll *a* fluorescence and quantified the critical temperature ( $T_{crit}$ ) of photosystem II damage – a measure of leaf photosynthetic heat tolerance – for wheat genotypes grown in multiple field experiments, as well as a controlled environment experiment. The field experiments demonstrated the extent of variation in  $T_{crit}$  over the course of a single day, as well as across several crucial stages of phenological development. They also showed that the region of origin of wheat genotypes were unrelated to  $T_{crit}$  in three representative Australian wheat growing regions, and that sowing time (and thus, growth temperature) was responsible for significant variation in  $T_{crit}$ . Delayed sowing (i.e. elevated growth temperature) was generally associated with increases in  $T_{crit}$ , resulting in higher thermal safety margins at both field sites. When two genotypes were subjected to a sudden heat shock in a controlled environment, we observed a slight difference between genotypes in the speed with which  $T_{crit}$  increased. However, both genotypes exhibited a similar peak  $T_{crit}$  value during this heat shock. Finally, when combining these data with previously published wheat  $T_{crit}$  data, as well as unpublished data from other experiments conducted in controlled environment facilities at The Australian National University, we found that the absolute latitude of pedigrees of wheat genotypes were not significantly linked with variation in  $T_{crit}$  for either cool or warm grown plants.

#### *Wheat $T_{crit}$ exhibits plasticity over both short- and long-term timescales*

Wheat  $T_{crit}$  varied significantly over the course of a single day, declining by an average of 1.7°C over the 18 hours from solar noon to sunrise (Fig. 1A). This pattern resembles the extent of change in  $T_{crit}$  in a temperate tree species reported by Hüve *et al.* (2006); specifically, a linear increase over 14 hours, from a low point at 5 am to a peak at 7 pm. Taken together, these findings suggest that  $T_{crit}$  generally increases to a peak during the late afternoon before declining to a minimum between midnight and dawn. Hüve *et al.* (2006) linked this diel variation in  $T_{crit}$  with daily variation in leaf sugar content, and demonstrated that  $T_{crit}$  increased when leaves were fed sugar solutions. The link between leaf sugar content and PSII heat tolerance likely stems from the stabilising effect that sugars have on thylakoid membrane thermostability, with higher molecular weight sugars having a greater protective effect during temperature stress (Santarius, 1973). Further work is needed to determine if the diel variation in  $T_{crit}$  that we observed in wheat was also influenced by corresponding variation in leaf sugar content.

It is also interesting to compare the extent of variation in  $T_{crit}$  that was observed over the course of a single day with the extent of variation that was observed across phenological stage. In the 18 hours between solar noon and sunrise  $T_{crit}$  declined by 1.7°C (Fig. 1A), a fluctuation that was similar in size to the 1.5°C rise in  $T_{crit}$  that we observed from heading to anthesis (Fig. 1B). This comparison highlights the high level of plasticity in  $T_{crit}$ , and that variation in  $T_{crit}$  is clearly responsive to factors on both an hours-long timescale (i.e. diurnal fluctuations in leaf sugar content) and a longer term weeks-long scale (as evidenced by changes in  $T_{crit}$  from heading to anthesis and grain filling, possibly linked to changes in membrane fatty acid composition). Anthesis is widely considered the phenological stage at which high temperature has the most severe consequences for wheat yield (Ferris *et al.*, 1998; Thistlethwaite *et al.*, 2020), with this vulnerability largely due to a reduction of sink strength to import and utilize assimilates within the reproductive organs, rather than of assimilate supply from leaf photosynthesis per se (Li *et al.*, 2012; Ruan *et al.*, 2012). While this increase could reflect an ongoing rise in heat tolerance coinciding with seasonal warming, there was no significant difference in  $T_{crit}$  between plants undergoing anthesis versus those at the grain filling stage. Therefore, it is possible that anthesis may be the phenological stage at which  $T_{crit}$  peaks, potentially reflecting an acclimation pattern where the timing of peak PSII heat tolerance is synchronised with the most vulnerable stage of development.

#### *Drivers of variation in wheat $T_{crit}$*

The field site at which plants were grown was the most significant source of variation in  $T_{crit}$ ; the overall average  $T_{crit}$  at Narrabri was 1.8°C higher than recorded at Dingwall and 0.8°C higher than at Barraport West. In addition to environment, genotype had significant effect on  $T_{crit}$  at the Barraport West and Narrabri sites. These results suggests that environment, genotype, and most likely the genotype-by-environment interactions (GxE) may play large roles in determining wheat flag leaf  $T_{crit}$ . Breeding for genotypes with greater photosynthetic heat tolerance (i.e. higher  $T_{crit}$ ) may be challenging if variation in  $T_{crit}$  is also influenced by GxE effects. GxE effects have been reported for other abiotic stress tolerance traits including lodging tolerance in spring wheat (Dreccer *et al.*, 2020), and drought tolerance in maize (Dias *et al.*, 2018).

#### *Genotypes maintain moderate photosynthetic thermal safety margins*

We observed variation in the thermal safety margins of wheat genotypes, predominantly associated with differences between field sites and the effect of sowing time at these sites. The thermal safety margin was 2.1°C when averaged across all genotypes (Fig. 2). Thermal safety margins in three representative Australian wheat-growing regions were at least 2–4°C for all genotypes.  $T_{crit}$  was always several degrees greater than the hottest recorded air temperature during the typical month of anthesis at each site (Narrabri, 40.8°C, Dingwall/Barraport West 40°C; denoted by the blue dot-dash lines in Fig. 2). Under the IPCC's RCP 4.5 intermediate emission scenario for Eastern Australia by 2090, most genotypes would maintain a positive, yet reduced, thermal safety margin in the studied growing regions. However, under the high emission RCP 8.5 scenario, the thermal safety margins of most genotypes grown at the Dingwall site and a few genotypes at the Barraport West site would be exceeded (Fig. 2A & 2B). For genotypes grown at the Narrabri site, thermal safety margins under the RCP 8.5 scenario would be drastically reduced and, in some cases, disappear (Fig. 2C). According to our  $T_{crit}$  observations, only genotypes originating from Obregón and Aleppo would retain positive thermal safety margins under the RCP 8.5 scenario when sown at either optimal or delayed sowing times. The rise in  $T_{crit}$  with delayed sowing (and thus increased growth temperature) that we observed in the majority of genotypes indicates a widespread capacity for the thermal acclimation of wheat flag leaf  $T_{crit}$ . This suggests that thermal safety margins for wheat photosynthetic heat tolerance could yet increase in response to warming under future climate scenarios. However, given that we also observed an apparent limit to the acclimation of  $T_{crit}$  following sudden heat shock (Fig. 4), it is possible that daytime maximum temperatures could approach this physiological thermal limit of wheat PSII if the most severe global warming predictions are borne out. A hard limit to the high temperature acclimation of  $T_{crit}$  could indicate a physiological limitation of PSII, or a temperature that represents the absolute maximum tolerance. Given that the considerable thermal plasticity of PSII electron transport has been closely linked with improving photosynthetic heat tolerance more generally (Yamasaki *et al.*, 2002), the prospect of air temperatures approaching the physiological threshold of PSII high temperature acclimation is concerning.

Thus far, in assessing thermal safety margins we have assumed parity between air and leaf temperatures; however, wheat leaf/canopy temperature can differ substantially from air temperature. Balota *et al.* (2007) reported canopy temperatures ranging from 3°C below noon air temperatures to 10°C above noon air temperatures in dryland wheat, and 3°C below

noon air temperatures to 5.7°C above noon air temperatures in irrigated wheat. Similarly, canopy temperatures of Australian wheat have also been recorded exceeding afternoon air temperature by 0.3–2.3°C (Ratley *et al.*, 2011) and 3–5°C (Rebetzke *et al.*, 2013). These examples, along with other previous instances (Rashid *et al.*, 1999; Thapa *et al.*, 2018), highlight the significant genotypic variation in canopy cooling and thus the potential for achieving gains in performance under high temperature by exploiting this variation. While greater levels of canopy cooling could increase thermal safety margins by limiting leaf temperature, achieving gains in wheat  $T_{crit}$  could also provide an avenue to maintaining positive thermal safety margins by increasing the threshold to PSII damage. Enhancing thermal safety margins by increasing  $T_{crit}$  could be particularly important in water-limited environments considering that heatwaves are frequently accompanied by drought, which increases stomatal closure and limits transpirational cooling, resulting in increased leaf temperature (Aspinwall *et al.*, 2019).

#### *$T_{crit}$ increases within hours of heat shock, and peaks after 3–4 days*

We observed widespread evidence of wheat  $T_{crit}$  plasticity following exposure to high temperature, including elevated growth temperature in the field (via delayed sowing, Fig. 2 & 3) and sudden heat shock under controlled conditions (Fig. 4). We also saw clear genotypic variation in the plasticity of  $T_{crit}$  across these experiments. In some genotypes  $T_{crit}$  rose by upwards of 4°C when sowing time was delayed by two months (Fig. 2B), while in others  $T_{crit}$  showed no change or even declined by up to 1.2°C from TOS 1 to TOS 3 (Fig. 2A). Similarly, following a heat shock imposed under controlled conditions we observed a difference between two genotypes in the speed at which  $T_{crit}$  increased despite the two genotypes eventually reaching a similar peak  $T_{crit}$  (Fig. 4). Genotypic variation is thus evident not only in wheat flag leaf  $T_{crit}$  under common non-stressful temperatures, but also in the extent of  $T_{crit}$  plasticity in response to sudden heat shock. Increases in  $T_{crit}$  with warming have been reported previously (O’Sullivan *et al.*, 2017; Zhu *et al.*, 2018) and these are considered examples of high temperature acclimation. That we observed similar patterns in wheat  $T_{crit}$ , as well as genotypic variation in this acclimation, suggests that the capacity to increase PSII heat tolerance could be a trait worth targeting for the development of wheat genotypes with greater heat tolerance. However, further work is needed to first investigate whether such acclimation is associated with enhanced performance under high temperature in the field.



One aspect of the current study that may aid such future efforts is the development of high throughput minimal chlorophyll *a* fluorescence assays that can be used for large-scale screening of wheat PSII heat tolerance. When combined with other burgeoning high throughput techniques for measuring photosynthetic characteristics (Sharma *et al.*, 2012; Silva-Pérez *et al.*, 2018; Fu *et al.*, 2019; McAusland *et al.*, 2019; Arnold *et al.*, 2021), it is becoming increasingly achievable to efficiently measure a range of traits that provide insight into the photosynthetic thermal tolerance of entire plots in crop breeding trials.

*Thermal environment of growth site may be more influential than genotype origin in determining variation in wheat flag leaf  $T_{crit}$*

Considering the potential benefits to wheat heat tolerance and performance under high temperature that could arise from achieving increases in  $T_{crit}$ , as well as the extent of variation that we observed in  $T_{crit}$  among 24 genotypes at three field sites, it would be beneficial to identify characteristics that predict high  $T_{crit}$  in wheat genotypes. Thus, we analysed whether the distinct regions from which our genotypes originated could reliably predict variation in  $T_{crit}$ . Previous studies of (mostly) woody, non-crop species found that  $T_{crit}$  was correlated with climate of origin (O'Sullivan *et al.*, 2017; Zhu *et al.*, 2018). In a similar vein, we found evidence of genotype region of origin significantly affecting  $T_{crit}$  at two of our field sites (Fig. 3A & 3C). One consistency at both of these sites was that genotypes originating from Roseworthy, Australia generally exhibited the lowest or second-lowest mean  $T_{crit}$  values. By contrast, the genotype from Aleppo exhibited the highest  $T_{crit}$  at the Narrabri site (Fig. 3C), while at the Barraport West site the genotypes originating from Narrabri had the highest mean  $T_{crit}$  across all times of sowing (Fig. 3A). However, it seems unlikely that the effect of genotype region of origin is the result of differences in temperature at these locations: for instance, the average daily maximum April temperature in Aleppo, Syria is 23°C (NOAA), while the average daily October maximum in Roseworthy, Australia is 23.8°C (Australian Bureau of Meteorology). Therefore, the observed variation associated with genotype origin is likely related to a more complex combination of environmental differences between locations (e.g. rainfall, temperature, soil quality, agricultural practices). Differences in the aims and methods of breeding programs across locations could also contribute to this variation. We also note that our experiments did not include genotypes originating from cooler environments, such as

wheat growing regions in Europe or Northern America, and so further work may be required to capture the full extent of global variation in wheat  $T_{crit}$ .

Upon combining our experimental data with data from the literature we also found no evidence of a relationship between wheat leaf  $T_{crit}$  and the latitude of genotype climate of origin, irrespective of thermal acclimation (Fig. 5). This contradicts previous results that reported a decrease in PSII heat tolerance with increasing latitude (O'Sullivan *et al.*, 2017; Lancaster and Humphreys, 2020). This discrepancy could be related to differences between cultivated and wild species: the O'Sullivan *et al.* (2017) and Lancaster and Humphreys (2020) studies demonstrated a relationship between heat tolerance and latitude based almost entirely on records of different wild species. By contrast, our study focuses solely on one domesticated species. Wheat is known as a crop with a particularly narrow genetic background (Tanksley and McCouch, 1997), but we observed a large range of  $T_{crit}$  in wheat here (up to 20°C) which compares with the approximately 30°C global range reported across 218 plant species spanning seven biomes reported by O'Sullivan *et al.* (2017). This large range of wheat leaf  $T_{crit}$  can be exploited to improve heat tolerance in modern crop varieties, as has been done recently in successful efforts to improve wheat drought tolerance (Reynolds *et al.*, 2015). Still, wheat is cultivated in a wide range of ecological and climatic conditions, covering over 220 million hectares, including areas where it is exposed to high temperature stress. As such, we predicted that the rise in  $T_{crit}$  that we observed with elevated growth temperature in our experimental data set (Fig. 1–4) would also be apparent in the meta-analysis. However, there was no evidence of any thermal acclimation response of  $T_{crit}$  in this larger data set. This could partly be due to diversity of experimental methods used to generate the data in Figure 5, as well as variation in the duration and intensity of elevated growth temperature treatments. Given that the plant thermal tolerance field uses a large and diverse range of experimental designs and assays (Geange *et al.*, 2021), the results of our systematic review of wheat  $T_{crit}$  could be further evidence of a need to better standardise the approaches used to measure and describe photosynthetic heat tolerance.

### *Conclusion*

Wheat leaf  $T_{crit}$  varied dynamically with changes in growth conditions, notably increasing in response to short and long-term high temperatures, and exhibited an upper ceiling in acclimating to heatwaves. There was also evidence of developmental, diel and genotypic

variation in  $T_{crit}$ . These results suggested a strong genotype-by-environment interaction effects on wheat leaf  $T_{crit}$  and potential links between  $T_{crit}$  and leaf sugar content. Interestingly, global wheat leaf  $T_{crit}$ , which spanned up to 20°C, was unrelated to genotype climate of origin and latitude, unlike reported associations with global interspecies variation in leaf  $T_{crit}$  of 171 plant species (*cf.* ~30°C). However, the observed genotypic variation and plasticity of wheat  $T_{crit}$ , combined with the recent development of a high throughput technique for measuring  $T_{crit}$  (Arnold et al 2021), indicate that this trait would be useful for high-throughput screening, understanding photosynthetic heat tolerance, and the development of heat tolerant wheat.

## Acknowledgements

We acknowledge and celebrate the First Australians on whose traditional lands this research was undertaken and pay our respect to the elders past and present. This work was supported by grants from the ARC Centre of Excellence in Plant Energy Biology (CE140100008), and the Australian Grains Research and Development Corporation (GRDC) projects Postdoctoral Fellowship: Photosynthetic Acclimation to High Temperature in Wheat (US1904-003RTX – 9177346) and National Wheat Heat Tolerance (US00080) and Australian Research Council (DP180103834). Bradley C. Posch was supported by the Australian Government Research Training Program. Onoride Coast also received support from Research England’s ‘Expanding Excellence in England’ (E3)-funded Food and Nutrition Security Initiative of the Natural Resources Institute, University of Greenwich. We are grateful to Claire Pickles and Amy Smith of Birchip Cropping Group, Victoria, for managing the trials in Victoria, and AGT and Sabina Yasmin for the trials in Narrabri. We are also grateful to the farmers who generously provided us with field sites for trials. Staff of the ANU Research School of Biology Plant Services team, especially Christine Larsen, Jenny Rath, Gavin Pritchard and Steven Dempsey are thanked for maintaining the plants in the controlled environments.

## References

**Addo-Bediako A, Chown SL, Gaston KJ.** 2000. Thermal tolerance, climatic variability and latitude. *Proceedings of the Royal Society of London. Series B: Biological Sciences* **267**, 739–745.

- Araújo MB, Ferri-Yáñez F, Bozinovic F, Marquet PA, Valladares F, Chown SL.** 2013. Heat freezes niche evolution (D Sax, Ed.). *Ecology Letters* **16**, 1206–1219.
- Armond PA, Schreiber U, Björkman O.** 1978. Photosynthetic Acclimation to Temperature in the Desert Shrub, *Larrea divaricata*. *Plant Physiology* **61**, 411–415.
- Arnold PA, Briceño VF, Gowland KM, Catling AA, Bravo LA, Nicotra AB.** 2021. A high-throughput method for measuring critical thermal limits of leaves by chlorophyll imaging fluorescence. *Functional Plant Biology* **48**, 634–646.
- Aspinwall MJ, Pfautsch S, Tjoelker MG, et al.** 2019. Range size and growth temperature influence *Eucalyptus* species responses to an experimental heatwave. *Global Change Biology* **25**, 1665–1684.
- Asseng S, Ewert F, Martre P, et al.** 2015. Rising temperatures reduce global wheat production. *Nature Climate Change* **5**, 143–147.
- Balota M, Payne WA, Evett SR, Lazar MD.** 2007. Canopy temperature depression sampling to assess grain yield and genotypic differentiation in winter wheat. *Crop Science* **47**, 1518–1529.
- Berry J, Björkman O.** 1980. Photosynthetic response and adaptation to temperature in higher plants. *Annual Review of Plant Physiology* **31**, 491–543.
- Brestic M, Zivcak M, Kalaji HM, Carpentier R, Allakhverdiev SI.** 2012. Photosystem II thermostability *in situ*: Environmentally induced acclimation and genotype-specific reactions in *Triticum aestivum* L. *Plant Physiology and Biochemistry* **57**, 93–105.
- Climate Change Australia** 2021. Climate change in Australia: Climate information, projections, tools and data. Available at: <https://www.climatechangeinaustralia.gov.au/en/>
- Coast O, Posch BC, Bramley H, Gaju O, Richards RA, Lu M, Ruan Y, Trethowan R, Atkin OK.** 2021. Acclimation of leaf photosynthesis and respiration to warming in field-grown wheat. *Plant, Cell & Environment* **44**, 2331–2346.
- Coast O, Shah S, Ivakov A, et al.** 2019. Predicting dark respiration rates of wheat leaves from hyperspectral reflectance. *Plant, Cell & Environment* **42**, 2133–2150.
- Colombo SJ, Timmer VR, Colclough ML, Blumwald E.** 1995. Diurnal variation in heat tolerance and heat shock protein expression in black spruce (*Picea mariana*). *Canadian Journal of Forest Research* **25**, 369–375.
- Cossani CM, Reynolds MP.** 2012. Physiological traits for improving heat tolerance in wheat. *Plant Physiology* **160**, 1710–1718.
- Deutsch CA, Tewksbury JJ, Huey RB, Sheldon KS, Ghalambor CK, Haak DC, Martin PR.** 2008. Impacts of climate warming on terrestrial ectotherms across latitude. *Proceedings of the National Academy of Sciences of the United States of America* **105**, 6668–6672.
- Dias KODG, Gezan SA, Guimarães CT, et al.** 2018. Estimating genotype × environment interaction for and genetic correlations among drought tolerance traits in maize via factor analytic multiplicative mixed models. *Crop Science* **58**, 72–83.
- Dickinson PJ, Kumar M, Martinho C, et al.** 2018. Chloroplast signaling gates thermotolerance in *Arabidopsis*. *Cell Reports* **22**, 1657–1665.
- Drake JE, Tjoelker MG, Vårhammar A, et al.** 2018. Trees tolerate an extreme heatwave via sustained transpirational cooling and increased leaf thermal tolerance. *Global Change Biology* **24**, 2390–2402.
- Dreccer MF, Condon AG, Macdonald B, et al.** 2020. Genotypic variation for lodging tolerance in spring wheat: wider and deeper root plates, a feature of low lodging, high yielding germplasm. *Field Crops Research* **258**, 107942.
- Feeley KJ, Martinez-Villa J, Perez T, Silva Duque A, Triviño Gonzalez D, Duque A.** 2020. The thermal tolerances, distributions, and performances of tropical montane tree species.

Frontiers in Forests and Global Change **3**, 25.

**Ferguson JN, McAusland L, Smith KE, Price AH, Wilson ZA, Murchie EH.** 2020. Rapid temperature responses of photosystem II efficiency forecast genotypic variation in rice vegetative heat tolerance. *Plant Journal* **104**, 839–855.

**Ferris R, Ellis RHR, Wheeler TR, Hadley P.** 1998. Effect of high temperature stress at anthesis on grain yield and biomass of field-grown crops of wheat. *Annals of Botany* **82**, 631–639.

**Figueroa FL, Conde-Álvarez R, Gomez I.** 2003. Relations between electron transport rates determined by pulse amplitude modulated chlorophyll fluorescence and oxygen evolution in macroalgae under different light conditions. *Photosynthesis Research* **75**, 259–275.

**Fu P, Meacham-Hensold K, Guan K, Bernacchi CJ.** 2019. Hyperspectral leaf reflectance as proxy for photosynthetic capacities: An ensemble approach based on multiple machine learning algorithms. *Frontiers in Plant Science* **10**, 1–13.

**Gabriel W, Lynch M.** 1992. The selective advantage of reaction norms for environmental tolerance. *Journal of Evolutionary Biology* **5**, 41–59.

**Geange SR, Arnold PA, Catling AA, et al.** 2021. The thermal tolerance of photosynthetic tissues: a global systematic review and agenda for future research. *New Phytologist* **229**, 2497–2513.

**Havaux M, Ernez M, Lannoye R.** 1988. Correlation between heat tolerance and drought tolerance in cereals demonstrated by rapid chlorophyll fluorescence tests. *Journal of Plant Physiology* **133**, 555–560.

**Hochman Z, Gobbett DL, Horan H.** 2017. Climate trends account for stalled wheat yields in Australia since 1990. *Global Change Biology* **23**, 2071–2081.

**Hoffmann AA, Chown SL, Clusella-Trullas S.** 2013. Upper thermal limits in terrestrial ectotherms: how constrained are they? *Functional Ecology* **27**, 934–949.

**Hüve K, Bichele I, Rasulov B, Niinemets U.** 2011. When it is too hot for photosynthesis: heat-induced instability of photosynthesis in relation to respiratory burst, cell permeability changes and H<sub>2</sub>O<sub>2</sub> formation. *Plant, Cell & Environment* **34**, 113–126.

**Hüve K, Bichele I, Tobias M, Niinemets Ü.** 2006. Heat sensitivity of photosynthetic electron transport varies during the day due to changes in sugars and osmotic potential. *Plant, Cell & Environment* **29**, 212–228.

**Iqbal M, Raja NI, Yasmeen F, Hussain M, Ejaz M, Shah MA.** 2017. Impacts of heat stress on wheat: A critical review. *Advances in Crop Science and Technology* **5**, 1–9.

**Kuznetsova A, Brockhoff PB, Christensen RHB.** 2017. lmerTest package: tests in linear mixed effects models. *Journal of Statistical Software* **82**.

**Lancaster LT, Humphreys AM.** 2020. Global variation in the thermal tolerances of plants. *Proceedings of the National Academy of Sciences of the United States of America* **117**, 13580–13587.

**Lenth R.** 2020. Estimated Marginal Means, aka Least-Squares Means. R package version 1.5.2-1.

**Leon-Garcia IV, Lasso E.** 2019. High heat tolerance in plants from the Andean highlands: Implications for paramos in a warmer world. *PLOS ONE* **14**, e0224218.

**Leung C, Rescan M, Grulois D, Chevin L.** 2020. Reduced phenotypic plasticity evolves in less predictable environments. *Ecology Letters* **23**, 1664–1672.

**Li QB, Guy CL.** 2001. Evidence for non-circadian light/dark-regulated expression of Hsp70s in spinach leaves. *Plant Physiology* **125**, 1633–1642.

**Li ZM, Palmer P, Martin M, Wang R, Rainsford F, Jin Y, Patrick JW, Yang YJ, Ruan Y-L.** 2012. High invertase activity in tomato reproductive organs correlates with enhanced sucrose

import into, and heat tolerance of, young fruit. *Journal of Experimental Botany* **63**, 1155–1166.

**Liu B, Martre P, Ewert F, et al.** 2019. Global wheat production with 1.5 and 2.0°C above pre-industrial warming. *Global Change Biology* **25**, 1428–1444.

**McAusland L, Atkinson JA, Lawson T, Murchie EH.** 2019. High throughput procedure utilising chlorophyll fluorescence imaging to phenotype dynamic photosynthesis and photoprotection in leaves under controlled gaseous conditions. *Plant Methods* **15**, 1–15.

**Melcarek PK, Brown GN.** 1979. Chlorophyll fluorescence monitoring of freezing point exotherms in leaves. *Cryobiology* **16**, 69–73.

**Muggeo VMR.** 2008. Segmented: an R package to fit regression models with broken-line relationships. *R News* **8**, 20–25.

**Neuner G, Pramsohler M.** 2006. Freezing and high temperature thresholds of photosystem II compared to ice nucleation, frost and heat damage in evergreen subalpine plants. *Physiologia Plantarum* **126**, 196–204.

**O’Sullivan OS, Heskell MA, Reich PB, et al.** 2017. Thermal limits of leaf metabolism across biomes. *Global Change Biology* **23**, 209–223.

**Ortiz-Bobea A, Wang H, Carrillo CM, Ault TR.** 2019. Unpacking the climatic drivers of US agricultural yields. *Environmental Research Letters* **14**, 064003.

**Perez TM, Feeley KJ.** 2020. Photosynthetic heat tolerances and extreme leaf temperatures. *Functional Ecology* **34**, 2236–2245.

**Perkins-Kirkpatrick SE, Lewis SC.** 2020. Increasing trends in regional heatwaves. *Nature Communications* **11**, 1–8.

**Raison JK, Roberts JKM, Berry JA.** 1982. Correlations between the thermal stability of chloroplast (thylakoid) membranes and the composition and fluidity of their polar lipids upon acclimation of the higher plant, *Nerium oleander*, to growth temperature. *BBA - Biomembranes* **688**, 218–228.

**Rashid FAA, Scafaro AP, Asao S, Fenske R, Dewar RC, Masle J, Taylor NL, Atkin OK.** 2020. Diel- and temperature-driven variation of leaf dark respiration rates and metabolite levels in rice. *New Phytologist* **228**, 56–69.

**Rashid A, Stark JC, Tanveer A, Mustafa T.** 1999. Use of canopy temperature measurements as a screening tool for drought tolerance in spring wheat. *Journal of Agronomy and Crop Science* **182**, 231–238.

**Rathey AR, Shorter R, Chapman SC.** 2011. Evaluation of CIMMYT conventional and synthetic spring wheat germplasm in rainfed sub-tropical environments. II. Grain yield components and physiological traits. *Field Crops Research* **124**, 195–204.

**Rebetzke GJ, Rathey AR, Farquhar GD, Richards RA, Condon AG.** 2013. Genomic regions for canopy temperature and their genetic association with stomatal conductance and grain yield in wheat. *Functional Plant Biology* **40**, 14–33.

**Rekika D, Monneveux E, Havaux M.** 1997. The in vivo tolerance of photosynthetic membranes to high and low temperatures in cultivated and wild wheats of the *Triticum* and *Aegilops* genera. *Journal of Plant Physiology* **150**, 734–738.

**Reynolds M, Tattaris M, Cossani CM, Ellis M, Yamaguchi-Shinozaki K, Pierre C Saint.** 2015. Exploring Genetic Resources to Increase Adaptation of Wheat to Climate Change. *Advances in Wheat Genetics: From Genome to Field*. Tokyo: Springer Japan, 355–368.

**Ruan Y-L, Patrick JW, Bouzayen M, Osorio S, Fernie AR.** 2012 Molecular regulation of seed and fruit set. *Trends in Plant Science* **17**, 656–665.

**Santarius K.** 1973. The protective effect of sugars on chloroplast membranes during

temperature and water stress and its relationship to frost, desiccation and heat resistance. *Planta* **113**, 105–114.

**Sastry A, Barua D.** 2017. Leaf thermotolerance in tropical trees from a seasonally dry climate varies along the slow-fast resource acquisition spectrum. *Scientific Reports* **7**, 11246.

**Scafaro AP, Atkin OK.** 2016. The Impact of Heat Stress on the Proteome of Crop Species. *Agricultural Proteomics Volume 2*. Cham: Springer International Publishing, 155–175.

**Scafaro AP, Negrini ACA, O’Leary BM, et al.** 2017. The combination of gas-phase fluorophore technology and automation to enable high-throughput analysis of plant respiration. *Plant Methods* **13**, 1–13.

**Scheiner SM.** 1993. Genetics and evolution of phenotypic plasticity. *Annual Review of Ecology and Systematics* **24**, 35–68.

**Schreiber U, Berry JA.** 1977. Heat-induced changes of chlorophyll fluorescence in intact leaves correlated with damage of the photosynthetic apparatus. *Planta* **136**, 233–238.

**Schreiber U, Colbow K, Vidaver W.** 1975. Temperature-jump chlorophyll fluorescence induction in plants. *Zeitschrift für Naturforschung C* **30**, 689–690.

**Sharkey TD.** 2005. Effects of moderate heat stress on photosynthesis: Importance of thylakoid reactions, rubisco deactivation, reactive oxygen species, and thermotolerance provided by isoprene. *Plant, Cell & Environment* **28**, 269–277.

**Sharma DK, Andersen SB, Ottosen CO, Rosenqvist E.** 2012. Phenotyping of wheat cultivars for heat tolerance using chlorophyll a fluorescence. *Functional Plant Biology* **39**, 936–947.

**Silva-Pérez V, Molero G, Serbin SP, Condon AG, Reynolds MP, Furbank RT, Evans JR.** 2018. Hyperspectral reflectance as a tool to measure biochemical and physiological traits in wheat. *Journal of Experimental Botany* **69**, 483–496.

**Slot M, Cala D, Aranda J, Virgo A, Michaletz ST, Winter K.** 2021. Leaf heat tolerance of 147 tropical forest species varies with elevation and leaf functional traits, but not with phylogeny. *Plant, Cell & Environment*, 2414–2427.

**Slot M, Krause GH, Krause B, Hernández GG, Winter K.** 2019. Photosynthetic heat tolerance of shade and sun leaves of three tropical tree species. *Photosynthesis Research* **141**, 119–130.

**Steer BT.** 1973. Diurnal variations in photosynthetic products and nitrogen metabolism in expanding leaves. *Plant Physiology* **51**, 744–748.

**Sunday JM, Bates AE, Dulvy NK.** 2011. Global analysis of thermal tolerance and latitude in ectotherms. *Proceedings of the Royal Society B: Biological Sciences* **278**, 1823–1830.

**Sunday JM, Bates AE, Kearney MR, Colwell RK, Dulvy NK, Longino JT, Huey RB.** 2014. Thermal-safety margins and the necessity of thermoregulatory behavior across latitude and elevation. *Proceedings of the National Academy of Sciences* **111**, 5610–5615.

**Tack J, Barkley A, Nalley LL.** 2015. Effect of warming temperatures on US wheat yields. *Proceedings of the National Academy of Sciences of the United States of America* **112**, 6931–6936.

**Tanksley SD, McCouch SR.** 1997. Seed banks and molecular maps: Unlocking genetic potential from the wild. *Science* **277**, 1063–1066.

**Thapa S, Jessup KE, Pradhan GP, Rudd JC, Liu S, Mahan JR, Devkota RN, Baker JA, Xue Q.** 2018. Canopy temperature depression at grain filling correlates to winter wheat yield in the U.S. Southern High Plains. *Field Crops Research* **217**, 11–19.

**Thistlethwaite RJ, Tan DKY, Bokshi AI, Ullah S, Trethowan RM.** 2020. A phenotyping strategy for evaluating the high-temperature tolerance of wheat. *Field Crops Research* **255**, 107905.

**Végh B, Marček T, Karsai I, Janda T, Darkó É.** 2018. Heat acclimation of photosynthesis in wheat genotypes of different origin. *South African Journal of Botany* **117**, 184–192.

- Way DA, Yamori W.** 2014. Thermal acclimation of photosynthesis: On the importance of adjusting our definitions and accounting for thermal acclimation of respiration. *Photosynthesis Research* **119**, 89–100.
- Weng JH, Lai MF.** 2005. Estimating heat tolerance among plant species by two chlorophyll fluorescence parameters. *Photosynthetica* **43**, 439–444.
- Yamasaki T, Yamakawa T, Yamane Y, Koike H, Satoh K, Katoh S.** 2002. Temperature acclimation of photosynthesis and related changes in photosystem II electron transport in winter wheat. *Plant Physiology* **128**, 1087–1097.
- Yamashita A, Nijo N, Pospíšil P, Morita N, Takenaka D, Aminaka R, Yamamoto Y, Yamamoto Y.** 2008. Quality control of photosystem II: Reactive oxygen species are responsible for the damage to photosystem II under moderate heat stress. *Journal of Biological Chemistry* **283**, 28380–28391.
- Zhao C, Liu B, Piao S, et al.** 2017. Temperature increase reduces global yields of major crops in four independent estimates. *Proceedings of the National Academy of Sciences of the United States of America* **114**, 9326–9331.
- Zhu L, Bloomfield KJ, Hocart CH, Egerton JGG, O’Sullivan OS, Penillard A, Weerasinghe LK, Atkin OK.** 2018. Plasticity of photosynthetic heat tolerance in plants adapted to thermally contrasting biomes. *Plant, Cell & Environment* **41**, 1251–1262.



## Supplementary material

**Table S1.** Pedigree information for wheat genotypes grown for the three field studies and one controlled environment study described in the materials and methods.

Reference no.	Pedigree	Note	Group, geographical origin
<b>Field studies</b>			
84	Sokoll/2/Sokoll/ 35888 M 500132	Backcross of a hexaploid synthetic derived wheat to a heat tolerant tetraploid <i>T. dicoccum</i> and a hexaploid type selected	Narrabri, Australia
1132	PBW550//C80.1/*2Batavia	Cross of heat tolerant Indian cultivar with rust resistant sources	Pune, India
1683	PBW343+L24+LR28/Lang	Same as above	Pune, India
1787	DBW16/Sunstate	Same as above	Pune, India
1898	DBW16/Annuello	Same as above	Pune, India
1943	DBW16/Gladius	Same as above	Pune, India
2062	ISR 812.8/Carinya (1, sister line)	Heat tolerant Mexican hexaploid landrace cross to Australian cultivar	Obregon, Mexico
2150	ISR 812.8/Carinya (2, sister line)	Same as above	Obregon, Mexico
2219	Ventura/Ido 637//Ventura	Low phytate mutant crossed to Australian cultivar - pre-screened for heat tolerance	Narrabri, Australia
2254	D67.2/P66.270//AE.Squarrosa (320)/3/Cunningham/4/Vorb	Heat tolerant in Mexico (Ciudad Obregon) and Narrabri, Australia. Origin CGIAR	Obregon, Mexico
2255	SLVS/Attila//WBLL1*2/3/Gondo/CBRD	Same as above	Obregon, Mexico
2328	Sokoll/2/Sokoll/35888 M 500132	Backcross of a hexaploid synthetic wheat to a heat tolerant tetraploid <i>T. dicoccum</i> and a hexaploid type selected	Narrabri, Australia
Corack		Commercial Australian cultivar, released in 2012	Roseworthy, Australia
Suntop		Same as above	Roseworthy, Australia
Trojan		Commercial Australian cultivar, released in 2013	Roseworthy, Australia
Mace	Wyalkatchem/Stylet//Wyalkatchem	Commercial Australian cultivar, released in 2008	Roseworthy, Australia
2475	Attila/3*BCN//Bav92/3/Tilhi/5/Bav92/3/PRL/Sara//TSI/Vee#5/4/Croc_1/Ae.Squarrosa (224)//2*Opata	Heat tolerant in Mexico (Ciudad Obregon) and Narrabri. Origin CGIAR	Obregon, Mexico
2355	Seri 82/Shuha's'//CM85295-0101TOPY-2M-0Y-0M-3Y-0M-OAP	Same as above	Aleppo, Syria
1964	DBW14/C80.1/2*SR2 Batavia	Cross of heat tolerant Indian cultivar with rust resistant sources	Pune, India
1704	PBW343+L24+LR28/Lang	Same as above	Pune, India

29	Berkut/2/Berkut/35883 M500110	Backcross of a hexaploid wheat to a heat tolerant tetraploid <i>T. dicoccum</i> and a hexaploid type selected	Narrabri, Australia
143	Waxwing*2/Kiritati /3/Waxwing*2/Kiritati /2/ 35888 M 500132	Same as above	Narrabri, Australia
2316	RAC 1192/4/2*Attila/3/Weaver*2/TSC//Weaver	Heat tolerant hexaploid; good performance in Mexico (Ciudad Obregon) and Narrabri, Australia. Origin CGIAR	Obregon, Mexico
<b>Field studies and controlled environment study</b>			
2267	Hubara-8///Mon's'/Ald's'//Bow's'	Heat tolerant hexaploid; good performance in Sudan and Narrabri. Origin CGIAR	Gezira, Sudan

**Table S2.** Analysis of variance of factors influencing wheat  $T_{crit}$  at two Australian field sites

	<b>Genotype</b>		<b>Time of day</b>		<b>Genotype × Time of day</b>	
	d.f.	<i>F</i> value	d.f.	<i>F</i> value	d.f.	<i>F</i> value
Dingwall, Victoria	5	3.7 **	3	15.8 ***	15	2 *
	<b>Genotype</b>		<b>Phenological stage</b>		<b>Genotype × Phenological stage</b>	
	d.f.	<i>F</i> value	d.f.	<i>F</i> value	d.f.	<i>F</i> value
Barraport West, Victoria	3	5.0 **	2	14.9 ***	6	2.2 *

\* $P < 0.05$ ; \*\* $P < 0.01$ ; \*\*\* $P < 0.001$ . Six out of the 20 genotypes sown at Dingwall in 2017 were sampled every six hours to measure diel variation in  $T_{crit}$  over the course of a day. Four of the 20 genotypes sown at Barraport West in 2018 were sampled from all three time of sowing plots to measure variation in wheat  $T_{crit}$  at varying phenological stages.

**Table S3.** Analysis of variance of effect of time of sowing and genotype on wheat  $T_{crit}$  at three Australian field sites

	<b>Time of sowing</b>		<b>Genotype</b>		<b>Time of sowing × Genotype</b>	
	d.f.	<i>F</i> value	d.f.	<i>F</i> value	d.f.	<i>F</i> value
Dingwall, Victoria	2	23.1 ***	19	0.5 <sup>ns</sup>	38	0.9 <sup>ns</sup>
Barraport West, Victoria	2	62.1 ***	19	2.1 **	38	2 **
Narrabri, New South Wales	1	13.7 ***	23	2.3 ***	23	1 <sup>ns</sup>

\* $P < 0.05$ ; \*\* $P < 0.01$ ; \*\*\* $P < 0.001$ ; <sup>ns</sup> = not significant. The same 20 genotypes that were sown in Dingwall and Barraport West were also sown at Narrabri in 2019, along with an additional four genotypes.

**Table S4.** Analysis of variance of effect of time of sowing and genotype origin on wheat  $T_{crit}$  at three Australian field sites

	<b>Time of sowing</b>		<b>Genotype origin</b>		<b>Time of sowing × Genotype origin</b>	
	d.f.	<i>F</i> value	d.f.	<i>F</i> value	d.f.	<i>F</i> value
Dingwall, Victoria	2	15.2 ***	4	0.2 <sup>ns</sup>	8	0.7 <sup>ns</sup>
Barraport West, Victoria	2	42.2 ***	4	2.5 *	8	1 <sup>ns</sup>
Narrabri, New South Wales	1	4.5 *	5	2.5 *	5	0.7 <sup>ns</sup>

\* $P < 0.05$ ; \*\* $P < 0.01$ ; \*\*\* $P < 0.001$ ; <sup>ns</sup> = not significant. The same 20 genotypes that were sown in Dingwall and Barraport West were also sown at Narrabri in 2019, along with an additional four genotypes.

## Statement of Contribution

This thesis is submitted as a Thesis by Compilation in accordance with [https://policies.anu.edu.au/ppl/document/ANUP\\_003405](https://policies.anu.edu.au/ppl/document/ANUP_003405)

I declare that the research presented in this Thesis represents original work that I carried out during my candidature at the Australian National University, except for contributions to multi-author papers incorporated in the Thesis where my contributions are specified in this Statement of Contribution.


Title: Wheat photosystem II heat tolerance reponds dynamically to short and long-term warming \_\_\_\_\_

Authors: Bradley C. Posch, Julia Hammer, Owen K. Atkin, Helen Bramley, Yong-Ling Ruan, Richard Trethowan, and Onoriode Coast \_\_\_\_\_

Publication outlet: Journal of Experimental Botany \_\_\_\_\_

Current status of paper: Accepted

Contribution to paper: O.K.A., H.B., and Y-L.R. secured grants; R.T. developed the seed materials; B.C.P., J.H., O.C., H.B., and O.K.A. designed experiments; B.C.P., J.H. and O.C. collected data; B.C.P., J.H. and O.C. analysed data; and B.C.P. and O.C. wrote the paper with contributions from all authors. \_\_\_\_\_

Senior author or collaborating authors endorsement:  (Dr. Onoriode Coast) 01 April 2022 \_\_\_\_\_

Bradley C. Posch

Candidate – Print Name



Signature

01-04-2022

Date

### Endorsed

PROFESSOR OWEN ATKIN

Primary Supervisor – Print Name



Signature

April 2nd 2022

Date

## **Chapter 4 – Wheat respiratory O<sub>2</sub> consumption falls with night warming alongside greater respiratory CO<sub>2</sub> loss and reduced biomass**

**Bradley C. Posch, Deping Zhai, Onoriode Coast, Andrew P. Scafaro, Helen Bramley, Peter B. Reich, Yong-Ling Ruan, Richard Trethowan, Danielle A. Way, and Owen Atkin**

Author Contributions: O.K.A., H.B., and Y-L.R. secured grants; R.T. developed seed material; B.C.P., O.C., A.P.S., and O.K.A. designed research; B.C.P., D.Z., A.P.S. performed research; B.C.P., O.C., A.P.S., and O.K.A. analysed data; and B.C.P. wrote the paper with contributions from all authors.

*This manuscript has been published in the Journal of Experimental Botany (Posch BC, Zhai D, Coast O, Scafaro AP, Bramley H, Reich PB, Ruan YL, Trethowan R, Way DA, Atkin OK. 2022. Wheat respiratory O<sub>2</sub> consumption falls with night warming alongside greater respiratory CO<sub>2</sub> loss and reduced biomass. Journal of Experimental Botany **73**, 915–926.)*

### **Abstract**

Warming nights are correlated with declining wheat growth and yield. A key determinant of plant biomass, respiration consumes O<sub>2</sub> as it produces ATP and releases CO<sub>2</sub> and is typically reduced under warming to maintain metabolic efficiency. We compared the response of respiratory O<sub>2</sub> and CO<sub>2</sub> flux to multiple night and day warming treatments in wheat leaves and roots, using one commercial (Mace) and one breeding cultivar grown in controlled environments. We also examined the effect of night warming and a day heatwave on the capacity of the ATP-uncoupled alternative oxidase (AOX) pathway. Under warm nights plant biomass fell, respiratory CO<sub>2</sub> release measured at a common temperature was unchanged (indicating higher rates of CO<sub>2</sub> release at prevailing growth

temperature), respiratory O<sub>2</sub> consumption at a common temperature declined, and AOX pathway capacity increased. The uncoupling of CO<sub>2</sub> and O<sub>2</sub> exchange and enhanced AOX pathway capacity suggest a reduction in plant energy demand under warm nights (lower O<sub>2</sub> consumption), alongside higher rates of CO<sub>2</sub> release under prevailing growth temperature (due to a lack of downregulation of respiratory CO<sub>2</sub> release). Less efficient ATP synthesis, teamed with sustained CO<sub>2</sub> flux, could thus be driving observed biomass declines under warm nights.

## Introduction

Over the last 50 years increases in daily minimum temperature (i.e. minimum night temperature) have outpaced the rise in daily maximum temperature across much of the globe (Davy *et al.*, 2017). Night warming has been associated with wheat and rice yield declines (Reynolds *et al.*, 1994; Peng *et al.*, 2004; Welch *et al.*, 2010; García *et al.*, 2015; Bahuguna *et al.* 2021) via reduced grain number, inhibited flowering, and decreased biomass accumulation up to physiological maturity, the latter of which is strongly correlated with wheat yield under high temperature (Pinto *et al.*, 2017). Plant respiration is key in determining biomass and yield and is also highly sensitive to temperature, making it an important trait for crop growth under warm nights. With this in mind, we investigated the effect of both night and day warming on rates of dark respiration in wheat leaves and roots.

Respiration is a principal determinant of plant biomass accumulation, with up to 50% of daily assimilated carbon expended on the same day via respiratory flux (Poorter *et al.*, 1990), and is highly sensitive to temperature. The short-term temperature response of mitochondrial dark respiration ( $R_{\text{dark}}$ ) is commonly expressed as the  $Q_{10}$  – the proportional change in  $R_{\text{dark}}$  per 10°C increase (but see Heskell *et al.* (2016) for a more precise quantification of such responses) – and has typically been observed to be approximately 2 (i.e.  $R_{\text{dark}}$  doubling per 10°C within a range of non-stressful temperatures;

Atkin & Tjoelker 2003). This reflects a rapid rise in energy demand for maintenance functions with rising temperature, potentially diverting a greater proportion of assimilated carbon away from growth. Importantly, plants can acclimate their respiratory metabolism to sustained warming. This generally results in lower rates of  $R_{\text{dark}}$  when measured at a common temperature (typically in the 20-25°C range), or a near-homeostasis of  $R_{\text{dark}}$  when comparing plants measured at their respective growth temperatures (Atkin and Tjoelker, 2003; Kurimoto *et al.*, 2004; Reich *et al.*, 2016, 2021). This may manifest as reduced respiratory O<sub>2</sub> consumption (indicative of a reduction in ATP production) and reduced CO<sub>2</sub> release (improving plant carbon use efficiency) (O’Leary *et al.*, 2019). Thus, high temperature acclimation maintains stable rates of  $R_{\text{dark}}$  during sustained periods of elevated temperature. However, despite our awareness of night warming trends, our understanding of the thermal acclimation response of leaf and root  $R_{\text{dark}}$  to night warming remains limited.

Daytime warming affects both photosynthesis and respiration as both processes are active during the day. However, while photosynthesis ceases at night, respiration continues. Thus, when warming occurs during the day, any subsequent increase in respiratory rate can be accompanied by an equivalent increase in carbon assimilation, thus maintaining metabolic balance (Wang *et al.*, 2020). By contrast, when warming occurs at night respiration relies upon assimilates fixed and stored the previous day, with no immediate photosynthetic carbon gain to offset increased respiratory carbon release. Night warming can increase demand for photosynthetic products by accelerating processes that require respiratory energy (e.g. nocturnal protein turnover), providing impetus for increased photosynthetic rate during the day to meet this increased demand (Turnbull *et al.*, 2002, 2004). This sink demand will be influenced by the extent of adjustment (i.e., acclimation) of demand for respiratory energy during the night (e.g. through a reduction in protein turnover rates). Therefore, increases in night temperature could potentially be even more consequential than day warming for gas-exchange and, by extension, plant growth. While a recent study in rice by Bahuguna *et al.* (2021)

supports this notion, investigations of the response of respiration to night warming in plant species have been limited, particularly in wheat.

Past  $R_{\text{dark}}$  thermal acclimation studies have largely relied upon  $\text{CO}_2$  efflux measurements ( $R_{\text{dark-CO}_2}$ ; Gifford, 1995; Impa et al., 2019; Slot & Kitajima, 2015). Though respiratory  $\text{O}_2$  consumption ( $R_{\text{dark-O}_2}$ ) is also worthy of attention, a comparatively less studies have reported impacts of growth temperature on  $R_{\text{dark-O}_2}$  (Covey-Crump *et al.*, 2002; Armstrong *et al.*, 2006). Coast *et al.* (2021) observed a discrepancy between these two measures in field-grown wheat; namely,  $R_{\text{dark-O}_2}$  declined under elevated growth temperature while  $R_{\text{dark-CO}_2}$  did not, though the role of night warming in the  $R_{\text{dark-O}_2}$  acclimation was unclear. Respiratory  $\text{O}_2$  consumption is closely tied to ATP synthesis via glycolysis, the TCA cycle, and mitochondrial electron transport, and so changes in  $R_{\text{dark-O}_2}$  with temperature provide insight into energy demand under elevated temperature (Plaxton and Podestá, 2006). Concurrent measurements of  $R_{\text{dark-O}_2}$  and  $R_{\text{dark-CO}_2}$  reveal the respiratory quotient (RQ) – the ratio of moles of  $\text{CO}_2$  released to moles of  $\text{O}_2$  consumed in mitochondrial respiration, which indicates the substrate being oxidised. Carbohydrates are the main plant respiratory substrate (Plaxton and Podestá, 2006) and have an RQ of 1 (Dilly, 2001). Any change in RQ with warming could imply a change in substrate use associated with thermal acclimation.

One relevant aspect of respiratory  $\text{O}_2$  metabolism that responds to elevated temperature is the alternative oxidase (AOX) pathway (Rachmilevitch *et al.*, 2007; Searle and Turnbull, 2011; Searle *et al.*, 2011). Most mitochondrial electron transport occurs via the cytochrome *c* oxidase (COX) pathway, which couples electron transport with ATP production. The AOX pathway differs as its capacity for electron flow is far more limited, and  $\text{O}_2$  uptake via the AOX pathway is not coupled to ATP synthesis. The absence of proton translocation in the AOX pathway means that it is not directly controlled by adenylate limitation, with increased AOX activity resulting in decreased ATP production per  $\text{O}_2$  consumed (Atkin *et al.*, 2002). Exposure to various environmental stressors, including low temperature, drought, and nutrient deficiency, increase AOX pathway capacity (Vanlerberghe, 2013; Del-Saz *et al.*, 2018). Some have suggested AOX pathway



capacity rises under high temperature to combat reactive oxygen species accumulation associated with the over-reduction of mitochondrial electron transfer chain components (Fedyaeva *et al.*, 2014; O’Leary *et al.*, 2019). Murakami and Toriyama (2008) found over-expression of the *AOX1a* gene was associated with improved growth in rice seedlings following short-term and long-term high temperature exposure. However, a detailed understanding of the AOX pathways role in plant high temperature response – including to night warming – remains elusive.

We measured leaf and root  $R_{\text{dark-O}_2}$ , as well as leaf  $R_{\text{dark-CO}_2}$ , in plants grown under night temperatures ranging from 14 to 25°C, and day temperatures from 20 to 26°C. A subset of plants were also exposed to a three-day 38°C daytime heatwave and used to measure leaf  $R_{\text{dark-O}_2}$  and AOX and COX pathway capacity. In this study, we aimed to: (1) compare acclimation of  $R_{\text{dark}}$  to three night and two day growth temperatures in leaves and roots; (2) observe the degree of acclimation of  $R_{\text{dark}}$  to night warming on both an O<sub>2</sub> and CO<sub>2</sub> basis; and (3) examine and compare the effect of night warming and a day heatwave on mitochondrial electron transport via the AOX pathway. Collectively, our results point toward night growth temperature playing a crucial role in driving acclimation of wheat respiratory O<sub>2</sub> metabolism, coupled with a lack of respiratory CO<sub>2</sub> flux acclimation, in aggregate associated with declining plant biomass as a response to warmer nights.

## Materials and methods

### *Plant material*

Two heat-tolerant wheat genotypes were chosen for this study, based on their use in a previous study of respiration and warming in field-grown wheat (Coast *et al.*, 2021). The previous study consisted of 20 wheat genotypes, 16 of which were part of a heat tolerance breeding program, and four of which are commercially available Australian genotypes. Mace (Australian Grain Technologies; pedigree: Wyalkatchem/Stylet//Wyalkatchem), is a widely grown commercially available

benchmark genotype that yields well in the field under high temperature and drought stress (Australian Grain Technologies, 2021) 8:ZWW11 is a genotype developed by the International Maize and Wheat Improvement Centre (CIMMYT; pedigree: D67.2/P66.270//AE.SQUARROSA (320)/3/CUNNINGHAM/4/VORBEY) and, based on preliminary field data provided by Prof. Richard Trethowan of the University of Sydney, is heat tolerant under Australian conditions. Mace was used in both experiments 1 and 2 while 8:ZWW11 was only used in experiment 1.

*Experiment 1 – warming night and day growth temperature*

Germinated seedlings of Mace and 8:ZWW11 were transferred into sixty 1.9 L pots (one seedling per pot) containing a mixture of steamed bark-based potting mix (80% composted bark, 10% sharp sand, 10% coir). Osmocote® Exact Mini fertiliser (ICL, Tel Aviv, Israel) was mixed through the potting mix at a ratio of 4 g of fertiliser per L of potting mix. Plants were watered following potting, and then watered every 1-2 days after that to minimise water-stress. After potting, all plants were grown for six weeks at the control temperature of 20/15°C, 60-90% relative humidity, ambient CO<sub>2</sub>, and photosynthetically active radiation of 700 - 800  $\mu\text{mol m}^{-2} \text{s}^{-1}$ . Day and night growth temperatures were then imposed for the next three to four weeks. The experimental design was an incomplete 2 x 3 factorial design, with two day (20 and 26°C), and three night (15, 20, and 25°C) temperature treatments. Treatment combinations were (day/night): 20/15, 20/20, 26/15, 26/20, and 26/25°C. Day and night temperatures were maintained for 12 h periods, with the first and last hours of each period used for a step-transition from day to night temperature, or vice versa. Treatment temperatures were chosen to provide a comparison of the effects of night versus day warming and to provide the greatest likelihood of eliciting acclimation responses, thus the night temperatures imposed were slightly greater than average night temperatures typically experienced in most spring wheat growing regions. Each of the five temperature treatments were allocated to a walk-in growth room (Phoenix Research, SA, Australia) in the Controlled Environment Facility at the Australian National University, Canberra, Australia. Within each growth room

plants were arranged in a randomised block design, and then randomly allocated to the measurement they would be sampled for. During the first and last hours of the day period, light was reduced to 65% intensity and day temperature was reduced to halfway between the daily maximum and nightly minimum temperature for each respective treatment. Overall a 12h photothermal period was maintained.

*Measurements of leaf ( $O_2$ - and  $CO_2$ -based) and root ( $O_2$ -based)  $R_{dark}$*

Sampling began after the plants had spent either three (plants in the 20/20, 26/20, and 26/25 treatments) or four (plants in the 20/15 and 26/15 treatments) weeks at their respective temperature treatments. Plants in the 20/15 and 26/15 treatments were given the additional week to ensure that all plants were at approximately the same phenological stage upon sampling (the stem elongation/node production stage of development – Zadok's stage 31-39; Zadoks, Chang, & Konzak, 1974), and only the most recently fully-expanded leaf on the main tiller that developed within the treatment periods were used for  $R_{dark}$  measurements. Four replicate plants were used for all measurements. Tissue used for measurements of  $R_{dark-O_2}$  was taken from plants separate to those that were used for measurements of  $R_{dark-CO_2}$ . In order to avoid any diurnal variation effect, leaves used for  $R_{dark-O_2}$  measurements were harvested at 9 am on every measurement day (photoperiod in the growth rooms ran from 6am–6pm). Previous work on rice has shown that the time of day that leaves are dark adapted and measured does not significantly affect thermal acclimation of leaf  $R_{dark-O_2}$  (Rashid *et al.*, 2020). Harvested leaves were temporarily stored in a darkened, chilled cooler in sealed plastic bags, and left to dark adapt for at least 30 minutes. Measurements of  $R_{dark-O_2}$  were taken using a Q2  $O_2$ -sensor (Astec Global, Maarsse, Netherlands), according to methods outlined in Scafaro *et al.* (2017). Leaves were cut into four equal sections (each section approximately  $2cm^2$ ) and weighed. Leaf sections were then placed within sealed 2 mL tubes containing 50  $\mu L$  of water to prevent desiccation.  $R_{dark-O_2}$  was measured at four temperatures (20, 25, 30, and 35°C), to which leaf sections were randomly allocated in the Q2  $O_2$ -sensor. In some instances, there was insufficient leaf tissue for four leaf sections so two leaf sections

were cut and measured at 25 and 35°C only. Fresh and dry mass of all leaf sections were used to estimate  $R_{\text{dark}}$  on per leaf mass basis.

Newly developed nodal roots were used for  $R_{\text{dark-O}_2}$  measurements. These were harvested 1-2 days after leaves for  $R_{\text{dark-O}_2}$  had been harvested. Roots were gently washed and divided into four equal portions, each containing 2-4 whole nodal root branches. Each of the four root portions (i.e. 2-4 whole nodal root branches) were then measured at the same four temperatures as were used for measuring leaf  $R_{\text{dark-O}_2}$  on the Q2 O<sub>2</sub>-sensor.

Leaf CO<sub>2</sub> evolution in darkness ( $R_{\text{dark-CO}_2}$ ) was measured with portable photosynthesis systems (Li-Cor 6400 and 6400XT infrared gas analysers; Li-Cor BioSciences, Lincoln, NE, USA). All leaf  $R_{\text{dark-CO}_2}$  measurements were taken on attached leaves of previously unsampled plants between 8:30am and 3pm. Plants were dark-adapted for 30 minutes, then CO<sub>2</sub> flux was measured in darkness at 25°C to indicate  $R_{\text{dark-CO}_2}$ . Throughout measurements of leaf  $R_{\text{dark-CO}_2}$  Li-Cor leaf chamber parameters were maintained as follows: flow rate 500  $\mu\text{mol s}^{-1}$ ; CO<sub>2</sub> concentration 400  $\mu\text{mol mol}^{-1}$ ; and relative humidity 60–80%. The growth stages of plants were monitored and scored according to the Zadok's scale (Zadoks *et al.*, 1974) throughout the experiment to guide the timing of measurements, ensuring that plants were measured at similar stages of development.

#### *Experiment 2 – night growth temperature warming and a daytime heatwave*

All plants in this experiment had a common day growth temperature of 26°C, and the experiment was a complete 2 x 2 factorial design: there were two night growth temperature treatments – 14°C and 21°C – and two temporary day heat stress treatments – a 38°C heatwave and a continuation of the 26°C control. Seeds of wheat genotype Mace were germinated for one week and seedlings planted in 6 L white rigid Polyvinyl chloride pots (diameter was 160mm, and height was 410mm) filled with the same potting mix used in Experiment 1. Potted seedlings were transferred into climate-controlled LED-lit Growth Capsules (Photo System Instruments, Brno, Czech Republic) at the Australian Plant

Phenomics Facility located within the Australian National University, Canberra. Night temperature within the capsules was either 14°C or 21°C, with a day temperature of 26°C for the first 10 weeks of growth. Capsules were maintained at 60-70% relative humidity, ambient CO<sub>2</sub>, and an average of 750 μmol m<sup>-1</sup> sec<sup>-1</sup> photosynthetically active radiation with a 12-hour day length from 6am to 6pm. Following 10 weeks of growth, at which point all plants were between early heading (Zadok's growth stage 51) and late anthesis (Zadok's growth stage 69), half of the plants from each night temperature treatment were exposed to a daytime heatwave event with a maximum temperature of 38°C. During the heatwave temperature ramped up gradually from 6am to 9am, then was maintained at 38°C from 9am to 3pm, and then ramped down toward the respective night temperature from 3pm to 6pm. The daytime heatwave lasted a total of five days. Plant management was as described for Experiment 1.

#### *Measurements of respiration with inhibitors*

Measurements of leaf  $R_{\text{dark-O}_2}$  were taken according to the method outlined in Experiment 1, aside from the following differences. Leaf  $R_{\text{dark-O}_2}$  was measured at 26°C and 38°C, representing the two daytime temperatures plants experienced in the capsules. Harvested leaves were sliced into two 3 cm long sections, which were either used in their entirety to measure  $R_{\text{dark-O}_2}$  as described in the previous experiment, or alternatively were sliced into 2 mm wide strips. These strips were then submerged in one of four solutions, depending on their respiratory inhibition treatment: leaf wounding buffer (20 mM HEPES pH 7.2, 10 mM MES, 2 mM CaCl<sub>2</sub>) as control, leaf wounding buffer + 10 mM potassium cyanide (KCN) to inhibit the COX pathway, leaf wounding buffer + 5 mM salicylhydroxamic acid (SHAM) to inhibit the AOX pathway, or leaf wounding buffer + 10 mM KCN + 5mM SHAM to inhibit both pathways (Lambers, 1980; Azcón-Bieto *et al.*, 1983). Immediately after submergence, leaves were vacuum infiltrated for five minutes to ensure uptake of solution. Remaining solution was then removed from measurement tubes, and tubes were sealed for measurement. The effectiveness of these concentrations of both KCN and SHAM for inhibiting  $R_{\text{dark-O}_2}$  was determined in

preliminary trials in which concentrations were systematically increased (Fig. S1). In order to control for any potential injury effects of slicing and vacuum infiltrating,  $R_{\text{dark-O}_2}$  of chemically inhibited leaves was expressed in proportion to  $R_{\text{dark-O}_2}$  of control leaf samples that were also sliced and infiltrated with only buffer.

### *Statistical analysis*

All leaf-based traits reported in Experiment 1 were arithmetic means of four individual leaves sampled from separate, previously unsampled plants. All measurements of traits in Experiment 2 were similarly taken from individual leaves of separate plants; however, the number of replicates was increased to five. Data analysis was carried out using linear mixed models within the R statistical environment (v. 3.4.4; R Core Team, 2018) using two-packages – lmerTest (Kuznetsova *et al.*, 2017) and emmeans (Lenth, 2020). This approach allowed us to examine the potential interactions of several experimental variables while also accounting for any variance associated with extraneous variables. Night and day temperature were considered fixed effects across all experiments, as well as genotype and inhibitor in Experiments 1 and 2, respectively. Random terms in the models were plant replicate (all experiments) and Li-Cor unit (for applicable traits) in order to account for any variation in  $R_{\text{dark}}$  associated with either within-genotype/treatment differences, or differences between Li-Cor units. Fisher's l.s.d. was used to assess the pairwise differences between factors of ANOVA while controlling the error rate to less than 0.05. Calculated l.s.d. values are presented alongside analyses of variance results. For leaves in which  $R_{\text{dark}}$  was measured at two temperatures,  $Q_{10}$  was calculated as:

$$Q_{10} = \left( \frac{R_{\text{dark } 2}}{R_{\text{dark } 1}} \right)^{\frac{10^\circ\text{C}}{T_2 - T_1}}$$

where  $R_{\text{dark } 2}$  is the  $R_{\text{dark}}$  of the leaf measured at the higher temperature, and  $R_{\text{dark } 1}$  is the  $R_{\text{dark}}$  of the leaf measured at the lower temperature, and  $T_2$  and  $T_1$  are the measuring temperatures for the respective leaves. For root  $R_{\text{dark}}$ , which was recorded at four measurement temperatures,  $Q_{10}$  was calculated as:

$$Q_{10} = e^{(10k)}$$

where  $k$  is the slope of natural log transformed root  $R_{\text{dark}}$  across the four measurement temperatures.

## Results

### *Above- and below-ground biomass was lower in plants grown at warmer night temperatures*

Night warming was associated with a decline in the total biomass of both above-ground (Fig. 1A) and below-ground tissue (Fig. 1B). A significant genotypic difference was observed only for above-ground biomass – specifically, that above-ground dry mass of 8:ZWW11 was consistently greater than that of Mace ( $P < 0.01$ ; Table S1). While biomass both above and below-ground fell significantly as night growth temperature increased, a 6°C increase in day growth temperature had comparatively little effect. Thus, plants grown under elevated night temperatures were smaller above and below-ground following an increase in night growth temperature.

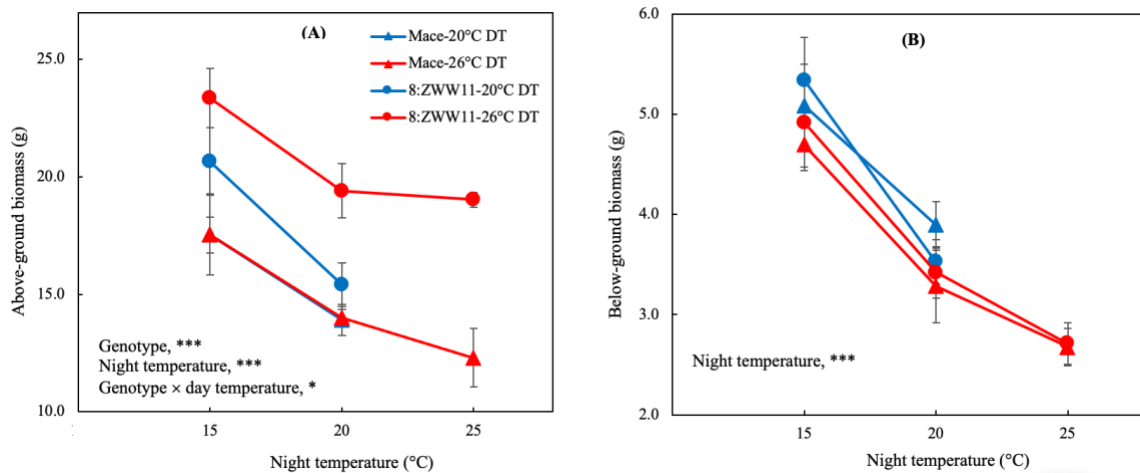


**Figure 1.** Above-ground (A) and below-ground (B) biomass for Mace and 8:ZWW11 plants grown under 15, 20, or 25°C nights, and 20 or 26°C days. All above-ground and below-ground tissue was harvested from previously unsampled plants following approximately four weeks under their respective temperature treatment. At this time all plants had largely stopped adding vegetative tissue and fell within the Zadok's growth stages of 45-59 (between booting and late heading). Indicated in each panel are the level of

significance difference for main treatment terms (genotype, night temperature, and day temperature) that were significant with \*, \*\*, and \*\*\*, representing  $P < 0.05$ ,  $P < 0.01$  and  $P < 0.001$ , respectively.  $n = 4$ , error bars denote s.e. See Table S1 for ANOVA results.

*R<sub>dark</sub> declined with night warming when measured as O<sub>2</sub> consumption, but not when measured as CO<sub>2</sub> flux*

Measured at 25°C, O<sub>2</sub>-based leaf dark respiration ( $R_{25-O_2}$ ) declined ( $P < 0.001$ ) as night temperature rose from 15°C to 20°C and from 20°C to 25°C (Fig. 2 and Table S1). This pattern was observed in both genotypes and for plants grown at both day temperatures of 20°C and 26°C, as well as when expressed as leaf dry mass-based  $R_{25-O_2}$  (Fig. 2A) or leaf area-based  $R_{25-O_2}$  (Fig. 2B). Thus, there was strong evidence of temperature acclimation of  $R_{25-O_2}$  to night temperature increase. A 6°C rise in day temperature from 20°C to 26°C did not cause down-regulation of  $R_{25-O_2}$ , either having no impact on leaf  $R_{25-O_2}$  (e.g., leaf dry mass basis) or increasing leaf  $R_{25-O_2}$  (leaf area basis,  $P < 0.01$ ). By contrast, CO<sub>2</sub>-based leaf dark respiration measured at 25°C ( $R_{25-CO_2}$ ) was not significantly affected by night or day warming in either genotype (Fig. 2D), exhibiting no evidence of temperature acclimation. The short-term temperature sensitivity of leaf  $R_{\text{dark-O}_2}$  (i.e.,  $Q_{10}$ ) significantly increased with rising night temperature ( $P < 0.01$ , Table S2), with cool-night grown plants exhibiting  $Q_{10}$  values near 1.7, while plants experiencing warmer nights exhibited  $Q_{10}$  values in the 2.2-2.4 range (Fig. S2). By contrast, the  $Q_{10}$  of leaf  $R_{\text{dark-O}_2}$  generally declined or remained constant as day temperature rose (Fig. S2). There were no significant first or second order interaction effects between genotype, night, or day temperature on leaf  $R_{\text{dark}}$  traits (Table S1).

Root  $R_{\text{dark-O}_2}$  measured at 25°C ( $R_{26-O_2}$ ) also declined significantly with night warming ( $P < 0.05$ , Table S1), despite this pattern being slightly less consistent across all contrasts than it was in leaves (Fig. 2C). Just as for leaf  $R_{25-O_2}$ , night warming had a far greater effect on root  $R_{25-O_2}$  than day warming did. The temperature sensitivity of root  $R_{\text{dark-O}_2}$  (Fig. S3) contrasted with that of leaf  $R_{\text{dark-O}_2}$  (Fig. S2). Specifically, whereas leaf  $Q_{10}$  increased with growth temperature, root  $Q_{10}$  values (which were in the 1.4-2.4 range)



either remained unchanged or fell with warming. Mace demonstrated a greater temperature sensitivity of root  $R_{\text{dark-O}_2}$  than 8:ZWW11 did.

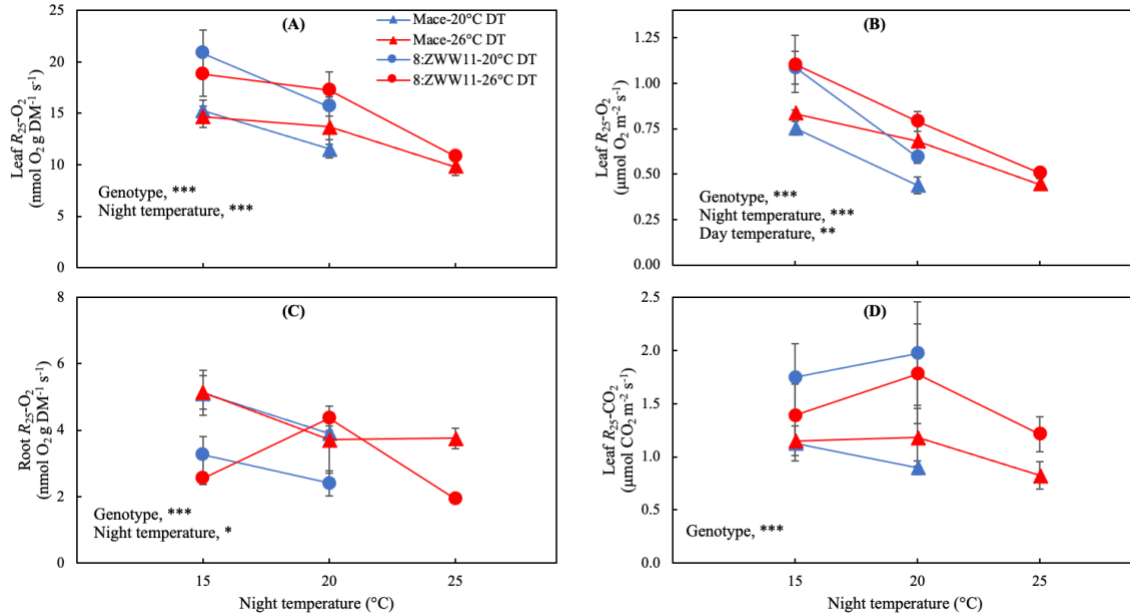


**Figure 2.** Dark respiration rates measured at 25°C ( $R_{25}$ ) of two wheat genotypes (Mace and 8:ZWW11) grown at night temperatures of 15, 20, or 25°C and day temperatures (DT) of 20 or 26°C.  $R_{\text{dark}}$  was measured as  $O_2$  consumption ( $R_{25-O_2}$ ) and expressed for leaf or root tissue per gram of leaf dry mass (DM; A);  $m^2$  of leaf area (B); or gram of root dry mass (C). Leaf  $R_{\text{dark}}$  was also measured as  $CO_2$  evolution ( $R_{25-CO_2}$ ) per  $m^2$  of leaf area (D). Indicated in each panel are the level of significance difference for main treatment terms (genotype, night temperature, and day temperature) that were significant with \*, \*\*, and \*\*\*, representing  $P < 0.05$ ,  $P < 0.01$  and  $P < 0.001$ , respectively.  $n = 4$ , error bars denote s.e. See Table S1 for ANOVA results.

In Experiment 2, night warming was again associated with a decline in leaf  $R_{\text{dark-O}_2}$  measured at a common temperature of 26°C ( $R_{26-O_2}$ ). Specifically, a 7°C rise in night growth temperature coincided with a 25% decrease ( $P < 0.05$ ) in leaf area-based  $R_{26-O_2}$  (Fig. 3; Table S2). Unlike in Experiment 1, the temperature sensitivity of leaf  $R_{\text{dark-O}_2}$  did not differ between night temperature treatments, with a  $Q_{10}$  close to 2 maintained in each treatment. Exposure to three consecutive days of daytime heatwave, during which the maximum temperature rose 12°C above the control daytime maximum, had no significant effect on leaf  $R_{\text{dark-O}_2}$  ( $P > 0.05$ ). Thus, these results echoed those of

Experiment 1; temperature-normalized rates of  $R_{\text{dark-O}_2}$  declined with night warming but not day warming, even when the latter took the form of a heatwave.

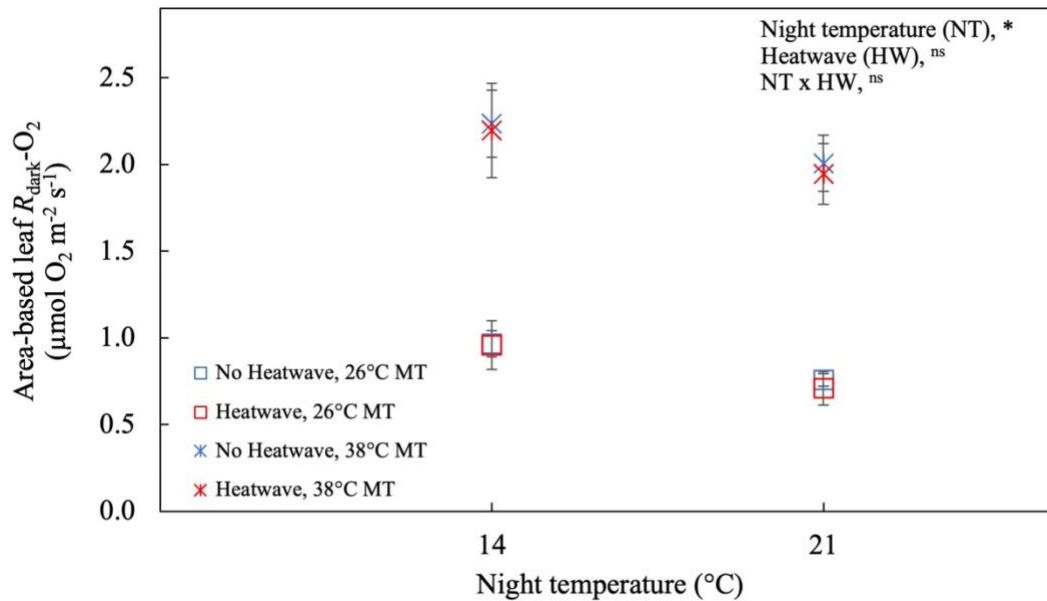


**Figure 3.** Leaf dark respiration rate of the wheat genotype Mace measured as  $O_2$  consumption ( $R_{\text{dark-O}_2}$ ) per  $m^2$  of leaf area, grown at night temperature (NT) of 14 or 21°C and day temperature of 26°C. Day temperature was increased to 38°C for three days prior to measurement for plants in heatwave treatment (HW; red data points). Measurement temperature (MT) of  $R_{\text{dark}}$  was 26 (squares) or 38°C (crosses). Significant difference in main treatment terms (NT = night temperature, HW = heatwave) or their interaction (NT x HW) is indicated by \* ( $P < 0.05$ ) or ns (not significant) for  $P > 0.05$ .  $n = 5$ , error bars denote s.e. See Table S1 for ANOVA results.

#### *Increased capacity of AOX pathway under warm nights*

Using KCN to inhibit the COX pathway resulted in 80-90% decline in leaf  $R_{26-O_2}$  from uninhibited rates, whereas inhibiting the AOX pathway with SHAM reduced  $R_{26-O_2}$  by less than 20% (Table 1), highlighting the dominant role of the COX pathway in leaf  $R_{\text{dark}}$ . For leaves that developed under the warmer night growth temperature, AOX capacity doubled relative to those grown under the control night. Specifically, when expressed as a percentage of uninhibited rates of  $O_2$  uptake, KCN-resistant  $R_{26-O_2}$  (i.e.,  $O_2$  consumption by the AOX pathway) increased from 8.1 to 18.3% in the 26°C grown plants, and 9.2 to 20.7% in the heatwave treated plants when night temperatures rose from 14 to 21°C (Fig.

4). This trend was observed regardless of whether or not plants had been exposed to a 38°C daytime heatwave. In contrast to the effect of increasing night temperature, exposure to the three-day 38°C daytime heatwave had no significant effect on KCN- and/or SHAM-resistant rates of leaf  $R_{26}\text{-O}_2$  (Fig. 4 and Table 1).

**Table 1.** KCN and SHAM resistant leaf dark respiration rate measured at 26°C ( $R_{26}$ ) as  $\text{O}_2$  consumption in plants grown under 14 or 21°C night temperatures and exposed to a 38°C three-day daytime heatwave or maintained at 26°C day. 10mM potassium cyanide (KCN) was used to inhibit COX pathway, and 5mM salicylhydroxamic acid (SHAM) was used to inhibit AOX pathway.

Day/night (°C)	Leaf $R_{26}$ ( $\mu\text{mol O}_2 \text{ m}^{-2} \text{ s}^{-1}$ )			Residual (KCN + SHAM)
	Uninhibited	KCN-resistant	SHAM-resistant	
26/14	0.67 ± 0.06	0.13 ± 0.06	0.56 ± 0.05	0.09 ± 0.04
26/21	0.58 ± 0.05	0.20 ± 0.05	0.52 ± 0.04	0.12 ± 0.04
38/14	0.63 ± 0.05	0.15 ± 0.05	0.61 ± 0.04	0.11 ± 0.03
38/21	0.61 ± 0.05	0.25 ± 0.06	0.62 ± 0.04	0.15 ± 0.04
LSD ( $P < 0.05$ )				
Night temperature (NT)	0.25 <sup>ns</sup>	0.05 <sup>***</sup>	0.23 <sup>ns</sup>	0.03 <sup>ns</sup>
Day heatwave (DH)	0.25 <sup>ns</sup>	0.05 <sup>ns</sup>	0.23 <sup>ns</sup>	0.03 <sup>ns</sup>
NT x DH	0.36 <sup>ns</sup>	0.07 <sup>ns</sup>	0.33 <sup>ns</sup>	0.04 <sup>ns</sup>

Rates of  $\text{O}_2$  uptake are expressed as a percentage of the  $R_{\text{dark-O}_2}$  of uninhibited leaves (leaf wounding buffer-infiltrated leaves), and minus residual  $R_{\text{dark-O}_2}$  (i.e.  $R_{\text{dark-O}_2}$  of leaves inhibited by both KCN and SHAM). LSD – Fisher’s Least Significant Difference. \*\*\* indicates significance at  $P < 0.001$ ; <sup>ns</sup> indicates non-significance,  $P > 0.05$ . Mean ± s.e.,  $n = 5$ .

Interestingly, there was no change in  $R_{\text{dark-O}_2}$  with night warming in uninhibited leaves that experienced the daytime heatwave (Table 1). Under control growth conditions (26/14°C day/night temperatures), the  $Q_{10}$  of both SHAM and KCN resistant  $\text{O}_2$  uptake was 1.5–1.6, suggesting that the temperature sensitivity of the AOX and COX was similar under control conditions. Night warming was associated with a significant change ( $P < 0.05$ ; Table S2) in  $Q_{10}$  from 1.5 to 2.1 for SHAM-resistant  $\text{O}_2$  uptake (pointing to an increase in the  $Q_{10}$  of the COX pathway) but no change in KCN-resistant  $R_{\text{dark-O}_2}$ . Irrespective of the night temperature, exposure to a three-day daytime heatwave did not significantly alter the  $Q_{10}$  of KCN-resistant  $R_{\text{dark-O}_2}$  (mean  $Q_{10} = 1.3$ ) or SHAM-resistant  $R_{\text{dark-O}_2}$  (mean  $Q_{10} =$

1.8). Collectively, these results point to AOX capacity increasing under elevated night growth temperature, a phenotype which may be indicative of increased utilisation of non-energy producing electron transport and thus a way of achieving metabolic homeostasis under warm nights.

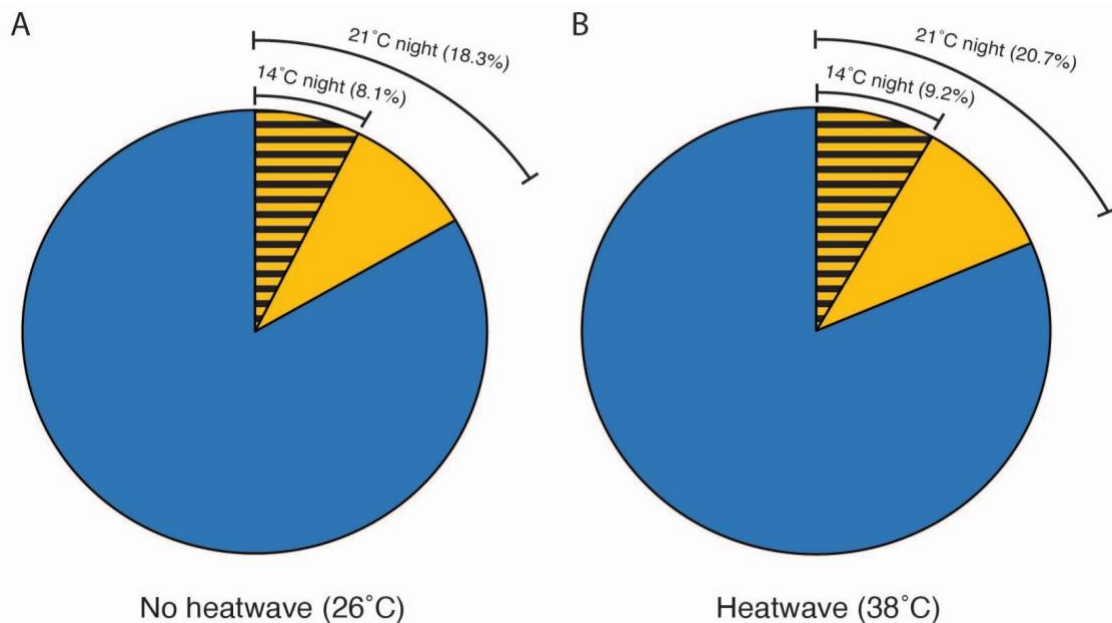


**Figure 4.** Representation of alternative oxidase (AOX) capacity (expressed as a percentage of uninhibited  $O_2$  uptake rates when measured at  $26^\circ C$ ) in wheat leaves grown at night temperatures of 14 or  $21^\circ C$  and a day temperature of  $26^\circ C$  or having been exposed to a maximum day temperature of  $38^\circ C$  for three days. (A) The yellow striped and unstriped sectors together show the AOX capacity percentage value following inhibition by KCN of leaf dark respiration measured at  $26^\circ C$ . AOX capacity more than doubled from 8% under  $14^\circ C$  night growth temperature (the striped sector) to 18% (the striped and yellow sector) at  $21^\circ C$  night. (B) A similar increase in AOX capacity (from 9 to 21%) with increase in night temperature (from 14 to  $21^\circ C$ ) was observed even when plants were also exposed to a  $38^\circ C$  daytime heatwave for three days.

## Discussion

### *Night warming, rather than day warming, is the major driver of respiratory acclimation*

In demonstrating a decline in rates of  $R_{\text{dark-}O_2}$  of leaves and roots measured under a common temperature in response to warming (Figs. 2 & 3), our results were consistent with previous descriptions of thermal acclimation of  $R_{\text{dark}}$  (Gifford, 1995; Atkin *et al.*, 2000;

Covey-Crump *et al.*, 2002; Armstrong *et al.*, 2006; Slot and Kitajima, 2015; Smith and Dukes, 2017; Dusenge *et al.*, 2018). However, we observed this thermal acclimation of  $R_{\text{dark}}$  only in response to night warming and not day warming, whereas most prior studies do not make this distinction. The strong effect of night warming on the acclimation of  $R_{\text{dark-O}_2}$  was also unlikely related to measurement time, as this was standardised across all experiments and also has been shown to be unrelated to the thermal acclimation of  $R_{\text{dark-O}_2}$  (Rashid *et al.*, 2020). Recent observational evidence from field-grown tree species also found that thermal acclimation of  $R_{\text{dark-CO}_2}$  was predominantly associated with prior night, but not day, temperatures (Reich *et al.*, 2021). Our results with wheat suggest that night and day temperatures play different roles in promoting respiratory acclimation, and thus that there may be different mechanisms underpinning the  $R_{\text{dark}}$  acclimation to night versus day temperature. Regarding the response of root  $R_{\text{dark-O}_2}$  to night warming, it is also worth noting that the warming imposed in our growth room experiment could potentially have a greater effect on the roots of pot-grown plants compared to the effect that equivalent ambient warming would have on the roots of field-grown plants. Thus, in order to confirm the observed decline in root  $R_{\text{dark-O}_2}$  with night warming, future experiments should look to replicate the insulation effect that is provided by soil in the field.

#### *Implications of the uncoupling of respiratory O<sub>2</sub> consumption and CO<sub>2</sub> release under warm nights*

We observed night warming to be associated with an uncoupling of respiratory O<sub>2</sub> and CO<sub>2</sub> flux. Despite the consistent decline in  $R_{\text{dark-O}_2}$  (at a standardized temperature) in response to night warming, the rate of  $R_{\text{dark}}$  did not change with growth temperature when measured as CO<sub>2</sub> flux at 25°C (Fig. 2D). The decline in O<sub>2</sub> consumption and the lack of change in CO<sub>2</sub> evolution in warm-night-grown leaves reflects an increase in respiratory quotient with night warming (RQ – the ratio of moles of CO<sub>2</sub> released to moles of O<sub>2</sub> consumed in mitochondrial respiration). We have not presented RQ values as they were calculated from O<sub>2</sub> and CO<sub>2</sub> flux measured by two separate instruments on different

individuals, thus the exact RQ numbers likely lacked precision. However, the decline in  $R_{\text{dark-O}_2}$  and lack of change in  $R_{\text{dark-CO}_2}$  following increases in night growth temperature were consistent across experiments, and thus we are confident that the ratio of  $\text{CO}_2$  released to  $\text{O}_2$  consumed did indeed increase with night growth temperature. Night warming was also associated with an increase in the capacity of the AOX pathway, a result that suggests a potential decline in the efficiency of ATP production.

Coast *et al.* (2021) described a similar rise in RQ in field-grown wheat that had experienced elevated growth temperatures. In that study, a two month delay in sowing led to plants experiencing a warmer average growth temperature over their lifespan, and this was associated with a reduced rate of  $R_{\text{dark-O}_2}$  but no change in  $R_{\text{dark-CO}_2}$  (Coast *et al.*, 2021). We confirmed this pattern in controlled environment grown wheat, while also identifying night warming as the key driver of this pattern. Given that glucose is the most common substrate in wheat (Plaxton and Podestá, 2006) and has an RQ of 1, an increase in RQ potentially reflects a change in respiratory substrate to a more oxygen-rich organic acid (Platenius, 1942; Berggren *et al.*, 2012). Both  $\text{C}_4$  and CAM plants use the organic acid malate as a form of photoassimilate storage in leaves, and recent evidence has suggested that  $\text{C}_3$  species such as *Arabidopsis* and rice may also employ malate in this way (Zell *et al.*, 2010; Rashid *et al.*, 2020); however the extent to which this might occur in wheat is unknown. Based on stoichiometry, switching substrate from glucose to malate would provide a way for a plant to reduce  $\text{O}_2$  consumption while maintaining the same rate of  $\text{CO}_2$  flux. Such a change in substrate could indicate that plants grown under warm nights experience a decline in ATP demand and release more  $\text{CO}_2$  per ATP generated, though fine scale simultaneous measurements of leaf  $\text{O}_2$  and  $\text{CO}_2$  flux are required to test this hypothesis and to provide more accurate RQ numbers.

#### *Why would night warming promote a decline in ATP demand?*

Reduced ATP demand under warm nights could arise from several processes associated with thermal acclimation. One of the most rapid forms of high temperature acclimation is the induction of heat shock proteins (HSPs), which accumulate within hours of

temperature increase (Vierling, 1991). HSPs stabilise and refold proteins (Wang *et al.*, 2004), as well preventing aggregating of mis-folded proteins (Trösch *et al.*, 2015). Energetic costs associated with protein turnover under high temperature, as well as total ATP demand, are likely reduced by these HSP functions. Warming may also decrease ATP demand by reducing protein synthesis and degradation costs due to accelerated rates of enzyme activity. For instance, Scafaro *et al.* (2021) illustrated how a 10°C rise in Arabidopsis growth temperature could lead to a 57% drop in Rubisco abundance and yet no change in enzymatic activity due to faster enzyme kinetics, resulting in the same enzyme activity levels being achieved for roughly half the ATP costs. Longer-term, heat acclimation involves alterations to lipid membrane fatty acid content (Los and Murata, 2004). Specifically, warming promotes increases in the degree of saturation of lipid membranes in an effort to preserve optimal membrane permeability (Larkindale and Huang, 2004). Increasing lipid membrane saturation under elevated temperature reduces proton leakage, thus decreasing the ATP requirement for maintaining proton gradients (Brookes, 2005). Though plants in the current manuscript were well-watered, it is still worth noting the potential for water stress to impact photosynthate availability and ATP demand given that water and heat stress commonly co-occur. Water stress has been associated with decreases in wheat photosynthetic rate and stomatal conductance, as well as plant height and grain size (Zhao *et al.*, 2020). By limiting intercellular CO<sub>2</sub> concentration and transpirational cooling (Reynolds *et al.*, 2010), drought-induced stomatal closure is likely to inhibit assimilate production and is thus a good example of how water stress may also negatively impact wheat respiration.

*Increased AOX capacity may reflect a drop in efficiency of ATP synthesis as nights warm*

The overall decline in leaf and root  $R_{26-O_2}$  rates as nights warmed coincided with a rise in AOX pathway capacity (i.e. specifically, an increase in the rate of KCN-resistant  $R_{26-O_2}$  as night growth temperature shifted from 14 to 21°C; Table 1). When considered as a proportion of total uninhibited leaf  $R_{26-O_2}$ , AOX capacity doubled under warm nights for plants grown under 26°C days (Fig 4A). It was also noteworthy that the night-warming-

induced increase in AOX capacity also occurred in plants exposed to a three-day 38°C daytime heatwave (Fig. 4B), further evidence of the importance of night warming, rather than day warming, in driving  $R_{26-O_2}$ . It should also be noted that  $R_{26-O_2}$  in the presence of inhibitors was expressed in proportion to  $R_{26-O_2}$  sliced and infiltrated in buffer, so the observed change in  $R_{26-O_2}$  is unlikely due to leaf injury.

The increased capacity of the AOX pathway that was observed under warm nights (Fig. 4) raises the possibility that a greater proportion of leaf  $R_{\text{dark}}$  is diverted through the AOX pathway under elevated night temperature. Macfarlane *et al.* (2009) found that the proportion of total  $R_{\text{dark}}$  accounted for by AOX activity was unchanged with short-term warming. However, we demonstrated an increase in AOX capacity following warming sustained over weeks, thus suggesting that engagement of the AOX pathway may only increase as part of a longer-term acclimation response. An increase in AOX use under elevated temperature could balance the redox poise of the ubiquinone pool in order to reduce ROS production while still maintaining TCA cycle activity (Millenaar and Lambers, 2003). Maintaining TCA cycle activity would be a priority over a 24-hour period if demand for C-skeletons was high during the day (Del-Saz *et al.*, 2018), which could possibly contribute to a lack of decline in  $\text{CO}_2$  flux as nights warmed. A rise in  $\text{CO}_2$  flux as night temperatures increase may reflect increased TCA cycle activity, which could require an increased pyruvate supply. Given that pyruvate and  $\alpha$ -keto acids are known to stimulate AOX pathway activity (Millar *et al.*, 1993, 1996), it is possible that the failure to acclimate  $R_{\text{dark-CO}_2}$  to night warming may have also influenced the increase in AOX capacity via pyruvate levels. Thus, when considering both an increase in AOX capacity and an overall decline in  $R_{\text{dark-O}_2}$ , we theorise that leaf  $R_{\text{dark}}$  may be both slower in rate and potentially less efficient in its energy production under elevated night growth temperatures. If true, it is likely that reduced ATP demand is driving these responses.

A decline in  $R_{\text{dark-O}_2}$  measured at a common temperature reflects acclimation to night warming, suggesting a homeostasis of ATP production across different night growth temperatures. By contrast, a lack of change in  $R_{\text{dark-CO}_2}$  measured at a given temperature may indicate a failure to maintain homeostasis of leaf  $\text{CO}_2$  release with rising night growth



temperature. We found that night warming was associated with consistent declines in above and below ground biomass (Fig. 1), recalling previously reported declines in crop biomass and yields that were attributed to night warming (Reynolds *et al.*, 1994; Peng *et al.*, 2004; Welch *et al.*, 2010; García *et al.*, 2015; Bahuguna *et al.* 2021). The disparate responses of O<sub>2</sub> and CO<sub>2</sub> flux under warm nights could thus be a contributing factor to these declines in biomass accumulation.

### *Conclusion*

By separating day and night warming we were able to demonstrate that night warming had a significantly greater impact than day warming on the temperature-normalized rates and short-term temperature sensitivity of leaf respiratory O<sub>2</sub> consumption, as well as driving declines in above- and below-ground biomass.  $R_{\text{dark-O}_2}$  measured at 25°C in both leaves and roots declined only in response to night warming, demonstrating a classic acclimation response to increased night temperature but not to increased day temperature. This points to a coordinated change in respiratory metabolism across the whole plant, likely in response to changes in energy demand within leaves and roots induced by warm nights. That night warming alters energy demand is further evidenced by the increase in capacity of the alternative respiratory pathway that was observed. Yet, despite clear patterns of O<sub>2</sub> consumption acclimating to night warming, temperature-normalized rates of  $R_{\text{dark-CO}_2}$  were unchanged with increased growth temperature. Thus, warm nights resulted in higher overall rates of realized  $R_{\text{dark-CO}_2}$  – a factor that would limit the daily accumulation of carbon (and thus growth). A lower efficiency of ATP synthesis, teamed with sustained flux of CO<sub>2</sub>, could thus be key factors contributing to biomass declines that have been observed under night warming. Future studies that combine simultaneous measurements of O<sub>2</sub> and CO<sub>2</sub> flux with fine-scale tracking of growth rate for plants grown under warm nights could provide confirmation as to the extent that these responses are contributing to the reduced growth phenotype that has been observed. Such work is urgent, as future climate projections indicate a much greater extent of night- than day-warming, and hence our ability to predict future crop responses

will hinge on improved understanding of night-time temperature impacts on all aspects of plant metabolism.

## **Acknowledgments**

This project was supported by grants from the Grains Research Development Corporation (GRDC) (US00080, and UOS1904-003RTX) and the Australian Research Council Centre of Excellence in Plant Energy Biology (CE140100008). BCP was supported by the Australian Government Research Training Program. OC received support from a GRDC Fellowship (UOS1904-003RTX) and Research England's 'Expanding Excellence in England' (E3)-funded Food and Nutrition Security Initiative of the Natural Resources Institute. DAW was also supported in part by the US Department of Energy contract number DE-SC0012704 to Brookhaven National Laboratory. PBR was supported in part by the by US National Science Foundation, Biological Integration Institutes grant NSF-DBI-2021898. D.Z. was supported by the China Scholarship Council. We are grateful to staff of the ANU Research School of Biology Plant Services Team for maintaining the plants in the controlled environments. We also thank the Australian Plant Phenomics Facility, which is supported under the National Collaborative Research Infrastructure Strategy of the Australian Government.

## **References**

**Armstrong AF, Logan DC, Atkin OK.** 2006. On the developmental dependence of leaf respiration: Responses to short- and long-term changes in growth temperature. *American Journal of Botany* **93**, 1633–1639.

**Atkin OK, Edwards EJ, Loveys BR.** 2000. Response of root respiration to changes in temperature and its relevance to global warming. *New Phytologist* **147**, 141–154.

**Atkin OK, Tjoelker MG.** 2003. Thermal acclimation and the dynamic response of plant respiration to temperature. *Trends in Plant Science* **8**, 343–351.

**Atkin OK, Zhang Q, Wiskich JT.** 2002. Effect of temperature on rates of alternative and cytochrome pathway respiration and their relationship with the redox poise of the quinone pool. *Plant Physiology* **128**, 212–222.

**Australian Grain Technologies.** 2021. Our Varieties - Older Varieties.

**Azcón-Bieto J, Lambers H, Day DA.** 1983. Effect of photosynthesis and carbohydrate status on respiratory rates and the involvement of the alternative pathway in leaf respiration. *Plant Physiology* **72**, 598–603.

**Bahuguna RN, Chaturvedi AK, Pal M, Chinnusamy V, Jagadish SVK, Pareek A.** 2021. Carbon dioxide responsiveness mitigates rice yield loss under high night temperature. *Plant Physiology*.

**Berggren M, Lapierre JF, Del Giorgio PA.** 2012. Magnitude and regulation of bacterioplankton respiratory quotient across freshwater environmental gradients. *ISME Journal* **6**, 984–993.

**Brookes PS.** 2005. Mitochondrial H<sup>+</sup> leak and ROS generation: An odd couple. *Free Radical Biology and Medicine* **38**, 12–23.

**Coast O, Posch BC, Bramley H, Gaju O, Richards RA, Lu M, Ruan Y, Trethowan R, Atkin OK.** 2021. Acclimation of leaf photosynthesis and respiration to warming in field-grown wheat. *Plant, Cell & Environment*, pce.13971.

**Covey-Crump EM, Attwood RG, Atkin OK.** 2002. Regulation of root respiration in two species of *Plantago* that differ in relative growth rate: The effect of short- and long-term changes in temperature. *Plant, Cell & Environment* **25**, 1501–1513.

**Davy R, Esau I, Chernokulsky A, Outten S, Zilitinkevich S.** 2017. Diurnal asymmetry to the observed global warming. *International Journal of Climatology* **37**, 79–93.

**Del-Saz NF, Ribas-Carbo M, McDonald AE, Lambers H, Fernie AR, Florez-Sarasa I.** 2018. An in vivo perspective of the role(s) of the alternative oxidase pathway. *Trends in Plant Science* **23**, 206–219.

**Dilly O.** 2001. Microbial respiratory quotient during basal metabolism and after glucose amendment in soils and litter. *Soil Biology and Biochemistry* **33**, 117–127.

**Dusenge ME, Duarte AG, Way DA.** 2018. Plant carbon metabolism and climate change: elevated CO<sub>2</sub> and temperature impacts on photosynthesis, photorespiration and respiration. *New Phytologist* **2**, 32–49.

**Fedyaeva A V., Stepanov A V., Lyubushkina I V., Pobezhimova TP, Rikhvanov EG.** 2014. Heat shock induces production of reactive oxygen species and increases inner mitochondrial membrane potential in winter wheat cells. *Biochemistry (Moscow)* **79**, 1202–1210.

**García GA, Dreccer MF, Miralles DJ, Serrago RA.** 2015. High night temperatures during grain number determination reduce wheat and barley grain yield: A field study. *Global Change Biology* **21**, 4153–4164.

**Gifford RM.** 1995. Whole plant respiration and photosynthesis of wheat under increased CO<sub>2</sub> concentration and temperature: long-term vs. short-term distinctions for modelling. *Global Change Biology* **1**, 385–396.

**Heskel MA, O’Sullivan OS, Reich PB, et al.** 2016. Convergence in the temperature response of leaf respiration across biomes and plant functional types. *Proceedings of the National Academy of Sciences* **113**, 3832–3837.

**Impa SM, Sunoj VSJ, Krassovskaya I, Bheemanahalli R, Obata T, Jagadish SVK.** 2019. Carbon balance and source-sink metabolic changes in winter wheat exposed to high night-time temperature. *Plant, Cell & Environment* **42**, 1233–1246.

**Kurimoto K, Day DA, Lambers H, Noguchi K.** 2004. Effect of respiratory homeostasis on plant growth in cultivars of wheat and rice. *Plant, Cell & Environment* **27**, 853–862.

**Kuznetsova A, Brockhoff PB, Christensen RHB.** 2017. lmerTest package: tests in linear mixed effects models. *Journal of Statistical Software* **82**.

**Lambers H.** 1980. The physiological significance of cyanide-resistant respiration in higher plants. *Plant, Cell & Environment* **3**, 293–302.

**Larkindale J, Huang B.** 2004. Changes of lipid composition and saturation level in leaves and roots for heat-stressed and heat-acclimated creeping bentgrass (*Agrostis stolonifera*). *Environmental and Experimental Botany* **51**, 57–67.

**Lenth R.** 2020. Estimated Marginal Means, aka Least-Squares Means. R package version 1.5.2-1.

**Los DA, Murata N.** 2004. Membrane fluidity and its roles in the perception of environmental signals. *Biochimica et Biophysica Acta - Biomembranes* **1666**, 142–157.

**MacFarlane C, Hansen LD, Florez-Sarasa I, Ribas-Carbo M.** 2009. Plant mitochondria electron partitioning is independent of short-term temperature changes. *Plant, Cell & Environment* **32**, 585–591.

**Millar AH, Hoefnagel M, Day DA, Wiskich JT.** 1996. Specificity of the Organic Acid Activation of Alternative Oxidase in Plant Mitochondria. *Plant Physiology* **111**, 613–618.

**Millar AH, Wiskich JT, Whelan J, Day DA.** 1993. Organic acid activation of the alternative oxidase of plant mitochondria. *FEBS Letters* **329**, 259–262.

**Millenaar FF, Lambers H.** 2003. The alternative oxidase: In vivo regulation and function. *Plant Biology* **5**, 2–15.

**Murakami Y, Toriyama K.** 2008. Enhanced high temperature tolerance in transgenic rice seedlings with elevated levels of alternative oxidase, OsAOX1a. *Plant Biotechnology* **25**, 361–364.

**O’Leary BM, Asao S, Millar AH, Atkin OK.** 2019. Core principles which explain variation in respiration across biological scales. *New Phytologist* **222**, 670–686.

**Peng S, Huang J, Sheehy JE, Laza RC, Visperas RM, Zhong X, Centeno GS, Khush GS, Cassman KG.** 2004. Rice yields decline with higher night temperature from global warming. *Proceedings of the National Academy of Sciences of the United States of America* **101**, 9971–9975.

**Pinto RS, Molero G, Reynolds MP.** 2017. Identification of heat tolerant wheat lines showing genetic variation in leaf respiration and other physiological traits. *Euphytica* **213**, 1–15.

**Platenius H.** 1942. Effect of temperature on the respiration rate and the respiratory quotient of some vegetables. *Plant Physiology* **17**, 179–197.

**Plaxton WC, Podestá FE.** 2006. The functional organization and control of plant respiration. *Critical Reviews in Plant Sciences* **25**, 159–198.

**Poorter H, Remkes C, Lambers H.** 1990. Carbon and nitrogen economy of 24 wild species differing in relative growth rate. *Plant Physiology* **94**, 621–627.

**Rachmilevitch S, Xu Y, Gonzalez-Meler MA, Huang B, Lambers H.** 2007. Cytochrome and alternative pathway activity in roots of thermal and non-thermal *Agrostis* species in response to high soil temperature. *Physiologia Plantarum* **129**, 163–174.

**Rashid FAA, Scafaro AP, Asao S, Fenske R, Dewar RC, Masle J, Taylor NL, Atkin OK.** 2020.

Diel- and temperature-driven variation of leaf dark respiration rates and metabolite levels in rice. *New Phytologist*.

**Reich PB, Sendall KM, Stefanski A, Wei X, Rich RL, Montgomery RA.** 2016. Boreal and temperate trees show strong acclimation of respiration to warming. *Nature* **531**, 633–636.

**Reich PB, Stefanski A, Rich RL, Sendall KM, Wei X, Zhao C, Hou J, Montgomery RA, Bermudez R.** 2021. Assessing the relevant time frame for temperature acclimation of leaf dark respiration: A test with 10 boreal and temperate species. *Global Change Biology*, 1–14.

**Reynolds MP, Balota M, Delgado MI, Amani I, Fischer RA.** 1994. Physiological and morphological traits associated with spring wheat yield under hot, irrigated conditions. *Journal of Plant Physiology* **21**, 717–30.

**Reynolds MP, Hays D, Chapman SC.** 2010. Breeding for adaptation to heat and drought stress. In: Reynolds MP, ed. *Climate Change and Crop Production*. Wallingford: CABI, 71–91.

**Scafaro AP, Fan Y, Posch BC, Garcia A, Coast O, Atkin OK.** 2021. Responses of leaf respiration to heatwaves. *Plant, Cell & Environment*, pce.14018.

**Scafaro AP, Negrini ACA, O’Leary BM, et al.** 2017. The combination of gas-phase fluorophore technology and automation to enable high-throughput analysis of plant respiration. *Plant Methods* **13**, 1–13.

**Searle SY, Bitterman DS, Thomas S, Griffin KL, Atkin OK, Turnbull MH.** 2011. Respiratory alternative oxidase responds to both low- and high-temperature stress in *Quercus rubra* leaves along an urban-rural gradient in New York. *Functional Ecology* **25**, 1007–1017.

**Searle SY, Turnbull MH.** 2011. Seasonal variation of leaf respiration and the alternative pathway in field-grown *Populus × canadensis*. *Physiologia Plantarum* **141**, 332–342.

**Slot M, Kitajima K.** 2015. General patterns of acclimation of leaf respiration to elevated temperatures across biomes and plant types. *Oecologia* **177**, 885–900.

**Smith NG, Dukes JS.** 2017. Short-term acclimation to warmer temperatures accelerates leaf carbon exchange processes across plant types. *Global Change Biology* **23**, 4840–4853.

**Trösch R, Mühlhaus T, Schroda M, Willmund F.** 2015. ATP-dependent molecular chaperones in plastids - More complex than expected. *Biochimica et Biophysica Acta - Bioenergetics* **1847**, 872–888.

**Turnbull MH, Murthy R, Griffin KL.** 2002. The relative impacts of daytime and night-time warming on photosynthetic capacity in *Populus deltoides*. *Plant, Cell & Environment* **25**, 1729–1737.

**Turnbull MH, Tissue DT, Murthy R, Wang X, Sparrow AD, Griffin KL.** 2004. Nocturnal warming increases photosynthesis at elevated CO<sub>2</sub> partial pressure in *Populus deltoides*. *New Phytologist* **161**, 819–826.

**Vanlerberghe GC.** 2013. Alternative oxidase: A mitochondrial respiratory pathway to maintain metabolic and signaling homeostasis during abiotic and biotic stress in plants. *International Journal of Molecular Sciences* **14**, 6805–6847.

**Vierling E.** 1991. *The Roles of Heat Shock Proteins in Plants*. Environment.

**Wang H, Atkin OK, Keenan TF, Smith NG, Wright IJ, Bloomfield KJ, Kattge J, Reich PB, Prentice IC.** 2020. Acclimation of leaf respiration consistent with optimal photosynthetic

capacity. *Global Change Biology*, 2573–2583.

**Wang W, Vinocur B, Shoseyov O, Altman A.** 2004. Role of plant heat-shock proteins and molecular chaperones in the abiotic stress response. *Trends in Plant Science* **9**, 244–252.

**Welch JR, Vincent JR, Auffhammer M, Moya PF, Dobermann A, Dawe D.** 2010. Rice yields in tropical/subtropical Asia exhibit large but opposing sensitivities to minimum and maximum temperatures. *Proceedings of the National Academy of Sciences of the United States of America* **107**, 14562–14567.

**Zadoks JC, Chang TT, Konzak CF.** 1974. A decimal code for the growth stages of cereals. *Weed Research* **14**, 415–421.

**Zell MB, Fahnenstich H, Maier A, et al.** 2010. Analysis of Arabidopsis with highly reduced levels of malate and fumarate sheds light on the role of these organic acids as storage carbon molecules. *Plant Physiology* **152**, 1251–1262.

**Zhao W, Liu L, Shen Q, Yang J, Han X, Tian F, Wu J.** 2020. Effects of water stress on photosynthesis, yield, and water use efficiency in winter wheat. *Water* **12**, 1–19.

## Supplementary material

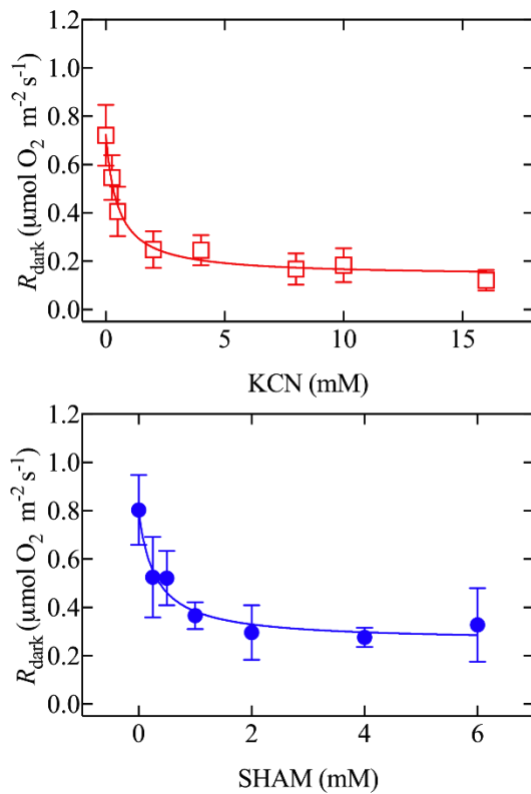


**Figure S1:** Curves showing the effectiveness of inhibition of wheat leaf  $R_{\text{dark-O}_2}$  at 26°C in the genotype Mace using increasing concentrations of potassium cyanide (KCN) and salicylhydroxamic acid (SHAM), respectively. Residual respiration in the presence of both inhibitors was  $0.12 \pm 0.02$  (mean  $\pm$  SD;  $n = 20$ ).

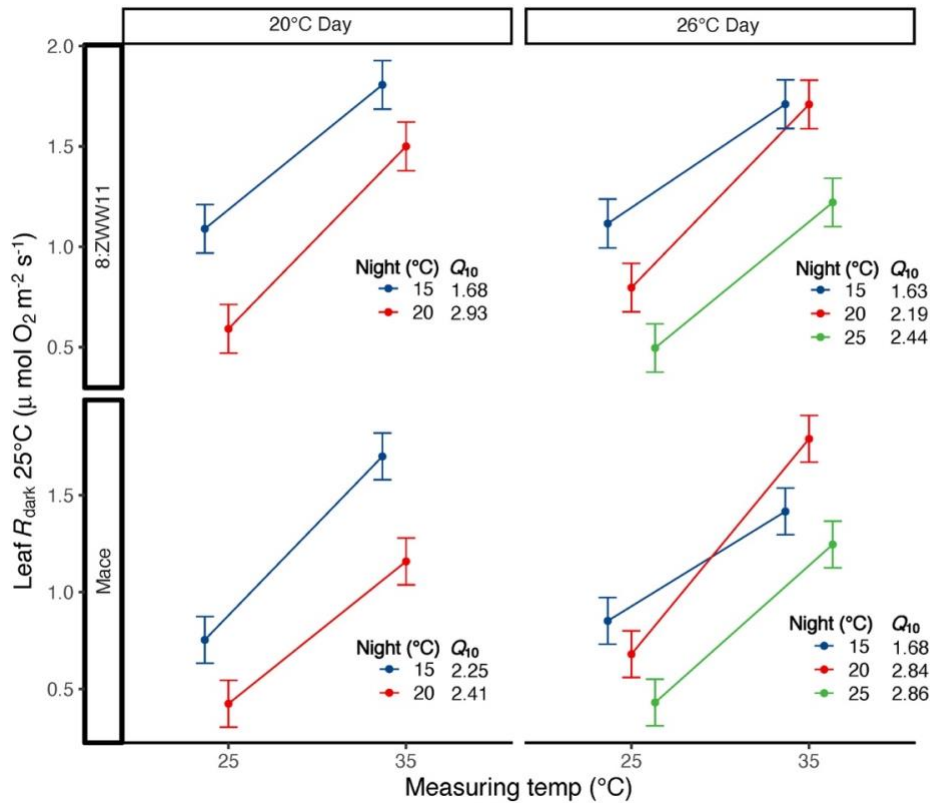


**Figure S2:** Sensitivity of leaf dark respiration  $R_{\text{dark-O}_2}$  to increasing measuring temperature in wheat genotypes 8:ZWW11 and Mace, grown under 15, 20, or 25°C nights, and 20 or 26°C days.  $R_{\text{dark-O}_2}$  was measured as per unit leaf area ( $\mu\text{mol O}_2 \text{ m}^{-2} \text{ s}^{-1}$ );  $n = 4$ ; error bars denote s.e;  $Q_{10}$  refers to the proportional increase in  $R_{\text{dark}}$  with a 10°C rise in measuring temperature.



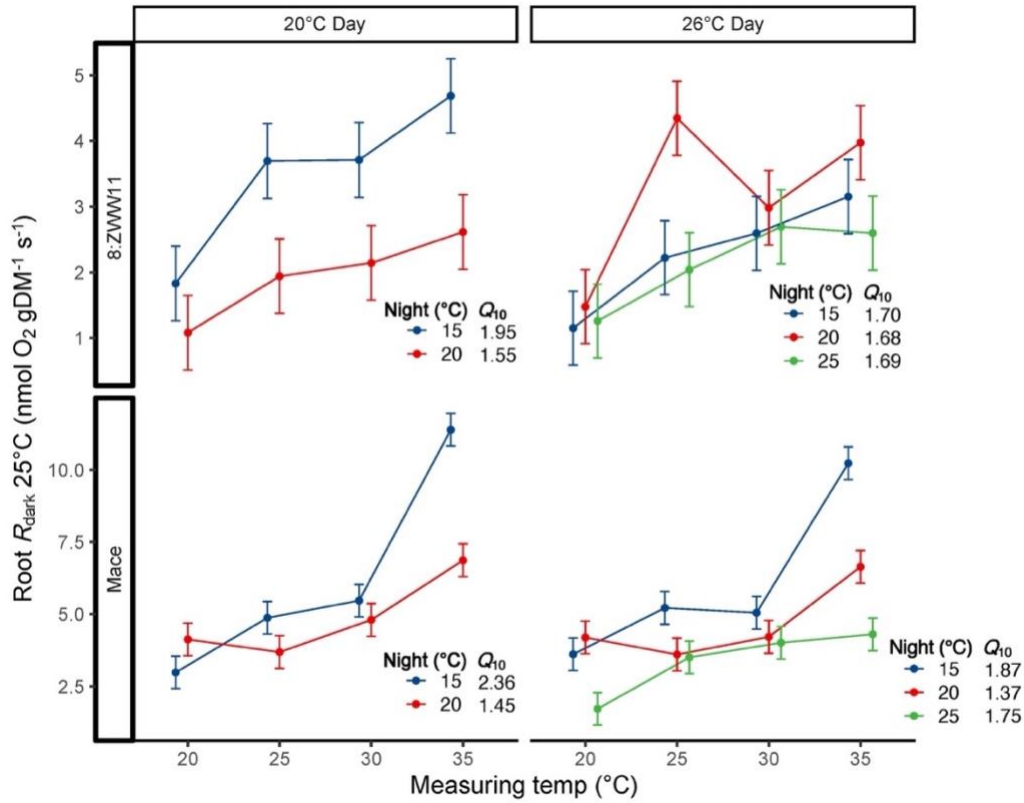


**Figure S3.** Root dark respiration ( $R_{\text{dark-O}_2}$ ): sensitivity of root  $R_{\text{dark-O}_2}$  to increasing measuring temperature in wheat genotypes 8:ZWW11 and Mace, grown under 15, 20, or 25°C nights, and 20 or 26°C days.  $R_{\text{dark-O}_2}$  was measured as per gram of root dry mass ( $\text{nmol O}_2 \text{ g DM}^{-1} \text{ s}^{-1}$ );  $n = 4$ ; error bars denote s.e.;  $Q_{10}$  refers to the proportional increase in  $R_{\text{dark}}$  with a 10°C rise in measuring temperature.

**Table S1:** Analysis of variance of traits for Mace and 8:ZWW11 wheat genotypes grown under warm night and/or day growth temperature in Experiment 1.

	Genotype		Night temperature		Day temperature	
	d.f.	F value	d.f.	F value	d.f.	F value
<b>Leaf</b>						
O <sub>2</sub> -based dry mass: $R_{25-O_2}$ ( $\mu\text{mol O}_2 \text{ gDM}^{-1} \text{ s}^{-1}$ )	1	16.5 <sup>***</sup>	2	20.8 <sup>***</sup>	1	0.7 <sup>ns</sup>
O <sub>2</sub> -based area: $R_{25-O_2}$ ( $\mu\text{mol O}_2 \text{ m}^{-2} \text{ s}^{-1}$ )	1	15 <sup>***</sup>	2	43.9 <sup>***</sup>	1	10.4 <sup>**</sup>
O <sub>2</sub> -based area: $Q_{10}$ of $R_{25-O_2}$ ( $\mu\text{mol O}_2 \text{ m}^{-2} \text{ s}^{-1}$ )	1	1.61 <sup>ns</sup>	4	4.9 <sup>**</sup>	4	1.35 <sup>ns</sup>
CO <sub>2</sub> -based area: $R_{25-CO_2}$ ( $\mu\text{mol CO}_2 \text{ m}^{-2} \text{ s}^{-1}$ )	1	19.8 <sup>***</sup>	2	1.5 <sup>ns</sup>	1	0.3 <sup>ns</sup>
<b>Root</b>						
O <sub>2</sub> -based dry mass: $R_{25-O_2}$ ( $\mu\text{mol O}_2 \text{ gDM}^{-1} \text{ s}^{-1}$ )	1	21.6 <sup>***</sup>	2	4 <sup>*</sup>	1	0.6 <sup>ns</sup>
O <sub>2</sub> -based dry mass: $Q_{10}$ of $R_{25-O_2}$ ( $\mu\text{mol O}_2 \text{ gDM}^{-1} \text{ s}^{-1}$ )	1	43.12 <sup>***</sup>	4	6.28 <sup>**</sup>	4	5.31 <sup>**</sup>
<b>Biomass</b>						
Above-ground biomass (g)	1	38.72 <sup>***</sup>	2	20.7 <sup>***</sup>	1	2.04 <sup>ns</sup>
Below-ground biomass (g)	1	0.03 <sup>ns</sup>	2	34.25 <sup>***</sup>	1	2.91 <sup>ns</sup>

\* $P < 0.05$ ; \*\* $P < 0.01$ ; \*\*\* $P < 0.001$ ; <sup>ns</sup> = not significant.  $n = 4$ .  $R_{25-O_2}$  – dark respiration measured as O<sub>2</sub> consumption at 25°C;  $R_{25-CO_2}$  – dark respiration measured as CO<sub>2</sub> consumption at 25°C;  $Q_{10}$  – proportional increase in  $R_{\text{dark}}$  with 10°C rise in measuring temperature. Night growth temperatures were 15, 20, and 25°C, while day growth temperatures were 20 and 26°C. No interactions between factors were significant for any leaf  $R_{\text{dark}}$  measurements, so these are not shown in the table. The genotype  $\times$  night temperature, and genotype  $\times$  night temperature  $\times$  day temperature interactions were significant for root  $R_{25-O_2}$  ( $P < 0.05$ ), and the genotype  $\times$  day temperature interaction was significant for above-ground biomass ( $P < 0.05$ ).

**Table S2:** Analysis of variance of O<sub>2</sub>-based leaf dark respiration ( $R_{\text{dark-O}_2}$ ) for Mace grown under warm nights and/or exposed to 3 days of daytime heatwave in Experiment 2.

	Night temperature (NT)		Day heatwave (DH)		NT x DH	
	d.f.	F value	d.f.	F value	d.f.	F value
Leaf $R_{26\text{-O}_2}$ ( $\mu\text{mol O}_2 \text{ m}^{-2} \text{ s}^{-1}$ )	1	7.72 *	1	0.11 <sup>ns</sup>	1	0.06 <sup>ns</sup>
SHAM-resistant $R_{26\text{-O}_2}$ (as percentage of uninhibited leaf $R_{26\text{-O}_2}$ )	1	1.48 <sup>ns</sup>	1	6.3 *	1	0.002 <sup>ns</sup>
KCN-resistant $R_{26\text{-O}_2}$ (as percentage of uninhibited leaf $R_{26\text{-O}_2}$ )	1	7.96 *	1	0.2 <sup>ns</sup>	1	0.03 <sup>ns</sup>
SHAM-resistant $Q_{10}$	1	8.8 *	1	0.08 <sup>ns</sup>	1	2.11 <sup>ns</sup>
KCN-resistant $Q_{10}$	1	0.66 <sup>ns</sup>	1	0.47 <sup>ns</sup>	1	2.93 <sup>ns</sup>

\* $P < 0.05$ ; \*\* $P < 0.01$ ; \*\*\* $P < 0.001$ ; <sup>ns</sup> = not significant.  $n = 5$ .  $R_{\text{dark-O}_2}$  at 26°C – leaf dark respiration measured as O<sub>2</sub> consumption per  $\text{m}^{-2} \text{ s}^{-1}$  at 26°C; SHAM - salicylhydroxamic acid, used to inhibit AOX pathway; KCN – potassium cyanide, used to inhibit COX pathway. Night growth temperature was 14°C or 21°C, control day growth temperature was 26°C, and heatwave day temperature was 38°C.

## Statement of Contribution

This thesis is submitted as a Thesis by Compilation in accordance with [https://policies.anu.edu.au/ppl/document/ANUP\\_003405](https://policies.anu.edu.au/ppl/document/ANUP_003405)

I declare that the research presented in this Thesis represents original work that I carried out during my candidature at the Australian National University, except for contributions to multi-author papers incorporated in the Thesis where my contributions are specified in this Statement of Contribution.

Title: Wheat respiratory O<sub>2</sub> consumption falls with night warming alongside greater respiratory CO<sub>2</sub> loss and reduced biomass \_\_\_\_

Authors: Bradley C. Posch, Deping Zhai, Onoriode Coast, Andrew P. Scafaro, Helen Bramley, Peter B. Reich, Yong-Ling Ruan, Richard Trethowan, Danielle A. Way, and Owen K. Atkin \_\_\_\_\_

Publication outlet: Journal of Experimental Botany \_\_\_\_\_

Current status of paper: Published

Contribution to paper: O.K.A., H.B., and Y-L.R. secured grants; R.T. developed seed material; B.C.P., O.C., A.P.S., and O.K.A. designed research; B.C.P., D.Z., A.P.S. performed research; B.C.P., O.C., A.P.S., and O.K.A. analysed data; and B.C.P. wrote the paper with contributions from all authors. \_\_\_\_\_

Senior author or collaborating authors endorsement: Owen Atkin April 2nd 2022

Bradley C. Posch

Candidate – Print Name

*B.P.L.*

Signature

01-04-2022

Date

### Endorsed

PROFESSOR OWEN ATKIN

Primary Supervisor – Print Name

*Owen Atkin*

Signature

April 2nd 2022

Date

## Chapter 5 – General discussion

### Recap of results

The literature review in Chapter 1 provided a snapshot of the current knowledge of the effects of high temperature of respiration and photosynthesis in wheat. A major takeaway from this was the disparity between the amount of work that has focussed on the high temperature response of respiration versus that focussing on the high temperature response of photosynthesis; specifically, far less is known regarding the effect of warming on wheat respiration. This lack of attention comes despite the crucial role of respiration in plant functioning, with variations in respiration having the potential to influence biomass accumulation and yield, as well as affecting the extent of warming of the climate around the globe. While there are previous papers detailing the high temperature acclimation responses of plant respiration in a variety of species (Atkin and Tjoelker, 2003; Reich *et al.*, 2016; O’Sullivan *et al.*, 2017), these have rarely included one of the world’s most widely consumed crops – wheat. Thus, a major aim of this thesis was to describe the response of wheat respiration to warming and determine whether wheat demonstrates a pattern of thermal acclimation of respiration similar to that described in other species.

Following the literature review, Chapter 2 described a multi-season field experiment in which delayed time of sowing was used to investigate the effect of elevated growth temperature on respiration and photosynthesis in 20 field-grown wheat genotypes. We reported on numerous leaf gas-exchange traits at anthesis, including flag leaf dark respiration rates measured as the rate of O<sub>2</sub> consumption ( $R_{\text{dark-O}_2}$ ) at multiple temperatures. We also measured a number of CO<sub>2</sub> flux based traits, including  $R_{\text{dark}}$  measured as the rate of CO<sub>2</sub> release at 25°C ( $R_{\text{dark-CO}_2^{25}}$ ), CO<sub>2</sub> assimilation rate at 25°C ( $A^{25}$ ), and maximum carboxylation rate at 25°C ( $V_{\text{cmax}}^{25}$ ). When measured at a common temperature  $R_{\text{dark-O}_2}$  declined with the later, warmer times of sowing, consistent with the predicted thermal acclimation response. However, we found no evidence of a similar downregulation for our CO<sub>2</sub>-based traits – across the two field seasons  $R_{\text{dark-CO}_2^{25}}$ ,  $A^{25}$ , and  $V_{\text{cmax}}^{25}$  were all either unchanged or increased from TOS 1 to either TOS 2 or 3. This apparent lack of acclimation of CO<sub>2</sub> flux to warming contradicted many previous descriptions of thermal acclimation – most notably the response of  $R_{\text{dark}}$  – and points to an uncoupling of O<sub>2</sub> and CO<sub>2</sub> flux under elevated growth temperature.

Chapter 3 continued with a focus on the temperature response of photosynthesis, though this time revolving around chloroplast electron transport and the heat tolerance of photosystem II (PSII). For this work, PSII heat tolerance was measured as  $T_{crit}$ , the critical temperature at which PSII begins to experience irreversible damage. We employed a high throughput assay to screen  $T_{crit}$  in multiple field experiments as well as under controlled conditions. In the field,  $T_{crit}$  was revealed to rise throughout the course of a day and peak close to sundown, before then declining through the night to a low point prior to dawn.  $T_{crit}$  also varied across wheat phenological stages; it rose significantly from the heading stage of development higher to the anthesis and grain filling stages. There was abundant evidence of  $T_{crit}$  increasing with elevated growth temperature, as well as of genotypic variation in the response of  $T_{crit}$  to warming. The genotypes that did increase their  $T_{crit}$  with warming enjoyed increased thermal safety margins at their respective field sites, at least when calculating margins based on current climate records. However, the majority of genotypes appear likely to lose their thermal safety margin if the warming predicted under high emission scenarios occurs. There was also limited evidence that geographical origin of genotype pedigrees was associated with observed variation in  $T_{crit}$  and the acclimation of  $T_{crit}$  to high temperature, and there appeared to be little correlation between mean temperature of origin sites and observed  $T_{crit}$  values. A growth cabinet experiment was employed to quantify the speed and threshold of  $T_{crit}$  rise following a heat stress of 36°C. In both genotypes measured  $T_{crit}$  had risen after only two hours of heat stress, and this rapid rise continued up to one day into the treatment. However, from this point on we observed a plateau in  $T_{crit}$  up to the five day mark, suggesting the existence of an upper acclimation threshold of  $T_{crit}$ . Though eventually reaching a similar upper threshold, the two genotypes that were measured differed in the speed of their  $T_{crit}$  rise, thus raising the potential of genotypic variation in the speed of acclimation of PSII in wheat. An analysis that brought together our experimental data with wheat  $T_{crit}$  data from the literature also demonstrated no relationship between the latitude of wheat genotype climate of origin and  $T_{crit}$ . This was contrary to previously reported studies of woody, non-crop species that described an increase in  $T_{crit}$  in plants that originated closer to the equator.

In Chapter 4, many of the results that were gathered in the field were followed up with controlled environment experiments that, among other things, aimed to examine the effects of daytime and night-time warming on wheat respiratory metabolism. Growing two

genotypes under one of three night temperatures (15, 20, or 25°C) and one of two day temperatures (20 or 26°C) for approximately one month, flag leaf and root  $R_{\text{dark}}$  was measured both as the rate of  $\text{O}_2$  consumption for leaves and roots, as well as the rate of  $\text{CO}_2$  release for leaves. Above and below ground plant biomass were also measured at the conclusion of temperature treatments. Just as was observed in the field, a typical respiratory acclimation response to warming (i.e. a downregulation) was observed in both leaves and roots when measuring  $R_{\text{dark-O}_2}$  at a common temperature. Interesting to note, however, was that this acclimation was associated only with night warming, rather than daytime warming. Also consistent with the fieldwork results was that there was no evidence of a similar acclimation response in the controlled environments when  $R_{\text{dark}}$  was measured as  $\text{CO}_2$  release. In addition, night warming was also associated with significant declines in both above and below ground biomass (measured at a common phenological stage), while daytime warming again had a far smaller, if any, effect. A follow up experiment was run to further investigate the effect of night warming on wheat leaf respiration, specifically focussing on the response of the non-energy producing mitochondrial alternative oxidase (AOX) electron transport pathway. Plants were grown for approximately 3 weeks under one of two night temperatures (14 or 20°C) and a common day temperature, before then being treated to a five-day 38°C daytime heatwave. Potassium cyanide (KCN) used to inhibit the cytochrome oxidase pathway, meaning that subsequent measurements of  $R_{\text{dark-O}_2}$  provided an insight into AOX pathway capacity. Once again, night warming appeared to have a larger influence than daytime warming (in this case, a daytime heatwave), with AOX pathway capacity of warm night grown plants double that of cool night grown plants.

### **The pros and cons of differing approaches to studying heat tolerance of wheat physiology**

The research described in the preceding chapters encompasses a diverse set of experimental approaches and designs, and many specific pros and cons of these approaches were discussed in the relevant chapters. However, a reflection on the broader benefits and drawbacks may also be useful for guiding future plant physiology/heat tolerance research. A fundamental consideration is whether experimental work is conducted in the field or in a controlled environment. When studying plant responses to warming, the environmental control that

growth cabinet experiments provide is invaluable. The ability to isolate warming from other environmental variables that often accompany it in the field, such as water stress, in order to more easily identify mechanisms that underlie physiological temperature responses is particularly useful. The results presented in Chapters 3 and 4 are a testament to this; in Chapter 3 growth chambers facilitated the imposition of a tightly controlled heat stress event, allowing a hard upper-limit to wheat PSII heat tolerance to be identified; in Chapter 4, walk-in growth rooms allowed us to compare the effect of night warming with that of day warming and a day heatwave by controlling each separately. Considering the difficulty of conducting such heat-manipulation experiments in the field (particularly outside the growth season), controlled environment experiments such as those conducted for this thesis have clear utility. However, despite great advances in the capabilities of controlled environment facilities, it remains near impossible to recreate the complexity of the field environment to the point where controlled studies could reliably predict real-world crop performance. Thus, field experiments remain a crucial aspect of crop physiology research. There are techniques that can be adopted to impose warming in the field, including exploiting seasonal warming by delaying sowing time, as described in Chapter 2. However, delaying sowing does not guarantee plants will experience warmer conditions; for example, during our 2017 field experiment in Dingwall average night temperature from sowing to anthesis did not change between time of sowing one and two. As previously discussed, delayed sowing also brings additional environmental variation, such as seasonal changes in light and precipitation patterns, making it more difficult to tease apart specific warming effects. Recent papers have demonstrated the viability of imposing warming in the field with portable heating chambers (Thistlethwaite *et al.*, 2020; Bahuguna *et al.*, 2022), a strategy that may mitigate some of these issues and thus provide even further insight into temperature responses in the field than that gained in Chapter 2.

While the concept of acclimation providing a benefit to wheat performance under warming conditions was a consistent theme throughout this thesis, it is important to note that acclimation is not necessarily a panacea. While it may lead to improved growth and yield under elevated temperature, it is important that future research also explores any costs associated with acclimation. This is particularly important in the context of crop breeding, because even if acclimation reduces yield losses suffered under high temperature, such gains could be negated by a decrease in yield under optimal/non-stressful conditions. More



broadly, some instances of thermal acclimation have been found to manifest as reductions in photosynthetic rate and been termed 'detractive adjustments' (Way and Yamori, 2014).

Though most of the work presented in this thesis was conducted at the leaf level, Chapter 4 demonstrated that root respiration responded similarly to night warming. In addition to cross-organ comparisons, plant development is another important consideration when describing wheat photosynthetic and respiratory responses to high temperature. This thesis contains physiological measurements taken at a range of wheat phenological stages, from the tillering stage in early vegetative development, to the critical stages of heading and anthesis. As mentioned in Chapter 1, previous work has shown that the temperature response of wheat respiration changes from the vegetative to reproductive stages (Todd 1982; Mitchell *et al.* 1991). Thus, it is important to consider phenological stage when researching wheat temperature acclimation, as  $R_{\text{dark}}$  might be expected to increase as plants approach the energy-intensive processes of reproduction, flowering, and grain filling. Longitudinal studies will be required if we are to fully understand how temperature effects changing respiratory demand over the course of wheat development.

### **Limits to acclimation/limits of life at high temperature**

Many of the results reported in this thesis raise interesting questions surrounding the upper thermal limits of the acclimation and function of plant physiological processes. This is no more apparent than in Chapter 3, in which an experiment was run to determine the upper threshold of  $T_{\text{crit}}$  increase following exposure to heat stress. As this experiment and previous publications (O'Sullivan *et al.*, 2017; Zhu *et al.*, 2018) demonstrated,  $T_{\text{crit}}$  often rises in response to increasing leaf temperature. This response is generally considered a form of thermal acclimation of PSII; however, whether there is an upper limit to this rise in  $T_{\text{crit}}$  and, if so, where this limit lies, was unclear up to this point. An upper limit to the high temperature-induced increase in  $T_{\text{crit}}$  of approximately 43.7°C was observed for two wheat genotypes in the in Chapter 3 experiment. While the existence of physiological limits to thermal acclimation is perhaps unsurprising, quantifying such limits provides valuable insight into the risks associated with future extreme heat events. This is illustrated by the thermal safety margin data presented in Chapter 3; while acclimation to elevated growth temperature improved current PSII thermal safety margins for the majority of wheat genotypes, such acclimation would be largely inadequate to maintain thermal safety margins under the more

severe warming scenarios that are predicted by climate modellers. Recent studies of a range of woody plant species reported maximum  $T_{crit}$  values of approximately 48°C (Marias *et al.*, 2017; Perez and Feeley, 2020). However, it is not clear if this number reflects PSII heat tolerance in warm-acclimated plants, and thus may not represent a hard threshold. Estimates of possible upper temperature limits for optimal CO<sub>2</sub> assimilation rates are also present in the literature (approximately 35°C for C<sub>3</sub> species and 40°C for C<sub>4</sub> species; Yamori *et al.*, 2014), though it is also unclear whether these are thresholds of warm-acclimated plants. If the thresholds from Marias *et al.* and Perez and Feeley did reflect the true upper limit of PSII heat tolerance of these species, it would suggest that this limit is fairly conserved across plant species. However, further work is required to verify the upper limits of PSII heat tolerance in a greater number of species in order to test this theory. Quantifying the physiological limits of thermal acclimation across plant species could thus prove useful for identifying the specific risks that future warming events pose for key plant processes such as photosynthetic electron transport. High-throughput methods for quantifying these limits, like the assay used in this thesis to measure  $T_{crit}$ , are crucial for collecting such measurements for large numbers of genotypes and species.

Like the upper limit of thermal acclimation of wheat PSII that was identified in Chapter 3, similar limits likely exist for the acclimation of other photosynthetic and respiratory processes. A recent study of *Quercus serrata* grown at high and low altitude by Yamaguchi *et al.* (2019) provided further evidence of upper limits to photosynthetic acclimation; in that study, the authors found that the optimum temperature of CO<sub>2</sub> assimilation initially rose with growth temperature before then plateauing. Additional examples of studies that have identified acclimation limits for either photosynthesis or respiration are scarce. However, given that increases in the maximum thermal tolerance of respiration ( $T_{max}$ ) must be driven primarily by increasing membrane fatty acid saturation (Arthur and Watson, 1976; Zhu *et al.*, 2018; Scafaro *et al.*, 2021), it is logical that such alterations could not persist unperturbed by continued warming. As leaf temperature approaches  $T_{max}$  proteins have typically begun to denature and adenylate supply is limited due to decreased membrane functionality (Scafaro *et al.*, 2021). Furthermore, while past estimates of  $T_{max}$  have generally fallen within the range of 50–60°C (O’Sullivan *et al.*, 2017), these estimates are likely inflated by the common practice of rapidly ramping leaf temperature (~1 min/°C) when determining  $T_{max}$ . When warming is more gradual, as is typical in nature, estimates of  $T_{max}$  are significantly lower (O’Sullivan *et al.*,

2013). The fact that many current approximations of  $T_{\max}$  may be overestimates is further evidence of the need for additional, targeted research on the upper thermal limits of plant physiology, similar to that which was conducted in this thesis.

### **Implications for crop breeding and wheat yield gains**

As well as being a useful tool for identifying the upper limits of acclimation, high-throughput phenotyping is central to crop breeding programmes seeking to protect and improve yields in a warming climate. While pursuing higher rates of CO<sub>2</sub> assimilation and lower rates of respiratory CO<sub>2</sub> release are popular goals when seeking to improve crop yields under high temperature (Wilson and Jones, 1982; Cossani and Reynolds, 2012; Reynolds *et al.*, 2012), methods of measuring gas-exchange have traditionally been too slow and cumbersome to effectively aid the large-scale phenotyping required in crop breeding programmes. However, the recent development of high-throughput methods for measuring photosynthetic and respiratory characteristics has begun to address this issue. Two of the assays used in this thesis highlight improvements in the efficiency of phenotyping gas-exchange parameters; the Q2 (Astec Global, Maarsse, The Netherlands) system used to measure respiratory O<sub>2</sub> consumption, and the FluorCam 800MF system (Photon System Instruments, Brno, Czechia) that measures  $T_{\text{crit}}$  of PSII. The use of the Q2's robotic fluorophore-sensing system to measure plant tissue respiration rates across a variety of temperatures is a relatively recent development (Scafaro *et al.*, 2017), yet it has already facilitated the screening of plant dark respiration in larger numbers than were possible with previous methods (O'Sullivan *et al.*, 2017; Coast *et al.*, 2019). Similarly, the FluorCam technique described in Chapter 3 combines traditional chlorophyll fluorescence imaging techniques with a 48-well heating block, thus providing a 48-fold improvement in the speed of measuring chlorophyll fluorescence-based traits (such as  $T_{\text{crit}}$ ) when compared with methods restricted to measuring samples individually (Zhu *et al.*, 2018). While these are good examples of how improved measurement speed and efficiency can bolster phenotyping efforts, further gains are yet required to significantly expand future crop breeding programmes.

Techniques based on leaf hyperspectral reflectance are an example of an approach that is comparatively closer to having significant impacts on real world phenotyping. These approaches are based on the fact that crop leaves reflect light within the near-infrared ranges

of 700-1100 nm and shortwave infrared up to 2500nm (Furbank and Tester, 2011). Exploiting the relationship of leaf reflectance signatures with traits such as chlorophyll or nitrogen content has become more common in plant science (Martin and Aber, 1997; Zarco-Tejada *et al.*, 2003; Yendrek *et al.*, 2017; Furbank *et al.*, 2021). While hyperspectral reflectance was initially mostly used to predict traits that directly alter leaf light absorption (e.g. chlorophyll content), more recent work has demonstrated that more complex physiological traits can also be predicted via leaf reflectance. For instance, recent papers have shown that models can be trained to use wheat leaf hyperspectral reflectance to accurately estimate photosynthetic characteristics such as maximum CO<sub>2</sub> carboxylation rate and chloroplast electron transport rate (Silva-Pérez *et al.*, 2018; Furbank *et al.*, 2021), both of which otherwise could only be collected with relatively slow gas-exchange measurements. A similarly successful approach has also been used to predict leaf dark respiration in wheat using hyperspectral reflectance signatures (Coast *et al.*, 2019). Given that the hand-held technique used by both Silva-Pérez *et al.* (2018) and Coast *et al.* (2019) allowed for the measurement of 100 leaves per hour, hyperspectral reflectance-based techniques can dramatically increase the scale of phenotyping efforts. Furthermore, the capacity to remotely sense leaf hyperspectral signatures – including through the use of satellites – has already been established (Blackburn, 2006), and so it is possible that continued progress in this area will allow for extremely high-throughput screening of entire fields and growing regions for complex physiological traits that have been identified as being heat-adaptive.

Identifying and understanding physiological traits that help to maintain or even enhance yield under high temperature, as well as the development of high-throughput methods to screen these traits, are key preliminary steps in breeding for heat tolerance in wheat (Cossani and Reynolds, 2012). This is particularly true given that, despite recent efforts to identify wheat genes or quantitative trait loci central to heat tolerance (Paliwal *et al.*, 2012; Zang *et al.*, 2018; Schmidt *et al.*, 2020), there are still no known genes that directly confer heat tolerance in wheat (Cossani and Reynolds, 2012). Thus, an alternative approach to breeding genotypes for increased heat tolerance relies upon crossing parents that each possess traits known to improve crop performance under high temperature. The theory behind this approach is that such crosses produce what Reynolds *et al.* (2009) term ‘cumulative gene action,’ giving rise to genotypes that enjoy the heat-adaptive traits of both parents. The parents for such crosses are often recombinant inbred lines, which themselves

undergo large scale screening to identify alleles that may confer (in this case) heat tolerance. Unintended consequences of these crosses must also be considered, particularly in light of environmental variability (Cossani and Reynolds, 2012). As mentioned above, rather than being solely controlled by a handful of individual genes heat tolerance is also influenced by environmental variability. Understanding and quantifying the variability in growth environment is thus also important in breeding efforts. This is because knowledge of the variation in environmental conditions can be included alongside traits of interest in parents (both heat-adaptive and otherwise) to model the potential benefits of particular crosses in a given environment (Chapman, 2008). Such thinking has led to success in the development of wheat genotypes with improved drought tolerance (Reynolds and Tuberosa, 2008), and so there is reason to believe similar gains could be achieved for wheat heat tolerance.

### **Improving models to represent plant carbon flux more accurately under warming**

In addition to their implications for crop breeding (as discussed in the previous section), the results presented in this thesis also raise concerns with how models represent plant gas exchange and growth in a warming climate. Specifically, while the preceding chapters contain many findings that portray the complexity of the relationship between respiration and photosynthesis and their responses to warming, most popular models used to predict crop growth do not currently capture any of this complexity (see Table 3 in Chapter 1 for a review of a number of these models). To take one example, the Agricultural Production Systems Simulator (APSIM) model developed in Australia in 1991 is prominently used to predict wheat growth and yield – there is even a modified version of the model called APSIM-wheat that is specifically used to predict wheat growth. However, APSIM is extremely limited in its representation of plant respiration when modelling plant biomass accumulation. In APSIM-Wheat, solar radiation, transpiration, and nitrogen availability are the factors that determine estimates of biomass accumulation, while respiration is only considered indirectly via the simulation of net photosynthesis (Brown *et al.*, 2021). Consideration of temperature stress is similarly limited relative to these other factors – water and N stressors are the primary limitations to net carbon assimilation and biomass accumulation, while the effect of warming on biomass accumulation is mostly relegated to its acceleration of the rate at which crops

progress through phenological stages (Brown *et al.*, 2021). However, the results described in Chapters 2 and 4 of this thesis demonstrate that the relationship between wheat respiration and photosynthesis is not necessarily fixed, and that warming (particularly when it occurs during the night) may cause the uncoupling of these processes. Specifically, we observed that night warming coincided with a downregulation of respiratory O<sub>2</sub> consumption but no such decline in CO<sub>2</sub> release. We also found that an increase in the capacity of the non-energy producing AOX mitochondrial electron transport pathway under warm nights. Together, these results suggested a potential reduction in the efficiency of ATP production per CO<sub>2</sub> release, driven perhaps by a reduced demand for ATP under warm nights. Such a response to warming has clear implications for plant biomass accumulation (as discussed at greater length in the discussion section of chapter four), and indeed the plants from which these measurements were taken also demonstrated significant declines in above- and below-ground biomass with increasing night temperature. In light of this, the practice adopted by the majority of current crop models – that of assuming fixed rates of respiration, or even ignoring respiration entirely – seems likely to be a source of increasing inaccuracy in a world in which night-time temperature continues to rise.

Crop models are not the only models that could stand to benefit from an improved understanding of respiration and its relationship with temperature and photosynthesis. Current models of ecosystem-level CO<sub>2</sub> exchange also contain potential inaccuracies stemming from their representations of plant respiration. Just like the majority of crop models, many popular terrestrial biosphere models incorporate rather rudimentary representations of plant respiration, its response to warming, and how it scales with photosynthesis. For instance, the Joint UK Land Environment Simulator (JULES) models the CO<sub>2</sub> flux between terrestrial vegetation and the atmosphere (Clark *et al.*, 2011). As in other similar models,  $R_{\text{dark}}$  is represented in JULES in relation to plant gross primary productivity; specifically,  $R_{\text{dark}}$  at the standard measuring temperature of 25°C is expressed as a fixed proportion of the maximum rate of carboxylation at 25°C ( $V_{\text{cmax}}^{25}$ ). Estimates of  $V_{\text{cmax}}^{25}$  are based on leaf N data and thus rely on the robust relationship between  $V_{\text{cmax}}$  and leaf N (Atkin *et al.*, 2015). Terrestrial biosphere models also often adopt the common practice of obtaining  $V_{\text{cmax}}$  estimates from gas-exchange data, namely using CO<sub>2</sub> response curves of photosynthesis (von Caemmerer and Farquhar, 1981). Through their analysis of a data set spanning 899 species across 20 global sites, Atkin *et al.* (2015) demonstrated that the  $R_{\text{dark}}^{25}-V_{\text{cmax}}^{25}$

relationship is reliably proportional. However, they also showed that this relationship can become significantly more variable with elevated growth temperature. The results presented in Chapters 2 and 4 of this thesis lend further support for incorporating the response of leaf respiration to warming into estimates of vegetative CO<sub>2</sub> flux in models such as JULES (Huntingford *et al.*, 2017). In fact, considering the evidence presented in this thesis that suggests that plant  $R_{\text{dark}}$  responds differently to night versus day warming, it may be prudent for modellers to consider independently represent the effects of day and night-time temperature on plant gas-exchange. This could become particularly useful in the context of current global warming trends, given that night warming continues to outpace daytime warming in many regions (Davy *et al.*, 2017).

As mentioned above, JULES considers  $R_{\text{dark}}$  to be directly proportional to  $V_{\text{cmax}}$ ; specifically,  $R_{\text{dark}}^{25}$  is assumed to be 1.5% of  $V_{\text{cmax}}^{25}$  (Atkin *et al.*, 2015). However, this assumption is reliant on another assumption – that all Rubisco in each leaf constantly remains 100% active. Yet, this seems unlikely, and indeed evidence has suggested this to be an overestimation (Sage *et al.*, 1990; Makino and Sage, 2007). Therefore, it is likely that many current models are underestimating the respiratory costs associated with maintaining the proportion of inactive Rubisco in leaves. Given the large total CO<sub>2</sub> fluxes moving between terrestrial vegetation and the atmosphere, even small inaccuracies in modelling the leaf-level  $R_{\text{dark}}-V_{\text{cmax}}$  relationship could give rise to significant errors when estimating flux at the ecosystem level (Piao *et al.*, 2010). Additionally, as observed throughout this thesis temperature exercises a strong influence over both respiration and photosynthesis, thus it is worth considering how warming might also affect the modelling of the  $R_{\text{dark}}-V_{\text{cmax}}$  relationship. In a study of rice Scafaro *et al.* (2016) found that Rubisco activation fell to approximately 40% following four hours of exposure to a 45°C heat stress. Recent work has also provided evidence that incorporating a greater account of thermal history in the JULES model improves the accuracy of  $V_{\text{cmax}}$ -based predictions of  $R_{\text{dark}}$  (Huntingford *et al.*, 2017). Such improvements highlight the value of physiology-level research that improves our understanding of the temperature response of trait-trait relationships in the larger effort to optimise the performance of terrestrial biosphere models in a rapidly warming climate. If patterns that were observed throughout much of this thesis in wheat – such as a reduced ATP demand and increased inefficiency of ATP production under warm nights – are common to other plant species, it could lead to considerable inaccuracies in modelled terrestrial biosphere CO<sub>2</sub> flux.

Considering the near-global trend of asymmetric warming (in which daily minimum temperatures have risen more rapidly than daily maximums), this is a research area worthy of further attention.

## Conclusion

In the first chapter of this thesis, literature on the high temperature responses of wheat photosynthesis and respiration was reviewed, and several gaps in the literature were identified. This review made clear the lack of existing knowledge of how wheat respiration responds to warming, including how important factors such as plant phenological stage and the timing of warming events interact with this response. While it was acknowledged that wheat photosynthetic high temperature responses are comparatively better understood, the ongoing trend of warming and increased incidents of heat stress events mean that crop breeding efforts will likely benefit from improved understanding in these areas. The experiments in Chapters 2–4 were thus designed to provide insight into the responses of wheat respiration and photosynthesis to warming, and to do so across various settings (e.g., in the field vs. controlled environments) and using a variety of approaches. Major findings from this research that help to fill existing knowledge gaps include: (1) wheat  $R_{\text{dark}}$   $\text{O}_2$  flux acclimated to warming as expected, yet leaf  $\text{CO}_2$  flux did not acclimate; (2) increases in average daily minimum temperature were more influential in driving respiratory acclimation than increases in daily maximum temperature; and (3), an upper limit to the high temperature acclimation of wheat photosystem II was identified. Despite these new contributions to our knowledge of wheat physiological temperature responses, there are still questions raised in Chapter 1 that remain unanswered. For instance, while the evidence published here confirms the occurrence of respiratory thermal acclimation in wheat, it remains to be seen whether the observed acclimation responses translate to improved yield following warming in field conditions. Further work is also required to better understand the extent to which thermal acclimation of respiration might prime plants for the longer, more intense heatwaves that are predicted to threaten wheat yields in the coming decades.

## References

**Arthur H, Watson K.** 1976. Thermal adaptation in yeast: growth temperatures, membrane



lipid, and cytochrome composition of psychrophilic, mesophilic, and thermophilic yeasts. *Journal of Bacteriology* **128**, 56–68.

**Atkin OK, Bloomfield KJ, Reich PB, et al.** 2015. Global variability in leaf respiration in relation to climate, plant functional types and leaf traits. *New Phytologist* **206**, 614–636.

**Atkin OK, Tjoelker MG.** 2003. Thermal acclimation and the dynamic response of plant respiration to temperature. *Trends in Plant Science* **8**, 343–351.

**Bahuguna RN, Chaturvedi AK, Pal M, Viswanathan C, Jagadish SVK, Pareek A.** 2022. Carbon dioxide responsiveness mitigates rice yield loss under high night temperature. *Plant Physiology* **188**, 285–300.

**Blackburn GA.** 2006. Hyperspectral remote sensing of plant pigments. *Journal of Experimental Botany* **58**, 855–867.

**Brown HE, Huth NI, Holzworth DP.** 2021. The APSIM Wheat Model.

**von Caemmerer S, Farquhar GD.** 1981. Some relationships between the biochemistry of photosynthesis and the gas exchange of leaves. *Planta* **153**, 376–387.

**Carmo-Silva E, Salvucci M.** 2011. The activity of Rubisco's molecular chaperone, Rubisco activase, in leaf extracts. *Photosynthesis Research* **108**, 143–155.

**Chapman SC.** 2008. Use of crop models to understand genotype by environment interactions for drought in real-world and simulated plant breeding trials. *Euphytica* **161**, 195–208.

**Clark DB, Mercado LM, Sitch S, et al.** 2011. The Joint UK Land Environment Simulator (JULES), model description – Part 2: Carbon fluxes and vegetation dynamics. *Geoscientific Model Development* **4**, 701–722.

**Coast O, Shah S, Ivakov A, et al.** 2019. Predicting dark respiration rates of wheat leaves from hyperspectral reflectance. *Plant, Cell & Environment* **42**, 2133–2150.

**Cossani CM, Reynolds MP.** 2012. Physiological Traits for Improving Heat Tolerance in Wheat. *Plant Physiology* **160**, 1710–1718.

**Crafts-Brandner S, Salvucci M.** 2000. Rubisco activase constrains the photosynthetic potential of leaves at high temperature and CO<sub>2</sub>. *Proceedings of the National Academy of Sciences* **97**, 13430-13435.

**Davy R, Esau I, Chernokulsky A, Outten S, Zilitinkevich S.** 2017. Diurnal asymmetry to the observed global warming. *International Journal of Climatology* **37**, 79–93.

**Degen GE, Orr DJ, Carmo-Silva E.** 2020a. Heat-induced changes in the abundance of wheat Rubisco activase isoforms. *New Phytologist*.

**Degen GE, Worrall D, Carmo-Silva E.** 2020b. An isoleucine residue acts as a thermal and regulatory switch in wheat Rubisco activase. *Plant Journal* **103**, 742–751.

**Furbank RT, Silva-Pérez V, Evans JR, Condon AG, Estavillo GM, He W, Newman S, Poiré R, Hall A, He Z.** 2021. Wheat physiology predictor: predicting physiological traits in wheat from hyperspectral reflectance measurements using deep learning. *Plant Methods* **17**, 1–16.

**Furbank RT, Tester M.** 2011. Phenomics - technologies to relieve the phenotyping bottleneck. *Trends in Plant Science* **16**, 635–644.

**Huntingford C, Atkin OK, Martinez-De La Torre A, et al.** 2017. Implications of improved representations of plant respiration in a changing climate. *Nature Communications* **8**, 1–11.

**Makino A, Sage RF.** 2007. Temperature response of photosynthesis in transgenic rice transformed with 'sense' or 'antisense' rbcS. *Plant and Cell Physiology* **48**, 1472–1483.

**Marias DE, Meinzer FC, Woodruff DR, McCulloh KA.** 2017. Thermotolerance and heat stress responses of Douglas-fir and ponderosa pine seedling populations from contrasting climates. *Tree Physiology* **37**, 301–315.

**Martin ME, Aber JD.** 1997. High spectral resolution remote sensing of forest canopy lignin,

nitrogen, and ecosystem processes. *Ecological Applications* **7**, 431–443.

**O’Sullivan OS, Heskell MA, Reich PB, et al.** 2017. Thermal limits of leaf metabolism across biomes. *Global Change Biology* **23**, 209–223.

**O’Sullivan OS, Weerasinghe KWLK, Evans JR, Egerton JJG, Tjoelker MG, Atkin OK.** 2013. High-resolution temperature responses of leaf respiration in snow gum (*Eucalyptus pauciflora*) reveal high-temperature limits to respiratory function. *Plant, Cell & Environment* **36**, 1268–1284.

**Paliwal R, Röder MS, Kumar U, Srivastava JP, Joshi AK.** 2012. QTL mapping of terminal heat tolerance in hexaploid wheat (*T. aestivum* L.). *Theoretical and Applied Genetics* **125**, 561–575.

**Paolacci AR, Tanzarella OA, Porceddu E, Ciaffi M.** 2009. Identification and validation of reference genes for quantitative RT-PCR normalization in wheat. *BMC Molecular Biology* **10**, 1–27.

**Perez T, Feeley K.** 2020. Photosynthetic heat tolerances and extreme leaf temperatures. *Functional Ecology* **34**, 2236–2245.

**Piao S, Luysaert S, Ciais P, Janssens IA, Chen A, Cao C, Fang J, Friedlingstein P, Luo Y, Wang S.** 2010. Forest annual carbon cost: a global-scale analysis of autotrophic respiration. *Ecology* **91**, 652–661.

**Reich PB, Sendall KM, Stefanski A, Wei X, Rich RL, Montgomery RA.** 2016. Boreal and temperate trees show strong acclimation of respiration to warming. *Nature* **531**, 633–636.

**Reynolds MP, Foulkes J, Furbank R, Griffiths S, King J, Murchie E, Parry M, Slafer G.** 2012. Achieving yield gains in wheat. *Plant, Cell and Environment* **35**, 1799–1823.

**Reynolds M, Manes Y, Izanloo A, Langridge P.** 2009. Phenotyping approaches for physiological breeding and gene discovery in wheat. *Annals of Applied Biology* **155**, 309–320.

**Reynolds MP, Tuberosa R.** 2008. Translational research impacting on crop productivity in drought-prone environments. *Current Opinion in Plant Biology* **11**, 171–179.

**Ruijter JM, Ramakers C, Hoogaars WMH, Karlen Y, Bakker O, van den Hoff MJB, Moorman AFM.** 2009. Amplification efficiency: linking baseline and bias in the analysis of quantitative PCR data. *Nucleic Acids Research* **37**, e45–e45.

**Sage RF, Sharkey TD, Seemann JR.** 1990. Regulation of ribulose-1,5-bisphosphate carboxylase activity in response to light intensity and CO<sub>2</sub> in the C<sub>3</sub> annuals *Chenopodium album* L. and *Phaseolus vulgaris* L. *Plant Physiology* **94**, 1735–1742.

**Scafaro AP, Bautsoens N, Boer B Den, Van Rie J, Gallé A.** 2019. A conserved sequence from heat-adapted species improves Rubisco activase thermostability in wheat. *Plant Physiology* **181**, 43–54.

**Scafaro AP, Fan Y, Posch BC, Garcia A, Coast O, Atkin OK.** 2021. Responses of leaf respiration to heatwaves. *Plant, Cell & Environment*, pce.14018.

**Scafaro AP, Gallé A, Van Rie J, Carmo-Silva E, Salvucci ME, Atwell BJ.** 2016. Heat tolerance in a wild *Oryza* species is attributed to maintenance of Rubisco activation by a thermally stable Rubisco activase ortholog. *New Phytologist* **211**, 899–911.

**Scafaro AP, Negrini ACA, O’Leary BM, et al.** 2017. The combination of gas-phase fluorophore technology and automation to enable high-throughput analysis of plant respiration. *Plant Methods* **13**, 1–13.

**Schmidt J, Tricker PJ, Eckermann P, Kalambettu P, Garcia M, Fleury D.** 2020. Novel Alleles for Combined Drought and Heat Stress Tolerance in Wheat. *Frontiers in Plant Science* **10**.

**Silva-Pérez V, Molero G, Serbin SP, Condon AG, Reynolds MP, Furbank RT, Evans JR.** 2018. Hyperspectral reflectance as a tool to measure biochemical and physiological traits in wheat. *Journal of Experimental Botany* **69**, 483–496.

- Thistlethwaite R, Tan DKY, Bokshi AI, Ullah S, Trethowan RM.** 2020. A phenotyping strategy for evaluating the high-temperature tolerance of wheat. *Field Crops Research* **255**, 107905.
- Vierling E.** 1991. The Roles of heat shock proteins in plants. *Annual Review of Plant Biology* **42**, 579–620.
- Way DA, Yamori W.** 2014. Thermal acclimation of photosynthesis: On the importance of adjusting our definitions and accounting for thermal acclimation of respiration. *Photosynthesis Research* **119**, 89–100.
- Wilson D, Jones J.** 1982. Effect of selection for dark respiration rate of mature leaves on crop yields of *Lolium perenne* cv. S23. *Annals of Botany* **49**, 313–320.
- Yamaguchi DP, Mishima D, Nakamura K, Sano J, Nakaji T, Hiura T, Hikosaka K.** 2019. Limitation in the Photosynthetic Acclimation to High Temperature in Canopy Leaves of *Quercus serrata*. *Frontiers in Forests and Global Change* **2**, 1–10.
- Yamori W, Hikosaka K, Way D.** 2014. Temperature response of photosynthesis in C<sub>3</sub>, C<sub>4</sub>, and CAM plants: Temperature acclimation and temperature adaptation. *Photosynthesis Research* **119**, 101–117.
- Yendrek CR, Tomaz T, Montes CM, Cao Y, Morse AM, Brown PJ, McIntyre LM, Leakey ADB, Ainsworth EA.** 2017. High-Throughput Phenotyping of Maize Leaf Physiological and Biochemical Traits Using Hyperspectral Reflectance. *Plant Physiology* **173**, 614–626.
- Zang X, Geng X, He K, et al.** 2018. Overexpression of the Wheat (*Triticum aestivum* L.) TaPEPKR2 Gene Enhances Heat and Dehydration Tolerance in Both Wheat and Arabidopsis. *Frontiers in Plant Science* **9**.
- Zarco-Tejada P., Pushnik J., Dobrowski S, Ustin S.** 2003. Steady-state chlorophyll a fluorescence detection from canopy derivative reflectance and double-peak red-edge effects. *Remote Sensing of Environment* **84**, 283–294.
- Zhu L, Bloomfield KJ, Hocart CH, Egerton JJG, O’Sullivan OS, Penillard A, Weerasinghe LK, Atkin OK.** 2018. Plasticity of photosynthetic heat tolerance in plants adapted to thermally contrasting biomes. *Plant, Cell & Environment*, 1–12.

## Appendix

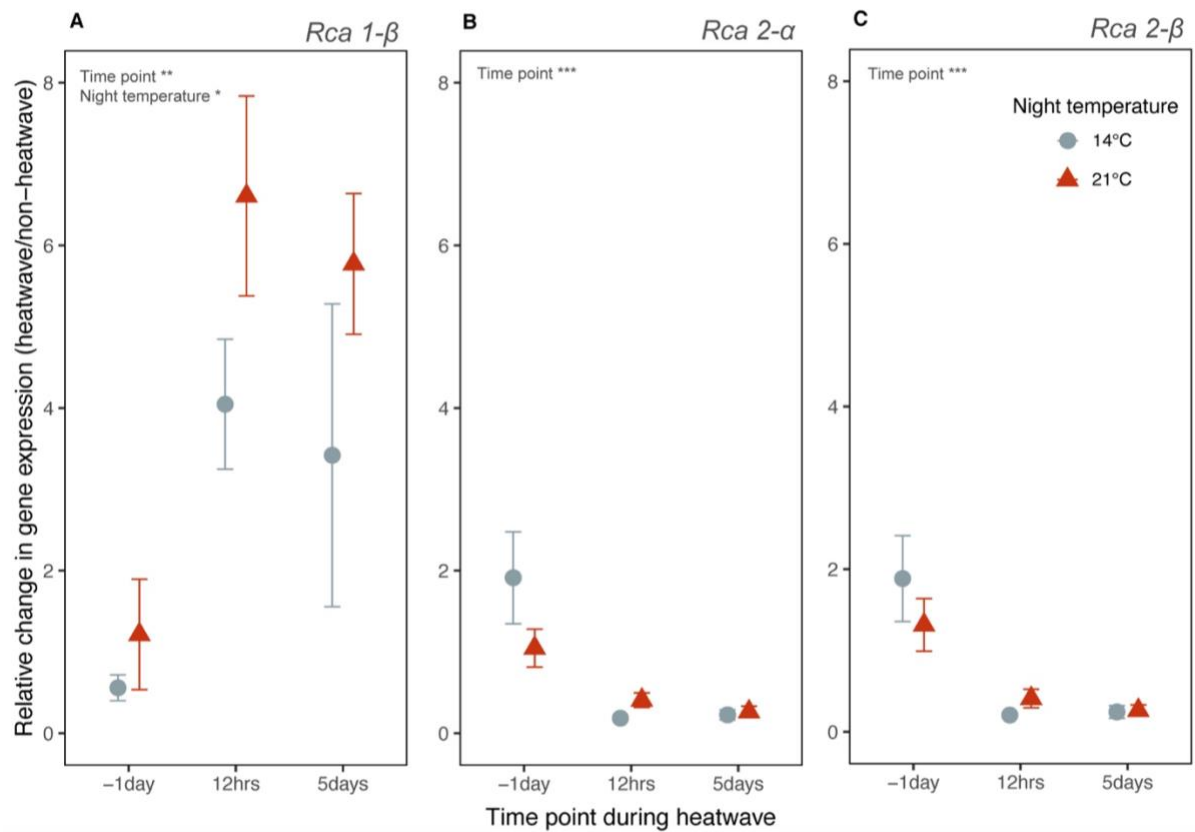
### The effect of night warming on Rubisco activase

While the results presented in the preceding chapters have provided insights into the temperature responses of respiration and photosynthesis at the leaf physiology level, effort was also made to briefly explore the biochemical mechanisms underpinning the observed responses to warming. Given how strong the influence of night warming appeared to be for leaf and root respiration, as well as biomass accumulation, an additional experiment was conducted to determine if night warming had a similarly significant influence on the wheat heat shock response during a daytime heatwave. Also of interest was the potential effects of night warming on photosynthesis – while it is rather straightforward that  $R_{\text{dark}}$  would be affected by warming during the night, it is less clear the extent to which night warming would affect photosynthetic processes that are restricted to the daytime. To explore these questions, tissues were sampled from plants grown in the daytime heatwave experiment described in Chapter 4 (in which plants were grown under cool and warm night temperatures and then exposed to a 5-day 38°C daytime heatwave).

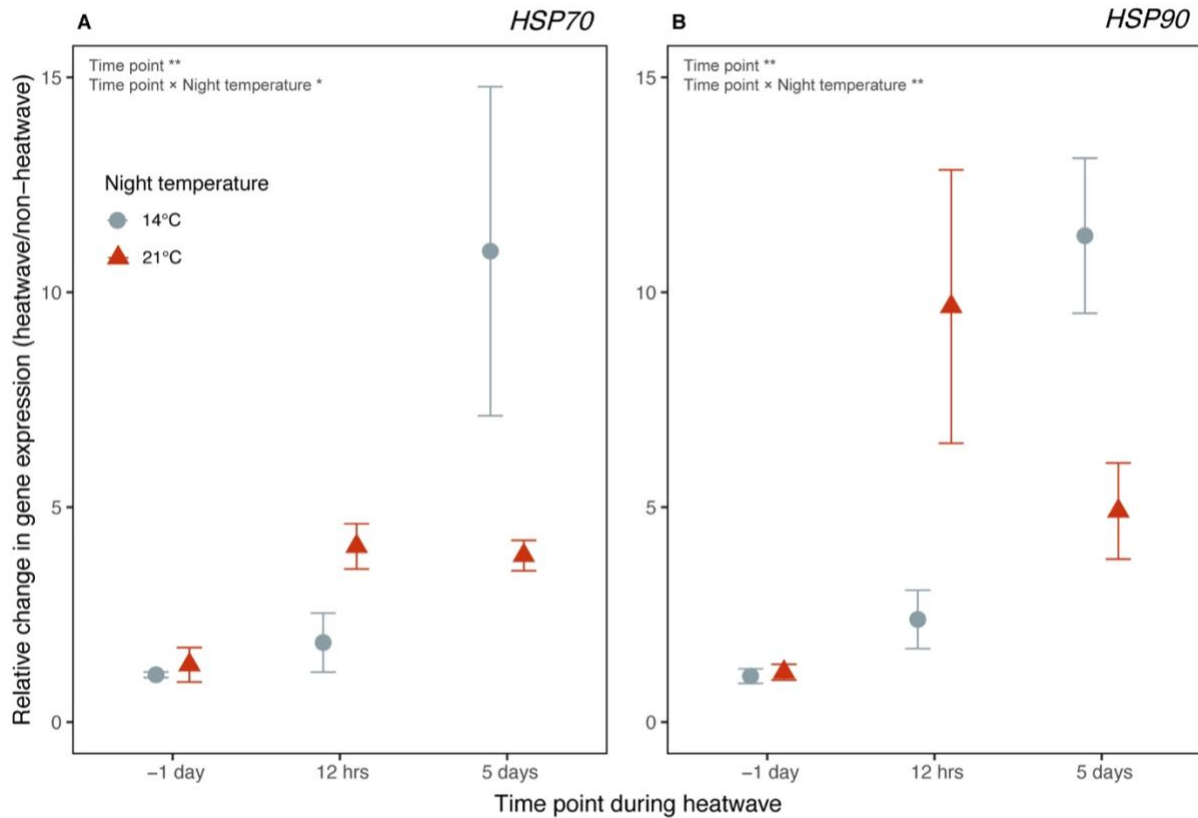
The gene- and protein-level responses of Rubisco activase (Rca) were chosen as the primary representation of photosynthesis at the biochemical level. This is because Rca is known to be critical for the function of Rubisco, particularly under high temperature (Carmo-Silva and Salvucci, 2011; Scafaro *et al.*, 2016). In fact, the heat susceptibility of Rca is far greater than that of Rubisco and is thus a major reason why carbon assimilation falls at temperatures beyond the photosynthetic optimum (Crafts-Brandner and Salvucci, 2000). Previous work identified three isoforms of Rca in wheat, including one (known as *Rca 1-β*) that is synthesised only following exposure to high temperature and that is able to remain active at temperatures beyond which the other two more abundant isoforms (*Rca 2-α* and *Rca 2-β*) begin to fail (Scafaro *et al.*, 2019; Degen *et al.*, 2020a). Based on these findings, we set out to determine if elevated night temperature influenced the expression of the *Rca 1-β* gene during a heatwave, as well as if this resulted in any increase in thermal tolerance of Rca at the protein level. Gene expression for heat shock proteins 70 and 90 (*HSP70* and *HSP90*, respectively) was also monitored to provide further insight into the effects of night warming

on the general wheat heat shock response, using genes that have been well-established as being part of the plant heat shock responses. Leaves of plants that had been grown at either 14 or 20°C nights for four weeks were sampled one day prior to the beginning of the 38°C daytime heatwave, then at 12 hours and five days after the heatwave began. qPCR analysis was used to quantify gene expression at each of these time points for the genes of interest (note: a complete description of the methodology employed for this work can be found in the Appendix).

The gene expression data showed that the daytime heatwave had the predicted impact on all genes of interest; significant increases in the expression of *HSP70*, *HSP90*, and *Rca 1-β* genes following just 12 hours of heat stress that were still apparent at the five-day mark of the heatwave, as well as declines in gene expression for the heat sensitive *Rca 2-α* and *Rca 2-β* in line with previous results (Scafaro *et al.*, 2019; Appendix Figs. 1 & 2). Interestingly, elevated night growth temperature was associated with greater increases in the expression of *Rca 1-β*, *HSP70*, and *HSP90* at the 12-hour point of the heatwave than occurred in the cool-night grown plants. The elevated expression of *Rca 1-β* in warm night plants was also observed five days into the heatwave (Appendix Fig. 1A), while for both HSPs gene expression in the cool-grown plants had exceeded that of the warm night plants by this point in the heatwave, though both maintained levels of expression significantly higher than control plants that has not experienced any heatwave (Appendix Fig. 2). Taken together, it thus appeared as if night warming had had a priming effect for these three genes, promoting faster and greater levels of expression once plants were challenged with a heatwave. The earlier decline in *HSP70* and *HSP90* levels in night warmed plants (evident five days into the heatwave) suggests not only a faster response but also a shorter time until full acclimation was realised, considering that HSP expression levels have been linked to the level of thermal stress (Vierling 1991).



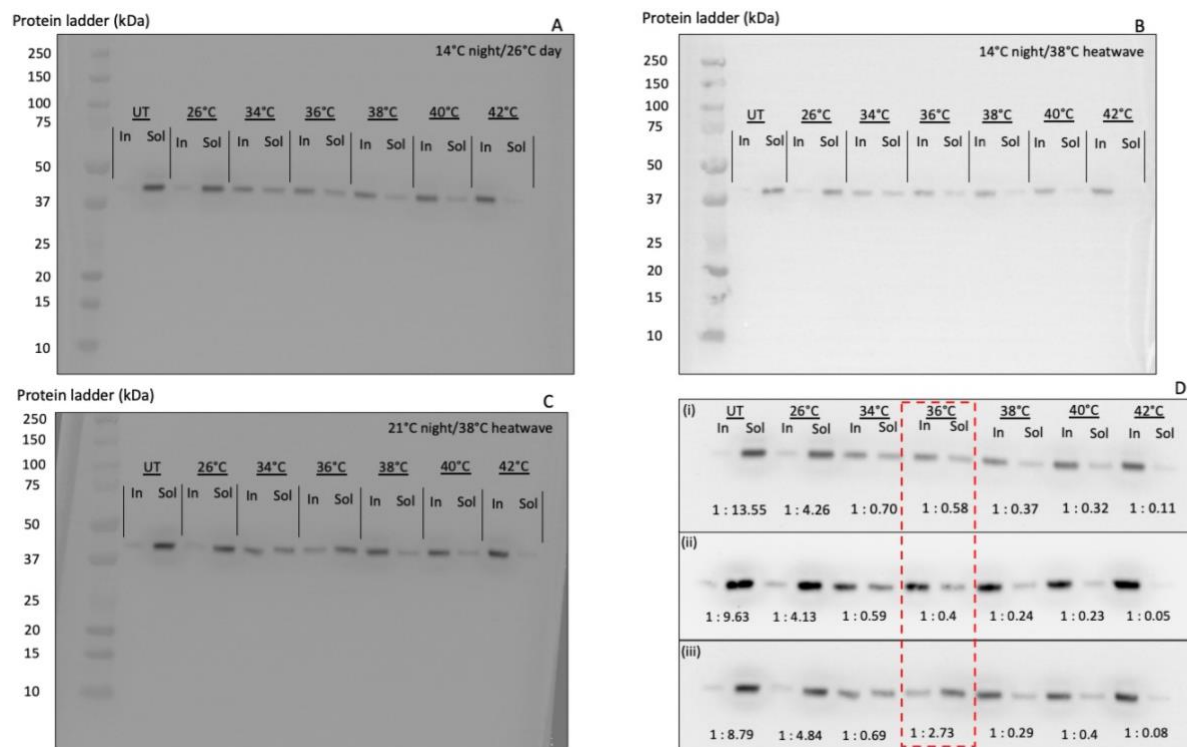
**Appendix Figure 1.** Relative change in gene expression of three wheat rubisco activase isoforms prior to and during a 38°C daytime heatwave for plants grown at 14°C or 21°C nights. Isoforms were *Rca-1β* (A), *Rca-2-α* (B), and *Rca 2-β* (C). Gene expression presented as change in plants that experienced daytime heatwave relative to expression in control plants that did not experience the heatwave (i.e. a value of one denotes expression was equal to that of control plant). Error bars denote s.e.,  $n = 5$ . Main treatment terms (time point and night temperature) are indicated in each panel when they have had a significant effect on gene expression, with \*, \*\*, and \*\*\* representing  $P < 0.05$ ,  $P < 0.01$ , and  $P < 0.001$ , respectively. See Appendix table 2 for analysis of variance results.



**Appendix Figure 2.** Relative change in gene expression of heat shock proteins 70 (A) and 90 (B) in wheat prior to and during a 38°C daytime heatwave for plants grown at 14°C or 21°C nights. Gene expression presented as change in plants that experienced daytime heatwave relative to expression in control plants that did not experience the heatwave (i.e. a value of one denotes expression was equal to that of control plant). Error bars denote s.e.,  $n = 5$ . Main treatment terms (time point and night temperature) are indicated in each panel when they have had a significant effect on gene expression, with \* and \*\* representing  $P < 0.05$  and  $P < 0.01$ , respectively. See Appendix table 2 for analysis of variance results.

To determine if the gene priming effect coincided with any difference in protein biochemistry, soluble leaf protein was extracted so that the thermostability of Rca could be determined at each time point for cool and warm grown plants (see Appendix for a detailed description of the methodology used). Regardless of plant growth temperature, incubating extracted leaf protein at temperatures of 38°C and above resulted in large drops in the ratio of soluble to insoluble extracted Rca protein (Appendix Fig. 3). For plants that had grown under 14°C nights the majority of Rca within extracted soluble leaf protein became insoluble following treatment at 34°C and 36°C for 10 minutes (Appendix Fig. 3A, 3B & 3D). However, the Rca of a warm night grown plant remained majority soluble following sample incubation at 36°C for 10 minutes. Thus, as well as being associated with an enhanced stimulation of

gene expression of the heat tolerant *Rca 1-β*, night warming was also linked to an increase in thermostability of the Rca protein.



**Appendix Figure 3.** Representative Western blots of wheat Rubisco activase for plants experiencing three different treatments: 14°C night/21°C day (no heatwave; A); 14°C night/38°C day heatwave (B); and 21°C night/38°C day heatwave (C). All plants were sampled five days after the beginning of the heatwave (or the equivalent time point for control plants that did not experience the heatwave). Extracted leaf protein was incubated at one of seven treatment temperatures, as denoted on blots – untreated (UT), 26°C, 34°C, 36°C, 38°C, 40°C, and 42°C. Bands for insoluble (In) and soluble (Sol) protein are shown for each treatment temperature. Precision Plus Protein Standards protein ladder (Bio-Rad, Hercules, CA, USA) is presented in panels A–C for reference. Intensity of soluble protein bands were expressed relative to the intensity of their equivalent insoluble protein band (D). The order of treatments show in panel D are: (i) 14°C night/21°C day; (ii) 14°C night/38°C day heatwave; and (iii) 21°C night/38°C day heatwave. Red broken line rectangle in panel D highlights bands of protein treated at 36°C.

While evidence at the gene and protein levels suggested that acclimation to elevated night growth temperature may have left wheat better equipped to cope with a daytime heatwave, it remains unclear whether these biochemical adjustments translate to tangible improvements in photosynthetic performance and plant growth. Although its superior heat tolerance and rapid induction following heat stress are evident, it should be noted that the *Rca 1-β* isoform makes up a relatively small proportion of overall Rca abundance; Degen *et al.* (2020a) reported the figure as 6% of the total pool of Rca in wheat flag leaves following



five days at 38°C. However, given that our results corroborate previous reports of upregulated expression of *Rca 1-β* coinciding with improved Rca thermotolerance (Scafaro *et al.*, 2019; Degen *et al.*, 2020b), it appears that this isoform may still be conferring benefits under high temperature. Furthermore, the observation reported above of night warming alone inducing *Rca 1-β* during a daytime heatwave is the first time such a response has been described. While it has yet to be determined if this reflected a response unique to elevated night growth temperature (as the effects of elevated day growth temperature prior to the heatwave were not explored), the fact that acclimation to night warming was associated with increased *Rca 1-β* expression and Rca thermotolerance illustrates that these daytime, photosynthetic processes are responsive to night-time warming. To address these unresolved questions, future research could examine whether *Rca-1-β* expression is associated with any change in photosynthetic capacity (i.e.  $V_{\text{cmax}}$ ) at high temperature. Also worth investigating is whether HSPs 70 and 90 (as well as additional HSPs) exhibit a change at the protein-level corresponding with our gene expression observations and, if so, what functional consequences this carries for leaves under high temperature.

#### *Materials & methods for biochemical work*

For a detailed description of plant material and growth conditions, see the Materials and Methods section in Chapter 4. Briefly, the wheat genotype Mace was established in controlled environment rooms under the control temperature of 26/14°C (day/night) for nine weeks following germination. An elevated night temperature of 21°C was then imposed on half of the plants, and plants were thus maintained at either 26/14°C or 26/21°C for the subsequent two weeks. At this point, a daytime heatwave in which the maximum temperature reached 38°C was imposed for five days. Flag leaves were sampled and snap frozen in liquid N<sub>2</sub> at the following time points: one day prior to the beginning of the heatwave at 12:00pm; 12 hours after the heatwave began at 5:30pm; and five days after the heatwave began at 12:00pm.

#### *Gene-expression*

Real-time quantitative polymerase chain reaction (qPCR) was performed to measure gene expression for the following genes: *Rca 1-β*, *Rca 2-α*, *Rca 2-β*, *HSP 70*, and *HSP 90*. Primers used are listed in *Appendix table 1*. For RNA extraction three frozen leaf discs of 0.96cm<sup>2</sup> were

ground with a TissueLyser II bead mill (Qiagen Hilden, Germany). RNA extraction followed protocol of RNeasy Plant Mini Kit (Qiagen, Hilden, Germany). Synthesis of cDNA was performed using SuperScript<sup>®</sup>III Reverse Transcriptase (Invitrogen, Waltham, MA, USA). qPCR was run using LightCycler<sup>®</sup> 480 SYBR Green I Master on a LightCycler 480 system (Roche Holding AG, Basel, Switzerland), following the manufacturer's recommended cycles for PCR run in a LightCycler<sup>®</sup> 480 Multiwell Plate 384. Five biological replicates were used for each treatment with three technical replicates. Wells contained 10 $\mu$ M F primer and R primer (0.5 $\mu$ L of each), 1 $\mu$ L cDNA (ranging in concentration from 5-35ng/ $\mu$ L), 5 $\mu$ L SYBR Master Mix, and 3 $\mu$ L H<sub>2</sub>O for a total of 10 $\mu$ L per reaction. Analysis of raw qPCR data was carried out using LinRegPCR (Ruijter *et al.*, 2009). Data was normalised to reference genes *Ta54227* and *Ta54238*, then expressed as change relative to non-heatwave conditions (Paolacci *et al.* 2009).

**Appendix table 1.** Primers used for qPCR analysis. Cell division control genes *Ta54227* and *Ta54238* were used as the reference genes which Rca and HSP expression were normalised against.

Gene	Forward primer	Reverse primer
<i>TaRca1-<math>\beta</math></i>	GGG TCG GCG AGA TCG GCG T	CCA GCA TGT GGC CGT ACT CCA TG
<i>TaRca2-<math>\alpha</math></i>	CCT TCT ACG GTA AAG GGG CAC AG	TGT AAA GGC AGC TCC CGT CGT
<i>TaRca2-<math>\beta</math></i>	CCA TAC ACA CCC ACC ATC TCT TGC	TGT AAA GGC AGC TCC CGT CGT
<i>TaHsp70</i>	AGG GTG AGG AGA AGC AGT TC	CAG TGG GCT CGT TGA TGA TG
<i>TaHsp90</i>	TAC TCC ATT GGC CAG CTC AA	ACC TCC TTG ATC ACC TTG CA
<i>Ta54227</i>	CAA ATA CGC CAT CAG GGA GAA CAT C	CGC TGC CGA AAC CAC GAG AC
<i>Ta54238</i>	TTC TTT TCT CAC AAC CCA ACG AC	GCC TCC CGA CAT TGC CAT CTG

#### *Thermally dependent solubility of rubisco activase in extracted leaf protein*

Soluble leaf protein was extracted from ground frozen leaf samples. One frozen leaf disc of 0.96cm<sup>2</sup> was homogenised in a 1.5mL Wheaton glass homogeniser in 1mL extraction buffer (50 mM HEPPEs pH 8, 5mM MgCl<sub>2</sub>, 1mM EDTA, 2% PVP, 1% plant protease inhibitor (Sigma, St. Louis, MO, USA), 25 $\mu$ M PMSF, and 4mM DTT. Samples were then immediately centrifuged for one minute at 4°C and 16000 rcf and supernatant kept on ice. Supernatant was then incubated for 10 minutes at one of the following temperatures: 26°C, 34°C, 36°, 38°C, 40°C, 42°C, or maintained at room temperature. Incubation temperatures were chosen based on previous work showing wheat Rca activity declining significantly at temperatures above 34°C (Scafaro *et al.*, 2019). Samples were then immediately spun at 4°C for 10 minutes at 19000

rcf. Soluble protein was diluted in 4x NuPAGE™ LDS Sample Buffer (Invitrogen, Waltham, MA, USA), while pellet was resuspended in 1x NuPAGE™ LDS Sample Buffer (Invitrogen, Waltham, MA, USA) in order to achieve the same final volume. Beta-mercaptoethanol (1/10 dilution) was added to all solutions, which were then heated for 10 minutes at 70°C. Proteins were further diluted 1/5 with 1x NuPAGE™ LDS Sample Buffer (Invitrogen, Waltham, MA, USA), then 5µl was loaded and separated by electrophoresis on a NuPAGE 4-12% Bis-Tris gel (Invitrogen, Waltham, MA, USA) in MES SDS Running Buffer (25mM MES, 25mM Tris, 1.7 mM SDS, 400 µM Na<sub>2</sub>EDTA). For immunoblotting, proteins were transferred from gels to Immobilon-P polyvinylidene fluoride membranes (Merck Millipore, MA, USA) using an XCell II Blot module (Invitrogen, Waltham, MA, USA) and transfer buffer (25 mM Bicine, 25 mM Bis-Tris, 0.8 mM EDTA, 10% (v/v) Methanol). Transfers were at 25 volts (150mA) for 120 minutes at 4°C. Membranes were then blocked for a minimum of two hours in solution of 5% (w/v) skim milk powder and TBS pH 7.6 (10mM Tris, 150 mM NaCl). Membranes were then incubated for 45 minutes in wheat Rca primary antibody diluted 1/3000 in solution of 12mL TBS and 3mL of 5% skim milk powder. Rca wheat antibody was provided courtesy of Prof. Spencer Whitney of the Australian National University. Membranes were then washed in TBS three times for 15 minute intervals, and then incubated for 45 minutes with goat anti-rabbit HRP secondary antibody diluted 1/3000 in solution of 12mL TBS and 3mL of 5% skim milk powder. After three more 15 minute TBS washes, membranes were prepared for imaging using ECL Western Blotting Substrate (Thermo Fisher Scientific, Waltham, MA, USA) and imaged on a ChemiDoc system (Bio-Rad, Hercules, CA, USA). Image analysis was carried out using Image Lab software (Bio-Rad, Hercules, CA, USA). Intensity of soluble protein bands was expressed relative to the intensity of insoluble protein bands for each sample at each treatment temperature. Precision Plus Protein Standards protein ladder (Bio-Rad, Hercules, CA, USA) was used for estimating molecular weights.

**Appendix table 2.** Analysis of variance of relativized gene expression for wheat *Rca 1-β*, *Rca 2-α*, *Rca 2-β*, *HSP70*, and *HSP90* prior to and during a five-day 38°C daytime heatwave.

	Time point		Night temperature		Time point × Night temperature	
	d.f.	F value	d.f.	F value	d.f.	F value
<i>Rca 1-β</i>	2	9.94 **	1	4.53 *	2	0.5 <sup>ns</sup>
<i>Rca 2-α</i>	2	15.1 ***	1	0.92 <sup>ns</sup>	2	0.11 <sup>ns</sup>
<i>Rca 2-β</i>	2	17.53 ***	1	0.28 <sup>ns</sup>	2	1.23 <sup>ns</sup>
<i>HSP70</i>	2	9.25 **	1	1.04 <sup>ns</sup>	2	5.45 *
<i>HSP90</i>	2	10.22 **	1	0.06 <sup>ns</sup>	2	9.28 **

\* $P < 0.05$ ; \*\* $P < 0.01$ ; \*\*\* $P < 0.001$ ; <sup>ns</sup> = not significant.  $n = 4$ . Time points were -1 day before heatwave, 12 hours after heatwave began, and 5 days after heatwave began. Night temperature was 14°C or 21°C.